Anomalies chromosomiques et leucémies lymphoïdes chroniques agressives : rôle des gènes TNFRSF10 dans la délétion 8p

Ludovic Jondreville

Thèse de doctorat

Spécialité Physiologie, Physiopathologie, Thérapeutique

Ecole doctorale 394

En vue de l'obtention du grade de

Docteur de Sorbonne Université

Présentée et soutenue par

Ludovic JONDREVILLE

le 04 avril 2023

Anomalies chromosomiques et leucémies lymphoïdes chroniques agressives : rôle des gènes *TNFRSF10* dans la délétion 8p

Devant un jury composé de

Pr. Guy GOROCHOV – Président du jury
Dr. Nadine VARIN-BLANK – Rapporteur
Pr. Romain GUIEZE – Rapporteur
Dr. Jozo DELIC – Examinateur
Dr. Lauren VERONESE – Examinateur
Pr. Florence NGUYEN-KHAC – Directrice de thèse

INSERM UMRS1138 – Centre de Recherche Biomédicale des Cordeliers

Thèse de doctorat

Spécialité Physiologie, Physiopathologie, Thérapeutique

Ecole doctorale 394

En vue de l'obtention du grade de

Docteur de Sorbonne Université

Présentée et soutenue par

Ludovic JONDREVILLE

le 04 avril 2023

Anomalies chromosomiques et leucémies lymphoïdes chroniques agressives : rôle des gènes *TNFRSF10* dans la délétion 8p

Devant un jury composé de

Pr. Guy GOROCHOV – Président du jury
Dr. Nadine VARIN-BLANK – Rapporteur
Pr. Romain GUIEZE – Rapporteur
Dr. Jozo DELIC – Examinateur
Dr. Lauren VERONESE – Examinateur
Pr. Florence NGUYEN-KHAC – Directrice de thèse

INSERM UMRS1138 – Centre de Recherche Biomédicale des Cordeliers

Remerciements

En premier lieu, je tiens à remercier le Pr Florence Nguyen-Khac pour m'avoir confié ce projet, et pour en avoir assuré la direction. Merci pour tes conseils, pour tes capacités organisationnelles (bien supérieures au miennes !) et pour ta disponibilité !! Merci pour tous les projets auxquels tu m'as associé, et pour ton soutien en chaque occasion !

Je remercie aussi particulièrement le Dr Santos Susin, pour tout le temps et l'énergie que tu as consacré (et que tu consacres encore) à rendre ton laboratoire polyvalent et autonome, et pour ton implication scientifique dans le projet « Del8p » ! Tes conseils ont toujours été précieux !

Je tiens également à remercier le Pr Romain Guièze et le Dr Nadine Varin-Blank pour avoir accepté de faire partie de mon jury en qualité de rapporteur. Je remercie également Dr Jozo Delic et le Dr Lauren Veronese pour avoir accepté le rôle d'examinateur, ainsi que Pr Guy Gorochov pour m'avoir fait l'honneur d'assurer la Présidence de ce jury !

Je souhaite ensuite adresser un immense merci à tous les membres de l'équipe 19 que j'ai eu l'occasion de côtoyer pendant ces 3 années. Tout d'abord, merci à Elodie Pramil pour m'avoir initié à la culture cellulaire et aux tests d'apoptose induite, pour avoir dédiabolisé les Western Blots et les qPCR. Merci d'avoir su me transmettre une petite partie de ton savoir-faire, et pour ta mémoire exceptionnelle qui nous a permis de retrouver des échantillons même 2 ans après ton départ, dans cette boîte rose au fond des -80°C. Un grand merci également à Marie-Noëlle Navas, pour m'avoir initié si rapidement à la biologie moléculaire et au CRISPR/Cas9, qui ont permis à un clinicien néophyte de produire ses premières lignées KO en partant de zéro, et en moins de 3 mois ! Un immense merci également au Dr Brigitte Bauvois, pour ta présence, tes conseils, la pertinence de tes remarques, et pour les projets auxquels tu m'as fait participer ! Merci de m'avoir fait réfléchir sur des sujets auxquels je ne connaissais pas grand-chose, et pour m'avoir montré que les qualités de raisonnement d'un esprit scientifique bien construit sont intemporelles ! Un merci tout particulier à Cécile Doualle : merci pour avoir supporté mon verbiage logorrhéique, merci pour m'avoir fait manger le midi (transitoirement), merci pour avoir été la

meilleure voisine de bureau qu'on puisse espérer, merci pour le chocolat, les gâteaux, la découverte de la gastronomie indonésienne, ta couleur de cheveux bizarre, le comptage des points « Cartman »… et merci aussi pour les manips (quand même !), les courbes de titration et les cahiers de lab… 'fin merci pour tout ! Egalement un immense merci à Leticia Koch-Lerner, pour m'avoir expliqué comment produire des séquençages corrects, et pour nos discussions quotidiennes, essentiellement scientifiques… mais aussi pour ta curiosité, pour ton esprit critique, pour cette voix si atypique qui a fait trembler plus d'une fois la verrerie du labo, pour le chocolat (aussi !), pour démontrer chaque jour qu'il ne faut pas se fier aux apparences (si si, elle est Brésilienne, j'vous dis !). Un très grand merci à Delphine, pour avoir su jouer à la fois le rôle de catalyseur et de régulateur au sein de ce petit groupe parfois un peu déjanté ! Merci d'avoir été de mon côté lorsqu'il fallait défendre un point de vue réac' lorsqu'on se retrouvait cernés par les wokistes… Enfin, merci à Christine pour ton travail, ta présence, ta sagesse et ton optimisme, quelle que soit la situation, et ta résilience exemplaire !

Je remercie également les membres de notre équipe travaillant dans l'unité de Cytogénétique de la Pitié-Salpêtrière, et tout particulièrement Elise Chapiro pour ses conseils et son soutien tout au long de ce travail. Merci pour tes remarques toujours pertinentes, et pour ta large contribution à la partie cytogénétique ! Merci également à Luce Smagghe, pour la réalisation des analyses et la tenue des tableaux récapitulatifs ! Merci à Frédéric Davi et à Michel Arock pour nos échanges lors des réunions d'équipe !

Je n'oublie pas les autres membres du Centre qui n'avaient pas le plaisir d'être associés à notre équipe ! Merci à François pour avoir été… François ! Merci pour tes conseils parfois, ton humour souvent, tes croquis si éloquents et pour le resto libanais ! Merci également à Estelle et Hélène pour leur aide sur la plateforme de tri cellulaire, les cellules survivantes leur sont reconnaissantes ! Merci à Edith Doucet, qui était sûre qu'on finirait par l'oublier après son départ… eh ben non, tu vois ! Une responsable « Hygiène et Sécurité » sympa et aidante, ça marque ! Je remercie également l'équipe de Direction du Centre de Recherche des Cordeliers, et tout particulièrement Tarik, Dominique et Véronique, à la fois pour leur accueil, leur

implication quand il s'est agi de me faire un contrat, et pour leur efficacité face aux affres de l'administration ou des pannes informatiques…

De même, je remercie très sincèrement l'équipe de recherche du Pr Olivier Bernard (U1170, Gustave Roussy), dans laquelle j'ai eu le plaisir d'effectuer mon stage de Master 2. Merci de m'avoir initié à la recherche, et merci tout particulièrement à Hussein Ghamlouch, Véronique Della-Valle et Marine Armand pour votre aide, y compris pendant cette thèse pour la mise au point des CRISPR double-KO !

Par ailleurs, je remercie mes collègues du service d'Hématologie de la Pitié-Salpêtrière ! Stéphanie, *the GOAT*, pour ton esprit brillant, ton appui permanent, ton humour décapant et tes propriétés anxiolytiques qui décidément persistent au fil des années ! Mais aussi les deux Véronique (Leblond et Morel), Madalina, Damien, Laetitia, Karim, Sylvain, Inès, Maya, Laurent, Nicolas, Floriane. Merci pour les échantillons, pour votre influence, et pour avoir été présents quand je devais prendre un peu de temps pour ce travail de thèse (réunions, rédaction, impression un jour de grève…).

Un grand merci également aux organismes qui ont financé directement ou indirectement ce projet : en particulier merci à la Fondation ARC pour avoir sélectionné puis soutenu mon projet, merci au FILO et au SiRIC CURAMUS.

Enfin, je voudrais finir par remercier ma famille et amis : mes parents, mon frère David, mes deux meilleurs acolytes Marc et Basile, et tous mes proches qui ont dû supporter autant mon absence (souvent) que ma présence (parfois) au cours de ces dernières années. Votre aide et votre soutien ont été inestimables ! Une pensée toute particulière pour mon grand-père Claude, qui n'aura pas vécu jusqu'à l'aboutissement de cette expérience, et pour mon oncle Gérard, dont l'état de santé s'avère malheureusement incompatible avec un déplacement jusque Paris. Ce travail vous est aussi dédié !

Table des matières

Abréviations

A

AA : Acide aminé
ADN : Acide désoxyribonucléique
ALK : *Anaplastic lymphoma kinase*
APAF-1 : *Apoptotic protease activating factor 1*
APRIL : *A proliferation inducing ligand*
ARN : Acide ribonucléique
ATM : *Ataxia telangiectasia mutated*
ATP : Adénosine triphosphate

B

BAD : *Bcl-2 Antgonist of cell death*
BAK : *Bcl-2 homologous antagonist/killer*
BAX : *Bcl-2 associated X*
BAFF : *B-cell activating factor of the TNF family*
BCL2 : *B-cell leukemia/lymphoma-2*
BCLXL : *B-cell lymphoma-extra large*
BCR : Récepteur aux cellules B
BID : *BH3 interacting domain death agonist*
BIRC3 : *Baculoviral IAP repeat containing 3*
BH : *Bcl-2 homology*
BR : Bendamustine + rituximab
BTK : *Bruton's tyrosine kinase*

C

CCL : *CC chemokine ligand*
CD : *Cluster of differentiation*
CDKN1A : *Cyclin dependent kinase inhibitor 1A*
CMH : Complexe majeur d'histocompatibilité
CXCL : *CXC chemokine ligand*

D

DcR : *Decoy receptor*
DISC : Complexe de signalisation induisant la mort
DLEU2 : *Deleted in Lymphocytic Leukemia-2*
DR : *Death receptor*

F

FADD : *Fas-associated protein with death domain*
Fc : Fragment constant des immunoglobulines
FCR : Fludarabine + cyclophosphamide + rituximab
FILO : *French innovative leukemia organization*
FISH : *Fluorescence in situ hybridation*
FLIP : *FLICE-like inhibitory protein*
FOXO3 : *Forkhead box O3*

H

HCDR3 : *heavy-chain complementarity-determining region 3*
HDACi : Inhibiteur d'histone désacétylase

I

IAP : Protéine inhibitrice de l'apoptose
Ig : Immunoglobuline
IGHV : région variable des chaines lourdes des immunoglobulines
ITAM : Motif d'activation des récepteurs immuns basé sur la tyrosine

K

KO : *Knock-out*

L

LDH : Lactate déshydrogénase

LL : Lymphome lymphocytique

LLC : Leucémie lymphoïde chronique

LPL-B : Leucémie prolymphocytaire B

LYN : *Lck/Yes novel tyrosine kinase*

M

MAPK : *Mitogen activated protein kinase*

MBL : Lymphocytose B monoclonale

MCL1 : *Myeloid cell leukemia-1*

MCP : Mort cellulaire programmée

MDM2 : *Mouse double minute 2*

MSH2 : *MutS homolog 2*

mTOR : *Mammalian target of rapamycin*

N

NF-κB : *Nuclear factor-kappa B*

NFAT2 : *Nuclear factor of activated T cells 2*

NK : *Natural killer*

NOTCH1 : *Neurogenic locus notch homolog protein 1*

P

PI3K : Phosphatidylinositide 3'OH kinase

PKC : Protéine kinase C

PLCγ2 : Phospholipase-C gamma 2

PUMA : *P53 upregulated modulator of apoptosis*

R

RANK(L) : *Receptor activator of nuclear factor- κB (ligand)*

S

SIDA : Syndrome d'immunodéficience acquise

Smac/DIABLO : *Second mitochondrial activator of caspases/direct IAP binding protein with low pI*

SYK : *Spleen tyrosine kinase*

T

TNF(-R) : *Tumor necrosis factor(-receptor)*

TNFRSF : *TNFR superfamily*

TRADD : *TNFR1A-associated death domain*

TRAF2 : *TNFR-associated factor 2*

TRAIL(-R) : *TNF-related apoptosis inducing ligand(-receptor)*

TP53 : *Tumor protein 53*

W

wt : *Wild-type*

X

XIAP : *X-linked inhibitor of apoptosis*

XPO1 : *Exportin 1*

Liste des tableaux

Liste des figures

Introduction

Chapitre I. Leucémie lymphoïde chronique

I.1. Rappel succinct sur la lymphopoïèse B

Les lymphocytes B (*bone-marrow-derived lymphocytes*) sont des cellules du système immunitaire humoral adaptatif, responsables de la production d'immunoglobulines spécifiques d'un antigène, et dont la production et la différenciation de la cellule souche hématopoïétique jusqu'au stade de lymphocyte B naïf s'effectuent dans la moelle osseuse hématopoïétique (**Figures 1 et 2**).

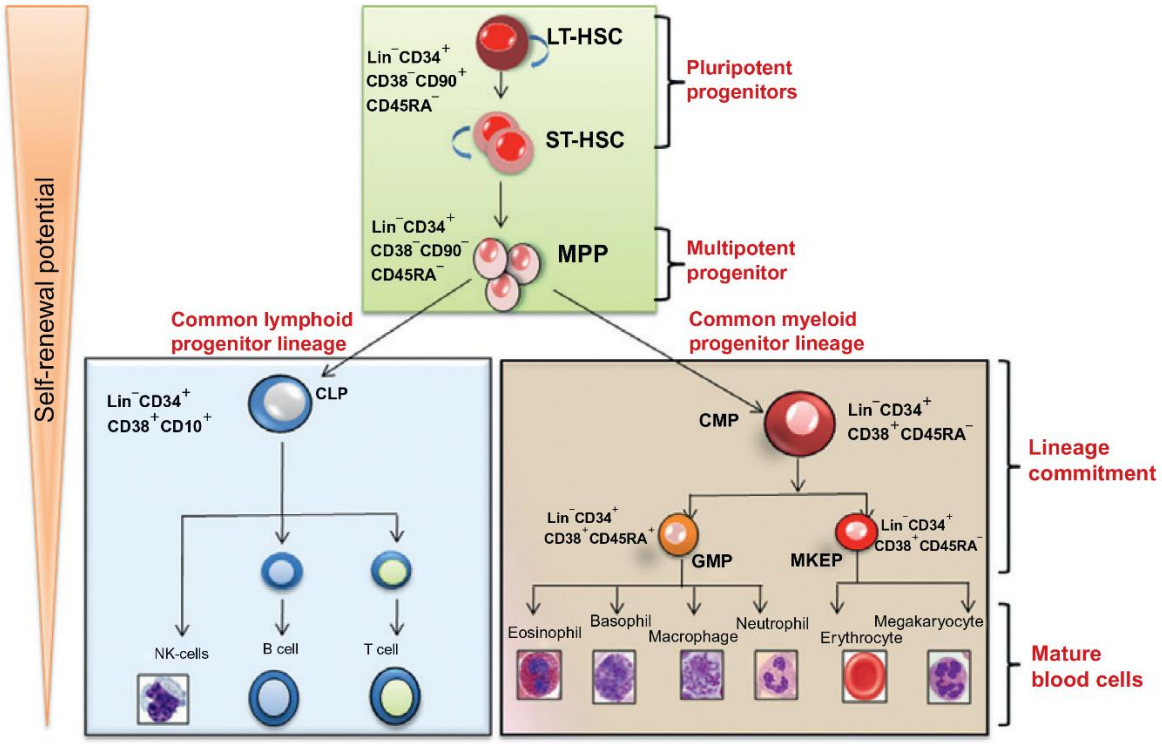

Figure 1. Hématopoïèse normale chez l'Homme (Wasnik, 2012[1]). Les cellules souches hématopoïétiques (HSC) prolifèrent et se différencient en progéniteurs multipotents (MPP), à partir desquels se différencient les progéniteurs lymphoïdes communs (CLP), qui donneront eux-mêmes naissance aux lymphocytes B, T et NK.

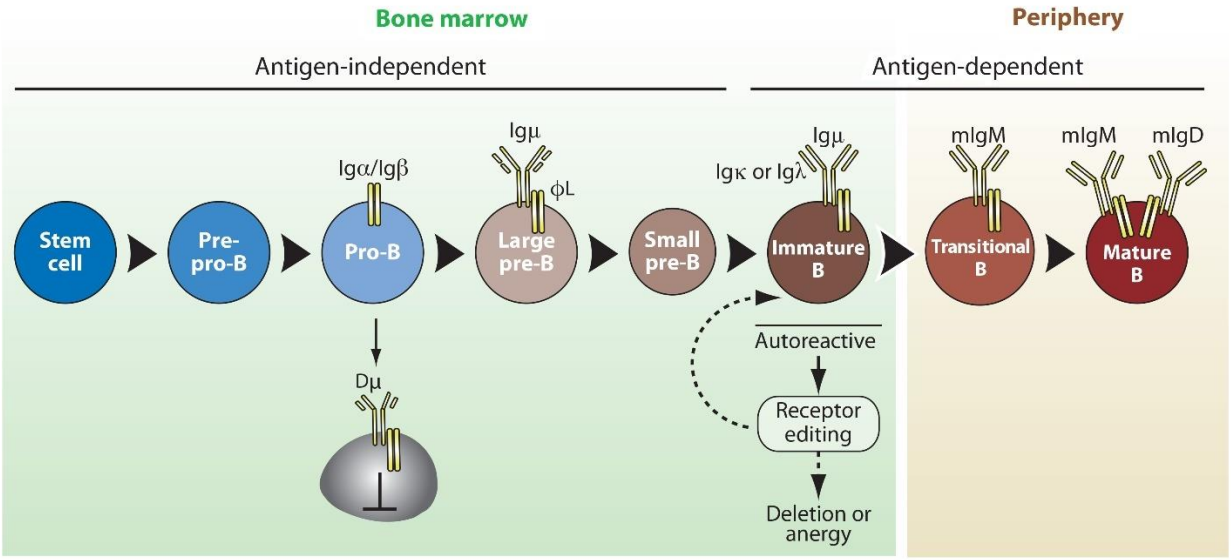

Figure 2. Différenciation lymphoïde B (Kurosaki, 2010[2]). La synthèse de l'immunoglobuline de surface commence par la synthèse de la chaîne lourde. La recombinaison DJ débute dans les progéniteurs lymphoïdes communs et les cellules pré-pro-B, suivie de la recombinaison V-DJ, et aboutit à la présence d'une chaîne lourde dans les cellules pré-B, qui s'associe aux chaînes légères de substitution pour constituer le pré-BCR. La signalisation efficace par ce pré-BCR induit la prolifération et la différenciation des petits lymphocytes pré-B, puis le réarrangement VJ de la chaîne légère d'immunoglobuline permettant la formation d'un BCR complet (IgM) à la surface des lymphocytes B naïfs. Les lymphocytes autoréactifs sont éliminés, et les lymphocytes B naïfs restants migrent vers les organes lymphoïdes secondaires pour se différencier en lymphocytes B matures (folliculaires, de zone marginale, ou B1), prêts à s'activer s'ils rencontrent leur antigène spécifique.

I.2. Généralités sur la leucémie lymphoïde chronique

La leucémie lymphoïde chronique (LLC) est un syndrome lymphoprolifératif chronique caractérisé par une prolifération clonale de lymphocytes B matures, et de leur accumulation, responsable d'une infiltration sanguine, médullaire, ganglionnaire et des autres organes lymphoïdes. En accord avec la classification OMS 2022 des néoplasies lymphoïdes, le diagnostic est porté lorsque la population lymphocytaire B de phénotype LLC est supérieure à 5 G/L dans le sang périphérique. En présence d'une atteinte tumorale exclusive (ganglionnaire, splénique ou extra-médullaire), non associée à une phase circulante > 5 G/L, on retient le diagnostic de lymphome

lymphocytique (LL). En l'absence de toute atteinte tumorale, la découverte d'une phase circulante inférieure au seuil de 5 G/L fait porter le diagnostic de lymphocytose B monoclonale (ou MBL, *monoclonal B cell lymphocytosis*). Un clone MBL « low count » ou expansion B clonale a un nombre de cellules B clonales inférieur à 0.5 G/L. Un clone MBL de type LLC/LL peut progresser vers une LLC/LL (0.5-2% par an), le risque étant plus élevé pour les clones avec un nombre de cellules B clonales plus important.

I.3. Présentation clinico-biologique et critères diagnostiques

Le diagnostic de LLC est porté dans la majorité des cas lors de la découverte fortuite d'une hyperlymphocytose au cours d'un examen de routine, en l'absence de tout symptôme. Certains patients présentent toutefois un syndrome tumoral au diagnostic (ganglionnaire, hépatique ou splénique), et/ou des cytopénies. La présence de signes généraux (altération de l'état général, fièvre et/ou sueurs nocturnes), de même qu'une augmentation rapide de la taille d'un ganglion, témoignent d'une maladie progressive et doivent faire évoquer une transformation en lymphome de haut grade (transformation de Richter).

Au plan biologique, le diagnostic est suspecté devant une hyperlymphocytose supérieure à 5 G/L, associée à d'éventuelles cytopénies (anémie, thrombopénie). Le frottis sanguin montre des cellules de petite taille, d'aspect mature, avec un rapport nucléo-cytoplasmique élevé, un cytoplasme basophile dépourvu de granulations, ainsi qu'une chromatine dense et mottée habituellement sans nucléole visible. À ces cellules s'associent classiquement des ombres nucléaires (« ombres de Gümprecht »), qui traduisent la fragilité des membranes cytoplasmiques et nucléaires des cellules leucémiques (**Figure 3**).

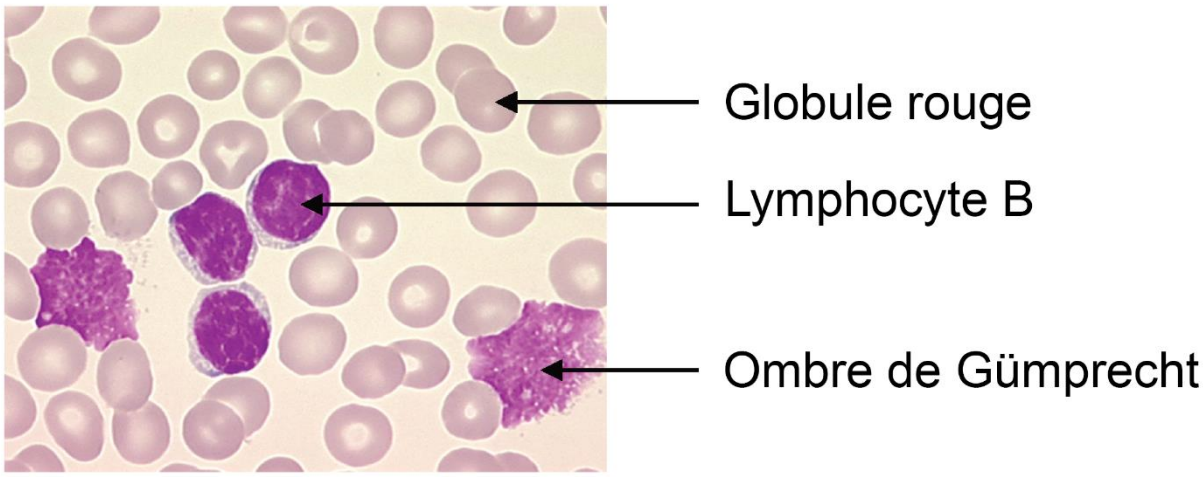

Figure 3. Frottis sanguin caractéristique d'un patient atteint de LLC.

La confirmation diagnostique requiert l'immunophénotypage des lymphocytes sanguins circulants, par cytométrie en flux. Les cellules leucémiques portent naturellement à leur surface les antigènes caractéristiques de la lignée lymphoïde B : le CD19 (marqueur pan-B) et le CD20 (marqueur des lymphocytes B matures), dont l'intensité d'expression est généralement diminuée. Chaque clone de cellule leucémique exprime à sa surface un même type de chaîne légère d'immunoglobuline, kappa ou lambda, composant le BCR, et dont l'intensité d'expression par le clone leucémique est également diminuée en comparaison avec les lymphocytes B normaux. La molécule CD5, antigène normalement exprimé par les cellules lymphoïdes T et par une sous-population de lymphocytes B naïfs, est retrouvée de façon presque constante à la surface des cellules LLC. Le CD23, récepteur de faible affinité du fragment Fc des IgE (FcεRII) et marqueur d'activation des lymphocytes B, est lui aussi habituellement présent. Le FMC7, présent sur les lymphocytes B physiologiques, est en revanche négatif. Enfin, le CD22 et le CD79b (composant le BCR) sont peu exprimés, voire absents. Tous ces critères phénotypiques entrent dans le calcul du score du Royal Marsden Hospital (RMH, ou score de Matutes[3]), qui attribue 1 point à la positivité du CD23 et du CD5, ainsi qu'à la négativité ou faible expression du FMC7 et du CD22 (ou du CD79b dans le score modifié par Moreau), et à la faible expression de la chaîne légère impliquée. Un score de 4 ou 5 sur 5 est compatible avec une LLC ; un score de 3 peut correspondre à une LLC de phénotype atypique ;

un score inférieur à 3 doit faire discuter d'autres syndromes lymphoprolifératifs B (**Tableau 1**).

Tableau 1. Calcul du score RMH (score de Matutes/Moreau).

Marqueur	+ 1 point	0 point
CD5	Positif	Négatif
CD23	Positif	Négatif
FMC7	Négatif	Positif
CD22 (ou CD79b)	Faible	Fort
Immunoglobulines de surface	Faible	Fort

I.4. Classifications

Les classifications de Binet[4] et de Rai[5] permettent la stratification pronostique des patients atteints de LLC. Ces classifications reposent cliniquement sur l'atteinte des aires lymphoïdes (adénopathies superficielles, hépatomégalie, splénomégalie) et biologiquement sur l'hémogramme (anémie, thrombopénie), afin de classer les patients en 3 stades (A, B ou C) pour la classification de Binet, ou en 5 stades (0 à IV) pour la classification Rai (**Tableaux 2 et 3**). En France, la classification de Binet reste la plus utilisée. Au diagnostic, environ 80% des patients sont en stade A et ne nécessitent qu'une simple surveillance. Environ la moitié d'entre eux évolueront vers un stade B ou C, et nécessiteront alors un traitement.

Tableau 2. Classification de Binet.

Stade	Aires lymphoïdes	Hémoglobine	Plaquettes	Médiane de survie
A	≤ 2	> 10 g/dL	> 100 G/L	> 10 ans
B	≥ 3	> 10 g/dL	> 100 G/L	7 ans
C	indifférent	< 10 g/dL	< 100 G/L	5 ans

Tableau 3. Classification de Rai.

Stade	Risque	Description	Médiane de survie
0	faible	Lymphocytose	> 10 ans
I	intermédiaire	Lymphocytose + lymphadénopathie	7 - 9 ans
II	intermédiaire	Stades 0-I + splénomégalie et/ou hépatomégalie	
III	élevé	Stade II + anémie (hémoglobine < 110 g/L)	< 5ans
IV	élevé	Stade III + thrombopénie (plaquette < 100 g/L)	

I.5. Epidémiologie

La LLC est la plus fréquente des leucémies de l'adulte dans les pays Occidentaux. En France, on a recensé 4674 nouveaux cas de LLC/LL en 2018 d'après l'Agence nationale de santé publique, soit près de 11% de l'ensemble des hémopathies malignes[6]. Il existe une prédisposition masculine, avec un sex-ratio proche de 2/1. La LLC concerne essentiellement les sujets âgés : l'âge médian au diagnostic est de 71 ans chez les hommes et 73 ans chez les femmes ; elle est exceptionnelle avant 50 ans.

Hormis l'âge avancé, il n'existe pas de facteur de risque formellement identifié qui favoriserait la survenue de la maladie. Le rôle de l'exposition aux radiations ionisantes ou aux agents chimiques dans l'incidence de la LLC n'est pas établi. Si la grande majorité des cas de LLC sont sporadiques, il existe vraisemblablement une susceptibilité génétique à la maladie, et des formes familiales de LLC peuvent être identifiées dans 5 à 10% des cas[7].

I.6. Physiopathologie de la LLC

I.6.1. Défaut d'apoptose

Les cellules de LLC circulantes sont quiescentes, arrêtées en phase G0 du cycle cellulaire. Elles sont essentiellement caractérisées par un défaut d'apoptose lié à la surexpression de protéines anti-apoptotiques telles que BCL2 (*B-cell*

leukemia/lymphoma-2) et MCL1 (*myeloid cell leukemia-1*). Les principaux mécanismes effecteurs de l'apoptose seront détaillés au Chapitre II de ce manuscrit. Les mécanismes aboutissant à la surexpression de ces protéines sont potentiellement multiples : hypométhylation du promoteur de *BCL2* décrite dans les cellules de LLC[8], stimulation de l'axe CD31/CD38 (cf. section I.7. Facteurs pronostiques biologiques) ou encore perte des microARNs *miR-15a/miR-16-1* avec la délétion 13q (cf. section I.8. Anomalies cytogénétiques).

I.6.2. Prolifération

Bien que l'accumulation de cellules de LLC soit principalement liée à un défaut d'apoptose, l'existence d'un pool prolifératif a également été proposée[9]. Il a été montré que les cellules tumorales proliféraient dans la moelle osseuse et dans les ganglions, générant chaque jour entre 0.1 et 1.75% de la population tumorale[10], ce qui contraste avec la quiescence des cellules sanguines circulantes.

I.6.3. Signalisation du BCR dans la LLC

Le BCR est un complexe protéique composé d'une immunoglobuline de surface associée à deux protéines transmembranaires Igα (CD79a) et Igβ (CD79b), nécessaires à la transduction du signal d'activation (**Figure 4**). Comme vu précédemment, l'expression des immunoglobulines de surface et du CD79b est souvent faible, voire indétectable. La stimulation du BCR par l'antigène correspondant induit l'activation de nombreuses tyrosine-kinases, en particulier LYN (de la famille des kinases SRC) et SYK[11]. Celles-ci phosphorylent en retour les motifs intracellulaires ITAM du CD79a et CD79b du BCR, ce qui active d'une part la tyrosine kinase de Bruton (BTK) puis la phospholipase C gamma 2 (PLCγ2) et les voies NF-κB, NFAT2 et PKC/MAPK, et d'autre part la phosphoinositide-3-kinase (PI3K) puis les voies AKT/mTOR et NF-κB (**Figure 5**).

Figure 4. Schéma du BCR.
(Xiong, 2014[12])

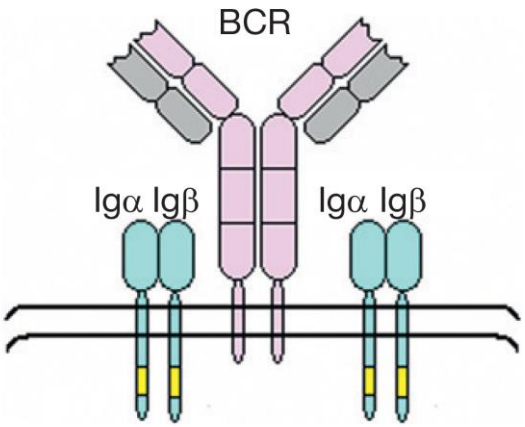

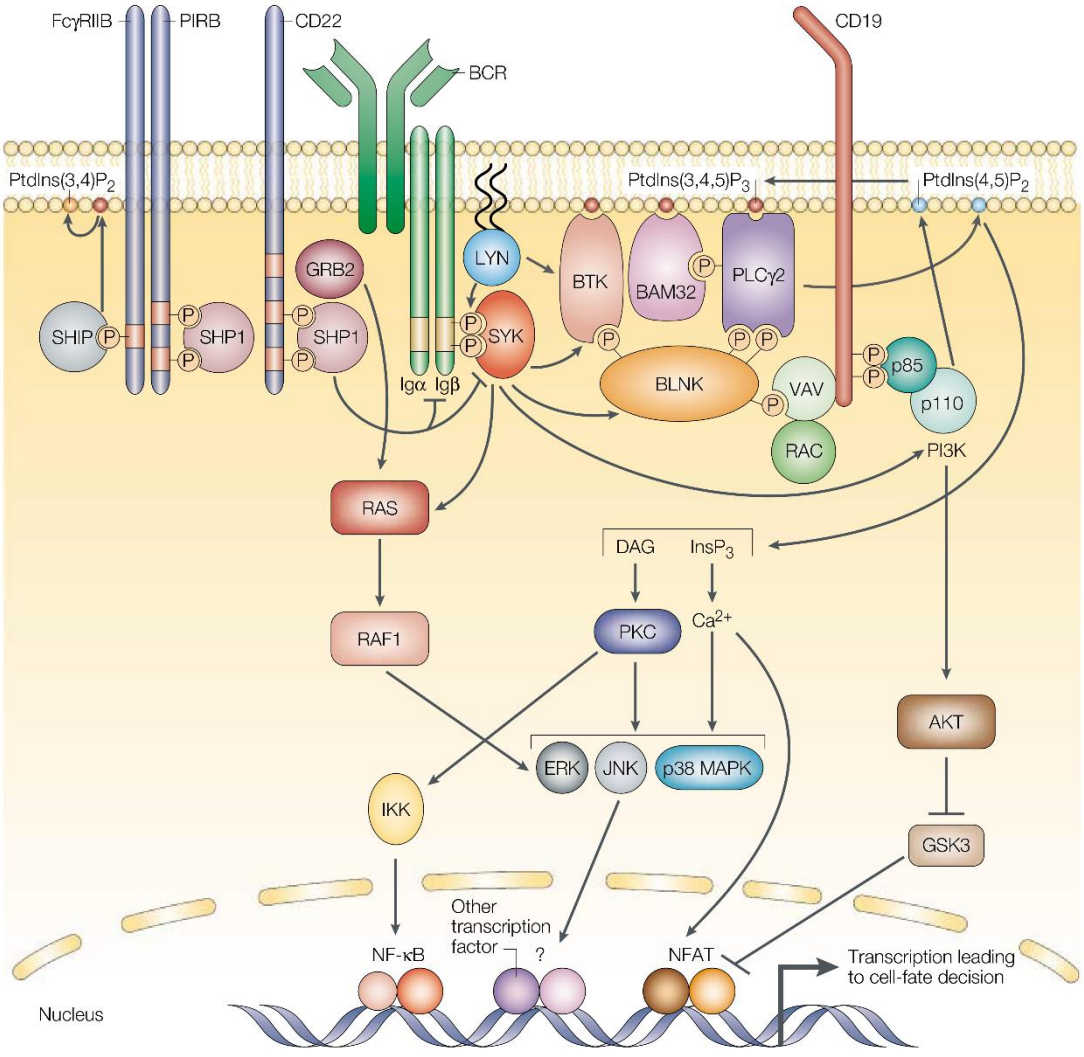

Figure 5. Signalisation en aval du BCR illustrant les principales voies d'aval : la voie BTK / PLCγ2 activant PKC puis NF-κB, NFAT et MAPK ; et PI3K activant principalement la voie AKT/mTOR. (Niiro, 2002[13])

Si la signalisation du BCR joue un rôle central dans la pathogénèse de la LLC, on distingue deux types de réponse à la stimulation du BCR, selon le statut mutationnel *IGHV* des patients. Le BCR des cellules *IGHV* mutées possède généralement une faible capacité de réponse à la stimulation antigénique. Il est en règle mono- ou oligo-réactif et de forte affinité. Sa stimulation *in vitro* n'entraîne pas ou peu de réponse en matière de survie cellulaire. A l'inverse, les cellules *IGHV* non mutées ont une capacité de réponse plus importante suite à la stimulation antigénique. Leur BCR est poly-réactif, de faible affinité, et sa stimulation *in vitro* s'accompagne d'une augmentation de la survie des cellules.
Par ailleurs, en plus de l'activation du BCR par les ligands antigéniques, il a été montré *in vitro* que certains épitopes intrinsèques du BCR (HCDR3) pouvaient être reconnus par un complexe BCR voisin, et déclencher une stimulation autonome à l'origine de la prolifération des cellules de LLC[14].

I.6.4. Microenvironnement tumoral

Les cellules de LLC présentent une survie prolongée *in vivo*, mais elles entrent rapidement en apoptose *in vitro*. Cette apoptose peut être prévenue par la co-culture des cellules LLC en présence de cellules stromales, ce qui souligne l'influence du micro-environnement dans la survie et la prolifération de ces cellules.
In vivo, le microenvironnement tumoral des cellules de LLC est constitué de cellules stromales mésenchymateuses (moelle osseuse), de cellules dendritiques folliculaires (ganglion, zone folliculaire), de fibroblastes réticulaires (ganglion, zone T) et de cellules dites « *nurse-like* », issues de la lignée myélo-monocytaire et apparentées à des macrophages d'origine monocytaire (moelle et ganglion).

Nous avons vu que les ganglions étaient le siège de la prolifération d'une partie des cellules leucémiques. Ceux-ci sont en effet infiltrés par les cellules leucémiques, regroupées en pseudo-follicules comprenant également des lymphocytes T et des cellules stromales, qui fournissent ainsi aux cellules de LLC les cytokines nécessaires à leur survie et leur maturation. Les cellules folliculaires dendritiques situées dans les

centres prolifératifs activent les cellules de LLC à la fois par leur capacité de présentation d'antigène et par la sécrétion de BAFF. Les cellules *nurse-like* promeuvent également la survie des cellules LLC tant par la sécrétion de facteurs (tels que CXCL12, CXCL13, BAFF et APRIL) que par leur capacité à présenter des antigènes stimulant le BCR (calréticuline, vimentine…) (**Figure 6A**). Enfin, il existe des interactions entre les lymphocytes B de LLC et les lymphocytes T du microenvironnement. Les cellules B de LLC produisent des chimiokines capables de recruter les lymphocytes T (CCL3, CCL4…), qui en retour vont favoriser la survie des lymphocytes B tumoraux en exprimant le CD40L (**Figure 6B**)[15].

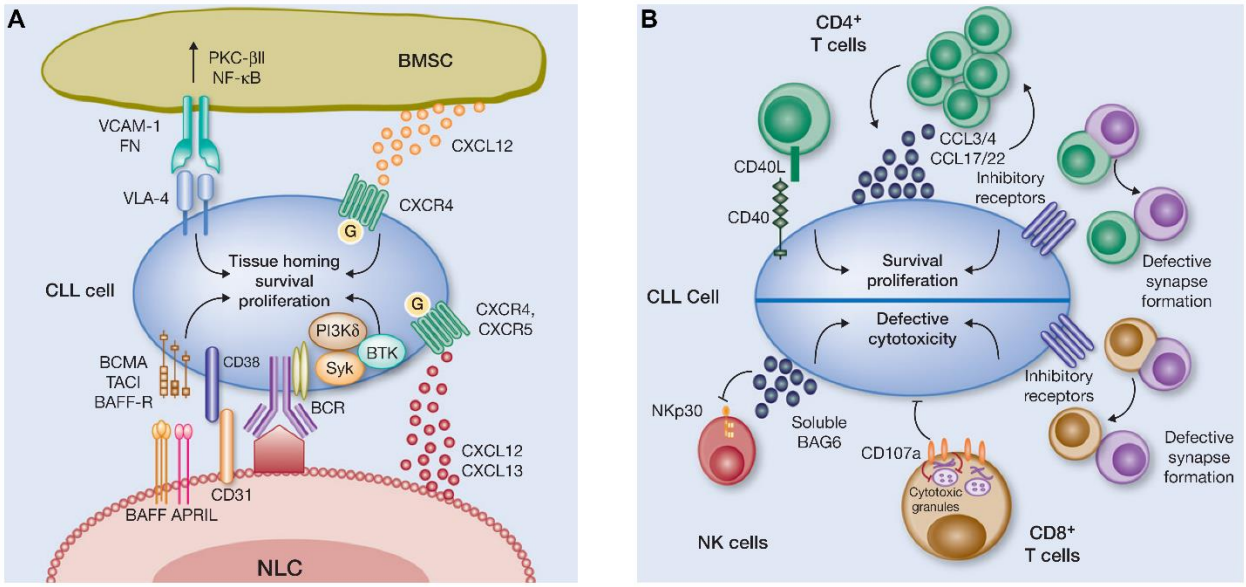

Figure 6. (**A**) **Schéma de l'interaction entre un lymphocyte B de LLC et une cellule « nurse-like »**. Ces dernières contribuent à la survie et à l'activation des lymphocytes leucémiques en stimulant le BCR (calréticuline, vimentine), et en exprimant BAFF / APRIL ainsi que des facteurs solubles (CXCL12, CXCL13). Les cellules stromales de la moelle osseuse (*bone-marrow stromal cells*, BMSC) jouent également un rôle de support. (**B**) Schéma de l'interaction entre un lymphocyte B de LLC et les lymphocytes T CD4, T CD8 et NK. Les lymphocytes T CD4 sont recrutés pour leur rôle de soutien (CD40L, CCL3, CCL4). Les lymphocytes T CD8 et NK voient en revanche leur fonction cytotoxique inhibée, ce qui concourt à l'évasion immunitaire des cellules de LLC. (Ten Hacken, 2014[15])

I.7. Facteurs pronostiques biologiques

La LLC est une maladie d'évolution clinique très hétérogène, même au sein des groupes définis par les classifications susmentionnées, avec des survies globales pouvant varier de quelques mois à plus de 20 ans. Cette variabilité peut être expliquée en grande partie par de nombreux facteurs biologiques, qui influencent le pronostic.

I.7.1. Marqueurs sériques

Plusieurs paramètres biologiques simples permettent d'évaluer le degré de prolifération des lymphocytes tumoraux, et donc l'agressivité de la maladie.
Le suivi de l'hémogramme permet le calcul du temps de doublement des lymphocytes sanguins. Les patients ayant un temps inférieur à 12 mois ont un pronostic moins bon (période sans traitement et survie globale plus courtes)[16].
La lactate-déshydrogénase (LDH) est une enzyme catalysant la transformation du pyruvate en lactate. Dans la LLC, comme dans d'autres hémopathies, son taux reflète la masse tumorale. Un taux élevé de LDH constitue donc un marqueur de mauvais pronostic, de mauvaise réponse au traitement, et peut faire suspecter une transformation en lymphome de haut grade (transformation de Richter)[17,18].
La β2-microglobuline est un constituant du CMH de classe I, retrouvé à la surface de toutes les cellules nucléées de l'organisme. Elle est synthétisée par les lymphocytes T CD8, les lymphocytes B et les cellules tumorales, et peut ainsi refléter la masse tumorale[19].

I.7.2. Marqueurs immunophénotypiques

Le CD38 est une glycoprotéine transmembranaire exprimée par de nombreuses cellules hématopoïétiques, notamment les lymphocytes B et T activés. En interagissant avec le CD31 présent à la surface des cellules stromales/endothéliales, il induit la prolifération et la différenciation immunoblastique des lymphocytes LLC, ainsi que la survie cellulaire en inhibant l'apoptose dans les centres germinatifs[20]. Dans la LLC, un niveau d'expression élevé du CD38 est fréquemment associé à une prolifération plus marquée[20–22], mais son intérêt reste discuté du fait d'une expression

inconstante au cours de la maladie et de l'absence de valeur seuil de positivité clairement définie.

I.7.3. Statut mutationnel des gènes des immunoglobulines

Les patients atteints de LLC peuvent être classés en deux groupes selon le caractère muté ou non muté de la séquence des gènes codant la partie variable des chaînes lourdes des immunoglobulines (gènes *IGHV*, *immunoglobulin heavy variable genes*). Pour établir ce statut mutationnel, le réarrangement *IGHV* est étudié par séquençage dans les lymphocytes B de LLC, et comparé aux séquences de référence en conformation germinale. Ainsi, un pourcentage d'homologie supérieur ou égal à 98% définit le caractère non muté, tandis qu'un pourcentage inférieur à 98% définit le statut muté. Ce statut muté est associé à un pronostic favorable, alors que les patients non mutés ont une moins bonne réponse aux traitements (en particulier à la chimiothérapie)[23–25].

I.8. Anomalies cytogénétiques

Le paysage génomique de la LLC est hétérogène. Cette hétérogénéité a été mise en évidence dès les années 1980, par analyse du caryotype d'échantillons issus de patients LLC, et utilisation de sondes fluorescentes spécifiques (FISH, *fluorescence in situ hybridization*)[26–28]. Si environ 20% des patients ont un caryotype normal, de nombreuses anomalies cytogénétiques récurrentes ont pu être identifiées.

I.8.1. Caryotype complexe

Il se définit par l'accumulation d'au moins 3 anomalies chromosomiques de nombre ou de structure dans un même clone. Au diagnostic de LLC, 11 à 18% des patients ont un caryotype complexe ; cette prévalence s'élève jusqu'à 40% en situation réfractaire ou en rechute. Il s'agit d'un groupe de patients très hétérogène, dont le pronostic est généralement mauvais, mais qui dépend en grande partie du détail des anomalies qui le constituent[26,27]. Par exemple, la présence d'une trisomie 12 avec une trisomie 19 est associée à un bon pronostic. En revanche, la présence d'au moins 5 anomalies

cytogénétiques – définissant un caryotype « hyper-complexe »[29] – est associée à un pronostic très défavorable. La valeur pronostique du caryotype complexe sera discutée en détail dans la section Résultats de ce manuscrit (cf. Article 3).

I.8.2. Délétion 13q14

Elle est retrouvée chez 50 à 60% des patients LLC au diagnostic. Sa présence est associée à un pronostic favorable, lorsqu'elle reste isolée (**Figure 7**). On la retrouve le plus souvent à l'état mono-allélique. La région minimale délétée inclut les micro-ARN *miR15a/16-1*, codés dans un intron du gène *DLEU2 (Deleted in Lymphocytic Leukemia 2)*. Il a été montré que leur délétion dans un modèle murin aboutissait au développement de lymphoprolifération B de phénotype semblable à la LLC et de profil plutôt peu agressif[30]. Ces micro-ARN fonctionnent comme des suppresseurs de tumeur : ils régulent négativement l'expression de la protéine anti-apoptotique BCL2 en induisant la dégradation de son transcrit. La perte de *DLEU2* et des *miR15a/16-1* aurait ainsi pour conséquence l'accumulation de BCL2, à l'origine d'un défaut d'apoptose permettant l'expansion clonale. A noter la présence dans cette région chromosomique du gène *RB1*, impliqué dans le contrôle du cycle cellulaire au moment de la transition G1-S, et dont la perte en cas de délétion de plus grande taille est associée à un pronostic plus défavorable.

I.8.3. Trisomie 12

Elle est retrouvée chez 10 à 15% des patients LLC au diagnostic. Elle est associée à un risque intermédiaire (**Figure 7**), superposable aux LLC de caryotype normal. Il s'agit d'une entité elle-même hétérogène, possiblement associée à la del13q, mais aussi à d'autres trisomies (en particulier tri19 et tri18) ou d'autres délétions (del17p, del11q, del14q)[31]. La trisomie 12 est volontiers associée aux mutations de *NOTCH1* (25%) et de *TP53* (8.5%), et s'associe plus fréquemment à un profil mutationnel *IGHV* non muté (66%).

I.8.4. Délétion 11q

Elle est retrouvée chez 6 à 20% des patients LLC au diagnostic. La région minimale de délétion est située en 11q22.3-q23.1, qui comporte le gène suppresseur de tumeur *ATM* (*Ataxia telangiectasia mutated*). La seconde copie d'*ATM* comporte des mutations dans 30% des cas[32]. La del11q peut impliquer la région 11q22.2, où se situe le gène *BIRC3* dont la fonction physiologique est de réguler négativement la voie NF-κB. La del11q était associée à un pronostic défavorable à l'ère de l'immunochimiothérapie (**Figure 7**), impliquant fréquemment une atteinte tumorale ganglionnaire et rapidement progressive[33].

I.8.5. Délétion 17p

Elle est retrouvée chez 5 à 10% des patients LLC au diagnostic, et jusqu'à 40% chez les patients en situation réfractaire ou en rechute. Elle implique la perte du gène *TP53* (17p13), un gène suppresseur de tumeur majeur (cf. section II.2. Mécanismes de l'apoptose). La del17p est associée dans plus de 90% des cas à des mutations inactivatrices de l'autre copie du gène *TP53*. Quel qu'en soit le mécanisme, une altération de la voie p53 est associée à un pronostic défavorable (**Figure 7**).

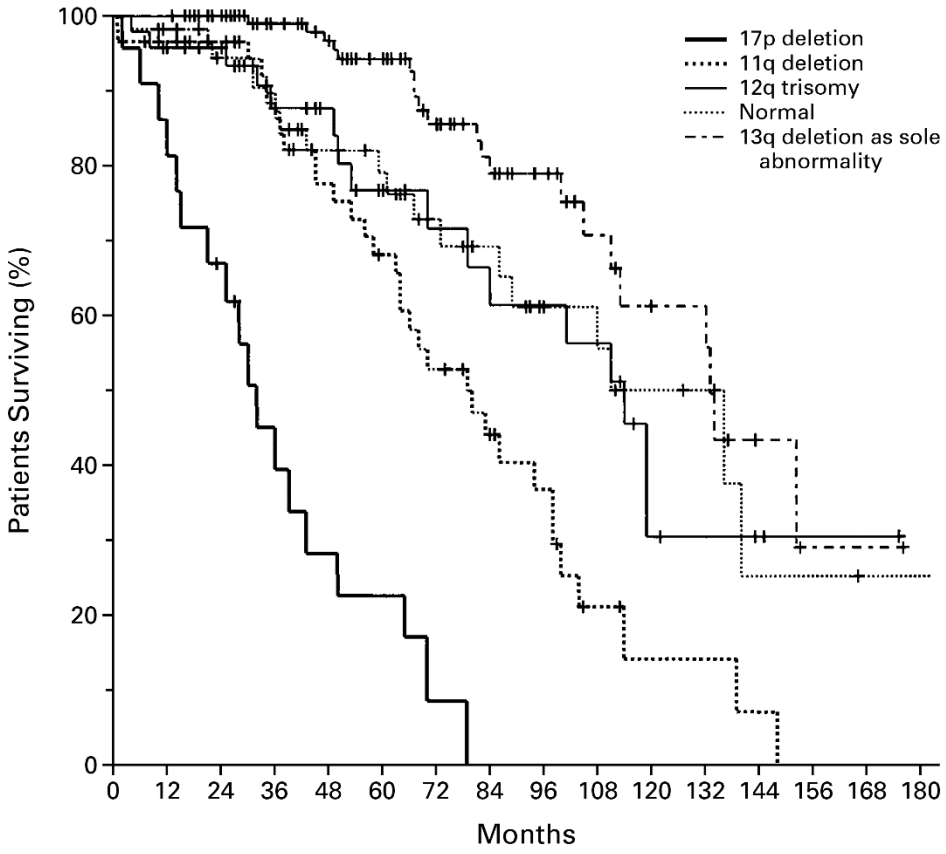

Figure 7. Courbes de survie des patients LLC stratifiés selon les anomalies cytogénétiques présentes : modèle hiérarchique de Döhner avant l'ère des thérapies ciblées (Döhner, 2000[34]). La médiane de survie des patients est de 133 mois pour les patients del13q (pronostic favorable), 114 mois pour les patients tri12 (pronostic intermédiaire), 79 mois pour les patients del11q (pronostic défavorable) et 32 mois pour les patients del17p (pronostic très défavorable).

I.8.6. Autres anomalies

D'autres anomalies chromosomiques récurrentes observées dans les LLC agressives pourraient participer à la résistance aux drogues.

I.8.6.1. Délétion 6q

La délétion 6q est retrouvée dans 3 à 7% des LLC, et s'intègre dans un caryotype complexe dans plus de 60% des cas. Bien que les cas rapportés présentent une

grande hétérogénéité de longueur et de régions impliquées, il semble que la région 6q21 soit la plus fréquemment concernée, dans plus de 70% des cas[35,36]. Elle est phénotypiquement associée à une expression plus forte du CD38[37], et cliniquement associée à une présentation clinique volontiers plus tumorale, ainsi qu'à une résistance aux traitements et une survie plus courte[38]. Parmi les gènes suppresseurs de tumeur imputables, il a été suggéré que la perte d'un haplotype du gène codant la protéine FOXO3, impliquée dans la voie de réparation des dommages de l'ADN (en amont d'ATM et de p53), entraîne un défaut de son activité pro-apoptotique dans les lymphocytes.

I.8.6.2. Gain 2p

Le gain 2p est une anomalie récurrente retrouvée chez environ 15% des cas selon les séries[39–41]. Cette anomalie est associée à des facteurs de mauvais pronostic, comme le statut *IGHV* non-muté, la del11q et la del17p. Le gain 2p semble également associé à la progression de la maladie, au risque de transformation en syndrome de Richter, et aurait un impact défavorable sur la survie globale. Plusieurs oncogènes sont localisés dans cette région (*ALK*, *MSH2*, *BCL11A*, *MYCN*, *REL*, *XPO1*). En particulier, le gène *XPO1*, codant l'exportine-1, a été décrit comme impliqué dans la résistance à la fludarabine ainsi qu'aux inhibiteurs du BCR (ibrutinib, idélalisib) dans la LLC[42].

I.8.6.3. Gain 8q

Le gain 8q24 est une anomalie rare (<5% des LLC au diagnostic[40], davantage à la rechute[43]) mais récurrente, impliquant l'oncogène *MYC*. Il est fréquemment associé aux délétions impliquant *ATM* et/ou *TP53*[44,45], mais confère également un mauvais pronostic de façon indépendante, avec une survie globale plus courte[46].

I.8.6.4. Délétion 8p

La del8p est une anomalie chromosomique rare dans la LLC, non recherchée de façon systématique, et donc peu étudiée. Elle est retrouvée dans environ 5% des cas, et jusqu'à 28% dans les LLC avec une del17p[44,47]. Sa fréquence pourrait être sous-estimée car elle est parfois difficile à repérer au sein d'un caryotype complexe, et elle

est volontiers sous-clonale (en particulier au diagnostic). Dans la majorité des cas, cette anomalie est décrite comme un événement secondaire, apparaissant dans l'évolution de la maladie[48]. Les LLC avec del8p ont un délai raccourci entre le diagnostic et le premier traitement, et l'association avec la del17p est corrélée à une survie diminuée par rapport aux patients LLC ayant une del17p sans del8p[44,47]. Elle a été enfin associée à la résistance au traitement par l'ibrutinib[49].

Le tableau 4 récapitule les données rapportées dans la littérature sur la délétion 8p dans la LLC, entre 2002 et 2021. En particulier, on note l'implication fréquente de la région 8p21.3 dans la région délétée, ce qui a poussé de nombreux auteurs à suggérer un rôle de la famille des gènes *TNFRSF10*, dont la structure et la fonction seront abordées plus loin (dans la section III. Voie TRAIL/TNFRSF10) de cette introduction. L'ensemble de ces données sera décrite de façon plus détaillée en discussion de l'Article 1 de la section Résultats, consacré à la del8p dans la LLC, à la lumière de nos propres résultats.

I.9. Prise en charge thérapeutique de la LLC

La LLC reste encore à ce jour une hémopathie incurable dans la très grande majorité des cas. Cependant, compte tenu de l'évolution clinique très hétérogène des patients, seule une minorité de patients recevront un traitement d'emblée, alors que les autres seront suivis sans traitement en consultation.

Lorsqu'il est nécessaire, le choix du traitement dépend de l'état général du patient (âge, comorbidités), de l'existence d'une altération de la voie p53, du statut mutationnel *IGHV*, et des éventuels traitements antérieurement reçus.

Tableau 4. Délétion 8p et LLC : revue de la littérature.

N of cases (%)	Analysis	Cytobands	Segment length	Discussed genes	Clonal subclonal	Prognosis	Reference
3/30 (10%) untreated CLL 4/9 (44%) RS	CGHa	8p21-p23 8p23-q11.2				nd	Bea S, Am J Pathol, 2002[50]
?/50 ?CLL NHL	CGHa	8p21.3	0.6Mb	*TNFRSF10A/B*			Rubio-Moscardo F, Blood, 2005[51]
5/18 (28%) untreated del17p CLL	SNPa	8p23.1-p23.3 8p21.1-p23.1 8p12	7.3 Mb 19Mb 1.3Mb	*TNFRSF10A/B*		TTFT, OS	Forconi F, BJH, 2008[44]
3/48 (6.25%) untreated CLL	CGHa	8p11.2-p12	5.49Mb (MDR)				Kay NE, Cancer genet cytogenet, 2010[52]
10/323 (3.1%) untreated CLL	SNPa	8p23.1-p21.2 8p21.2	12.4Mb 1.7Mb	*TNFRSF10A/B*		OS univariate	Rinaldi A, BJH, 2011[53]
4/57 (7%) untreated CLL	CGHa	8p				nd	O'Malley D, Int j lab, 2011[54]
6/369 (1.6%) untreated CLL	SNPa	8p11.2p23.3	38.5Mb (MDR)				Gunnarsson R, Haematologica, 2011[55]
7/255 (2.7%) untreated/treated CLL (78%+22%)	SNPa	8p					Ouillette P, Blood, 2011[56]
8/161 (5%) CLL (6 untreated CLL/8)	SNPa	8p23.2-q11.2	11-29.6 Mb	*TNFRSF10A/B* (decreased expression)		TTFT	Brown JR, Clin Can Res, 2012[47]
5/ 353 (1.4%) untreated CLL	SNPa	8p12 (MDR)	90.8kb			nd	Edelmann J, Blood, 2012[40]
5/228 (2%) untreated CLL	CGHa	8p23.3-p21.2	24.8 Mb			TTFT; OS univariate	Houldsworth J, Leuk Lymp, 2013[45]
4/77 (5%) / 1/55 (1.8%) CLL	SNPa			*DLC1*			Kawamata N, Int J oncol, 2013[57]
5% (5/111)	WES				Subclonal		Landau, Cell, 2013[48]
7/180 (3.8%)	SNPa	8p23.3-8q12.3	6.7-65Mb				Salaverria I, GCC, 2015[58]
16/501 (3.2%)	WES				Clonal ?	nd	Landau, Nature, 2015[59]
8 CLL	SNPa, FISH	8p21 (consensus region)		*TNFRSF10A/B*		Ibrutinib resistance	Burger JA, Nat commun, 2015[49]
11/75 (14.7%) del17p/TP53mut CLL	FISH	8p21 (LPL)		*TNFRSF10A/B*	Subclonal (/ % del17p)	OS univariate	Blanco, Oncotarget, 2016[60]
29/961 (3%) CLL	CGHa/SNPa	8p21.3-8p21.2 (MDR)	4.2Mb	(includes *TNFRSF10A/B*)		OS ns	Leeksma, Haematologica, 2021[46]
16/158 (10.1%) CK CLL	CGHa/SNPa	8p23.1-p22 (MDR)	3.3Mb	(does not include *TNFRSF10A/B*)		nd	Ramos-Campoy S, Haematologica, 2021[61]

CGHa, *comparative genomic hybridization array*; SNPa, *single nucleotide polymorphism array*; WES, *whole exome sequencing*; TTFT, *time to first treatment*; OS, *overall survival*; nd, *not determined*; MDR, *minimal deleted region*

I.9.1. Immunochimiothérapie

Les chimiothérapies utilisées dans la LLC comprennent essentiellement les analogues des purines (en particulier la fludarabine) et les agents alkylants (le cyclophosphamide, la bendamustine ou encore le chlorambucil). La fludarabine exerce son action essentiellement en s'insérant lors de la synthèse d'ADN au moment de la phase S ou lors des mécanismes de réparation, ce qui entraîne l'inhibition de la synthèse d'ADN, l'apparition de cassures, puis l'apoptose induite par la voie p53. Les agents alkylants ont la capacité de former des liaisons covalentes avec l'ADN, ce qui inhibe la réplication et la transcription, puis aboutit à des cassures, ce qui conduit également à l'apoptose des cellules de LLC.

En association avec ces chimiothérapies, les anticorps monoclonaux ont montré leur efficacité, et ont été de ce fait largement utilisés. Le premier d'entre à avoir trouvé sa place dans les schémas thérapeutiques a été le rituximab, ciblant le CD20, encore utilisé aujourd'hui en association avec la fludarabine et le cyclophosphamide (schéma FCR), ou avec la bendamustine (schéma BR). L'obinutuzumab, un anticorps monoclonal anti-CD20 recombinant humanisé, a également intégré les stratégies thérapeutiques en association le chlorambucil chez les patients les plus âgés[62].

I.9.2. Thérapies ciblées

I.9.2.1. Inhibiteurs de la voie du BCR

Compte tenu du rôle majeur de la signalisation du BCR dans le développement et la progression de la LLC, de nombreuses molécules ont été développées pour inhiber cette voie de signalisation.

L'ibrutinib est le premier inhibiteur de BTK à avoir obtenu l'autorisation de mise sur le marché, après avoir démontré son efficacité chez des patients LLC en rechute, ou en première ligne thérapeutique en présence d'une altération de la voie p53. Il agit de façon irréversible, en formant une liaison covalente avec un résidu cystéine situé dans le site fixant l'ATP de la protéine BTK. Bien qu'il s'agisse d'un traitement ciblé, on observe tout de même un effet inhibiteur non spécifique au-delà de BTK, en particulier

sur d'autres kinases de la famille TEK (plaquettes, cardiomyocytes), à l'origine de complications hémorragiques et/ou de fibrillation auriculaire. Dans le but d'améliorer l'efficacité et la tolérance de cette classe thérapeutique, d'autres inhibiteurs covalents de BTK dits de « seconde génération » ont été développés (acalabrutinib, zanubrutinib), de même que des inhibiteurs non-covalents de « troisième génération » (pirtobrutinib, vecabrutinib), permettant de contourner les éventuelles résistances liées à une modification du site de fixation en cas de mutation (cf. section I.9.3.2. Mutations de BTK et résistance à l'ibrutinib)[63–65].

Par ailleurs, une autre classe thérapeutique inhibant l'isoforme δ de la PI3K a été développée. Ayant pour chef de file l'idélalisib, ces inhibiteurs empêchent sélectivement la fixation de l'ATP sur la PI3Kδ, ce qui bloque la propagation du signal en aval du BCR. Ces inhibiteurs restent moins utilisés en raison d'une fréquence élevée de complications infectieuses pulmonaires, ainsi que de colites et d'hépatites auto-immunes secondaires au déficit en lymphocytes T régulateurs induites par ces traitements[66,67].

I.9.2.2. Inhibiteurs de la protéine anti-apoptotique BCL-2

Le vénétoclax est un BH3-mimétique antagoniste de la protéine anti-apoptotique BCL2. Il s'agit du premier inhibiteur de BCL2 disponible en clinique, utilisé en particulier chez les patients en rechute, et permettant d'obtenir des réponses complètes chez une bonne proportion de ces patients à haut risque. Une partie des patients traités semble même avoir obtenu une maladie résiduelle négative en cytométrie en flux[68]. L'intérêt de la combinaison du vénétoclax avec un anticorps monoclonal anti-CD20 est à l'étude ; ainsi l'essai clinique de phase 3 CLL14 a randomisé l'association obinutuzumab + vénétoclax contre obinutuzumab + chlorambucil chez des patients LLC en première ligne, montrant ainsi une meilleure survie sans progression dans le groupe obinutuzumab + vénétoclax[69]. D'autres molécules, telles que le lisaftoclax (APG-2575) sont en cours de développement[70].

I.9.3. Impact des altérations génétiques sur la résistance au traitement

I.9.3.1. Altération de la voie p53 et résistance à la fludarabine

Le lien entre altération de la voie p53 et la résistance à la fludarabine a été attesté par de nombreuses études. Ce lien s'explique par une incapacité des cellules à induire l'apoptose en réponse aux dommages de l'ADN provoqués par la fludarabine. Les cellules issues des clones portant des altérations du gène *TP53* survivent au traitement, puis s'expandent et deviennent majoritaire au moment de la rechute. La recherche de ces altérations est donc indispensable avant l'initiation de tout traitement, et leur présence contre-indique l'utilisation de schémas thérapeutiques à base de fludarabine au profit de thérapies ciblées[71,72].

I.9.3.2. Mutations de BTK et résistance à l'ibrutinib

Les mutations de BTK ciblent le site de liaison de l'ibrutinib : substitution d'une cystéine par une sérine en position 481, C481S. L'ibrutinib ne peut alors plus se lier de façon covalente, et échoue à bloquer le signal d'activation transmis par le BCR.
Il existe par ailleurs un autre groupe de mutations impliquant le gène *PLCG2*, codant une protéine homonyme située en aval de BTK dans la chaîne de transduction du signal du BCR. Il s'agit de mutations « gain de fonction », qui transmettent le signal d'activation indépendamment de l'inhibition de BTK en amont. Ces mutations de BTK et/ou de PLCG2 sont identifiées chez plus de 80% des patients résistants à l'ibrutinib[73,74].

I.9.3.3. Mutations de BCL2 et résistance au vénétoclax

Depuis le début de son utilisation, plusieurs mutations de BCL2 ont été rapportées, à commencer par la substitution d'une glycine par une valine en position 101 observée chez près de la moitié des patients résistants, ayant pour conséquence une perturbation de la liaison du vénétoclax sur sa cible[75,76]. Il a également été montré que l'hyperexpression d'autres molécules de la famille de BCL2 ayant également un rôle anti-apoptotique, telles que MCL1 (amplification 1q) ou BCLXL, pouvait compenser l'inhibition de BCL2[77].

I.9.4. Indication de traitement et schémas thérapeutiques

D’après les recommandations de l’IWLCLL (*International Workshop on Chronic Lymphocytic Leukemia*) actualisées en 2018, en dehors de tout essai clinique, les patients LLC de stade A selon la classification de Binet relèvent d’une simple surveillance clinico-biologique, sous réserve de l’absence de signe de progression franche de la maladie ou de symptômes reliés. La majorité des patients de stade B ont une indication thérapeutique, mais certains d’entre eux restant asymptomatiques et stables aux plans clinique et biologique peuvent être simplement surveillés de façon rapprochée. Les patients de stade C doivent être traités, tout comme ceux présentant des signes de progression tumorale clinique rapide, un temps de doublement lymphocytaire court et/ou des signes généraux[78].

Des recommandations récentes du groupe FILO ont récapitulé les principaux schémas thérapeutiques à privilégier en première ligne et au-delà[79]. Brièvement, l’immuno-chimiothérapie est essentiellement réservée aux patients jeunes sans comorbidité, présentant une LLC de profil *IGHV* muté, et en l’absence d’altération de la voie p53. Le schéma FCR est alors le traitement de référence. Chez les patients âgés ou présentant des comorbidités, ou en présence d’une altération de *TP53*, l’utilisation de la fludarabine est contre-indiquée et on privilégie l’ibrutinib (Figure 8A). En rechute, on choisira le plus souvent l’ibrutinib si la première ligne consistait en une immuno-chimiothérapie, ou le vénétoclax après échec de l’ibrutinib (Figure 8B). Malgré les avancées récentes, l’incidence de rechute restée élevée, ce qui justifie la poursuite des efforts dans la compréhension des mécanismes de résistance aux traitements, le développement de nouvelles molécules et l’optimisation des stratégies thérapeutiques.

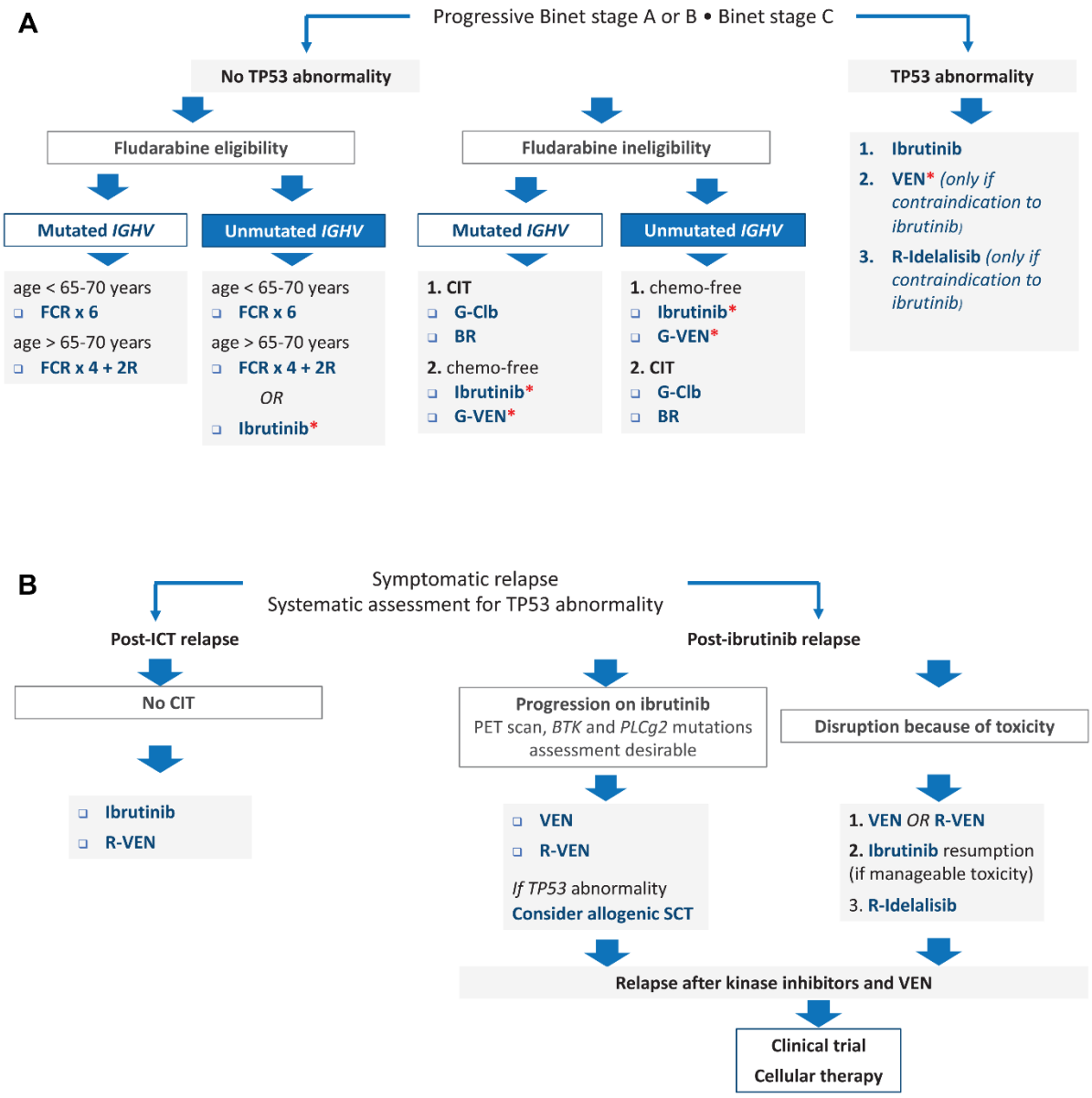

Figure 8. (**A**) Algorithme de prise en charge de la LLC en première ligne. (**B**) Algorithme de prise en charge de la LLC en seconde ligne et au-delà. (Quinquenel, 2020[79])

Chapitre II. Apoptose

II.1. Mort cellulaire et apoptose

La mort cellulaire est un processus correspondant à l'arrêt des fonctions de la cellule. Elle peut survenir en conditions physiologiques (vieillissement cellulaire, embryogenèse, homéostasie cellulaire…) ou pathologiques (maladie, traumatisme local, ou mort du tissu ou de l'organisme dont elle fait partie). L'existence de programmes de mort cellulaire est donc essentielle au bon fonctionnement de tout organisme pluricellulaire complexe, pour éliminer les cellules surnuméraires ou dysfonctionnelles.

Historiquement, le terme « nécrose » désignait tout type de mort cellulaire. En 1971, Kerr, Wyllie et Currie observent au microscope une mort cellulaire physiologique permettant l'élimination focale de cellules lors du développement embryonnaire ainsi que lors de processus tumoraux : spontanés et induits par les traitements. Ces observations sont publiées l'année suivante, et cette forme de mort cellulaire est baptisée « apoptose »[80].

De nos jours, la nomenclature des différents types de mort cellulaire s'est considérablement enrichie selon les mécanismes impliqués[81], mais l'apoptose reste la principale forme de mort cellulaire programmée (MCP).

Les exemples physiologiques sont nombreux. Lors de l'embryogenèse, elle est impliquée dans l'élimination des cellules des espaces interdigitaux permettant l'individualisation des doigts, ou dans l'élimination des neurones qui ne sont pas parvenus à établir de liaison synaptique utile avec les cellules voisines. Après la naissance et tout au long de la vie de l'organisme, l'apoptose est requise dans de nombreuses situations, telles que la défense contre certains pathogènes infectant des cellules (virus, certaines bactéries…) ou contre l'engagement de cellules vieillissantes ou tumorales vers une prolifération incontrôlée. Concernant les lymphocytes, on la retrouve également impliquée lors de la constitution du répertoire immunologique dans le thymus, avec l'élimination des lymphocytes T incapables de reconnaître le complexe majeur d'histocompatibilité du soi (sélection positive) puis de ceux ayant une trop forte affinité pour les antigènes du soi (sélection négative), ou encore dans le contrôle de la réponse immunitaire et de la prolifération cellulaire après stimulation du système immunitaire.

II.2. Mécanismes de l'apoptose

L'entrée d'une cellule en apoptose dépend d'un équilibre complexe entre signaux de survie et signaux de mort cellulaire.

II.2.1. Principaux acteurs

La protéine p53 est un facteur de transcription jouant un rôle majeur dans la régulation du cycle cellulaire et de l'apoptose. En l'absence de stress cellulaire, sa fonction est inhibée par MDM2 (murine double minute 2), une E3 ubiquitine ligase qui se lie à p53, provoque son transport du noyau vers le cytoplasme, et sa destruction dans le protéasome.

Les protéines issues de la famille des gènes *BCL2* jouent également un rôle régulateur primordial. Ses membres partagent au moins un des quatre « domaines d'homologie avec BCL2 » (domaines BH). Les protéines anti-apoptotiques, dont BCL2 mais aussi BCLXL ou MCL1, conservent au moins les domaines BH1 et BH2. Les protéines pro-apoptotiques peuvent contenir plusieurs domaines BH (telles que BAX ou BAK), ou uniquement le domaine BH3 (telles que BID, BAD, PUMA, NOXA…) nécessaire pour la dimérisation avec les autres protéines de la famille BCL2, en particulier pour inhiber les membres anti-apoptotiques (**Figure 9**). En l'absence de stress cellulaire, les protéines pro-apoptotiques sont inactives, et BAX est séquestrée dans le cytoplasme par BCL2.

Les principaux acteurs effecteurs de l'apoptose sont des protéines appartenant à la famille des protéases à cystéine, identifiées dans les années 1990 et dénommées « caspases »[82]. Il s'agit d'endoprotéases présentes de façon constitutive dans le cytoplasme des cellules sous forme inactive (procaspase ou zymogène). On distingue les caspases inflammatoires (caspases-1, -4, -5, -11, -12, -13 et -14) des caspases apoptotiques, elles-mêmes subdivisées en caspases initiatrices (caspases-2, -8, -9 et -10) à long pro-domaine contenant des motifs d'interaction protéine-protéine, et caspases exécutrices (caspases-3, -6 et -7), à pro-domaine plus court, et dont

l'activation mène au clivage de milliers de protéines substrats, à l'origine des évènements biochimiques et morphologiques de l'apoptose[83].

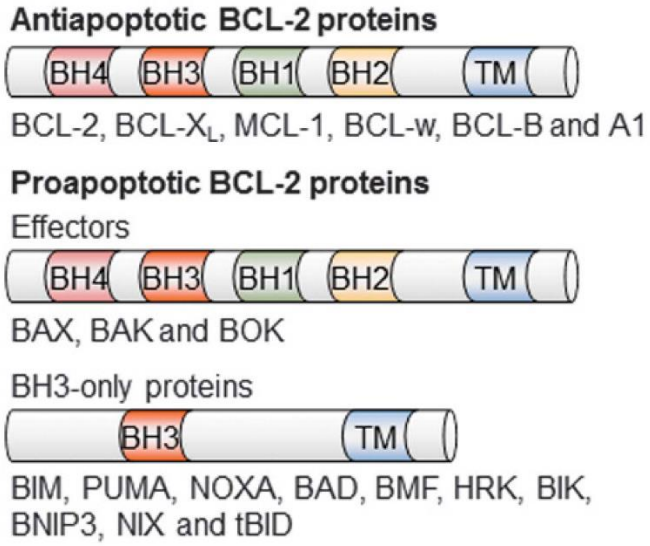

Figure 9. Structure des principales protéines de la famille BCL2 (BCL-2) (Pihán, 2017[84]).

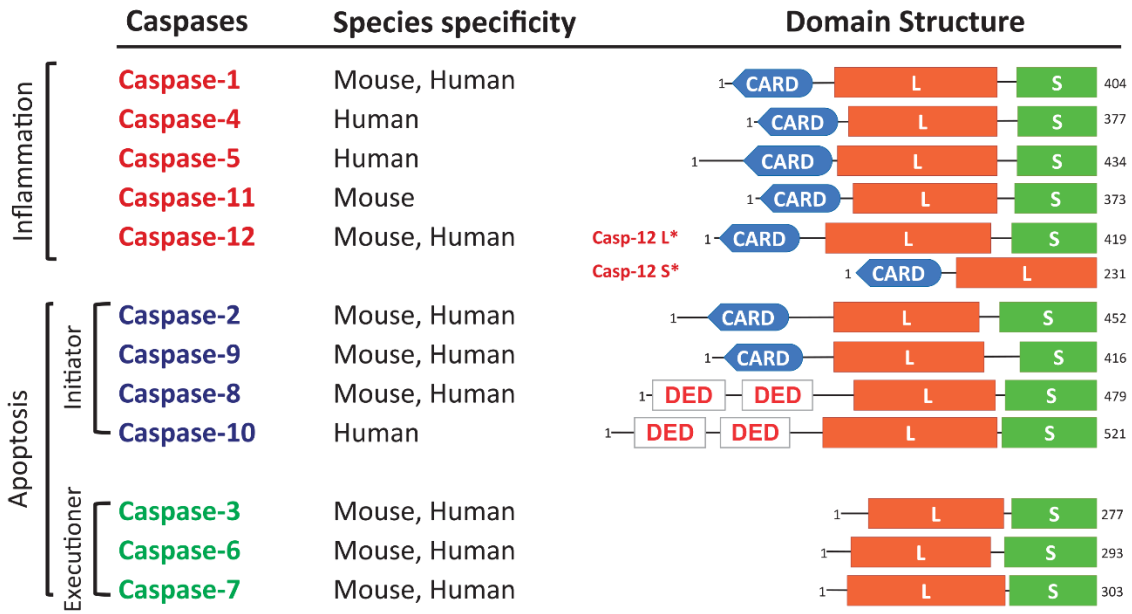

Figure 10. Rôles et structure des principales caspases (Shalini, 2015[85]).

L'apoptose peut être déclenchée par des signaux internes à la cellule (voie intrinsèque), ou par des signaux externes (voie extrinsèque).

II.2.2. Voie intrinsèque

La voie intrinsèque est déclenchée suite à la perte d'intégrité membranaire des mitochondries en contexte de stress cellulaire, comme suite à des dommages importants de l'ADN ou à un stress métabolique.
En présence de dommages de l'ADN, la protéine ATM est capable à la fois de phosphoryler MDM2, ce qui abolit son interaction inhibitrice avec p53, et de phosphoryler p53 elle-même, à l'origine de nombreuses modifications post-traductionnelles lui permettant alors d'exercer son activité transcriptionnelle sur ses nombreux gènes-cibles. Parmi eux, on peut citer p21/CDKN1A (cyclin-dependant kinase inhibitor 1A) dont la principale fonction est l'arrêt du cycle cellulaire, le temps de la résolution de la cause du stress cellulaire. Si la résolution n'est pas possible, p53 active l'expression de BAX, qui s'intègre dans la membrane mitochondriale et la perméabilise, ce qui aboutit à la libération de cytochrome C dans le cytoplasme. Celui-ci se lie à APAF-1 (apoptotic protease activating factor-1), dont l'oligomérisation permet le recrutement de la procaspase-9 et la formation de l'apoptosome. La procaspase-9 est alors clivée, et la caspase-9 active à son tour d'autres caspases exécutrices : les caspases-3, -6 et -7, ce qui aboutit à la mort cellulaire (**Figure 11**).
A noter que MDM2 fait partie des gènes dont la transcription est favorisée par p53, ce qui permet un rétrocontrôle négatif à la fois de p53 et des autres gènes cibles.

II.2.3. Voie extrinsèque

La voie extrinsèque repose sur l'activation de récepteurs membranaires par leurs ligands respectifs, dont les plus courants sont les récepteurs Fas/CD95 activés par FasL (Fas ligand), les récepteurs TNFR1 (tumor necrosis factor receptor-1) activés par TNFα, et les récepteurs TNFRSF10 (tumor necrosis factor receptor superfamily member 10) activés par TRAIL (tumor-necrosis-factor related apoptosis inducing ligand). L'activation de ces recepteurs entraîne le recrutement de la protéine adaptatrice FADD (Fas-associated death domain) et des procaspases-8 et -10,

permettant la formation d'un complexe protéique DISC (death-inducing signaling complex), qui active les caspases initiatrices (caspase-8 et/ou -10). A leur tour, ces caspases activent les caspases exécutrices (caspases -3, -6 et -7), ce qui aboutit à la mort cellulaire.

A noter qu'il existe des interactions entre les voies intrinsèque et extrinsèque. En particulier, parmi les substrats de la caspase-8 (voie extrinsèque), se trouvent plusieurs protéines de la famille de BCL-2, telles que BID, dont le clivage active la voie mitochondriale (intrinsèque) qui vient alors renforcer le signal pro-apoptotique (**Figure 11**).

Les cellules qui entrent en apoptose se caractérisent par de nombreux changements morphologiques : diminution du volume cellulaire, condensation puis dégradation de la chromatine, regroupement des organites intra-cellulaires, bouillonnement de la membrane plasmique puis scission de la cellule en corps apoptotiques. De façon précoce, les résidus phosphatidylsérine de la couche lipidique interne de la membrane plasmique sont externalisés, et restent exposés à la surface des corps apoptotiques, qui seront phagocytés par les cellules adjacentes et/ou par les cellules immunitaires.

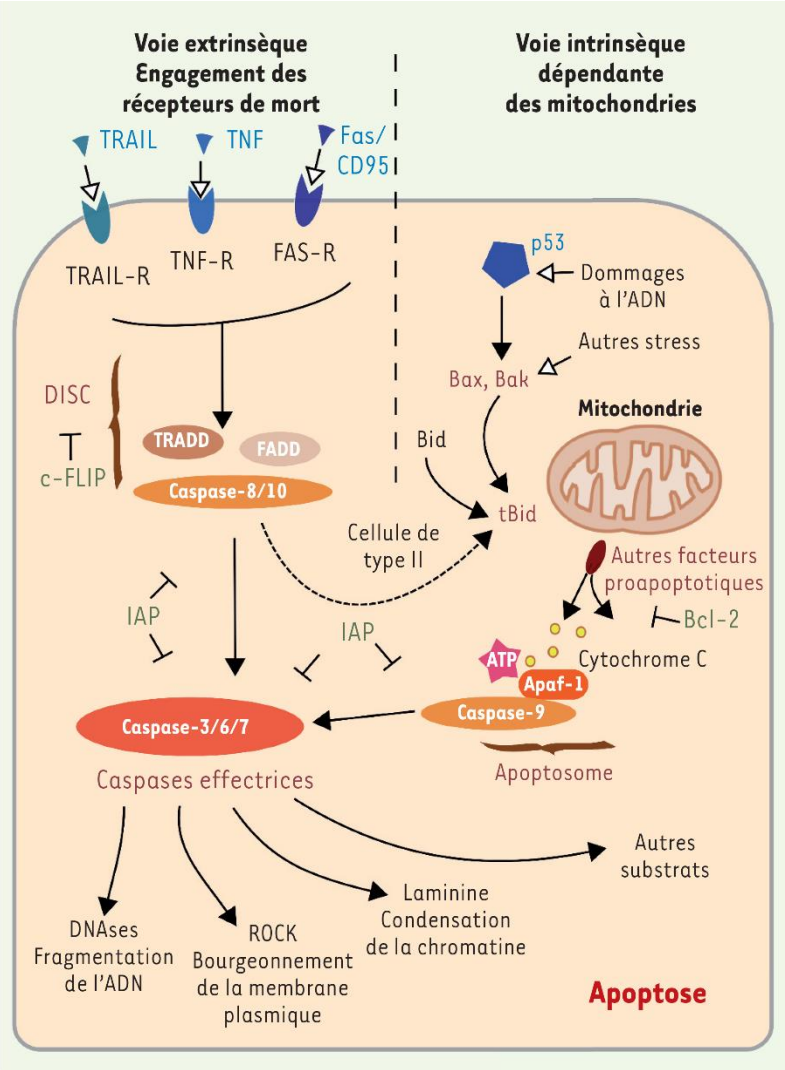

Figure 11. Schéma des voies extrinsèque et intrinsèque de l'apoptose (Cabon, 2013[86]). La voie extrinsèque est activée par les récepteurs membranaires et aboutit à l'activation des caspases-8 et -10 au sein du DISC, tandis que la voie intrinsèque est activée par des signaux internes (dommages de l'ADN, stress cellulaire) et implique la mitochondrie, puis la formation de l'apoptosome comprenant APAF-1, le cytochrome c et la caspase-9. Les deux voies aboutissent à l'activation des caspases effectrices (caspases-3, -6 et -7).

II.2.4. Autres mécanismes de régulation

La régulation de la mort cellulaire programmée met en jeu de nombreux autres acteurs et mécanismes.

La plupart des récepteurs à domaine de mort existent sous forme soluble, ou sous forme membranaire tronquée, pouvant capter une partie de leur ligand mais sans possibilité d'induction des voies effectrices d'aval. De plus, ces récepteurs sont souvent plus efficaces lorsqu'ils sont regroupés au sein de « radeaux lipidiques », micro-domaines membranaires riches en sphingolipides, favorisant le regroupement des domaines de mort et le recrutement de FADD et des procaspases nécessaires à la formation du DISC.

Par ailleurs, les IAPs (*inhibitor of apoptosis proteins*) sont des protéines capables de se lier directement aux caspases initiatrices et exécutrices, et d'empêcher leur activité de clivage, inhibant ainsi la mort cellulaire. Ces IAPs sont elles-mêmes inactivées par la protéine Smac/DIABLO (*second mitochondrial activator of caspases/direct IAP binding protein with low pI*), qui possèdent donc un rôle pro-apoptotique propre.

II.3. Apoptose pathologique

II.3.1. Excès d'apoptose

Une apoptose excessive a été associée à de nombreuses pathologies, au premier rang desquelles de nombreuses maladies neurodégénératives telles que la maladie d'Alzheimer, la démence à corps de Lewy ou encore la chorée de Huntington. L'apoptose joue également un rôle majeur dans le remodelage ventriculaire et le développement d'une insuffisance cardiaque post-infarctus du myocarde[87], ou après un accident vasculaire cérébral ischémique[88]. Enfin, l'infection des lymphocytes T CD4+ par le virus de l'immunodéficience humaine entraîne leur apoptose, à l'origine des infections opportunistes caractéristiques du stade SIDA.

II.3.2. Défaut d'apoptose

A l'opposé, un défaut d'apoptose peut également être à l'origine de diverses pathologies tumorales ou non.

Parmi les pathologies non tumorales, on peut citer le syndrome auto-immun lymphoprolifératif (ALPS, *auto-immune lymphoproliferative syndrome*), résultant d'une mutation de *FAS* (type Ia) ou de *FASLG* (type Ib), à l'origine d'un défaut d'élimination des lymphocytes auto-réactifs, d'où l'apparition d'adénopathies, d'une splénomégalie, d'une hypergammaglobulinémie et de manifestations auto-immunes chez l'enfant ; ou encore la lymphohistiocytose hémophagocytaire familiale, dont une partie des cas sont secondaires à une mutation du gène de la perforine (*PRF1*), responsable d'une activité cytotoxique réduite des lymphocytes T CD8+, qui s'accumulent dans les organes lymphoïdes et dans le système nerveux central, avec une hémophagocytose et les signes clinico-biologiques de l'activation histio-lymphocytaire.

Par ailleurs, de nombreux dysfonctionnements de l'apoptose ont été décrits comme associés au développement de pathologies tumorales. Le gène *TP53* est un gène suppresseur de tumeur majeur, dont des mutations sporadiques sont retrouvées dans 5 à 50% de la grande majorité des tumeurs malignes chez l'Homme[89]. Le gène codant BCL2 est localisé sur le bras long du chromosome 18 (18q21). La translocation t(14;18)(q32;q21) place l'expression de BCL-2 sous le contrôle de l'enhancer du gène des chaînes lourdes des immunoglobulines (situé en 14q32), ce qui aboutit à une surexpression de BCL2, inhibant ainsi la mort cellulaire et favorisant l'accumulation des cellules, tout en empêchant la réponse immunitaire antitumorale. On retrouve cette translocation dans différentes hémopathies lymphoïdes B, en particulier dans environ 90% des lymphomes folliculaires et 20% des lymphomes B diffus à grandes cellules. Des mutations somatiques de *FAS* et de *TNFRSF10* ont été rapportées dans plusieurs types d'hémopathies et de cancers solides[90,91].

II.4. Apoptose dans la LLC

II.4.1. Physiopathologie

Nous avons vu précédemment que la LLC se caractérise par l'expansion clonale de lymphocytes B. Cette expansion résulte essentiellement d'une incapacité des cellules à entrer en apoptose, qui peut s'expliquer par la conjonction de deux grands types de

mécanismes : une dysfonction des voies de l'apoptose dans les cellules leucémiques, et une stimulation anormale du micro-environnement tumoral.

Dans la LLC, la grande majorité des cellules leucémiques surexpriment BCL2. L'origine de cette surexpression semble être la délétion ou un défaut d'expression des micro-ARN *MIR15A* et *MIR16-1*, agissant normalement comme des inhibiteurs de BCL2[92]. Certaines LLC s'accompagnent également d'anomalies cytogénétiques et/ou moléculaires impliquant des acteurs majeurs de l'apoptose. C'est notamment le cas des gènes *ATM* et *TP53*, délétés et/ou mutés dans respectivement 10% et 5% des LLC de novo (et davantage en rechute).

Par ailleurs, nous avons évoqué précédemment l'importance du micro-environnement tumoral et des cellules qui le composent. Les cellules *nurse-like* sécrètent un ensemble de cytokines et de molécules d'adhérence (intégrine VLA4, L-sélectine, IL-4, CD40L, BAFF, CXCL12…) qui agissent comme des signaux de survie en activant les voies NF-kB ou PI3K/AKT des lymphocytes B, et favorisent leur *homing* dans la moelle et les ganglions[93]. L'activation de ces voies de survie aboutit à la transcription et à la surexpression de nombreuses molécules anti-apoptotiques, en particulier de XIAP (X-linked IAP) responsable de l'inactivation des caspases, et MCL1 qui agit comme un inhibiteur de BAX indépendamment de BCL2[94].

II.4.2. L'apoptose comme cible thérapeutique ?

Nous avons déjà vu les principaux traitements actuellement utilisés en routine dans le traitement des LLC en première ligne et en rechute. Parmi les stratégies déjà décrites, on peut rappeler que les chimiothérapies ont pour effet principal d'activer la mort cellulaire par l'induction de dommages de l'ADN (alkylants) et l'inhibition de la synthèse d'ADN et d'ARN (analogue des purines). En inhibant sélectivement BCL2, le vénétoclax (BH3-mimétique) exerce un effet cytotoxique en restaurant l'apoptose.
De façon plus expérimentale, d'autres stratégies thérapeutiques sont en cours de développement.

Un siRNA inhibiteur de BCL2, l'oblimersen, a été testé cliniquement chez 120 patients atteints de LLC en rechute ou réfractaires, en association avec la fludarabine et le

cyclophosphamide, dans le cadre d'un essai clinique de phase III randomisé, contre 121 patients dans le groupe contrôle recevant fludarabine et cyclophosphamide seuls[95]. Dans cette étude, l'oblimersen semblait montrer une efficacité en augmentant les taux de réponse complète et partielle, mais l'utilisation de ce traitement n'a finalement pas été approuvée pour une utilisation généralisée en pratique clinique.

Un essai de phase I a testé l'utilisation d'un antagoniste de MDM2, le RG7112, chez 19 patients atteints de LLC réfractaire ou en rechute, permettant d'obtenir une réponse partielle chez 1 patient, et une maladie stable chez 15 autres[96]. Bien qu'une diminution transitoire des lymphocytes ait été observée chez plusieurs patients, les doses plasmatiques étaient généralement inférieures aux cibles thérapeutiques, rendant difficile l'analyse des résultats.

Les inhibiteurs de XIAP semblent avoir une efficacité *in vitro* pour induire l'apoptose en combinaison avec TRAIL dans les cellules de LLC[97], mais aucun essai clinique n'a été réalisé sur une population de patients LLC.

Chapitre III. La voie TRAIL/TNFRSF10

Nous avons vu précédemment que les récepteurs de la famille TNFRSF10 (*tumor necrosis factor receptor superfamily member 10*) faisaient partie des récepteurs de mort localisés sur la membrane plasmatique, impliqués dans la voie extrinsèque de l'apoptose, et ayant en commun une capacité de reconnaissance d'un même ligand : TRAIL.
Ces récepteurs sont issus d'une famille de gènes homonymes, et comprennent 4 membres : TNFRSF10A (antérieurement appelé DR4, Apo2, TRAIL-R1 ou CD261), TNFRSF10B (DR5, TRAIL-R2 ou CD262), TNFRSF10C (DcR1, TRAIL-R3 ou CD263) et TNFRSF10D (DcR2, TRAIL-R4 ou CD264).

III.1. Le ligand TRAIL

TRAIL (également appelé TNFSF10, *TNF superfamily member 10*) est une cytokine de 281 AA, capable de se lier aux quatre membres de la famille de récepteurs TNFRSF10. Son gène (*TNFSF10*) est localisé sur le chromosome 3, en région 3q26.3. La protéine synthétisée existe sous forme membranaire, à la surface de nombreuses cellules (essentiellement dans la rate, les poumons et la prostate), ou sous forme soluble (sécrétée principalement par les monocytes et les lymphocytes NK). Quelle que soit sa forme, TRAIL joue son rôle en formant un homotrimère, qui interagit avec son récepteur également homotrimérisé[98,99].

III.2. Structure des récepteurs de TRAIL

III.2.1. Famille des gènes TNFRSF10

Les gènes de la famille *TNFRSF10* sont localisés sur le bras court du chromosome 8, en région 8p21.3.

Le **gène *TNFRSF10A*** contient 34 651 paires de bases (chr8:23,190,452-23,225,102 ; brin antisens, (GRCh38:CM000670.2)). Il permet de générer un transcrit de 2690

bases (TNFRSF10A-201) contenant 10 exons, à partir duquel sera codée une protéine de 468 acides aminés (AA) : TNFRSF10A. Cette protéine contient un peptide signal (AA 1-23), un domaine extracellulaire (AA 24-239) permettant la fixation de TRAIL (3 régions riches en cystéines : TNFR-Cys1, 2 et 3 ; AA 107-188), un domaine transmembranaire (AA 240-262) et un domaine intracellulaire (AA 263-468) contenant un domaine de mort (AA 365-448) capable de recruter FADD, à la base de la formation du DISC (**Figure 12**).

Le **gène *TNFRSF10B*** contient 48 899 paires de bases (chr8:23,020,133-23,069,031 ; brin antisens). Il permet de générer un transcrit de 3998 bases (TNFRSF10B-201) contenant 9 exons, à partir duquel sera codée une protéine de 440 AA : TNFRSF10B. Structurellement proche de TNFRSF10A, cette protéine contient un peptide signal (AA 1-55), un domaine extracellulaire (AA 56-210) permettant la fixation de TRAIL (3 régions riches en cystéines : TNFR-Cys1, 2 et 3 ; AA 57-178), un domaine transmembranaire (AA 211-231) et un domaine intracellulaire (AA 232-440) contenant un domaine de mort (AA 339-422) capable de recruter FADD de façon analogue à TNFRSF10A (**Figure 12**).

Le **gène *TNFRSF10C*** contient 14 525 paires de bases (chr8:23,102,921-23,117,445 ; brin sens). Il permet de générer un transcrit de 1395 bases (TNFRSF10C-201) contenant 5 exons, à partir duquel sera codée une protéine de 259 AA : TNFRSF10C. Cette protéine contient un peptide signal (AA 1-25), un domaine extracellulaire (AA 26-235) permettant la fixation de TRAIL (3 régions riches en cystéines : TNFR-Cys1, 2 et 3 ; AA 29-149), et un domaine transmembranaire (AA 236-258). Cependant, à la différence de TNFRSF10A et TNFRSF10B, il ne contient pas de domaine intracellulaire, et ne peut de ce fait transduire aucun signal (**Figure 12**).

Le **gène *TNFRSF10D*** contient 28 440 paires de bases (chr8:23,135,588-23,164,027 ; brin antisens). Il permet de générer un transcrit de 3535 bases (TNFRSF10D-201) contenant 9 exons, à partir duquel sera codée une protéine de 386 AA : TNFRSF10D. Cette protéine contient un peptide signal (AA 1-55), un domaine extracellulaire (AA 56-211) permettant la fixation de TRAIL (3 régions riches en cystéines : TNFR-Cys1, 2 et 3 ; AA 58-180), un domaine transmembranaire (AA 212-232) et un domaine

intracellulaire (AA 233-386) contenant un domaine de mort tronqué (340-366) et par conséquent non fonctionnel (**Figure 12**).

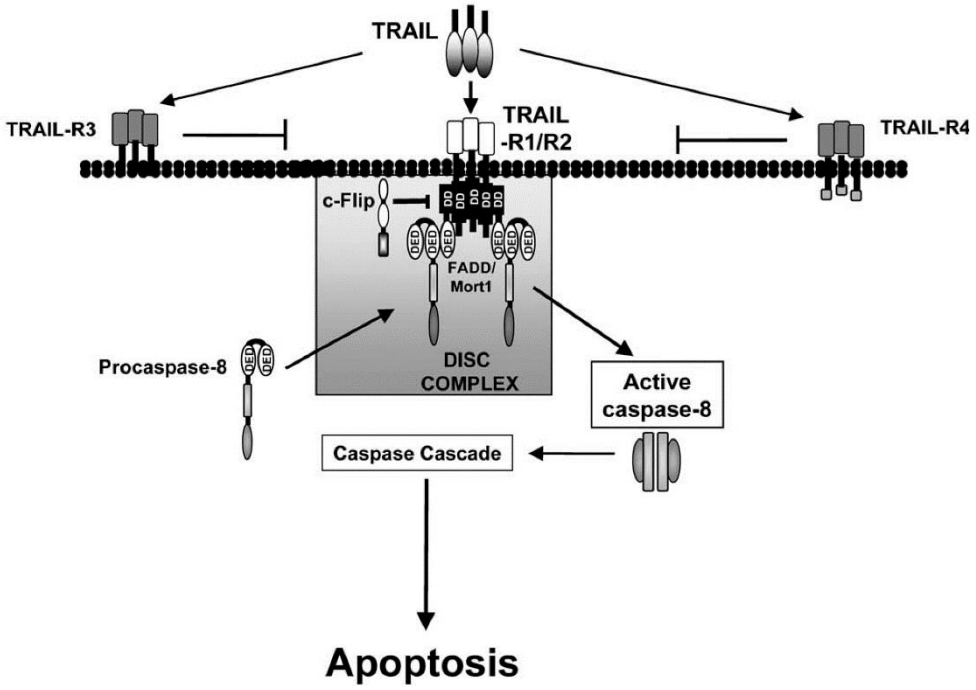

Figure 12. Schéma fonctionnel des récepteurs de la famille TNFRSF10. Seuls TNFRSF10A (TRAIL-R1) et TNFRSF10B (TRAIL-R2) ont un domaine intracellulaire complet et fonctionnel, permettant une réponse en présence du ligand TRAIL. (TRAIL-R3 = TNFRSF10C ; TRAIL-R4 = TNFRSF10D) (adapté de MacFarlane, 2003)[100]

Nous avons vu que seuls TNFRSF10A et TNFRSF10B possèdent un domaine de mort complet et fonctionnel, capable de recruter FADD et ainsi d'induire l'apoptose suite à leur activation par TRAIL. TNFRSF10C et TNFRSF10D ont un domaine intracellulaire respectivement absent ou tronqué, et ne peuvent jouer qu'un rôle de leurre, en captant une partie de TRAIL sans pouvoir déclencher d'apoptose en aval.

Bien que la formation du DISC soit une étape critique dans l'induction de l'apoptose, il est important de noter que c-FLIP (*cellular FLICE inhibitory protein*) peut également se lier à FADD (en compétition avec la procaspase-8), et recruter d'autres protéines (RIP, TRADD, TRAF2) pour former un complexe protéique secondaire à l'origine de

l'activation de voies de survie cellulaire, en particulier la voie NF-κB[101,102] (**Figure 13**). La capacité d'activation de la voie NF-κB par le domaine tronqué de TNFRSF10D est controversée[103,104].

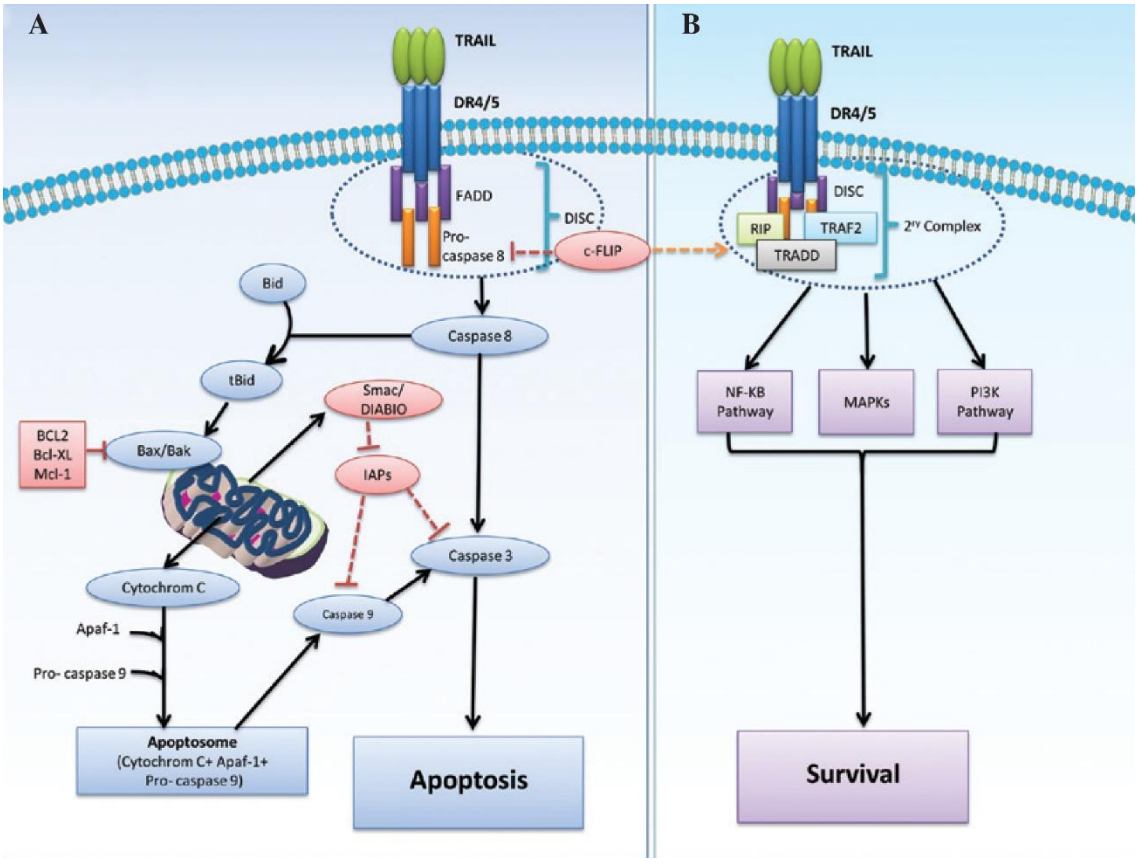

Figure 13. Signalisation de la voie TRAIL par les récepteurs TNFRSF10A (DR4) et TNFRSF10B (DR5). (**A**) Signalisation apoptotique. (**B**) Signalisation alternative, impliquant la fixation au DISC de protéines additionnelles (RIP, TRADD, TRAF2) favorisée par c-FLIP, qui aboutit finalement à l'activation des voies de survie et contrebalance l'effet pro-apoptotique. (Refaat, 2014[102])

III.2.2. L'ostéoprotégérine (TNFRSF11B)

Il existe un cinquième récepteur potentiel de TRAIL : l'ostéoprotégérine (ou TNFRSF11B), le récepteur soluble de RANK-ligand (*receptor activator of NF-kB-ligand*, RANKL). Dans la moelle osseuse, RANKL est exprimé par les cellules

stromales médullaires et les ostéoblastes. Son rôle est de favoriser la résorption osseuse en stimulant la différenciation des précurseurs des ostéoclastes (ostéoclastogenèse) et leur activation. L'ostéoprotégérine est également sécrétée par les cellules stromales et les ostéoblastes, et joue un rôle antagoniste de RANKL. Elle inhibe ainsi l'ostéoclastogenèse, et favorise l'apoptose des ostéoclastes[105]. L'ostéoprotégérine reconnaît également TRAIL comme ligand (20 à 34% d'homologie avec RANKL). Dans la moelle osseuse, TRAIL aurait donc un rôle de leurre, qui protègerait RANKL et promouvrait ainsi la résorption osseuse.

III.3. Régulation de la voie TRAIL/TNFRSF10

Des modèles in vitro utilisant des lignées cellulaires ont montré que sous l'influence des interférons de type I (essentiellement alpha) et de l'interféron gamma, de nombreux acteurs du système immunitaire (en particulier les lymphocytes T, B et NK, ainsi que les cellules dendritiques plasmacytoïdes et les monocytes) pouvaient augmenter leur expression de TRAIL et déclencher une réponse cytotoxique antitumorale et anti-infectieuse[106–109]. Ces cellules immunitaires activées tendent à exprimer également les récepteurs antagonistes TNFRSF10C et TNFRSF10D pour se protéger elles-mêmes de l'apoptose[110].

L'expression des récepteurs TNFRSF10 est contrôlée par p53. En présence d'un stress cellulaire, p53 stimule directement la synthèse de TNFRSF10A et de TNFRSF10B, afin de favoriser la réponse apoptotique[111,112].

L'activité pro-apoptotique des récepteurs TNFRSF10 est également modulée par leur concentration à la surface membranaire. Ces récepteurs voient leur efficacité augmentée lorsqu'ils sont regroupés au sein de radeaux lipidiques[113–116].

III.4. Rôles physiologiques de la voie TRAIL

Une part importante des connaissances actuelles quant au fonctionnement de la voie TRAIL/TNFRSF10 provient de l'étude de modèles murins.

Chez la souris, cette voie est beaucoup plus simple que chez l'Homme : il n'existe qu'un seul récepteur de TRAIL capable d'induire l'apoptose (mTRAIL-R, homologue à TNFRSF10A et TNFRSF10B)[117] ; les souris possèdent également deux récepteurs dépourvus de domaines intracellulaires fonctionnels (mDcTRAIL-R1 et mDcTRAIL-R2, dont les séquences d'acides aminés sont cependant assez éloignées des récepteurs humains TNFRSF10C et TNFRSF10D) ainsi que l'ostéoprotégérine.

III.4.1. Rôle dans l'immunité antitumorale

Les souris KO pour TRAIL ($TRAIL^{-/-}$) sont viables et fertiles, ce qui suggère l'absence de rôle crucial dans le développement et la reproduction[118,119].
En revanche, Cretney et al. ont rapporté que des souris $TRAIL^{-/-}$ allogreffées avec des cellules tumorales rénales ou mammaires montraient une croissance tumorale plus forte et un nombre de métastases hépatiques et pulmonaires augmenté, en comparaison avec des souris « contrôle » ($TRAIL^{+/+}$). Cette sensibilité accrue aux tumeurs serait au moins en partie liée à un défaut de toxicité des lymphocytes NK chez des souris $TRAIL^{-/-}$ ou traitées par anticorps monoclonaux inhibiteurs de TRAIL[120].

A l'instar des souris déficientes en TRAIL, les souris KO pour TRAIL-R ($TRAIL\text{-}R^{-/-}$) ont un développement normal, y compris de leur système immunitaire.
Cependant, tout comme les souris $TRAIL^{-/-}$, les souris $TRAIL\text{-}R^{-/-}$ tendent à développer des tumeurs malignes plus agressives[121].

Finnberg et al. ont montré que la perte d'un seul allèle de TRAIL-R chez des souris ayant une prédisposition aux lymphomes (Eμ-myc) était associée à une réduction significative de la survie sans lymphome. Ces tumeurs étaient également plus agressives[119].

Il semble donc que la voie TRAIL/TNFRSF10 contribue à la protection antitumorale assurée par le système immunitaire.

III.4.2. Rôle dans l'immunité anti-infectieuse

Lors de la réaction inflammatoire, l'expression de TRAIL est augmentée à la surface des cellules immunitaires (en particulier les lymphocytes NK, T CD8 et les polynucléaires neutrophiles), stimulée en particulier par les interférons de type I produits lors des infections virales. En parallèle, les cellules infectées expriment souvent davantage les récepteurs TNFRSF10 agonistes de l'apoptose[122–125]. Ces éléments plaident pour une participation de la voie TRAIL à l'immunité anti-infectieuse.

III.4.3. Rôle immunorégulateur

Les souris TRAIL$^{-/-}$ présentent un défaut de sélection thymique au moment de la constitution du répertoire T (par défaut d'apoptose), et sont sujettes à des réponses immunitaires dérégulées voire à un certain degré d'auto-immunité[126].
De la même façon, les souris TRAIL-R$^{-/-}$ ont une prédisposition pour certaines maladies auto-immunes, en particulier des encéphalomyélites[127]. Ces souris présentent également des réponses immunitaires innées dérégulées après stimulation[118].

Lors de la réponse immunitaire humorale, la sélection des lymphocytes B dans le centre germinatif, ainsi que la régulation de l'expansion clonale permettant le maintien de l'homéostasie humorale, impliquent des mécanismes d'apoptose essentiellement médiés par la voie Fas. Cependant, chez les souris déficientes en Fas-ligand, le KO de TRAIL aboutit à des lymphoprolifération extrêmes et à des thrombopénies auto-immunes, ce qui indique que la voie TRAIL peut prendre le relais de la voie Fas lorsque cette dernière est déficiente[128].

La voie TRAIL pourrait ainsi prévenir certaines maladies auto-immunes par inhibition des lymphocytes auto-réactifs. Malgré cela, aucune maladie auto-immune n'a été associée avec des mutations de *TRAIL* chez l'Homme.

III.4.4. Expression des récepteurs TNFRSF10 à la surface des lymphocytes

Chez l'Homme, l'expression des récepteurs TNFRSF10 est rapportée à la surface des lymphocytes T et B[129,130], ainsi que de celle de nombreux autres types cellulaires[131].

Cependant, la plupart de ces cellules sont peu sensibles à l'apoptose induite par TRAIL en l'absence de transformation ou d'infection[132–134].

Staniek et al. ont montré qu'au sein des lymphocytes B circulants, les récepteurs TNFRSF10A et B sont tous deux exprimés dans des proportions faibles mais variables. Cette expression a été décrite comme augmentée au sein des lymphocytes dérivant du centre germinatif, en particulier de TNFRSF10B. Ces récepteurs sont tous les deux fonctionnels, et contribuent à l'apoptose par voie caspase-3 dépendante. Bien que les lymphocytes B activés soient sensibles à TRAIL, ce n'est pas le cas des lymphocytes B quiescents[135].

III.5. Implications de la délétion 8p et de la voie TRAIL/TNFRSF10 dans les hémopathies lymphoïdes B

III.5.1. Détection de la del8p dans les hémopathies lymphoïdes B

Une délétion 8p impliquant la région 8p21.3 est retrouvée dans de nombreuses lignées cellulaires dérivant d'hémopathies lymphoïdes B (leucémie pro-lymphocytaire B : JVM2, JVM13 ; lymphome folliculaire : PR1, OCI-Ly8 ; lymphome B diffus à grandes cellules : MD-901 ; lymphome à cellules du manteau : Z-138 ; lymphome de Burkitt : NAMALWA)[51].

Cette délétion a également été décrite dans des cellules primaires issues de patients atteints de lymphomes B (folliculaire, à cellules du manteau, de la zone marginale splénique, B diffus à grandes cellules, Burkitt), de leucémies lymphoïdes chroniques, et de myélome multiple, avec des prévalences rapportées de 5 à 29%, voire jusqu'à près de 80% pour les formes blastoïdes de lymphomes à cellules du manteau[44,47,50,136–140].

III.5.2. Implication des gènes TNFRSF10A/TNFRSF10B dans la délétion 8p

Parmi les gènes suppresseurs de tumeur présents sur le chromosome 8p, l'implication des gènes *TNFRSF10* dans la tumorigenèse a rapidement été suspectée. Ainsi, la

perte d'un allèle de *TNFRSF10B* a été rapportée dans de nombreux types de cancer solides (broncho-pulmonaire, sein, côlon, prostate, hépatocellulaire…[141–144]), mais également dans de nombreuses hémopathies, comme nous allons le voir.

Plusieurs études ont rapporté l'existence de mutations de *TNFRSF10A* et *TNFRSF10B* chez certains patients atteints de cancers solides[91,145]. Cependant, il est important de noter qu'à la différence du modèle de Knudson, qui suggère que la nature récessive de la plupart des mutations « perte de fonction » impose l'altération des deux allèles d'un même gène suppresseur de tumeur au sein d'une cellule (« *two-hit » hypothesis*), les délétions 8p sont en règle hétérozygotes, et ne s'accompagnent pas de mutations associées des séquences des gènes *TNFRSF10* sur l'allèle restant[51]. Il semble donc que la perte d'un seul allèle soit suffisante pour faire apparaître les conséquences péjoratives en matière de résistance à l'apoptose et de tumorigenèse – on parle d'haploinsuffisance.

III.5.2.1. Dans la LLC

Les cellules de leucémie lymphoïde chronique expriment à la fois TNFRSF10A et TNFRSF10B. Les effets de TRAIL *in vitro* sur cellules primaires de LLC sont cependant inconstants, pouvant parfois induire une apoptose significative dans une minorité de cas, mais n'ayant le plus souvent aucun effet – voire promouvant la survie des cellules[146–148].

Johnston et al. ont montré, d'une part, que l'exposition de cellules primaires de LLC à certains traitements comme le chlorambucil et la fludarabine pendant 48 heures augmentait l'expression des récepteurs TNFRSF10A et TNFRSF10B ; et, d'autre part, que l'apoptose induite par ces traitements était corrélée à l'expression de ces deux récepteurs. De plus, si les cellules primaires étaient peu sensibles à l'apoptose induite par TRAIL, il existait en revanche une synergie en combinant TRAIL avec le chlorambucil et la fludarabine[149].
Cependant, s'il est reconnu que TNFRSF10A et TNFRSF10B sont tous les deux fonctionnels et que TNFRSF10B est davantage présent à la surface des cellules que TNFRSF10A, la contribution relative de ces récepteurs à l'apoptose est toujours controversée. MacFarlane et al. ont montré qu'après sensibilisation de cellules

primaires issues de 8 patients LLC par un inhibiteur d'HDAC (depsipeptide), l'utilisation d'un anticorps monoclonal agoniste spécifique de TNFRSF10A induisait l'apoptose, alors qu'un autre anticorps agoniste spécifique de TNFRSF10B était moins efficace[150]. Ce résultat semblait confirmé par la synthèse de variants de TRAIL spécifiques de TNFRSF10A ou TNFRSF10B, dont l'utilisation à fortes doses (1 µg/mL) montrait une apoptose induite par TNFRSF10A plus importante que TNFRSF10B[151]. En revanche, aucune différence n'était mesurée à la concentration de 100 ng/mL. Il a ensuite été montré par la même équipe que l'induction d'apoptose médiée par un anticorps monoclonal agoniste spécifique de TNFRSF10B était possible, à condition d'un cross-linking dudit anticorps, favorisé par l'oligomérisation des récepteurs TNFRSF10B[152].

III.5.2.2. Dans les lymphomes B

Rubio-Moscardo et al. ont montré une diminution d'expression de *TNFRSF10A* et *TNFRSF10B in vitro* sur cellules primaires issues de lymphomes B avec délétion 8p, ainsi qu'une résistance à l'apoptose induite par TRAIL des lignées cellulaires porteuses de la délétion. Cette résistance était réversible après restauration de l'expression de ces deux gènes par transfection de plasmides contenant *TNFRSF10A* ou *TNFRSF10B*[51].

III.5.2.3. Dans le myélome multiple

Dans le myélome, la délétion 8p impliquant la région 8p21 a été associée à une diminution de la sensibilité au bortézomib, associée à une altération de l'expression des récepteurs TNFRSF10A et TNFRSF10B sur cellules primaires de myélome[153].

III.6. La voie TNFRSF10/TRAIL comme cible thérapeutique ?

III.6.1. Rationnel

Plusieurs études ont montré que l'action pro-apoptotique de TRAIL ciblait préférentiellement les cellules néoplasiques, épargnant les cellules saines, ce qui pourrait s'avérer utile dans un objectif thérapeutique[154,155]. Cette différence d'action

peut s'expliquer par une expression accrue des récepteurs inducteurs d'apoptose (TNFRSF10A et TNFRSF10B) à la surface des cellules tumorales, alors que l'expression des récepteurs antagonistes (TNFRSF10C et TNFRSF10D) est plus importante à la surface des cellules normales.

De nombreuses études pré-cliniques, sur lignées cellulaires et modèles animaux, ont confirmé l'effet pro-apoptotique de TRAIL sur des cellules tumorales issues de cancers du côlon, du poumon, de la prostate, du sein, du pancréas, du système nerveux central, de la thyroïde, de cellules leucémiques ou de myélome[155–159]. L'un des avantages de la voie TRAIL/TNFRSF10 est qu'elle pourrait, en théorie, déclencher l'apoptose indépendamment de la voie p53, souvent altérée dans les cellules tumorales. Son utilisation, en combinaison avec la radiothérapie et/ou la chimiothérapie, pourrait ainsi contribuer de façon synergique à renforcer la réponse, et à réduire le risque d'apparition de résistances[160,161].

III.6.2. Anticorps monoclonaux agonistes

Plusieurs anticorps monoclonaux agonistes spécifiques de TNFRSF10A ou TNFRSF10B ont été développés[162,163]. Certains ont pu être testés lors d'essais cliniques de phase I[164–166], mais leur efficacité en monothérapie était globalement décevante. Le mapatumumab (agoniste de TNFRSF10A) a pu être étudié lors d'un essai clinique de phase II dans les lymphomes non Hodgkiniens en rechute, permettant d'obtenir des réponses essentiellement dans le sous-groupe des patients atteints de lymphome folliculaire[167]. Il n'a en revanche pas démontré de réponse significative dans deux autres essais de phase II concernant des cancers broncho-pulmonaires ou colo-rectaux[168,169]. Le conatumumab (agoniste de TNFRSF10B) n'a pas montré de bénéfice significatif dans des essais de phase II portant sur des cancers broncho-pulmonaires et pancréatiques[170,171]. Le tigatuzumab (agoniste de TNFRSF10B) a montré une faible proportion de réponses partielles chez des patients atteints de cancer du pancréas lors d'un essai de phase II[172], mais aucun bénéfice significatif chez d'autres atteints de cancers broncho-pulmonaires[173].

III.6.3. Variants recombinants de TRAIL

Des variants recombinants de TRAIL soluble ont également été synthétisés. A titre d'exemple, la dulanermine a été utilisée en association avec la vinorelbine et le cisplatine en première ligne thérapeutique chez des patients atteints de cancers broncho-pulmonaires non à petites cellules dans le cadre d'un essai thérapeutique de phase III, et montré une amélioration significative des taux de réponse globale et de la survie sans progression, avec une tolérance clinique acceptable[114]. Un nouvel agoniste de TRAIL, nommé AGP350, caractérisé par sa capacité à lier 6 récepteurs par molécule, a également été étudié *in vitro* et *in vivo* dans l'adénocarcinome canalaire du pancréas. La molécule était efficace pour induire l'apoptose sur lignées cellulaires. Sur modèle murin, après xénogreffe tumorale, l'APG350 a montré une réduction significative du volume tumoral et une réduction du risque de récidive et/ou d'extension métastatique. Cet effet était renforcé en association avec un BH-3 mimétique, le navitoclax (inhibiteur de BCL2 et de BCLXL)[174]. L'effet antitumoral semblait par ailleurs plus important en comparaison avec TRAIL soluble.

III.6.4. Perspectives d'amélioration des stratégies

III.6.4.1. Améliorer la biodisponibilité

L'un des freins à l'efficacité des molécules de TRAIL recombinantes est leur courte demi-vie (inférieure à une heure après leur administration), liée à la fois à leur faible poids moléculaire entraînant leur élimination rénale rapide, et au caractère non covalent de leur liaison aux récepteurs TNFRSF10. On peut également supposer que les récepteurs antagonistes peuvent réduire leur effet simplement par captation. Les anticorps monoclonaux permettent d'éviter ce problème, et ont une durée de vie significativement plus longue (de plusieurs jours à quelques semaines). Mais leur efficacité reste limitée dans les essais, vraisemblablement en raison d'un cross-linking insuffisant de ces anticorps bivalents sur des récepteurs dont la trimérisation est nécessaire à la constitution d'un DISC fonctionnel[175]. Une autre raison pourrait être le manque de soutien des cellules immunitaires exprimant le FcγR, nécessaire au déclenchement de l'apoptose par certains anticorps monoclonaux agonistes tels que le conatumumab ou le drozitumab[176,177]. Enfin, en aval de la voie TRAIL/TNFRSF10, les mécanismes d'apoptose impliquent la mitochondrie et les caspases effectrices. Par conséquent, la surexpression des membres anti-apoptotiques de la famille BCL2 et/ou

des IAPs contribue à altérer la réponse apoptotique induite par l'activation des récepteurs de TRAIL.

Pour tenter d'outrepasser ces limites, plusieurs stratégies sont en cours de développement[178].

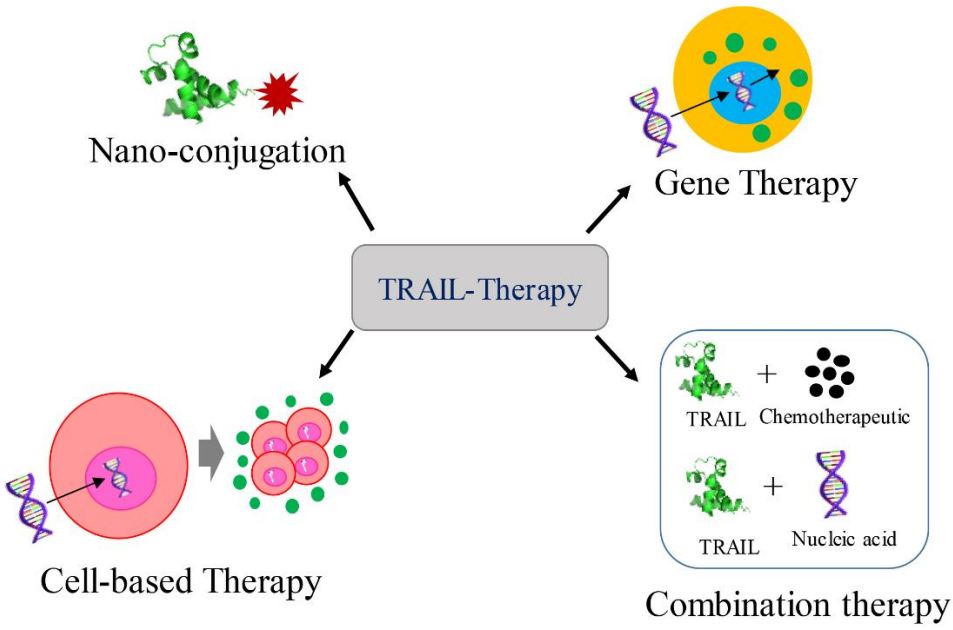

Figure 14. Perspectives d'utilisation et d'optimisation de TRAIL en thérapeutique. (Thapa, 2020[178])

De nouveaux peptides TRAIL recombinants ont ainsi été synthétisés, avec l'adjonction d'un peptide « tag » afin d'améliorer leur demi-vie, voire de favoriser leur homo-trimérisation : FLAG (FLAG-TRAIL)[179], poly-histidine (SuperKillerTRAIL)[180], ou leucine/isoleucine zipper (LZ-TRAIL/izTRAIL)[155]. Une tentative de liaison covalente avec le polyéthylène glycol (PEGylation) a également été employée afin d'accroître la demi-vie et d'améliorer l'efficacité de TRAIL[181]. De même, l'utilisation de vésicules extracellulaires issues de cellules souches mésenchymateuses capables d'exprimer des molécules de TRAIL recombinantes est en cours de développement, et pourrait être une piste intéressante pour résoudre le problème de la biodisponibilité[182].

D’autres approches de type thérapie génique ont consisté à conceptualiser des plasmides permettant l’expression de TRAIL, en vue de les administrer au patient afin d’augmenter de façon continue la quantité de TRAIL disponible dans le microenvironnement tumoral. Pour cela, des vecteurs viraux et non-viraux ont été développés, mais ces techniques sont encore au stade pré-clinique[183–186].

III.6.4.2. Associations thérapeutiques

Plus classiquement, de nombreuses associations avec d’autres traitements (chimiothérapie, radiothérapie) ont été étudiées, dans l’espoir de sensibiliser les cellules tumorales à TRAIL. Parmi les options les plus intéressantes, on peut citer l’association aux inhibiteurs de BCL2 ou aux inhibiteurs de XIAP, mentionnées précédemment. Le bortézomib, inhibiteur du protéasome, serait également un bon candidat en particulier dans le myélome, compte tenu de son effet inhibiteur puissant de la voie NF-κB[187]. Les inhibiteurs d’histone désacétylase (HDACi) semblent aussi jouer un rôle synergique intéressant, en favorisant l’expression de c-MYC, ce qui aboutit à un effondrement de l’expression de c-FLIP et permet donc l’activation de la caspase-8 au niveau du DISC[188,189]. Dans la LLC, il a également été montré qu’un pré-traitement par inhibiteur d’HDAC suivie de la stimulation de TNFRSF10A favorisait le recrutement de FADD, et donc l’apoptose[190]. Par ailleurs, puisque l’expression des récepteurs TNFRSF10A et TNFRSF10B est favorisée par p53, il est possible que tout traitement permettant l’activation de cette voie puisse favoriser l’efficacité de TRAIL. Appuyant cette hypothèse, une synergie entre la voie TRAIL et la radiothérapie a été décrite in vitro dans des lignées de cancer du sein, vraisemblablement par l’augmentation des récepteurs TNFRSF10B selon un mécanisme p53-dépendant[160,191].

Objectifs de la thèse

Objectifs de la thèse

La LLC est une maladie hétérogène, principalement du fait de ses caractéristiques cytogénétiques et moléculaires. Si certains patients peuvent rester de nombreuses années sans traitement, d'autres au contraire présentent des formes plus agressives, nécessitant souvent plusieurs lignes thérapeutiques en raison de la sélection de cellules de plus en plus résistantes, et pouvant à terme engager le pronostic vital.

Les LLC avec altération de *TP53* (17p) ou *ATM* (11q) ont été largement décrites comme associées à un pronostic défavorable. Bien que moins étudiés, d'autres facteurs de mauvais pronostic ont été rapportés, comme la délétion 8p et les anomalies 8q24. Enfin, le caryotype complexe a récemment été décrit comme nouveau facteur pronostic à prendre en compte dans les choix thérapeutiques.

Mon projet de thèse avait pour but d'approfondir la compréhension de ces facteurs d'agressivité dans la LLC. Il sera présenté en 3 parties : un article soumis sur le rôle de TNFSRF10 dans la délétion 8p ; un article publié sur un type de leucémie agressive, la leucémie prolymphocytaire B, associée à des anomalies du gène *MYC* en 8q24 ; et une revue de la littérature publiée sur les caryotypes complexes.

Résultats

Article 1

Del8p and TNFRSF10B loss are associated to poor prognosis and drug resistance in chronic lymphocytic leukemia

(en cours de finalisation)

La délétion 8p (del8p) est une anomalie cytogénétique rare (< 5% des LLC au diagnostic) mais récurrente dans les LLC agressives. Dans cet article, notre objectif était de caractériser la del8p dans la LLC, afin de déterminer le pronostic, le(s) gène(s) impliqué(s) et les mécanismes de résistance aux traitements.

Pour cela, nous avons constitué une cohorte de 57 patients LLC avec del8p (plus large cohorte à ce jour), que nous avons comparée à une cohorte contrôle de 155 patients LLC non-del8p. J'ai construit des lignées TNFRSF10 KO par CRISPR/Cas9 à partir de la lignée cellulaire de LLC OSU-CLL. Les mesures d'expression des gènes et les tests fonctionnels d'apoptose induite in vitro ont été réalisés à partir d'échantillons des lignées OSU-CLL wt et KO et de cellules primaires issues des patients des deux cohortes.

Nous avons ainsi montré que la del8p était fréquemment associée à d'autres facteurs « classiques » de mauvais pronostic, tels que le caryotype complexe, les anomalies *TP53* et le statut *IGHV* non muté. Nous avons confirmé que les patients LLC del8p présentaient des survies globale et sans progression raccourcies, et avaient un risque élevé de transformation de Richter. Par ailleurs, en comparant les patients traités par (immuno)chimiothérapie à base de fludarabine dans les deux cohortes, ceux avec une LLC del8p avaient une survie globale et un temps jusqu'au prochain traitement diminués. J'ai montré que les gènes de la famille *TNFRSF10*, codant les récepteurs du ligand TRAIL, étaient impliqués dans la région délétée chez la majorité des patients del8p (91% dans notre cohorte). Dans nos modèles de lignée, TNFRSF10A et TNFRSF10B étaient tous deux capables d'induire l'apoptose en réponse à la stimulation par TRAIL. Sur cellules primaires LLC non-del8p, la culture en présence de fludarabine entraînait principalement une augmentation d'expression de TNFRSF10B, et une sensibilisation des cellules à TRAIL. En revanche, les cellules primaires LLC del8p avaient perdu leur capacité à surexprimer TNFRSF10B, et

apparaissaient ainsi résistantes à TRAIL. Nous avons montré que le lien entre la fludarabine et la voie TRAIL passe probablement par l'intermédiaire de la protéine P53, dont plusieurs gènes cibles voient leur expression augmentée dans les LLC non-del8p après exposition à la fludarabine, ce que nous n'avons pas observé dans les LLC del8p.

Discussion

Les données clinico-biologiques, cytogénétiques et analyses de survie, ont confirmé le pronostic défavorable conféré par la del8p. Les gènes de la famille *TNFRSF10*, en particulier *TNFRSF10B*, fonctionnent comme des suppresseurs de tumeur, et sont haploinsuffisants dans la del8p : une délétion hétérozygote suffit à entraîner une diminution d'expression mesurable de ces gènes.

Nous avons mis en évidence in vitro une synergie entre la fludarabine et la voie TRAIL au sein des cellules LLC non-del8p, et une efficacité diminuée de la fludarabine chez les LLC del8p (indépendamment de toute autre anomalie cytogénétique ou moléculaire). De façon intéressante, les patients avec LLC del8p étaient mauvais répondeurs in vivo aux traitements à base de fludarabine. A l'heure actuelle, les patients avec LLC sans anomalie *TP53* et avec un statut *IGHV* muté sont éligibles à l'immunochimiothérapie fludarabine-cyclophosphamide-rituximab ; nous recommandons alors dans ce contexte de rechercher de façon systématique une délétion 8p, ce qui n'est pas fait en routine. Enfin une perspective d'association entre fludarabine et traitements activateurs de la voie TRAIL en cours de développement pourrait profiter aux patients LLC non-del8p dont la capacité à surexprimer TNFRSF10B est conservée.

Del8p and TNFRSF10B loss are associated with a poor prognosis and drug resistance in chronic lymphocytic leukemia

Ludovic Jondreville[1], Lea Deghane[1], Cecile Doualle[1], Luce Smagghe[1], Beatrice Grange[2], Frederic Davi[1,2], Leticia Koch Lerner[1], Delphine Garnier[1], Clotilde Bravetti[1,2], Olivier Tournilhac[3], Damien Roos-Weil[1,4], Marouane Boubaya[5], Elise Chapiro[1,2]*, Santos A Susin[1]*, Florence Nguyen-Khac[1,2]*

[1] Drug Resistance in Hematological Malignancies, Centre de Recherche des Cordeliers, UMRS 1138, INSERM, Sorbonne Université, Université Paris Cité, F-75006 Paris, France
[2] Service d'Hématologie Biologique, Hôpital Pitié-Salpêtrière, AP-HP, Paris, France
[3] Service d'Hématologie Clinique, CHU Estaing, 1 place Lucie et Raymond Aubrac, 63003 Clermont-Ferrand
[4] Service d'Hématologie Clinique, Hôpital Pitié-Salpêtrière, AP-HP, Paris, France
[5] Unité de Recherche Clinique, Hôpitaux Universitaires Paris Seine-Saint-Denis, AP-HP, Bobigny, France

Corresponding authors: Florence Nguyen-Khac, Service d'Hématologie Biologique, Hôpital Pitié-Salpêtrière, 83 Boulevard de l'Hôpital, 75013, Paris, France; email: florence.nguyen-khac@aphp.fr; Phone :+33 142162451 ; Fax : +33142162453. Santos A Susin, Centre de Recherche des Cordeliers, 15 rue de l'Ecole de Médecine, 75014 Paris, France; email: santos.susin@sorbonne-universite.fr. Elise Chapiro, Service d'Hématologie Biologique, Hôpital Pitié-Salpêtrière, 83 Boulevard de l'Hôpital, 75013 Paris, France; email: elise.chapiro@aphp.fr

**Shared senior co-authorship*

Competing Interests
The authors have nothing to disclose.

Word counts
Text: 4786
Abstract: 208
Table: 1
Figures: 5

Abstract

Chronic lymphocytic leukemia (CLL) is a heterogeneous disease, the prognosis of which varies according to the cytogenetic group. We characterized a rare chromosomal abnormality (del8p, deletion of the short arm of chromosome 8) in the context of CLL. By comparing the largest cohort of del8p CLL to date (n=57) with a non-del8p control cohort (n=155), del8p was significantly associated with a poor prognosis, a shorter time to first treatment, worse overall survival (OS), and a higher risk of Richter transformation. For patients treated with fludarabine-based regimens, the next-treatment-free survival and the OS time were shorter in del8p cases (including those with mutated *IGHV* genes). We found that one copy of the *TNFRSF10B* gene (coding for a pro-apoptotic receptor activated by TRAIL) was lost in 91% of del8p CLL. *TNFRSF10B* is haploinsufficient in del8p CLL, and is involved in the modulation of fludarabine-induced cell death - as confirmed by our experiments in primary cells and in CRISPR-edited *TNFRSF10B* knock-out CLL cell lines. Lastly, we found that del8p abrogates the synergy between fludarabine and TRAIL-induced apoptosis. Our results highlight del8p's value as a prognostic marker and suggest that fit CLL patients (i.e. with mutated *IGHV* and no *TP53* disruption) should be screened for del8p before the initiation of fludarabine-based treatment.

INTRODUCTION

Chronic lymphocytic leukemia (CLL, the most common adulthood leukemia in Western countries) is characterized by the accumulation of malignant CD5+ B cells in the blood, bone marrow, and secondary lymphoid tissues. Recurrent chromosomal abnormalities (CAs) have a key role in CLL oncogenesis and drug resistance. The 8p deletion (del8p) is found in approximately 5% of newly discovered CLL cases, 28% of cases of CLL with del17p (1, 2), and up to 44% of cases of Richter transformation (RT) (3), and is associated with a short time to first treatment (TTFT) and poor overall survival (OS) (1, 2, 4, 5). Given its rarity, del8p has only been described in small CLL case series, and an extensive analysis has not previously been performed. However, this CA is known to be a clonal or subclonal driver alteration (6, 7). A minimal deleted region of 4.2 Mb at 8p21 includes the *TNFRSF10A/B* genes coding for apoptotic TRAIL receptors (1, 2, 8-12). The haploinsufficiency of *TNFRSF10A/B* that results from del8p might contribute to ibrutinib resistance (10).

By combining clinical data with *ex vivo* and *in vitro* molecular analyses, we evaluated this recurrent CA in the largest-yet series of CLL patients with del8p. We observed correlations between cytogenetic findings, clinical outcomes, and *in vivo* responses to drug treatment. Furthermore, we determined the spectrum of anti-CLL drug responses in primary cells with del8p. Lastly, the results of our complementary *in vitro* experiments on CRISPR/Cas9-edited cell lines underlined the relevance of the *TNFRSF10A* and *TNFRSF10B* genes in del8p-related drug resistance.

METHODS

Patients

CLL patients diagnosed and/or treated at Pitié-Salpêtrière Hospital (Paris, France) between 1992 and 2020 were screened for del8p using cytogenetic techniques (karyotyping (K) and/or fluorescence *in situ* hybridization (FISH) and/or a single nucleotide polymorphism array (SNPa)). We also compiled data on a control group of 155 CLL patients without del8p. The diagnosis of CLL was based on lymphocytosis and the immunophenotyping analysis, according to the International Workshop on CLL (13). Patients were routinely tested for *IGHV* status and *TP53* mutations. In line with the ethical tenets of the Declaration of Helsinki, all the patients provided their written, informed consent to participation in the study. The study was approved by the local institutional review board (AP-HP, Paris, France; reference: BPD2018DIA008).

Cytogenetic analyses

To obtain R-banded chromosomes, cells prepared from peripheral blood samples were stimulated with CpG-oligonucleotides and interleukin-2 (Amplitech, Compiegne, France) in culture for 72 hours, using standard techniques. A complex karyotype (CK) was defined as 3 or more CAs, and a highly

complex karyotype (HCK) as 5 or more CAs. The specific probes and procedures for standard FISH are detailed in the Supplemental Data. SNPa analyses were performed as described previously (14).

Samples, cell lines, and cell culture

Mononuclear cells were isolated from blood samples (provided by nine healthy donors) using Ficoll-Paque density gradient centrifugation, and CD19+ cells were sorted by magnetic separation with anti-CD19 microbeads (Miltenyi Biotech). Cryopreserved primary CLL cells and OSU-CLL cells were cultured in RPMI medium supplemented with 10% fetal bovine serum, 100 U/mL penicillin and 100 µg/mL streptomycin (15). The characteristics of samples from CLL patients are summarized in Supplementary Table S1.

Digital droplet PCR (ddPCR)

Levels of *TNFRSF10A*, *TNFRSF10B*, *TNFRSF10C* and *TNFRSF10D* mRNA expression were measured using a Bio-Rad ddPCR system, according to the manufacturer's instructions (Supplemental Data).

Generation of stable *TNFRSF10A* and/or *TNFRSF10B* knock-out (KO) cell lines

We generated an inducible Cas9-expressing OSU-CLL cell line (OSU-iCas9) by transduction with Lenti-iCas9-neo (a gift from Qin Yan, New Haven, USA (16); Addgene plasmid # 85400). Next, we designed CRISPR guides that targeted the first exon of the *TNFRSF10A* and *TNFRSF10B* genes. These guide RNAs were cloned into the Lenti-multi-Guide plasmid (Addgene_# 85401) (16) and transduced into OSU-iCas9 cells. Cells were induced with doxycycline and sorted according to their GFP expression. After expansion, single KO-cells were sorted using flow cytometry and anti-TNFRSF10A or anti-TNFRSF10B antibodies, cloned, expanded and screened. For functional studies, at least three different clones harboring loss-of-function mutations were chosen for each CRISPR-generated cell line (Supplemental Data).

***In vitro* cell death analysis**

To induce cell death, the OSU cell lines were treated with TRAIL (25 ng/mL for 24 h; Enzo Life Sciences). Alternatively, primary CLL cells were treated for 24 h with fludarabine (10 µM; Selleckchem, TX, USA), ibrutinib (10 µM; Selleckchem), venetoclax (1 nM; Selleckchem) or bendamustine (30 µM; MedChemExpress, NJ, USA), and $2x10^6$ cells were harvested to quantify the drug-induced expression of *TNFRSF10A/B* (using ddPCR, as described above). The remaining cells were treated for 6 h with 200 ng/mL TRAIL, and cell death was measured with flow cytometry (FACSCanto II; BD Biosciences) and annexin V/propidium iodide (PI) co-staining. Data were analyzed using FlowJo software (Tree Star, Ashland, OR, USA).

Statistical analysis

The median follow-up time was estimated using the reverse Kaplan-Meier method. OS, next-treatment-free survival (NTFS), and TTFT were estimated using the Kaplan-Meier method, and survival curves were compared in a log-rank test. The frequency of RT was estimated using the cumulative incidence method, and Gray's test was used to compare cumulative incidence curves. Potential risk factors for mortality in del8p patients were evaluated using univariate and multivariate Cox proportional hazards models. The chi-squared test or Fisher's exact test were used to compare categorical variables, and Mann-Whitney U test was used to compare continuous variables. All tests were two-sided, and the threshold for statistical significance was set to $p<0.05$. Statistical analyses were carried out using R software (version 4.0.3, R Foundation for Statistical Computing; URL https://www.R-project.org/) (Supplemental Data).

RESULTS

A total of 57 CLL patients with del8p (as evidenced by karyotyping, FISH and/or SNPa analyses) were included in the present study (Table 1 and Supplementary Table S1). Of the 55 patients for whom clinical data were available, 27 (49%) had not been treated before the detection of del8p, and the median time interval between diagnosis and detection of del8p was 3.7 years (range: 0-22.6).

Del8p is associated with cytogenetic factors linked to a poor prognosis (CK, HCK and del17p)

Forty-six of the 57 del8p CLL patients had been successfully karyotyped. The del8p was identified precisely by karyotyping and FISH in 37 of these 46 cases, including two cases with two different 8p aberrations in independent clones. Thirty-one (80%) of the 39 identified 8p aberrations were unbalanced translocations. A translocation t(8;8) or an isochromosome 8 involving the long arm of chromosome 8 (8q) and that resulted in both del8p and 8q gain was observed in 13 (33%) of the 39 cases. The other recurrent 8p translocation partners were chromosomes 2, 3, 13 and 17. The del8p was subclonal in 30 (61%) of the 49 cases (Supplementary Table S2) and was frequently found within a CK or an HCK (33 out of 46 (72%) and 20 out of 46 (44%), respectively) (Supplementary Figure S1); these frequencies were significantly higher than those in the non-del8p control CLL group (Table 1). Deletion 11q and del17p were significantly more frequent in the del8p group than in the non-del8p group (52% vs. 17%, $p<.001$; 36% vs. 10%, $p<.001$, respectively) (Table 1). Furthermore, in the treatment-naive patients, the frequencies of CKs, HCKs, del11q and del17p were significantly higher ($p<.001$) in del8p than in non-del8p CLL (Supplementary Table S3). Gains of 8q (including the *MYC* gene, and resulting (or not) from a t(8;8)) and gains of 2p were also significantly more frequent in the del8p patients (both treated and treatment-naive) than in the non-del8p patients (Table 1 and

Supplementary Table S3). Taken as a whole, these results indicate that the del8p is associated with high-risk cytogenetic aberrations, including CKs, HCKs and del17p.

Del8p involves the *TNFRSF10* genes in the majority of cases of CLL, and a large del8p and *TP53* disruption are associated with poor OS

By using SNPa (in seven cases) and FISH probes for several genes in 8p22, 8p21.3 and 8p11, we found that the *TNFRSF10A/B/C/D* genes in 8p21.3 had been lost in 51 (91%) of the 56 cases of del8p (Supplementary Table S3, Figure 1A). We classified the patients into four categories, depending on the size of the deletion: group 1, del 8p10-8pter (the whole short arm) (8 out of 56 (14%)); group 2, del 8p11-8pter (21 out of 56 (38%)); group 3, del 8p21-8pter (17 out of 56 (30%)); and group 4, other deletions (10 out of 56 (18%)). There were no significant differences between the four groups, except for the presence of more *TP53* disruptions in group 1 and a trend toward a higher frequency of *MYC* gain in group 3 (Supplementary Table S4, Supplementary Figure S1). The translocation t(8;8) had two different breakpoints on the 8p: one between *TNFRSF10* and *FGFR1* (n=8) and the other between *FGFR1* and the centromere of chromosome 8 (n=5) (Figure 1A).

We observed that OS was significantly shorter in the patients with a large deletion (i.e. one that included *FGFR1*: groups 1 and 2) than in patients with smaller deletions (groups 3 and 4). This was true when considering the time from the detection of the del8p (10-year OS: 11% in groups 1+2 vs. 52% in groups 3+4; p=.019) or the time from diagnosis (43% vs 79%, respectively; p=.012) (Figure 1B and Supplementary Figure S2). In a univariate analysis, other factors associated with poor OS were *TP53* disruption (deletion and/or mutation) and the number of CAs (Supplementary Table S5). In a multivariate analysis, *TP53* disruption was still significantly associated with a shorter OS (Supplementary Figure S3), and a large del8p (groups 1+2) tended be associated with shorter OS (albeit not significantly; p=0.06).

Del8p is associated with a shorter TTFT, shorter OS, and more frequent Richter transformation

We next compared the clinical outcomes in our del8p cohort vs. the control non-del8p CLL cohort (n=155). The two cohorts did not differ significantly with regard to age, sex ratio, Binet stage at diagnosis, or treatment before karyotyping. Unmutated *IGHV* status was significantly more frequent in del8p patients (35 out of 48 (73%) than in non-del8p patients (70 out of 151 (46%); p=.002) (Table 1). The median [95% confidence interval (CI)] follow-up time was 12.3 years [10.2-15.6] in del8p patients and 11.9 years [11.0-13.9] in non-del8p patients. The OS after detection of del8p was shorter than the OS after karyotyping in the non-del8p CLL group (10-year OS rate: 30% vs 82%, respectively; median OS time: 6.8 years vs. not reached, respectively; p<.0001) (Figure 2A). The difference was also significant when considering solely patients who were treatment-naive before

the detection of del8p or (for non-del8p patients) karyotyping (10-year OS rate: 33.0% vs. 85.9%, respectively; median OS time: 7.7 years vs. not reached, respectively; p<.0001) (Figure 2B). In treatment-naive patients, the TTFT was shorter in del8p patients than in non-del8p patients (median OS time: 0.25 years vs. 1.7 years, respectively; p=.007) (Figure 2C). Similar results were obtained when comparing del8p and non-del8p patients with regard to OS following diagnosis, which was shorter in del8p patients (10-year OS rate: 61% vs. 93% in non-del8p patients; median OS time: 12.7 years vs. not reached, respectively; p<.0001). The TTFT was also shorter in del8p patients than in non-del8p patients (median: 1.7 years vs. 3.3 years, respectively) (Supplementary Figure S4A, S4B). Lastly, the risk of progression to RT (calculated from the time of diagnosis onwards) was significantly higher in del8p patients than in non-del8p patients (cumulative incidence at 10 years: 22% vs. 5.5%, respectively; p=.034) (Figure 2D). The cumulative incidence of RT at 10 years (calculated from the time of del8p detection or first karyotyping onwards) was 18% in del8p patients and 7% in non-del8p patients (p=.18, Supplementary Figure S4C).

Del8p CLL patients (including those with mutated *IGHV*) treated with fludarabine-based regimens have worse NTFS and OS.

Our patients with del8p CLL received a median of two lines of treatment (range: 0-7): 35 of the 55 (64%) had been treated with fludarabine-based regimens (first-line treatments in 31 (89%) cases), 20 (36%) had been treated with ibrutinib (at relapse in 19 (95%) cases), and 5 (9%) had been treated with venetoclax (all at relapse) (Supplementary Figure S5). Among the fludarabine-treated patients, the NTFS and OS rates were significantly shorter in the del8p CLL group than in the non-del8p CLL group (10-year NTFS rate: 3.7% vs 21.5%, respectively; p=.002) (Figure 2E); 10-year OS rate: 45.9% vs. 81.6%, respectively; p<.001 (Figure 2G)). Interestingly, the negative effect of the del8p on NTFS after fludarabine treatment was only significant in the subgroup of CLL patients with mutated *IGHV* (hazard ratio [95%CI]: 2.85 [1.2-6.79]; p=.015) (Figure 2F). Among the ibrutinib-treated patients, there was no difference between del8p and non-del8p patients with regard to NTFS or OS; however, only one patient had received first-line treatment with ibrutinib (data not shown). The small numbers of venetoclax-treated patients in the del8p subgroup prevented us from assessing the response to this drug.

***TNFRSF10A* and *TNFRSF10B* are haploinsufficient in del8p CLL**

One copy of the *TNFRSF10A/B/C/D* genes had been deleted in 91% of the del8p patients. To determine whether these genes were haploinsufficient, we measured their mRNA expression levels in healthy and CLL primary B cells (Figure 3). In healthy B cells, *TNFRSF10A* and *TNFRSF10B* were both strongly expressed, with a slight predominance of *TNFRSF10A* (median ratio: 2.33) over *TNFRSF10B*

(median ratio: 1.72). In non-del8p CLL cells, the expression of *TNFRSF10A* was similar to that seen in normal B cells (median ratio: 2.73 vs 2.33, respectively; p=.54) but the expression level of *TNFRSF10B* was significantly higher (median ratio: 3.66 vs 1.72, respectively, i.e. a 2.13-fold relative increase; p<.001). Hence, *TNFRSF10B* was more strongly expressed than *TNFRSF10A* (median ratio: 3.66 vs 2.73, i.e. a 1.3-fold relative increase). The expression level of *TNFRSF10B* was significantly lower in del8p CLL cells than in non-del8p CLL cells (median ratio: 1.52 vs 3.66, respectively, i.e. a 2.41-fold relative decrease; p<.001), whereas the expression level of *TNFRSF10A* was only slightly lower (median ratio: 2.29 vs 2.73, respectively, p=.15). Compared with *TNFRSF10A/B*, the expression levels of *TNFRSF10C* and *TNFRSF10D* were negligible in normal B cells and were not significantly higher in non-del8p or del8p CLL cells (Supplementary Figure S6). No major non-del8p vs. del8p differences in *TNFRSF10A* or *TNFRSF10B* expression were observed when stratifying patients according to karyotype complexity, del13q, del11q, tri12, *TP53* disruption (deletion and/or mutation), and *IGHV* status (Supplementary Figure S7).

***TNFRSF10A* and *TNFRSF10B* are both functional in CLL**

To analyze the clinical relevance and functional consequences of the inactivation of *TNFRSF10A* and *TNFRSF10B*, we used CRISPR/Cas9 to selectively inactivate the two genes in the well-characterized OSU-CLL cell line (15, 17). The baseline *TNFRSF10A* and *TNFRSF10B* expression profiles in OSU-CLL cells were similar to those observed in primary CLL cells (Supplementary Figure S8). We generated three cell lines (OSU-CLL *TNFRSF10A*$^{-/-}$ (hereafter "OSU A-KO"), OSU-CLL *TNFRSF10B*$^{-/-}$ ("OSU B-KO") and OSU-CLL *TNFRSF10A*$^{-/-}$ and *TNFRSF10B*$^{-/-}$ ("OSU AB-KO")), together with the OSU empty vector control cell line. The three KO cell lines' deficient phenotype was confirmed by flow cytometry of a bulk suspension (Supplementary Figure S9), whereas Sanger sequencing of clones derived from these cell lines confirmed the presence of the frameshift (Supplementary Table S6).

To functionally confirm the absence of TNFRSF10A and TNFRSF10B receptors in our OSU KO models, we used flow cytometry to test the various CRISPR-edited cell lines' mortality following exposure to the cell-death-activating TNFRSF10A and TNFRSF10B ligand TRAIL. Relative to the control OSU empty vector cell line, OSU A-KO and B-KO cells were less sensitive to TRAIL treatment and OSU AB-KO cells were completely resistant (Figure 4)**.** These data indicate that both TNFRSF10A and TNFRSF10B receptors were able to induce cell death in CLL cells (i.e., TNFRSF10A was functional when TNFRSF10B was inactivated, and vice versa) but that no compensation or up-regulation occurred when either gene was lost. Moreover, we observed that the level of cell death was slightly but reproducibly higher in OSU A-KO cells than in OSU B-KO cells; this might have been related to the higher level of TNFRSF10B expression observed in this cell line.

TNFRSF10B is involved in fludarabine-induced cell death

We initially supposed that low expression of the TNFRSF10B receptor on the surface of del8p primary CLL cells (relative to non-del8p cells) leads to lower sensitivity to TRAIL and thus promotes cell survival. However, the preliminary data from the *in vitro* cytotoxicity assay performed with TRAIL and primary non-del8p CLL cells showed that TRAIL sensitivity was low (Supplementary Figure S10) and suggested that TRAIL alone cannot induce cell death in primary CLL cells. We therefore hypothesized that exposure of the cells to anti-CLL drugs modulates TNFRSF10A and/or TNFRSF10B receptor expression and increases sensitivity to TRAIL (18). Accordingly, we cultured primary CLL cells in the presence of fludarabine, ibrutinib, or venetoclax. In non-del8p cells, we did not observe any significant differences in *TNFRSF10A* expression after treatment with these anti-CLL drugs (Supplementary Figure S11). However, *TNFRSF10B* expression was significantly greater after exposure to fludarabine (by a factor of 2.8; median ratio: 6.36, vs. 2.31 in the absence of the drug) but not after exposure to ibrutinib or venetoclax (Figure 5A). In contrast, treatment with fludarabine, ibrutinib, or venetoclax was not associated with significantly greater levels of *TNFRSF10A* or *TNFRSF10B* expression in almost all del8p CLL samples (all of which had a deletion spanning the TNFRSF10 locus) (Figure 5B). Remarkably, the two del8p CLL samples showing slightly greater levels of *TNFRSF10B* mRNA expression after fludarabine treatment had the lowest proportion of 8p-deficient cells (less than 20%, according to FISH). The other del8p CLL samples (with a negligible enhancement in *TNFRSF10B* expression) contained more than 50% of del8p-bearing cells (Figure 5C, Supplementary Table S1). Taken as a whole, these data indicate that *TNFRSF10B* modulation is involved in fludarabine-induced cell death but not in ibrutinib- or venetoclax-induced cytotoxicity. In contrast, *TNFRSF10A* expression is not modulated by these anti-CLL drugs.

Del8p abrogates the synergy between fludarabine and the TRAIL pathway

In view of the results described above, we sequentially evaluated the cytotoxic effect of the TRAIL-fludarabine combination. Cells were treated with fludarabine for 24h and then with TRAIL for 6h). With the unmodified OSU-CLL cell line, the TRAIL-induced decrease in viability was higher for fludarabine-treated cells than for control cells (43.3% vs. 33.9%, respectively; Supplementary Figure S12). None of the primary cell samples from 15 patients with non-del8p CLL showed a significant (>10%) decrease in cell viability after treatment with TRAIL alone. In contrast, sequential treatment with fludarabine and then TRAIL resulted in a significant decrease in cell viability (Figure 5D). TRAIL had an additional cytotoxic effect in 13 of the 15 (87%) non-del8p samples. When we applied the same approach to seven CLL B samples from del8p CLL patients (Figure 5E), TRAIL treatment alone had no significant cytotoxic effect (i.e. as with non-del8p CLL cells). Sensitivity to fludarabine alone was also similar to that observed for non-del8p CLL cells. However, in contrast to the results for non-

del8p CLL cells, the sequential fludarabine + TRAIL regimen failed to elicit a synergistic cytotoxic effect in most del8p CLL cell samples. Thus, it appears that del8p abrogates the synergistic effect on cell viability induced by the fludarabine + TRAIL combination in CLL. In similar experiments on del8p and non-del8p CLL samples, the combination of TRAIL with the BTK or BCL2 inhibitors ibrutinib or venetoclax did not have a synergistic effect on cell death. We therefore conclude that in del8p CLL cells specifically, the lack of fludarabine-induced overexpression of TNFRSF10B abrogates the synergy between the purine analog and TRAIL.

del8p CLL cells do not show an fludarabine-induced increase in p53 target gene expression, regardless of their *TP53* status

We next looked for the link between fludarabine treatment and enhanced *TNFRSF10B* expression and hypothesized that it was p53 - a protein commonly activated by DNA-damaging cell death inducers like fludarabine (19). To check p53's activation after fludarabine treatment in our CLL cohorts, we measured the expression of three well-known p53 target genes: *MDM2*, *BAX* and *CDKN1A*. As shown in Figure 6, the exposure of non-del8p CLL cells to fludarabine induced significantly greater expression of all three genes: 12.5-fold (33.9, vs. 2.71 for control cells, p=0.007), 4.3-fold (14.3 vs. 3.34, p=0.007) and 8.7-fold (11.0 vs. 1.27, p=0.002) for *MDM2*, *BAX* and *CDKN1A,* respectively. In contrast, the fludarabine-induced expression of *MDM2*, *BAX* and *CDKN1A* was substantially lower in del8p CLL cells: 2.2-fold (3.98, vs. 1.82 for control cells, p=0.15), 1.0-fold (2.89 vs. 2.80, p=0.55) and 3.4-fold (1.65 vs. 0.49, p=0.22) for *MDM2*, *BAX* and *CDKN1A,* respectively (Figure 6A). Thus, del8p in CLL appeared to interfere with the p53-dependent gene expression induced by fludarabine.

To further corroborate the specific relationships between del8p and p53 activation in fludarabine-treated CLL cells, we analyzed *MDM2*, *BAX* and *CDKN1A* expression in del8p CLL cells harboring del17p or not. As shown in Figures 6B and 6C, our results indicated that irrespectively of the presence or the absence of del17p, fludarabine failed to modulate the expression of p53 targets in del8p CLL cells. Furthermore, the absence of p53 pathway activation in del8p cells treated with fludarabine was closely correlated with the lack of *TNFRSF10B* overexpression in both the presence and absence of del17p. Lastly, our results also showed that fludarabine did not enhance *TNFRSF10B* expression in non-del8p/del17p CLL cells (Supplementary Figure S13); this observation substantiated the direct link between fludarabine treatment, p53 pathway activation, and *TNFRSF10B* overexpression.

DISCUSSION

In a retrospective analysis of the largest yet reported series of CLL patients with del8p, we characterized the molecular features and clinical significance of this rare, insufficiently studied CA. We first found that del8p was overlooked in about 20% of our karyotypes. The most common CA leading to 8p deletion is an unbalanced translocation, such as t(8;8). Moreover, as mentioned above, our results showed that del8p can be clonal or subclonal (6, 7, 9).

Del8p is associated with conventional factors for a poor prognosis in CLL, such as del11q, *TP53* aberrations, unmutated *IGHV*, and CK/HCK. Although *MYC* gain is frequently found together with del8p (4, 8, 9), the corresponding patients in our cohort did not always have a poor outcome; hence, del8p is an independent oncogenic factor and does not solely represent collateral damage in t(8;8). We also showed that del8p CLL patients have a shorter TTFT and shorter OS than non-del8p CLL patients. Our results fully substantiate the reports on the poor prognosis associated with del8p in small CLL cohorts (1, 2, 4, 8). Strikingly, we found that large 8p deletions (i.e. those in our patient groups 1+2) were associated with a shorter OS in CLL. This association strongly suggests that the loss of several genes in the 8p region is required for a poor prognosis. Similar results have been published in studies of hepatocellular carcinoma, where the concomitant deletion of several tumor suppressor genes on 8p synergistically promoted tumor growth (20). A detailed analysis of our large del8p CLL cohort revealed that del8p is associated with a higher risk of RT. This finding is consistent with the high prevalence of del8p observed in this aggressive transformation of CLL (3).

Del8p CLL patients treated with fludarabine-based regimens had shorter NTFS and OS times than non-del8p CLL patients; this was even true for del8p CLL patients with *IGHV* mutations, who generally respond well to fludarabine regimens. This finding underlines the prognostic importance of this genetic aberration in CLL. In contrast to a previous study (10), we found that del8p and non-del8p CLL patients responded in a similar manner to ibrutinib.

Several groups have used chromosomal microarrays to identified a minimal region of loss in 8p; it includes the *TNFRSF10* genes at 8p21 (1, 2, 4, 8-10, 12). We confirmed this finding in our large cohort: the *TNFRSF10* genes were deleted in 91% of cases. The *TNFRSF10* genes encode four membrane-bound TRAIL receptors: two induce apoptosis (*TNFRSF10A* and *TNFRSF10B*) and the other two are decoy receptors (*TNFRSF10C* and *TNFRSF10D*) (21). The TRAIL pathway has been extensively characterized over the last 20 years. Its activation can lead to pro- or anti-apoptotic outcomes, depending on the type of stimulation and the cellular/microenvironmental context (21, 22). In our cohort, we found that both *TNFRSF10A* and *TNFRSF10B* are expressed in malignant CLL cells, with *TNFRSF10B* more strongly expressed than *TNFRSF10A*. In line with previous studies, our results also confirmed that *TNFRSF10B* is expressed more strongly in CLL cells than in normal B cells and that the expression of *TNFRSF10C*/*D* is negligible in both normal and CLL B cells (21). These findings prompted us to focus our mechanistic work on *TNFRSF10A/B*. To this end, we used CRISPR/Cas9 to knock out

the *TNFRSF10A/B* genes in the OSU-CLL cell line and found that the OSU-*TNFRSF10A* KO cell line was less resistant to TRAIL treatment than the OSU *TNFRSF10B* KO cell line. This is consistent with reports on other cancers and indicates that TNFRSF10B is more effective than TNFRSF10A in inducing death (23). However, our results challenge the report by MacFarlane *et al* (24) in which agonistic antibodies against TNFRSF10A (but not against TNFRSF10B) induce apoptosis in primary CLL cells. Although we cannot rule out a difference in TNFRSF10A/B triggering between primary cells and our edited cell lines or a difference in agonistic activity between the anti-TNFRSF10A antibody and the anti-TNFRSF10B antibody, our CRISPR/Cas9 cellular models usefully enabled us to directly investigate the effect of the physiological TNFRSF10 ligand TRAIL.

As expected, we showed that del8p is associated with low *TNFRSF10A/B* expression in primary CLL cells. Although several studies have designated *TNFRSF10A/B* as candidate genes in the minimal deleted region on 8p21, few have evidenced their low expression in primary CLL cells (10). In line with previous studies (21, 25, 26), we also found that TRAIL alone does not strongly induce the apoptosis of primary CLL cells *in vitro*. This low level of efficacy suggests that other contributors (such as natural killer cells) are needed to activate this death pathway (27).

Our results endorse previous reports in which (i) chemotherapy (including fludarabine treatment) produced an increase in *TNFRSF10A/B* mRNA expression in primary CLL cells and (ii) treatment with a combination of fludarabine and TRAIL resulted in a synergistic apoptotic response (18). In our hands, fludarabine exposure specifically increased *TNFRSF10B* expression but did not change *TNFRSF10A* expression. Moreover, enhanced *TNFRSF10B* expression was accompanied by greater induction of apoptosis by the fludarabine-TRAIL combination. We found similar results with this combination in the OSU-CLL cell line. The known mechanisms of TRAIL resistance include downregulation of agonistic receptors, mutations within critical domains, expression of antagonistic receptors, and deregulation of downstream effectors (28). The present study is the first to have demonstrated that del8p in CLL prevents the increase in expression of the TNRSF10B receptor and thus abrogates the apoptogenic synergy between fludarabine and TRAIL. These *in vitro* results are in line with our *in vivo* data showing that del8p CLL patients treated with fludarabine-based regimens have shorter NTFS and OS times.

Del8p is often associated with del17p, which involves *TP53*. Our present results showed that fludarabine-induced *TNFRSF10A/B* expression is lower in *TP53*-disrupted CLL cells (i.e. del17p) than in non-*TP53* disrupted CLL cells. However, del8p *per se* was sufficient to abrogate the fludarabine-induced expression of p53 target genes (represented here by *MDM2*, *BAX*, and *CDKN1A*) and the synergistic effect of fludarabine and TRAIL. It is not clear why these p53 target genes are less strongly expressed, and specific research is warranted. Nevertheless, our new data indicate clearly that *TP53*

dysfunction and del8p are independent but critical genetic events in the regulation of *TNFRSF10* gene expression in CLL.

In contrast to fludarabine treatment, we found that ibrutinib or venetoclax treatment were not synergistic with TRAIL. This contrasts with Burger et al.'s suggestion whereby haploinsufficiency of *TNFRSF10* (as a consequence of del8p) might result in TRAIL insensitivity and might contribute to ibrutinib resistance (10). Assuming that the concentration of TRAIL is higher in blood than in lymph nodes (29), Burger et al. suggested that the ibrutinib-induced migration of CLL cell from lymph nodes to the blood might be a significant component in ibrutinib-induced cell death in CLL and would be lost in the event of del8p. Since this hypothesis does not involve any ibrutinib-related intracellular pathways, we could not test it in our *in vitro* model. However, we did not observe any *in vivo* influence of ibrutinib treatment on NTFS and OS when comparing non-del8p and del8p CLL patients.

In conclusion, our analysis of a large cohort of del8p CLL cases and the *in vitro* study of molecular mechanisms associated with del8p showed that this rare but recurrent CA is associated with other factors linked to a poor prognosis, such as a CK, an HCK, del11q, *TP53* aberrations, unmutated *IGHV* status, short TTFT and OS, and RT. We also demonstrated that TNFRSF10B has an important role in fludarabine resistance in del8p CLL. In patients who could benefit from the classical Fludarabine-cyclophosphamide-rituximab treatment but who harbor del8p, other treatments (such as ibrutinib and venetoclax) might be more effective than fludarabine.

Acknowledgments

The present research was funded by Roche Diagnostics, Force Hemato (grant reference: 03-2022), French Innovative Leukemia Organization (FILO) group, and SIRIC-CURAMUS (Cancer United research Associating Medecine, University and Society; grant reference: INCA-DGOS-INSERM_12560). L.J. and L.D. received PhD fellowships from Fondation ARC and SIRIC-CURAMUS, respectively. L. K. L. received a postdoctoral fellowship from Fondation de France. L.S. was funded by the FILO group and the SIRIC-CURAMUS. The funders had no role in study design, data collection and analysis, decision to publish, or preparation of the manuscript.

Author Contributions

F.N-K. and S.A.S designed the study. L.J. and E.C. performed experiments and analyzed data. L.D., C.D., L.S., B.G., F.D., L.K.L., D.G., C.B. performed experiments. O.T. and D.R-W. provided samples and clinical data. M.B. performed statistical analyses. F.N-K., S.A.S., E.C. and L.J. wrote the manuscript.

Competing Interests

The authors declare no competing financial interests.

References

1. Brown JR, Hanna M, Tesar B, Werner L, Pochet N, Asara JM, et al. Integrative genomic analysis implicates gain of PIK3CA at 3q26 and MYC at 8q24 in chronic lymphocytic leukemia. Clinical cancer research : an official journal of the American Association for Cancer Research. 2012;18(14):3791-802. Epub 2012/05/25.
2. Forconi F, Rinaldi A, Kwee I, Sozzi E, Raspadori D, Rancoita PM, et al. Genome-wide DNA analysis identifies recurrent imbalances predicting outcome in chronic lymphocytic leukaemia with 17p deletion. British journal of haematology. 2008;143(4):532-6.
3. Bea S, Lopez-Guillermo A, Ribas M, Puig X, Pinyol M, Carrio A, et al. Genetic imbalances in progressed B-cell chronic lymphocytic leukemia and transformed large-cell lymphoma (Richter's syndrome). Am J Pathol. 2002;161(3):957-68.
4. Houldsworth J, Guttapalli A, Thodima V, Yan XJ, Mendiratta G, Zielonka T, et al. Genomic imbalance defines three prognostic groups for risk stratification of patients with chronic lymphocytic leukemia. Leukemia & lymphoma. 2014;55(4):920-8. Epub 2013/09/21.
5. Leeksma AC, Baliakas P, Moysiadis T, Puiggros A, Plevova K, Van der Kevie-Kersemaekers AM, et al. Genomic arrays identify high-risk chronic lymphocytic leukemia with genomic complexity: a multi-center study. Haematologica. 2021;106:87-97.
6. Landau DA, Carter SL, Stojanov P, McKenna A, Stevenson K, Lawrence MS, et al. Evolution and impact of subclonal mutations in chronic lymphocytic leukemia. Cell. 2013;152(4):714-26. Epub 2013/02/19.
7. Landau DA, Tausch E, Taylor-Weiner AN, Stewart C, Reiter JG, Bahlo J, et al. Mutations driving CLL and their evolution in progression and relapse. Nature. 2015;526(7574):525-30. Epub 2015/10/16.
8. Rinaldi A, Mian M, Kwee I, Rossi D, Deambrogi C, Mensah AA, et al. Genome-wide DNA profiling better defines the prognosis of chronic lymphocytic leukaemia. British journal of haematology. 2011;154(5):590-9.
9. Blanco G, Puiggros A, Baliakas P, Athanasiadou A, Garcia-Malo M, Collado R, et al. Karyotypic complexity rather than chromosome 8 abnormalities aggravates the outcome of chronic lymphocytic leukemia patients with TP53 aberrations. Oncotarget. 2016;7(49):80916-24. Epub 2016/11/09.
10. Burger JA, Landau DA, Taylor-Weiner A, Bozic I, Zhang H, Sarosiek K, et al. Clonal evolution in patients with chronic lymphocytic leukaemia developing resistance to BTK inhibition. Nature communications. 2016;7:11589. Epub 2016/05/21.
11. Leeksma AC, Baliakas P, Moysiadis T, Puiggros A, Plevova K, Van der Kevie-Kersemaekers AM, et al. Genomic arrays identify high-risk chronic lymphocytic leukemia with genomic complexity: a multi-center study. Haematologica. 2021;106(1):87-97. Epub 2020/01/25.
12. Rubio-Moscardo F, Blesa D, Mestre C, Siebert R, Balasas T, Benito A, et al. Characterization of 8p21.3 chromosomal deletions in B-cell lymphoma: TRAIL-R1 and TRAIL-R2 as candidate dosage-dependent tumor suppressor genes. Blood. 2005;106(9):3214-22. Epub 2005/07/30.
13. Hallek M, Cheson BD, Catovsky D, Caligaris-Cappio F, Dighiero G, Dohner H, et al. iwCLL guidelines for diagnosis, indications for treatment, response assessment, and supportive management of CLL. Blood. 2018;131(25):2745-60. Epub 2018/03/16.
14. Cosson A, Chapiro E, Belhouachi N, Cung H-A, Keren B, Damm F, et al. 14q deletions are associated with trisomy 12, NOTCH1 mutations and unmutated IGHV genes in chronic lymphocytic leukemia and small lymphocytic lymphoma. Genes, chromosomes & cancer. 2014;53(8):657-66.
15. Hertlein E, Beckwith KA, Lozanski G, Chen TL, Towns WH, Johnson AJ, et al. Characterization of a new chronic lymphocytic leukemia cell line for mechanistic in vitro and in vivo studies relevant to disease. PloS one. 2013;8(10):e76607. Epub 2013/10/17.
16. Cao J, Wu L, Zhang SM, Lu M, Cheung WK, Cai W, et al. An easy and efficient inducible CRISPR/Cas9 platform with improved specificity for multiple gene targeting. Nucleic acids research. 2016;44(19):e149. Epub 2016/11/02.

17. Boudny M, Zemanova J, Khirsariya P, Borsky M, Verner J, Cerna J, et al. Novel CHK1 inhibitor MU380 exhibits significant single-agent activity in TP53-mutated chronic lymphocytic leukemia cells. Haematologica. 2019;104(12):2443-55. Epub 2019/04/13.
18. Johnston JB, Kabore AF, Strutinsky J, Hu X, Paul JT, Kropp DM, et al. Role of the TRAIL/APO2-L death receptors in chlorambucil- and fludarabine-induced apoptosis in chronic lymphocytic leukemia. Oncogene. 2003;22(51):8356-69. Epub 2003/11/14.
19. Rosenwald A, Chuang EY, Davis RE, Wiestner A, Alizadeh AA, Arthur DC, et al. Fludarabine treatment of patients with chronic lymphocytic leukemia induces a p53-dependent gene expression response. Blood. 2004;104(5):1428-34. Epub 2004/05/13.
20. Xue W, Kitzing T, Roessler S, Zuber J, Krasnitz A, Schultz N, et al. A cluster of cooperating tumor-suppressor gene candidates in chromosomal deletions. Proceedings of the National Academy of Sciences of the United States of America. 2012;109(21):8212-7. Epub 2012/05/09.
21. Secchiero P, Tiribelli M, Barbarotto E, Celeghini C, Michelutti A, Masolini P, et al. Aberrant expression of TRAIL in B chronic lymphocytic leukemia (B-CLL) cells. Journal of cellular physiology. 2005;205(2):246-52. Epub 2005/05/12.
22. MacFarlane M. TRAIL-induced signalling and apoptosis. Toxicology letters. 2003;139(2-3):89-97. Epub 2003/03/12.
23. Kelley RF, Totpal K, Lindstrom SH, Mathieu M, Billeci K, Deforge L, et al. Receptor-selective mutants of apoptosis-inducing ligand 2/tumor necrosis factor-related apoptosis-inducing ligand reveal a greater contribution of death receptor (DR) 5 than DR4 to apoptosis signaling. The Journal of biological chemistry. 2005;280(3):2205-12. Epub 2004/11/03.
24. MacFarlane M, Inoue S, Kohlhaas SL, Majid A, Harper N, Kennedy DB, et al. Chronic lymphocytic leukemic cells exhibit apoptotic signaling via TRAIL-R1. Cell death and differentiation. 2005;12(7):773-82. Epub 2005/04/30.
25. Irmler M, Thome M, Hahne M, Schneider P, Hofmann K, Steiner V, et al. Inhibition of death receptor signals by cellular FLIP. Nature. 1997;388(6638):190-5. Epub 1997/07/10.
26. Olsson A, Diaz T, Aguilar-Santelises M, Osterborg A, Celsing F, Jondal M, et al. Sensitization to TRAIL-induced apoptosis and modulation of FLICE-inhibitory protein in B chronic lymphocytic leukemia by actinomycin D. Leukemia. 2001;15(12):1868-77. Epub 2001/12/26.
27. Kaufmann SH, Steensma DP. On the TRAIL of a new therapy for leukemia. Leukemia. 2005;19(12):2195-202. Epub 2005/10/15.
28. Droin N, Guery L, Benikhlef N, Solary E. Targeting apoptosis proteins in hematological malignancies. Cancer letters. 2013;332(2):325-34. Epub 2011/07/20.
29. Herbeuval JP, Nilsson J, Boasso A, Hardy AW, Vaccari M, Cecchinato V, et al. HAART reduces death ligand but not death receptors in lymphoid tissue of HIV-infected patients and simian immunodeficiency virus-infected macaques. Aids. 2009;23(1):35-40. Epub 2008/12/04.

Table 1. Characteristics of the del8p group and the control non-del8p group.

Variable	Del8p N=57	Non-del8p N=155	P-value
Sex (female)	24/57 (42%)	61/155 (39%)	*.84*
Age at diagnosis, years, median (range)	59 (31-86)	60 (25-94)	*.91*
Binet stage at diagnosis			*.10*
A	26/36 (72%)	97/115 (84%)	
B	8/36 (22%)	17/115 (15%)	
C	2/36 (6%)	1/115 (1%)	
Treated	48/55 (87%)	138/155 (89%)	*.92*
Number of lines of treatment, median (range)	2 (0-7)	2.0 (0-9)	*.31*
Not treated before the detection of del8p or the first karyotyping	27/55 (49%)	124/155 (80%)	***<.001***
Time between diagnosis and the detection of del8p or the first karyotyping, years, median (range)	3.7 (0-22.6)	0.8 (0-29.6)	*.11*
CK (≥3 CAs)	33/46 (72%)	34/155 (22%)	***<.001***
HCK (≥5 CAs)	20/46 (44%)	12/155 (8%)	***<.001***
Number of CAs detected by karyotyping, median (range)	4 (1-14)	1 (0-8)	***<.001***
Classical CAs detected by FISH			
del13q	32/54 (59%)	97/155 (63%)	*.79*
tri12	4/53 (8%)	34/154 (22%)	*.03*
del11q	27/52 (52%)	27/155 (17%)	***<.001***
del17p	20/55 (36%)	16/154 (10%)	***<.001***
8q24 (*MYC*) gain	25/57 (44%)	6/155 (4%)	***<.001***
2p gain	14/56 (25%)	6/155 (4%)	***<.001***
unmutated *IGHV*	35/48 (73%)	70/151 (46%)	***.002***
***TP53* mutation**	15/40 (38%)	17/92 (19%)	***.03***
***TP53* disruption (deletion and/or mutation)**	22/47 (74%)	25/97 (26%)	***.02***

The results were calculated with all the available data for each variable (i.e. N varies from one variable to another). The p-values were obtained from comparisons of the two cohorts using a chi-squared test, Fisher's exact, or the Mann-Whitney test. CK: complex karyotype; HCK: highly complex karyotype, CA: chromosomal abnormality.

Figure legends

Figure 1. Constitution of four groups of patients as a function of the size of del8p, with intergroup differences in survival. **A**. Schematic representation of the chromosome 8 abnormalities identified in 56 of the 57 del8p patients using FISH and/or SNPa; for one patient (CLL_69), FISH was not informative and SNPa was not performed. Black lines correspond to the deleted regions, and red circles correspond to the *MYC* gains in each individual del8p patient. The patients were divided in four groups, according to the size of the del8p. *MYC gain due to t(8;8). [1] Two clones with del8p of different sizes. **B**. Overall survival in the del8p groups (1 + 2 vs. 3 + 4), starting from when the del8p was first detected.

Figure 2. Survival of del8p vs. non-del8p patients. **A**. OS; **B**. OS in treatment-naive patients; **C**. TTFT; **D**. Cumulative incidence of RT (**A**, **B**, **C**: calculated from the date of del8p detection or (for the non-del8p cohort) the first karyotyping, **D**: calculated from the date of CLL diagnosis). **E.** NTFS after treatment with fludarabine-based regimens in the whole cohort. **F.** NTFS after treatment with fludarabine-based regimens in *IGHV*-mutated patients. **G.** OS after treatment with fludarabine-based regimens.

Figure 3. *TNFRSF10B* is overexpressed in non-del8p CLL cells. mRNA was purified from B cells from healthy donors (n=9), from non-del8p CLL cells (n=33) or del8p CLL cells (n=9). The mRNA expression levels were determined using digital droplet PCR. *ABL1* mRNA expression was used to normalize the *TNFRSF10* data. The box corresponds to the interquartile range, the central line corresponds to the median, and the whiskers correspond to the range. Values were compared in a Mann-Whitney U test. ***, $P < .001$.

Figure 4. Inactivation of *TNFRSF10A* and *TNFRSF10B* induces resistance to TRAIL in the OSU-CLL cell line. The effects of *TNFRSF10A* and/or *TNFRSF10B* inactivation on TRAIL-mediated programmed cell death (25 ng/mL for 6 h) were studied in the OSU-CLL cell line transduced with empty vector (EV) or edited using CRISPR/Cas9 (as described in the Material and Methods section) to target *TNFRSF10A* and/or *TNFRSF10B* (A-KO; B-KO; AB-KO cells). Cell death was measured using co-positive annexin-V/PI staining and expressed as the mean ± SD (n=6). *, $P < .05$; **, $P < .01$.

Figure 5. Fludarabine treatment induces *TNFRSF10B* expression in primary non-del8p CLL cells but del8p specifically abrogates the decrease in cell viability induced by the fludarabine-TRAIL combination. (**A**) Primary non-del8p CLL cells were treated (or not) with 10 µM fludarabine (n=13), 10 µM ibrutinib (n=6) or 1 nM venetoclax (n=3). mRNA was purified 24 h after treatment, and *TNFRSF10B* expression (relative to control non-treated cells; n=14) was measured by ddPCR. *ABL1* mRNA expression was used to normalize the *TNFRSF10B* data. Cells treated with fludarabine showed significantly greater *TNFRSF10B* expression than untreated control cells. (**B**) Primary del8p CLL cells were treated (or not) with 10 µM fludarabine (n=7), 10 µM ibrutinib (n=4), or 1 nM venetoclax (n=6). mRNA was purified as in (**A**), and *TNFRSF10B* expression (relative to non-treated cells; n=7) was measured using ddPCR. *ABL1* mRNA expression was used to normalize the *TNFRSF10B* data. The box corresponds to the interquartile range, the central line corresponds to the median, and the whiskers correspond to the range. Significantly greater *TNFRSF10B* expression was never observed. Values

were compared in a Mann-Whitney U test. ***, P < .001. (**C**) Representation of the correlation between the percentage of cells with 8p deletion (measured using FISH) in primary CLL samples and the decrease in fludarabine-induced TNFRSF10B mRNA expression (P = 0.0068). Primary non-del8p (**D**) or del8p (**E**) CLL cells purified from various patients were treated (or not) with 10 µM fludarabine, 10 µM ibrutinib, or 1 nM venetoclax for 24 h and then cultured in the presence (200 ng/mL) or absence of TRAIL for 6h. The graphs show the cell viability (the percentage of viable cells, with co-negative annexin-V/PI staining) measured using flow cytometry. A cell viability decrease ≥ 10% in cells treated with TRAIL vs. cells not exposed to TRAIL was considered to be significant and is represented with a red line. Upon, treatment with fludarabine + TRAIL, we observed a significant decrease in viability in non-del8p CLL cells but not in del8p CLL cells. In similar experiments with ibrutinib and venetoclax, no significant non-del8p vs. del8p differences were observed.

Figure 6. Del8p abolishes fludarabine-induced p53-dependent gene expression. We studied the expression of three p53 target genes in primary CLL cells treated (or not) with fludarabine. (**A**) Primary non-del8p CLL cells (n=7, triangles) and del8p CLL cells (n=6, squares) were treated with fludarabine for 24h. mRNA expression of the *MDM2*, *BAX* and *CDKN1A* genes was measured using ddPCR. *ABL1* mRNA expression was used to normalize the data. B-cells with del17p are shown in orange, and those without are shown in purple. It is noteworthy that the fludarabine-induced expression of the three genes was lower in del8p samples than in non-del8p samples. The fludarabine-induced gene expression ratio (normalized against data from untreated cells, for each sample) was correlated with the percentage of cells harboring del17p (**B**) and del8p (**C**). The box corresponds to the interquartile range, the central line corresponds to the median, and the whiskers correspond to the range.

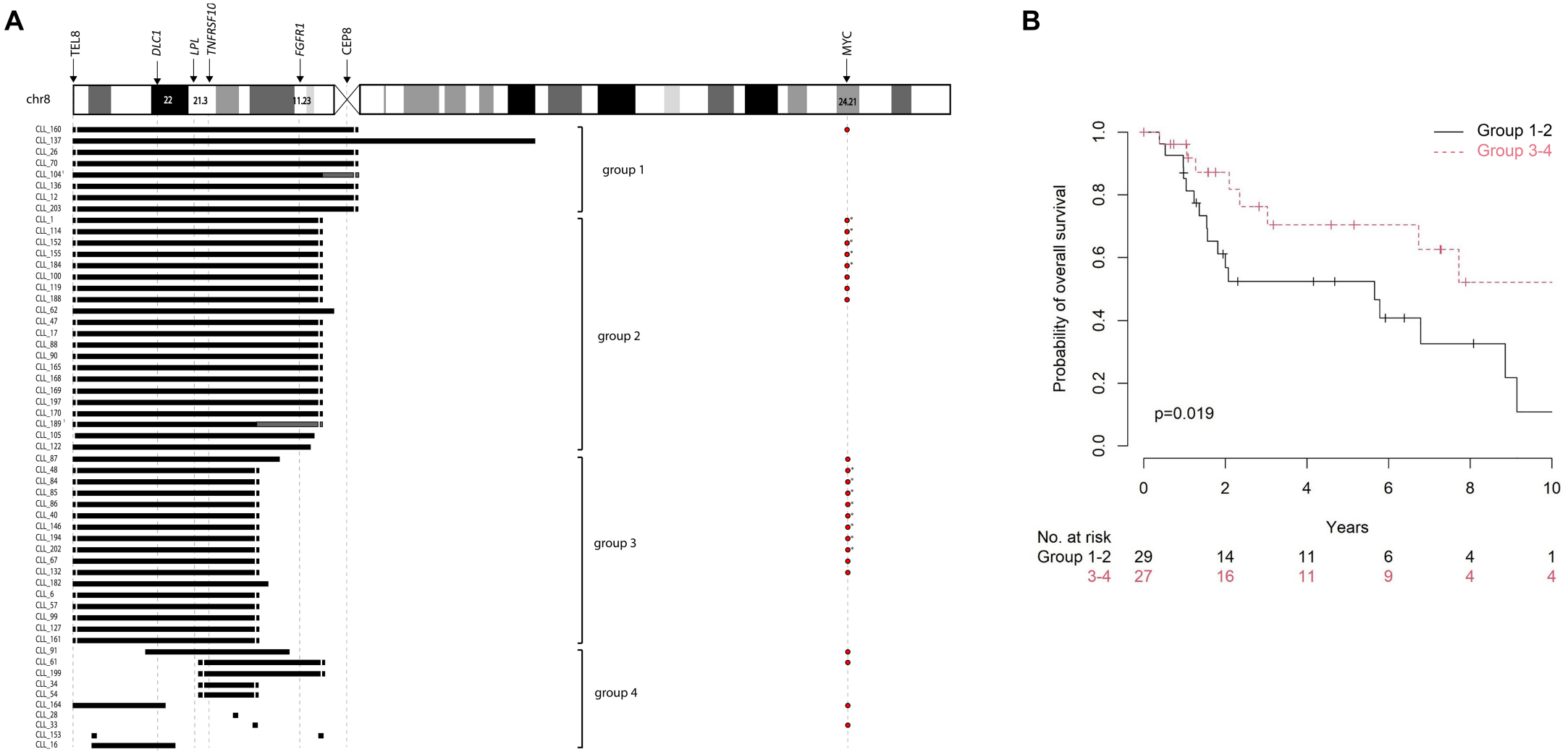

Figure 1. Delineation of the 8p deletions identifies 4 groups that have distinct impact on survival.

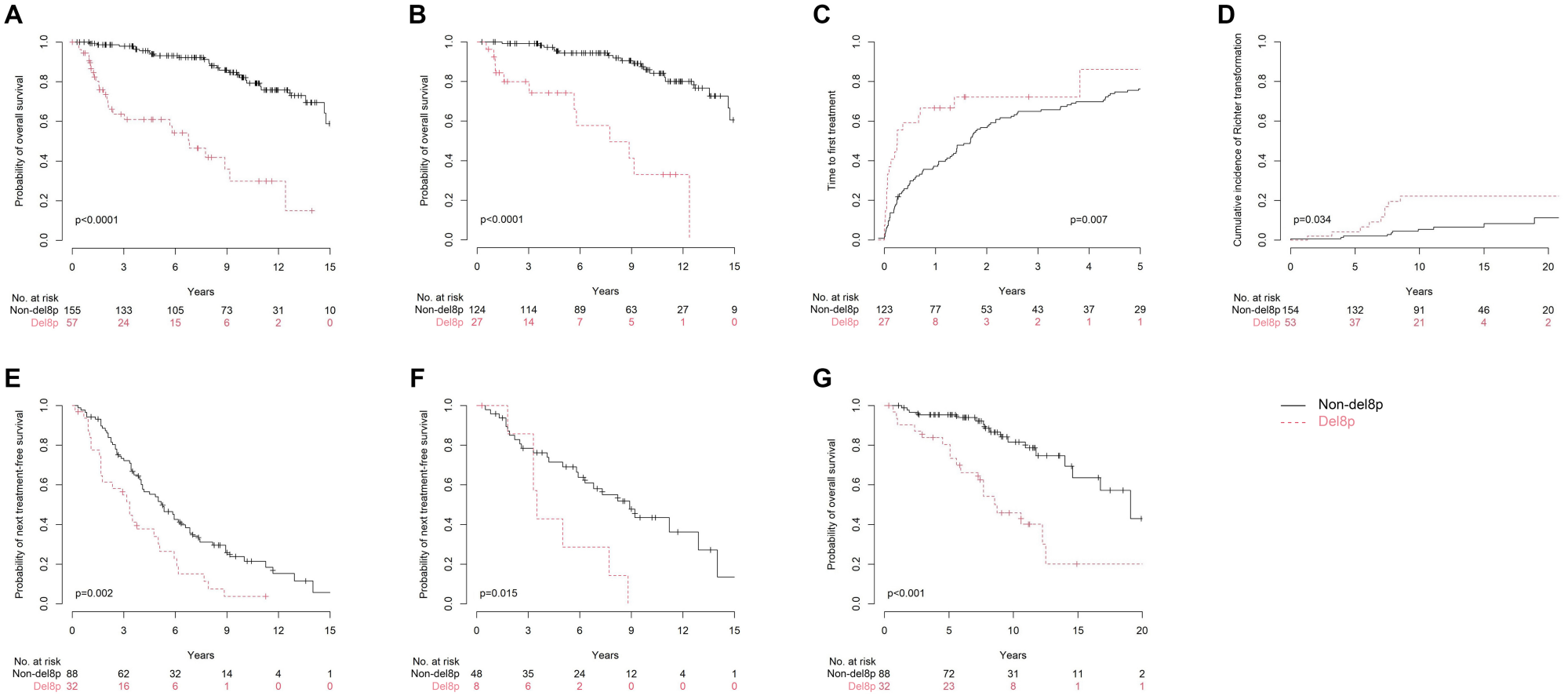

Figure 2. Survival analyses comparing del8p and non-del8p patients.

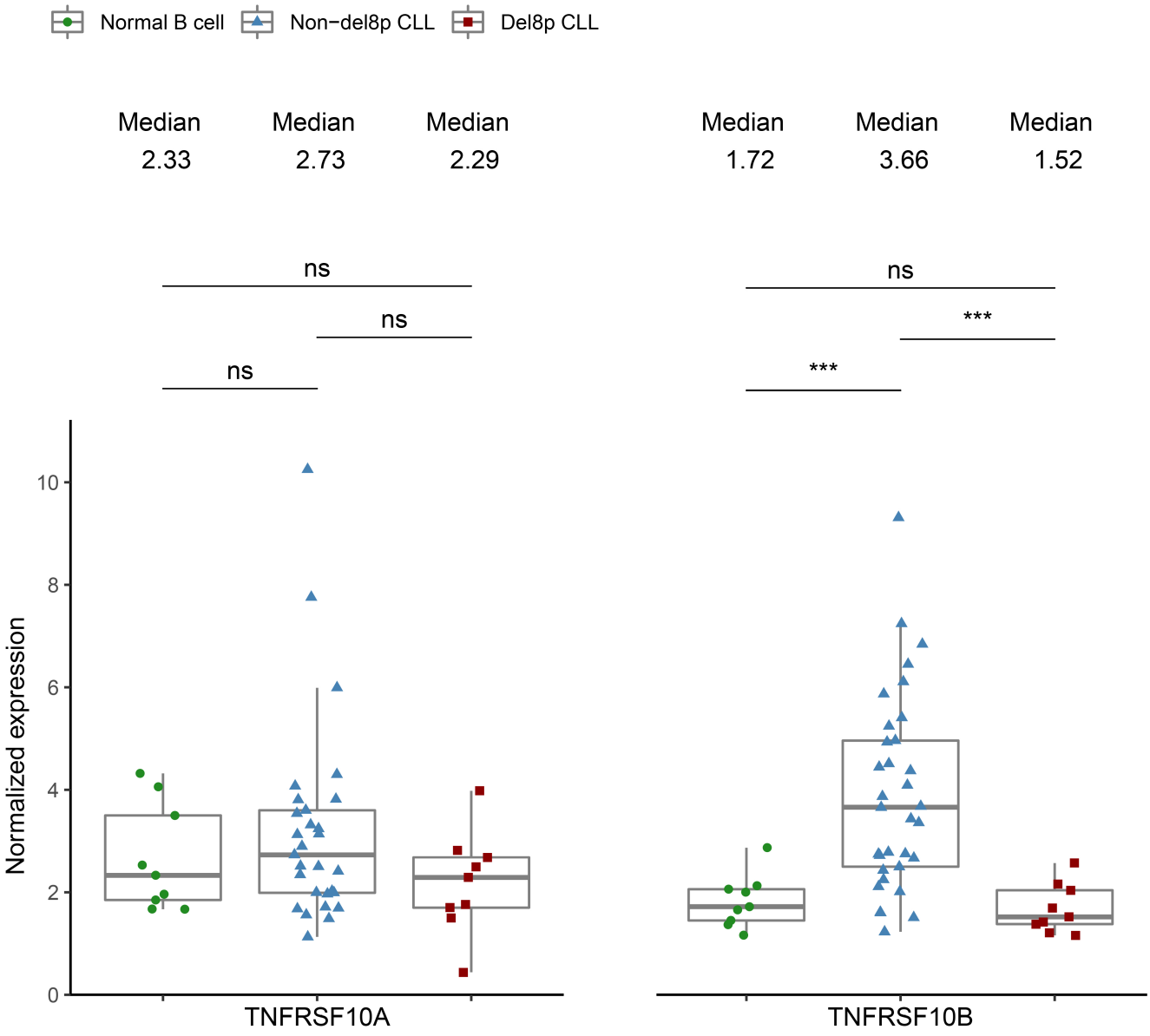

Figure 3. *TNFRSF10B* is overexpressed in non-del8p CLL cells.

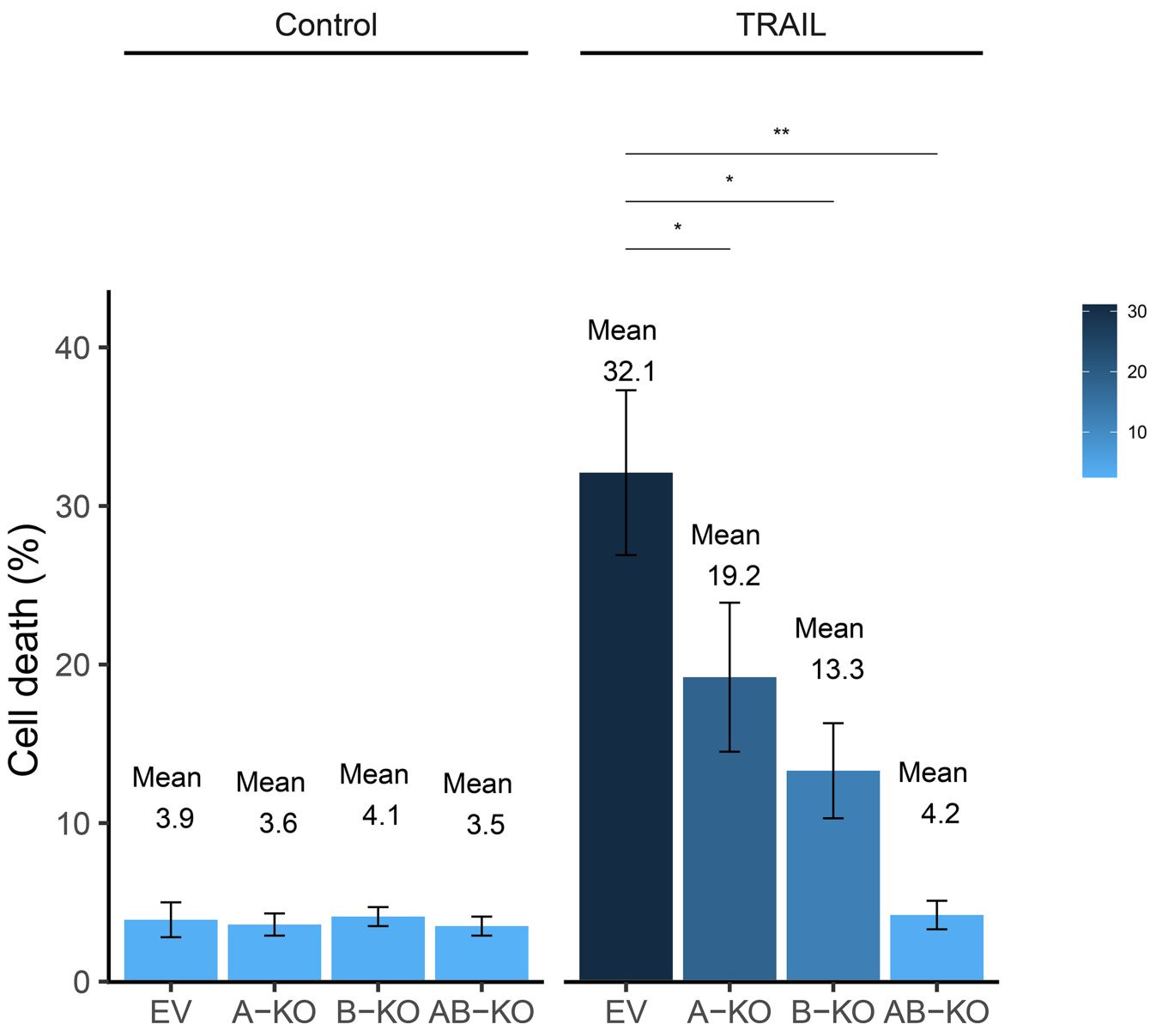

Figure 4. Inactivation of *TNFRSF10A* and *TNFRSF10B* induces resistance to TRAIL in the OSU-CLL cell line.

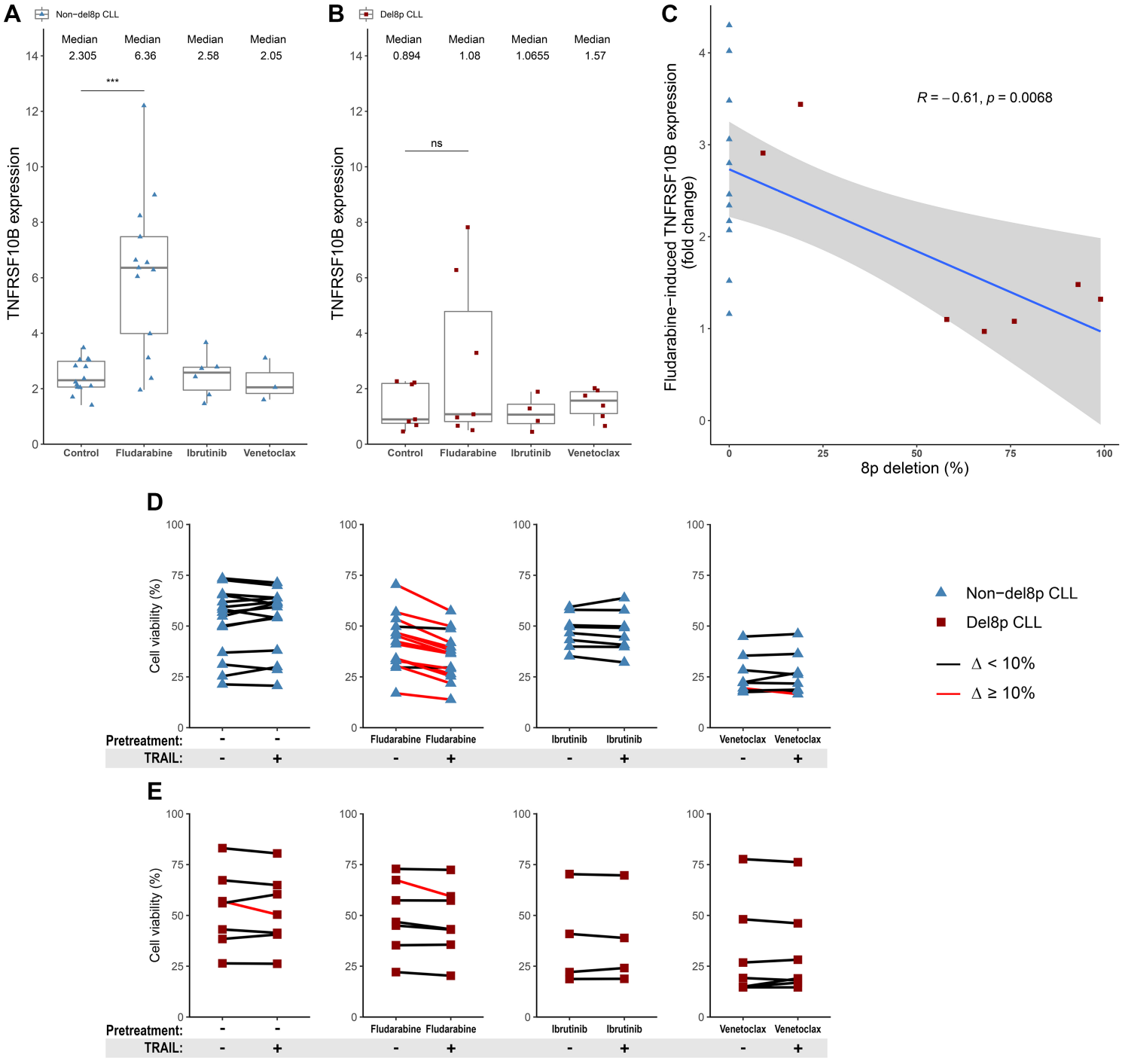

Figure 5. Fludarabine treatment induces *TNFRSF10B* expression in primary non-del8p CLL cells, but del8p specifically abrogates the cell viability loss induced by the combination fludarabine and TRAIL.

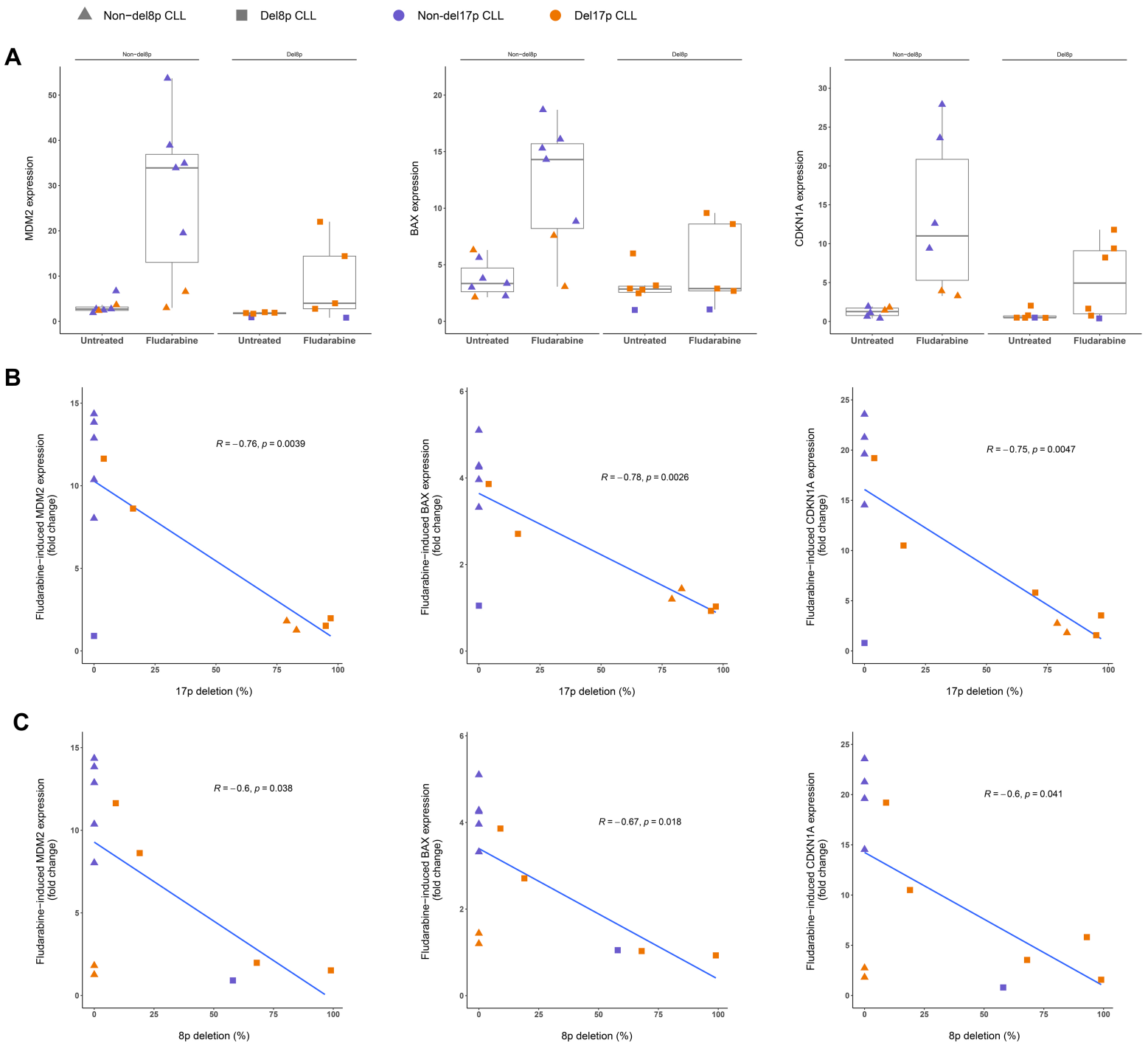

Figure 6. Del8p abolish fludarabine-induced p53-dependent gene expression. Expression of three p53-target genes in primary CLL cells treated or not with fludarabine.

SUPPLEMENTARY INFORMATION

Del8p and TNFRSF10B loss are associated with a poor prognosis and drug resistance in chronic lymphocytic leukemia

Ludovic Jondreville[1], Lea Deghane[1], Cecile Doualle[1], Luce Smagghe[1], Béatrice Grange[2], Frederic Davi[1,2], Leticia Koch Lerner[1], Delphine Garnier[1], Clotilde Bravetti[1,2], Olivier Tournilhac[3], Damien Roos-Weil[1,4], Marouane Boubaya[5], Elise Chapiro[1,2]*, Santos A Susin[1]*, Florence Nguyen-Khac[1,2]*

[1] Drug Resistance in Hematological Malignancies, Centre de Recherche des Cordeliers, UMRS 1138, INSERM, Sorbonne Université, Université Paris Cité, F-75006 Paris, France
[2] Service d'Hématologie Biologique, Hôpital Pitié-Salpêtrière, AP-HP, Paris, France
[3] Service d'Hématologie Clinique, CHU Estaing, 1 place Lucie et Raymond Aubrac, 63003 Clermont-Ferrand
[4] Service d'Hématologie Clinique, Hôpital Pitié-Salpêtrière, AP-HP, Paris, France
[5] Unité de Recherche Clinique, Hôpitaux Universitaires Paris Seine-Saint-Denis, AP-HP, Bobigny, France

Content

Figure S5. Time course of diagnosis and treatment for 55 patients with del8p CLL.

Figure S6. Expression of *TNFRSF10C* and *TNFRSF10D* genes in normal and CLL B-cells.

Figure S7. Expression of *TNFRSF10A* and *TNFRSF10B* genes, as a function of the presence of conventional cytogenetic and molecular risk factors in CLL.

Figure S8. Expression of *TNFRSF10A/B/C/D* genes in the OSU-CLL cell line.

Figure S9. Expression of TNFRSF10A and TNFRSF10B (measured by flow cytometry) in OSU-CLL cells.

Figure S10. TRAIL fails to induce cell viability loss in non-del8p primary CLL cells.

Figure S11. *TNFRSF10A* expression was not modulated in primary CLL cells by treatment with fludarabine, ibrutinib or venetoclax.

Figure S12. Fludarabine treatment potentiates TRAIL-induced cell death in the wild-type OSU-CLL cell line.

Figure S13. Del8p abolishes fludarabine-induced increase in *TNFRSF10B* expression in CLL cells, independently of del17p status.

A- Supplementary methods

FISH

Standard FISH was performed on interphase nuclei and metaphases using the commercial probes LPL (8p21) (Abbott Molecular, Des Plaines, IL), FGFR1 (8p11) (MetaSystems Probes, Altlussheim, Germany), CEP8 (MetaSystems), MYC (8q24) (ZytoVision GmbH, Bremerhaven, Germany), MYCN (2p24) (MetaSystems), D13S319,CEP12,ATM,TP53 (MetaSystems), TelVysion 8p (Abbott Molecular, Des Plaines, IL), and in-house bacterial artificial chromosome probes for the *TNFRSF10A/B* (8p21) (RP11-892A7+RP11-692J4), *DLC1* (8p22) (RP11-634E9 + RP11-1142J1), *REL* (2p16) (RP11-373L24) and *XPO1* (2p15) (RP11-240F4+RP11-477N2) genes. Probes were selected using the University of California Santa Cruz Genome Browser (http://www.genome.ucsc.edu/ NCBI37/hg19 build) and obtained from Genoscope (Evry, France). Extraction, labeling, and hybridization procedures were performed as described previously(1).

RNA extraction and droplet digital PCR (ddPCR)

Cells were thawed, and total RNA was extracted using a NucleoSpin RNA kit (Macherey-Nagel, Düren, Germany) or an AllPrep DNA/RNA Mini Kit (Qiagen, Hilden, Germany). Second-strand cDNA synthesis was performed using SuperScript IV reverse transcriptase (Invitrogen). ddPCR was performed using Supermix for probes (No dUTP) (Bio-Rad Laboratories) and probes (Applied Biosystems) against TNFRSF10A (Hs00269492_m1; exon boundary 2-3), TNFRSF10B (Hs00366278_m1; exon boundary 8-9 variant 1, 9-10 variant 2), TNFRSF10C (Hs00182570_m1) and TNFRSF10D (Hs00388742_m1) genes, all labelled with FAM dye. The housekeeping gene *ABL1* was used as the reference, and the corresponding VIC dye-labelled probe (Hs01104728_m1) was added concomitantly to each mix. Droplets were generated with a QX200 Droplet Generator (Bio-Rad), and the emulsified samples were transferred to ddPCR 96-well plates according to manufacturer's instructions (Bio-Rad). The cycling protocol included an enzyme activation step (95°C for 10 min), followed by 40 two-step cycles (95°C for 30 s and 60°C for 1 min, with a 2°C/s ramp between each step). Droplets containing PCR products were then analyzed using a QX200 Droplet Reader and QuantaSoft 1.7.4 software (Bio-Rad). The results were expressed as the absolute quantity of DNA per sample (copies/µL) for both the investigated and reference genes in each well. The normalized ratios were then calculated.

Generation of stable TNFRSF10A and/or TNFRSF10B KO cell lines

We first generated an inducible Cas9-expressing OSU-CLL cell line by transduction with Lenti-iCas9-neo (a gift from Qin Yan, New Haven, USA (2); Addgene plasmid # 85400) and geneticin (200 µg/mL) selection of cells, which we named "OSU-iCas9". We then designed CRISPR guides targeting the first exon of *TNFRSF10A* and *TNFRSF10B* genes and selected the most effective guides using the Guide-it

single-guide RNA (sgRNA) Screening Kit (Takara Bio, Inc). The sequences of sgRNAs targeting TNFRSF10A were 5'-CTTCAAGTTTGTCGTCGTCG-3' and 5'-GCGGGGAGGATTGAACCACG-3' but only one sgRNA was required for targeting TNFRSF10B (5'-AGAACGCCCCGGCCGCTTCG-3'). The sgRNAs were cloned into the Lenti-multi-Guide plasmid (Addgene plasmid # 85401)(2), to obtain simple TNFRSF10A/B or double TNFRSF10AB KO cells. Lentiviral particles were prepared using HEK293T cells and transduced into OSU-iCas9 cells. After puromycin (0.5 µg/mL) selection, resistant cells were induced with doxycycline (1 µg/mL for 24 hours, for the temporary expression of Cas9) and sorted according to their GFP expression (FACS Aria III, Becton Dickinson Biosciences, San Jose, CA). Five to seven days later, cells were stained with an anti-TNFRSF10A antibody (N°130-109-085; Miltenyi Biotec) and/or an anti-TNFRSF10B antibody (ab243080; Abcam), and the negative fractions containing KO cells (TNFRSF10A-KO, TNFRSF10B-KO or TNFRSF10AB-KO) were harvested by flow cytometry (bulk sorting and cloning).

gDNA extraction, PCR amp, cloning, and Sanger sequencing

Genomic DNA was isolated from clones derived from KO cell lines using an AllPrep DNA/RNA Mini Kit (Qiagen). The regions containing the sgRNA cleavage sites were amplified by PCR and cloned into pCR™-Blunt II-TOPO® vectors (Invitrogen, Inc), which were transformed into NEB Stable Competent *E. coli* (New England Biolabs) according to the manufacturer's protocol. Plasmids were then extracted with Plasmid Plus Midi Kit (Qiagen) and sent for Sanger sequencing (Genewiz, Leipzig, Germany).

Statistical analysis

Associations between characteristics of the del8p and control non-del8p populations were assessed using a chi-squared test for categorical data and a Mann–Whitney U test for continuous data. The median follow-up time was estimated using the reverse Kaplan-Meier method. Overall survival (OS), next treatment-free survival and time-to-first-treatment (TTFT) were estimated using the Kaplan-Meier method, and survival curves were compared using the log-rank test. The analysis of the frequency of Richter transformation (RT) took account of the competing risk of death. The frequency of RT was estimated using the cumulative incidence method, and Gray's test was used to compare the two populations' respective cumulative incidence curves. Potential risk factors for mortality in del8p patients were evaluated using univariate and multivariate Cox proportional hazards models, and the results were reported as hazard ratios (HRs). To account for the missing data in the multivariate model, multiple imputation by chained equations was applied. Due to multicollinearity, *TP53* disruption (rather than *TP53* mutation and del17p) was included in this model. For the data from *in vitro* assays, a chi-squared test or Fisher's exact test were used to compare categorical variables, and the Mann-Whitney U test was used to compare continuous variables. All tests were

two-sided, and the threshold for statistical significance was set to $p < 0.05$. Statistical analyses were carried out using R software (version 4.0.3, R Foundation for Statistical Computing, https://www.R-project.org/).

References

1. Cosson A, Chapiro E, Belhouachi N, Cung H-A, Keren B, Damm F, et al. 14q deletions are associated with trisomy 12, NOTCH1 mutations and unmutated IGHV genes in chronic lymphocytic leukemia and small lymphocytic lymphoma. Genes, chromosomes & cancer. 2014;53(8):657-66.
2. Cao J, Wu L, Zhang SM, Lu M, Cheung WK, Cai W, et al. An easy and efficient inducible CRISPR/Cas9 platform with improved specificity for multiple gene targeting. Nucleic acids research. 2016;44(19):e149. Epub 2016/11/02.

B- Supplementary Tables

Table S1.

Supplemental Table S1. Molecular and cytogenetic characteristics of patients used in in vitro experiments: non-del8p patients.

ID	Karyotype	CK (≥ 3 CA)	HCK (≥ 5 CA)	Del13q	Tri12	Del11q	Del17p (% FISH)	*TP53* mutation	*TP53* disruption	*IGHV* status	Figures 3, S6	Figure S7	Figure S10	Figures 5, S11	Figure 6	Figure 7
CLL_7	46,XX[20]	-	-	-	-	-	-	-	-	UM	x	x				
CLL_13	46,XY,t(11;13)(q23;q14)[9]/46,XY[11]	-	-	+	-	-	-	-	-	M	x	x				
CLL_214	46,XX[20]	-	-	+	-	-	-	ND	NA	M	x	x				
CLL_215	46,XY,del(13)(q14q?21)[1]/46,idem,t(9;13;14)(q?31;q14;q?24)[11]/46,XY[8]	-	-	+	-	-	-	ND	NA	M	x	x				
CLL_243	46,XY[20]	-	-	+	-	-	-	ND	NA	M				x	x	x
CLL_216	46,XX[20]	-	-	+	-	-	-	ND	NA	ND	x	x				
CLL_217	44,XY,add(11)(q23),t(14;19)?dic(14;19)(14qter->14p11::19?qter->19?pter),der(16)t(16;17)(q2??3;q?21),-17,-19[17]/46,XY[3]	+	+	-	-	-	+ (51%)	ND	+	ND				x	x	
CLL_218	failed	NA	NA	-	-	-	-	ND	NA	UM	x	x				
CLL_219	47,XX,+12[19]/46,XY[1]	-	-	-	+	-	-	ND	NA	UM	x	x				
CLL_220	47,XX,+12[17]/46,XX[3]	-	-	-	+	-	-	-	-	UM	x	x				
CLL_221	failed	NA	NA	+	-	-	-	ND	NA	M	x	x				
CLL_222	46,XX[20]	-	-	+	-	-	-	-	-	UM	x	x				
CLL_37	46,XY,del(11)(q1?4;q2?3)[20]	-	-	+	-	+	-	+	+	UM	x	x				
CLL_223	46,XX,t(12;16)(q13;q2?4)[2]/46,XX,del(6)(q1?3q2?4)[1]/46,XX[17]	-	-	-	-	-	-		NA	UM	x	x				
CLL_42	47,XY,+12,t(14;19)(q32;q13)[2]/47,sl,add(2)(p?23),add(6)(p?22),der(17)[10]/47,sl,add(3)(p?24)[6]/47,XY,-3,?t(4;13)(?q21;q?13),t(?5;14;19)(?;q32;q13),-9,+12,del(17)(p11),add(18)(q?),+2mar[2]	+	+	+	+	-	+ (14%)	+	+	UM	x	x	x			
CLL_52	46,XY,t(2;4)(p12;p15),del(11)(q13q24)[7]/46,sl,der(3)(?::6q?->6q21::3p26->3qter),del(6)(q1?4)[14]/46,sdl,t(13;17)(q13;q2?5)[2]	+	+	+	-	+	-	-	-	UM	x	x	x	x	x	x
CLL_59	46,XX,der(13)t(13;14)(q13;q31),der(14)t(13;14)(q21;q31)[3]/46,sl,t(2;6;10)(p24;q12;p11)[4]/46,XX[14]	+	-	+	-	-	-	ND	NA	M			x	x		
CLL_224	ND	NA	NA	-	-	-	-	-	-	M	x	x				
CLL_73	89~90,XXXX,der(3),-3,-4,-4,der(17)t(4;17)(q?31;p11)x2[cp19]/46,XX[1]	+	+	+	-	-	+ (33%)	+	+	M	x	x				
CLL_225	46,XX,t(2;18)(p11;q21)[1]/46,idem,t(12;13)(q24;q14)[17]/46,XX[2]	-	-	-	-	-	-	ND	NA	ND	x	x				
CLL_82	47,XY,+12[16]/48,sl,t(14;18)(q32;q21),+21[4]	+	-	-	+	-	-	ND	NA	UM				x	x	
CLL_244	ND	NA	NA	+	-	-	-	ND	NA	M				x	x	x
CLL_226	46,XX,del(1)(q?21q?41)[8]/46,XX[12]	-	-	-	-	-	-	ND	NA	UM	x	x				
CLL_108	46,XY,der(3)t(3;18)(p22;q12)[13]/46,idem,del(14)(q21q31)[5]/46,XY,t(3;18)(p22;q12),add(12)(p13)[cp2]	+	-	-	-	-	-	ND	NA	M				x	x	
CLL_227	46,XX,del(11)(q2?2)[1]/46,sl,t(3;8)(q1?3;q24)[12]/46,XX[7]	-	-	-	-	+	-	ND	NA	UM			x	x	x	
CLL_109	46,XY,dup(2)(p1?6p2?5),del(11)(q14q22)[8]/46,XY[12]	-	-	-	-	+	-	ND	NA	UM				x	x	
CLL_228	46,XX,der(1)t(1;2;13)(q10;q10;q14)ins(2;13)(q?22;q14q?31),der(2)t(1;2;13),der(13)t(1;2;13)[3]/46,XX[17]	+	-	+	-	-	-	-	-	UM	x	x	x	x	x	x
CLL_229	46,XY,del(11)(q?14q?22)[15]/46,XY[5]	-	-	+	-	+	-	ND	NA	NA				x	x	
CLL_230	ND	NA	NA	ND	ND	ND	ND	ND	ND	M	x	x				
CLL_231	46,XX,del(11)(q2?1q24),dup(8)(q?13q24)[18]/47,XX,del(11)(q2?1q24),+del(8)(p?12p22)[2]	+	-	+	-	+	-	-	-	UM	x	x				
CLL_134	46,XX,del(11)(q1?3q2?3),add(12)(q2?4),del(17)(p12)[2]/47,XX,add(2)(p2?4),del(11)(q1?3q2?3),del(17)(p12),+mar1[cp7]/48,XX,del(11)(q1?3q2?3),del(17)(p12),+mar1,+mar2[cp3]/46,XX,del(17)(p12),-16,+mar3[cp4]	+	+	+	-	-	+ (79%)	ND	+	M				x	x	x
CLL_138	46,XX,der(17)t(8;17)(q2?1;p11)[12]/46,idem,del(6)(q1?6q2?3)[4]/46,XX[4]	-	-	-	-	-	+ (61%)	ND	+	M	x	x				
CLL_232	ND	NA	NA	ND	ND	-	+ (NA)	+	+	UM	x	x	x			
CLL_233	46,XX[20]	-	-	+	-	-	-	-	-	UM	x	x	x		x	
CLL_166	47,XY,+12,del(17)(p12)[16]/47,sl,add(3)(q2?6)[2]/46,XY[2]	+	-	-	+	-	+ (83%)	+	+	UM				x	x	x
CLL_234	46,XX,del(11)(q21q22),t(12;13)(p1?3;q13)[15]	-	-	+	-	+	-	ND	NA	ND	x	x				
CLL_235	46,XX,i(17)(q10)[16]	-	-	-	-	-	+ (98%)	ND	+	ND	x	x				
CLL_180	45,XX,der(16)t(16;17)(p11;q11),dup(16)(?q12?q24),-17[17]/45,idem,t(3;19)(q11;q11),t(4;13)(q?24;q14)[3]	+	+	+	-	-	+ (97%)	ND	+	M	x	x				

ID	Karyotype	CK (≥ 3 CA)	HCK (≥ 5 CA)	Del13q	Tri12	Del11q	Del17p (% FISH)	*TP53* mutation	*TP53* disruption	*IGHV* status	Figures 3, S6	Figure S7	Figure S10	Figures 5, S11	Figure 6	Figure 7
CLL_181	46,XX[20]	-	-	+	-	-	-	ND	NA	M	x	x				
CLL_236	ND	NA	NA	ND	ND	ND	ND	ND	NA	M				x	x	
CLL_237	46,XY,del(6)(p22),del(13)(q14q33)[7]/47,XY,del(13)(q14q33),+mar1[3]/47,XY,add(7)(p?21),del(13)(q14q33),+mar1[2]/46,XY,-7,add(19)(?q14),+mar2[cp3]/46,XY,add(16)(p1?3)[2]/46,XY,t(12;15)(q24;q21)[1]/46,XY[2]	+	+	+	-	-	-	ND	NA	UM	x	x				
CLL_238	46,XY,del(11)(q?21q?25)[20]	-	-	+	-	+	-	ND	NA	UM	x	x				
CLL_200	46,XX[20]	-	-	-	-	-	-	ND	NA	M				x	x	x
CLL_239	46,XY,del(11)(q14q24)[1]/46,sl,inv(1)(p3?5q?32),der(18)t(2;18)(p11;p10)[13]/46,sdl,-inv(1),del(6)(q16q24)[5]/46,XY[1]	+	-	-	-	+	-	-	-	UM	x	x				
CLL_240	46,XX,t(1;16)(p11;p12),del(11)(q14q24)[2]/46,XX[18]	-	-	+	-	+	-	-	-	M	x	x				
CLL_241	ND	NA	NA	-	+	-	-	ND	NA	UM	x	x				

ND: not down; NA: not applicable; +: yes; -: no; CK: complex karytopye; HCK: highly CK; CA: chromosomal abnormalities

Supplemental Table S1. Molecular and cytogenetic characteristics of patients used in in vitro experiments: del8p patients.

ID	Karyotype	CK (≥ 3 CA)	HCK (≥ 5 CA)	Del8p (% FISH) (TNFRSF10)	Del13q	Tri12	Del11q	Del17p (% FISH)	*TP53* mutation	*TP53* disruption	*IGHV* status	Figures 3, S6	Figure S7	Figure S10	Figures 5, S11	Figure 6	Figure 7
CLL_1	45,XY,?der(4),?der(6),?der(8),+i(8)(q10),?der(9),add(11)(q),?der(12),-13,der(14),add(17)(p),-18,+mar[cp6]	+	+	76	+	-	+	+ (94%)	+	+	UM				x	x	
CLL_17	failed	NA	NA	9	+	-	-	+ (4%)	ND	+	M	x			x	x	x
CLL_242	45,XY,der(8;17)(q10;q10)[3]/46,XY[17]	-	-	19	+	-	-	+ (16%)	+	+	M		x		x	x	x
CLL_48	46,XY,del(11)(q22),add(13)(p13)[cp5]/46,sl,del(6)(q14)[cp5]/46,sdl,t(4;19)(q?26;?q13),der(8)t(8;8)(p?21;q2?3)[cp3]/46,sl,add(2)(q?33)[cp2]/46,XY[5]	+	+	10	+	-	+	+ (32%)	-	+	UM	x	x				
CLL_213	46,XX,der(2)(2pter->2p2?::?::2p2?->2q10::8q21->8qter),-8,+12,i(17)(q10)[9]/46,XX[1]	+	-	14	-	+	-	+ (71%)	+	+	UM	x	x				
CLL_90	46,XY,der(8)t(8;8)(p11;q21),del(13)(q1?3q2?2),add(17)(p11)[10]/46,sl,add(15)(q2?5)[5]/46,sl,?add(12)(p12)[4]/46,sl,add(1)(q2?2)[3]	+	+	92	+	-	+	+ (70%)	+	+	UM				x	x	x
CLL_104	46,XX,add(7)(q35),r(8),t(9;16)(p11;p11),der(17)t(8;17)(q?22;p11)[17]/46,XX[3]	+	-	68	+	-	-	+ (97%)	ND	+	M	x	x		x	x	x
CLL_119	45,XX,dup(2)(p?15p?21),add(15)(q2?5),-17,add(17)(p11),-18,add(18)(p1?),+mar[cp12]/46,XX[2]	+	+	8	+	-	+	+ (81%)	+	+	UM	x	x				
CLL_132	47,XX,der(8)t(8;18)(p1?2;q1?1),i(17)(q10),-18,+2mar[7]/47,XX,add(8)(q?24),t(?;15)(?;q?),i(17)(q10),add(18)(p1?1),+mar[cp6]/46,XX[7]	+	+	64	-	-	-	+ (43%)	ND	+	NA	x	x				
CLL_146	47,XY,+12[15]/47,sl,der(4)?inv(4)(p?13q?22)t(4;17)(?q31;q22)[4]/46,XY[1]	-	-	5	+	+	-	-	+	NA	M	x	x				
CLL_152	46,XX,dup(1)(q22q4?1),der(3)t(3;12)(p25;q11),der(6)t(6;7)(q15;q34),der(7)t(6;7)(q22;q34)[6]/46,XX[14]	+	-	58	-	-	-	-	-	-	M	x	x		x	x	x
CLL_197	43,XX,add(3)(p?12),t(7;13)(q2?1;q1?3),add(8)(p2?3),-9,t(10;13)(q26;q2?1),-15,der(17)t(9;17)(q2?1;p11),t(17;18)(q2?1;q1?2),-21[cp14]/43,sl,der(5)[3]/43,sl,del(1)(q4?1),der(9)[3]	+	+	99	-	-	-	+ (95%)	ND	+	NA	x	x		x	x	x

ND: not down; NA: not applicable; +: yes; -: no; CK: complex karytopye; HCK: highly CK; CA: chromosomal abnormalities

Table S2. Description of the 8p abnormalities.

Successful/informative K	46/57 (81%)
Number of patients with 8p abn identified by K and F	37/46 (78.2%)
Subclonal abn detected by K and/or F	30/49 (61.2%)
Number of identified 8p abn by K and/or F	39§
t(8;v)	31/39 (80%)
t(8;8)/i(8)(q) (K+F)	13/39 (33%)
t(8;17)	3/39 (8%)
t(3;8)§	3/39 (8%)
t(8;13)§	2/39 (5%)
t(2;8)	2/39 (5%)
Other partners*	5/39 (13%)
Unidentified partner: add(8p)	3/39 (8%)
Del(8p)	5/39 (13%)
Ring chromosome 8	2/39 (5%)
Monosomy 8	1/39 (2%)
FISH/SNPa analyses	
del TNFRSF10 (8p21.3)	51/56 (91%)
del LPL (8p21.3)	47/56 (84%)
del DLC1 (8p22)	49/56 (88%)
del FGFR1 (8p11)	31/56 (55%)

Abn: abnormality, K: karyotype, F:FISH, del: deletion, add: addition, SNPa: single-nucleotide polymorphism array

§ Two patients had two 8p abnormalities in two distinct clones: one had both t(3;8) and t(8;13) (CLL_189); one has del(8p) and t(2;8) (CLL_169)

* Chromosome partners: 10, 11, 12, 16 and 18 (one case of each)

Table S3. Comparison of CLL with and without del8p in patients not treated before the diagnosis of del8p or (for the non-del8p cohort) before karyotyping.

Variables	Del8p N=27	Non-del8p N=124	P-value
Sex (female)	12/27 (44%)	45/124 (36%)	*.57*
Age at diagnosis, years, median (range)	61 (31-86)	61 (25-94)	*.41*
Binet stage at diagnosis			***.015***
A	11/18 (61%)	81/95 (85%)	
B	5/18 (28%)	13/95 (14%)	
C	2/18 (11%)	1/95 (1%)	
Treated	20/27 (74%)	107/124 (86%)	*.14*
Number of lines of treatment, median (range)	1 (0-5)	1 (0-9)	*.065*
CK (≥3 CAs)	10/17* (59%)	25/124 (20%)	***.007***
HCK (≥5 CAs)	5/17*(29%)	8/124 (7%)	***.016***
Number of CAs detected by K, median (range)	3 (1-13)	1.0 (0-8)	***<.001***
Classical CAs detected by FISH			
del13q	14/24 (58%)	77/124 (62%)	*.91*
tri12	2/24 (8%)	26/123 (21%)	*.25*
del11q	10/23 (44%)	20/124 (16%)	***.009***
del17p	5/25 (20%)	10/123 (8%)	*.14*
8q24 (*MYC*) gain	8/27 (30%)	5/124 (4%)	***<.001***
2p gain	7/27 (26%)	3/124 (2%)	***<.001***
unmutated *IGHV*	18/26 (69%)	57/123 (46%)	*.057*
***TP53* mutation**	5/22 (23%)	11/76 (15%)	*.35*
***TP53* disruption (deletion and/or mutation)**	5/22 (23%)	15/78 (19%)	*.77*

The p-values came from a chi-squared test, Fisher's exact test, or a Mann-Whitney test comparing the two cohorts. *: 17 of the 27 treatment-naive del8p CLL cases were successfully karyotyped. K: karyotype; CK: complex karyotype; HCK: highly complex karyotype; CA: chromosomal abnormality

Table S4. Characteristics of the four subgroups of del8p patients.

	del8p size subgroups (n=56*)					
Variables	**1 n=8**	**2 n=21**	**3 n=17**	**4 n=10**	**OR [95%CI]**	**p-value**
Sex (female)	5/8 (63%)	10/21 (48%)	4/17 (245%)	5/10 (50%)	0.57 [0.21-1.54]	*.27*
Age at diagnosis, median (range)	58 (48-86)	56.5 (31-77)	63.5 (42-82)	52.0 (46-82)	1.00 [0.96-1.05]	*.92*
Treated	7/8 (88%)	17/20 (85%)	13/16 (81%)	10/10 (100%)	1.51 [0.38-5.9]	*.56*
Number of lines of treatment, median (range)	4 (0-5)	2 (0-5)	2.5 (0-7)	1.5 (1-4)	0.83 [0.62-1.11]	*.20*
Not treated before detection of del8p	4/8 (50%)	9/20 (45%)	6/16 (38%)	8/10 (80%)	1.68 [0.63-4.48]	*.30*
CK (≥3 CAs)	6/6 (100%)	13/18 (72%)	9/15 (60%)	4/6 (67%)	0.5 [0.16-1.55]	*.15*
HCK (≥5 CAs)	4/6 (67%)	7/18 (39%)	5/15 (33%)	3/6 (50%)	0.74 [0.25-2.18]	*.50*
Number of CAs by K, median (range)	6.0 (3 -14)	4.0 (1-13)	3 (1-12)	4 (2-7)	0.87 [0.74-1.01]	*.07*
Classical CAs by FISH						
del13q	5/8 (63%)	11/20 (55%)	7/16 (44%)	8/9 (89%)	1.41 [0.53-3.78]	*.49*
tri12	0/8 (0%)	0/19 (0%)	3/16 (19%)	1/9 (11%)	4.22 [0.75-23.65]	*.10*
del11q	4/8 (50%)	10/19 (53%)	9/16 (56%)	4/8 (50%)	1.06 [0.39-2.87]	*.91*
del17p	4/8 (50%)	8/21 (38%)	5/16 (31%)	2/9 (22%)	0.52 [0.18-1.46]	*.21*
8q24 (*MYC*) gain	1/8 (13%)	8/21 (38.1%)	11/17 (65%)	4/10 (40%)	2.31 [0.87-6.15]	*.09*
2p gain	0/8 (0%)	5/21 (24%)	6/17 (35%)	3/10 (30.0%)	2.3 [0.78-6.77]	*.13*
unmutated *IGHV*	7/8 (88%)	14/18 (78%)	7/12 (58%)	7/9 (78%)	0.6 [0.19-1.9]	*.38*
***TP53* mutation**	4/5 (80%)	6/14 (43%)	2/11 (18%)	2/9 (22%)	0.21 [0.06-0.8]	***.02***
***TP53* disruption (deletion and/or mutation)**	5/6 (83%)	8/16 (50%)	5/14 (36%)	3/10 (30%)	0.32 [0.1-0.95]	***.04***

The results were calculated with all the available data for each variable (i.e. N varies from one variable to another). The subgroups were defined according to the size of the del8p in 56 of the 57 patients (*one case could not be evaluated): 1: del 8p10-8pter (the whole short arm); 2: del 8p11-8pter; 3: del 8p21-8pter; and 4: other deletions. The odds ratios (OR) [95% confidence interval (CI)] and p-values were calculated in univariate ordinal logistic regressions. K: karyotype, CA: chromosomal abnormality, CK: complex karyotype; HCK: highly complex karyotype

Table S5. Univariate and multivariate analyses of potential risk factors for death in del8p patients.

	Univariate analysis		Multivariate analysis		N
Variables	**HR [95%CI]**	**p-value**	**HR [95%CI]**	**p-value**	
Sex (female)	1.79 [0.82-3.88]	.14			57
Age at diagnosis, median (range)	1.01 [0.97-1.04]	.76			53
Del8p subgroup 1 or 2	2.62 [1.13-6.05]	**.024**	2.36 [1.01-5.52]	.060	56
CK (≥3 CAs)	3.47 [0.99-12.22]	.053			46
HCK (≥5 CAs)	2.33 [0.91-5.97]	.077			46
Number of CAs by K	1.27 [1.09-1.47]	**.002**			46
Classical CAs by FISH					
del13q	0.61 [0.28-1.34]	.22			54
del11q	1.59 [0.7-3.6]	.27			52
del17p	2.81 [1.21-6.49]	**.016**			55
8q24 (*MYC*) gain	1.11 [0.5-2.45]	.80			57
2p gain	0.61 [0.24-1.54]	.30			56
Subclonal abnormality by K and/or F	0.95 [0.4-2.26]	.91			49
***IGHV* unmutated**	1.65 [0.61-4.43]	.32			48
***TP53* mutation**	4.27 [1.42-12.86]	**.010**			40
***TP53* disruption (deletion and/or mutation)**	4.14 [1.53-11.23]	**.005**	2.61 [1.06-6.4]	**.049**	47

Survival was calculated as the time interval between detection of the del8p and death or last follow-up. Trisomy 12 was not included because too few patients harbored this abnormality. K: karyotype, CA: chromosomal abnormality, CK: complex karyotype; HCK: highly complex karyotype

Table S6. Summary of CRISPR-mediated genetic alterations in OSU-CLL KO clones.

	TNFRSF10A (NM_003844.4)		TNFRSF10B (NM_003842.5)	
OSU A-KO				
Clone 8	c.140delC	c.140dupC	-	-
Clone 9	c.140delC	c.140delC	-	-
Clone 10	c.133_146del	c.140delC	-	-
OSU B-KO				
Clone 8	-	-	c.34dupT	c.27_42del
Clone 9	-	-	c.34dupT	c.34_271delinsX*
Clone 20	-	-	c.24_40del	c.15_39del
OSU AB-KO				
Clone 4	c.140delC	c.140delC	c.22_92del	c.34dupT
Clone 5	c.130_151del	c.140delC	c.29_99del	c.22_92del
Clone 8	c.140delC	c.140_146del	c.34dupT	c.34dupT

* X: CCTAGCGAACTTTTTGTATTTTTAGTAGAGACGGGGTTTCACCGTGTTAGCCAGGATGGTCTGGCTCGTGATCTGCC

C- Supplementary Figures

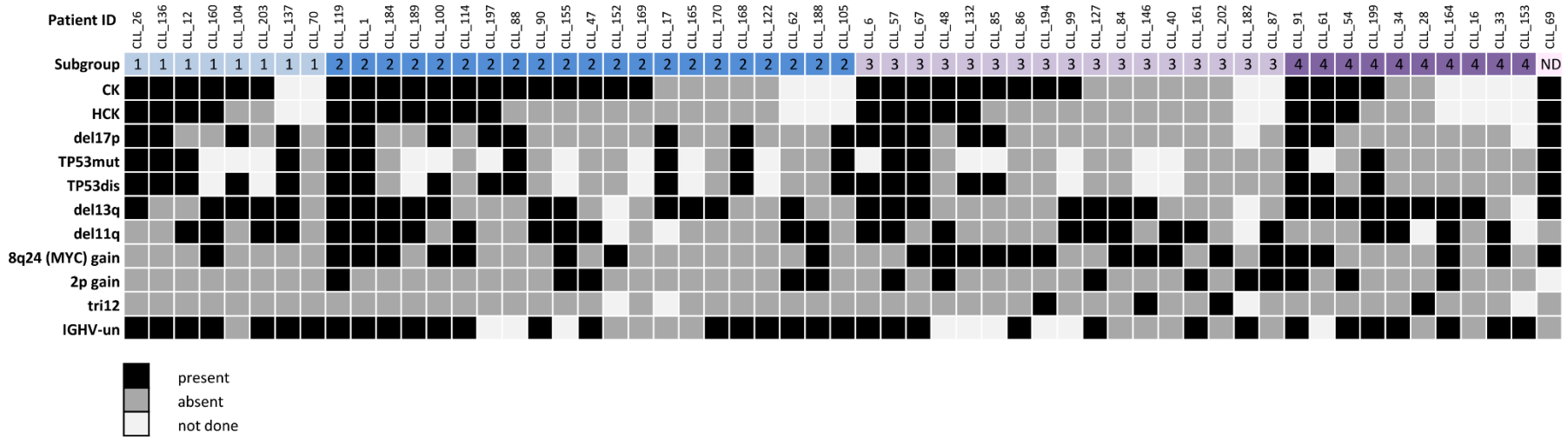

Figure S1. The genetic abnormalities detected in the 57 del8p CLL patients. Each column corresponds to a patient, and each row corresponds to a genetic variable. The colored row indicates membership of the four del8p size subgroups. CK: complex karyotype (≥3 chromosomal abnormalities), HCK: highly complex karyotype (≥5 chromosomal abnormalities), del: deletion, mut: mutated, dis: disruption (deletion and/or mutation), tri: trisomy, un: unmutated.

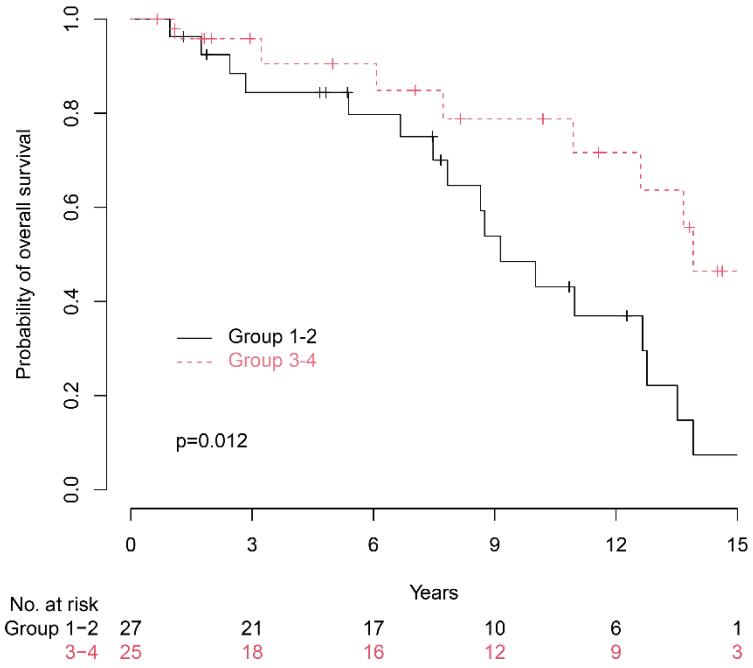

Figure S2. **Overall survival in patients with del8p as a function of the size of the deletion**, calculated from the date of diagnosis.

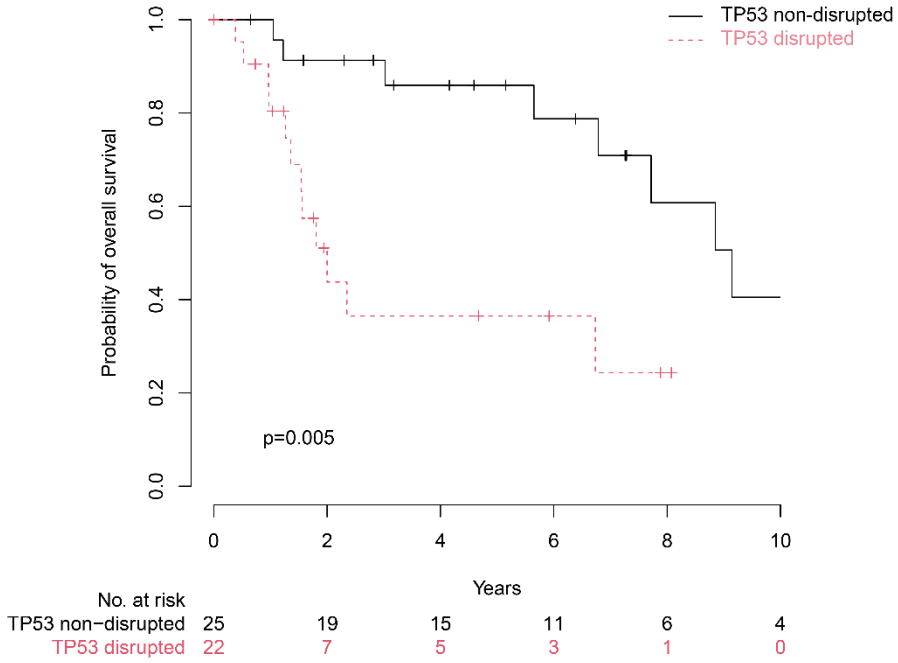

Figure S3. Overall survival in patients with del8p, as a function of the presence of *TP53* disruption (deletion and/or mutation), calculated from the date of del8p detection.

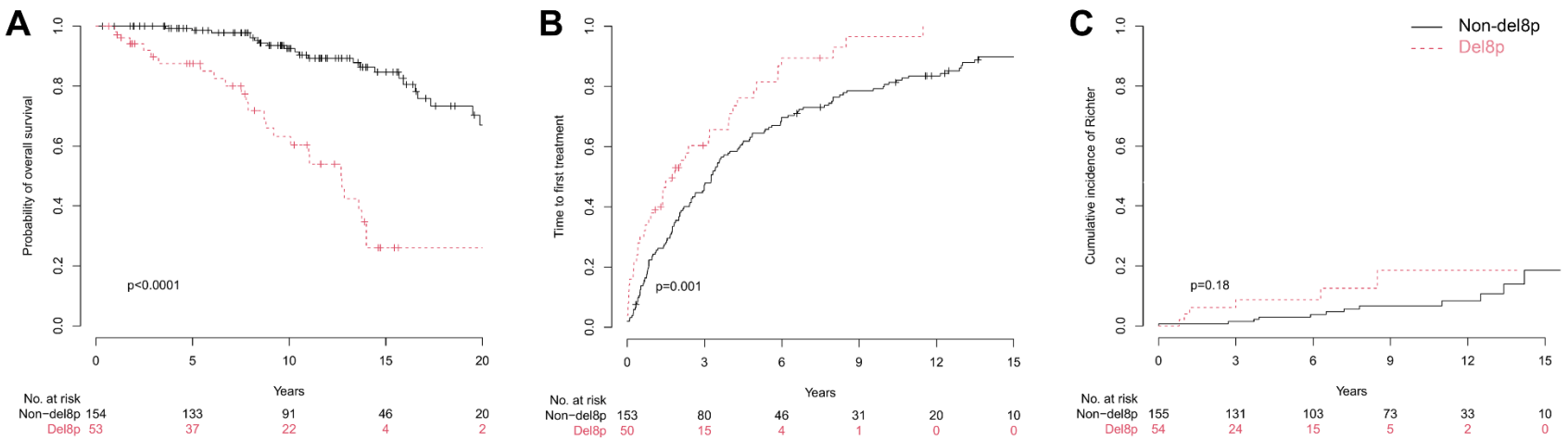

Figure S4. Survival analyses for del8p vs. non-del8p patients. A-B. Overall survival and time-to-first-treatment were calculated from the date of CLL diagnosis onwards. **C.** Cumulative incidence of Richter transformation calculated from the date of del8p detection or (for non-del8p patients) the date of karyotyping.

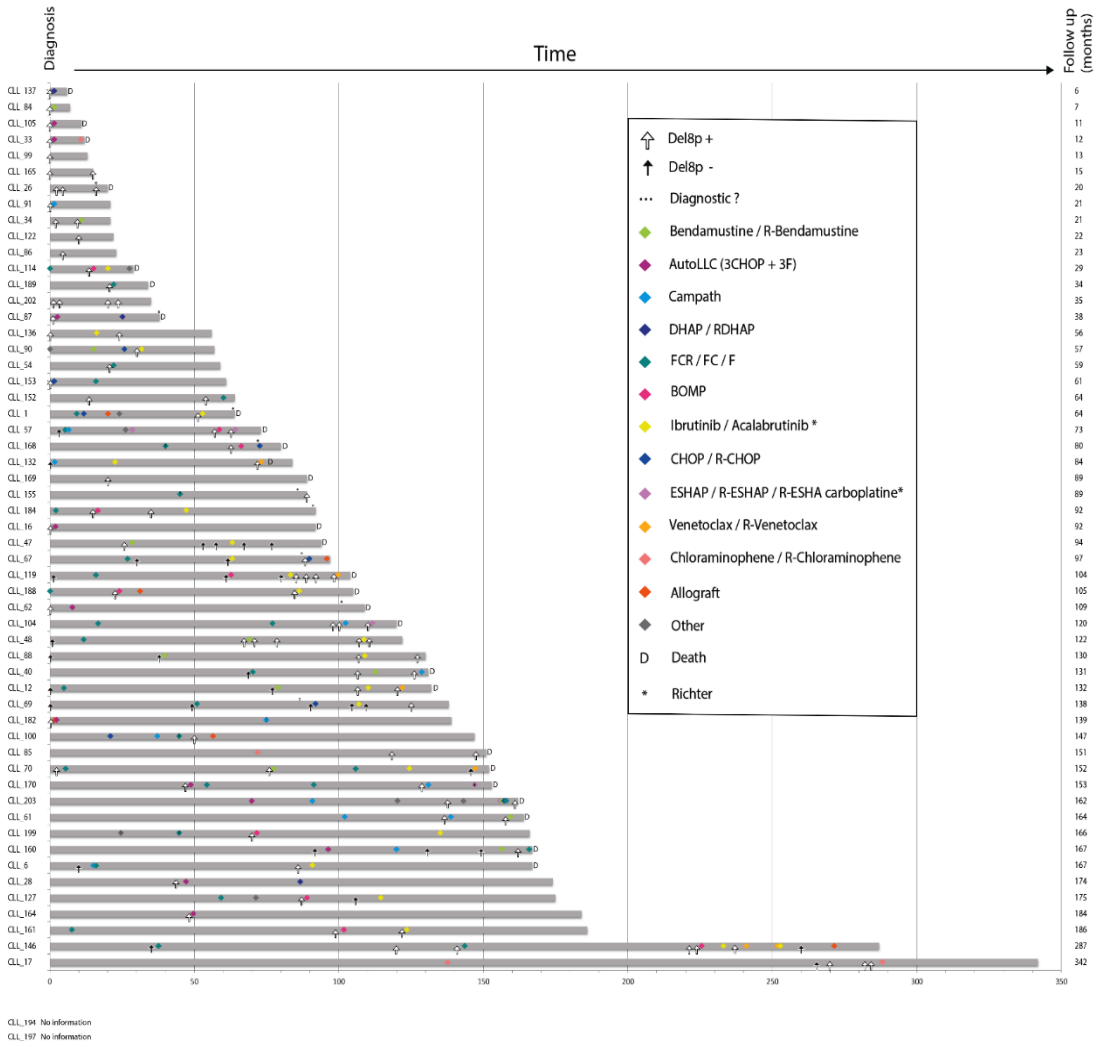

Figure S5. Time course of diagnosis and treatment for 55 patients with del8p CLL. R: rituximab; DHAP: dexamethasone/high-dose cytarabine & cisplatin; F: fludarabine; C: cyclophosphamide; CHOP: cyclophosphamide/doxorubicin hydrochloride/vincristine & prednisone, ESHAP: etoposide/methylprednisolone/high dose cytarabine & cisplatin; BOMP: bendamustine/ofatumumab & methylprednisolone.

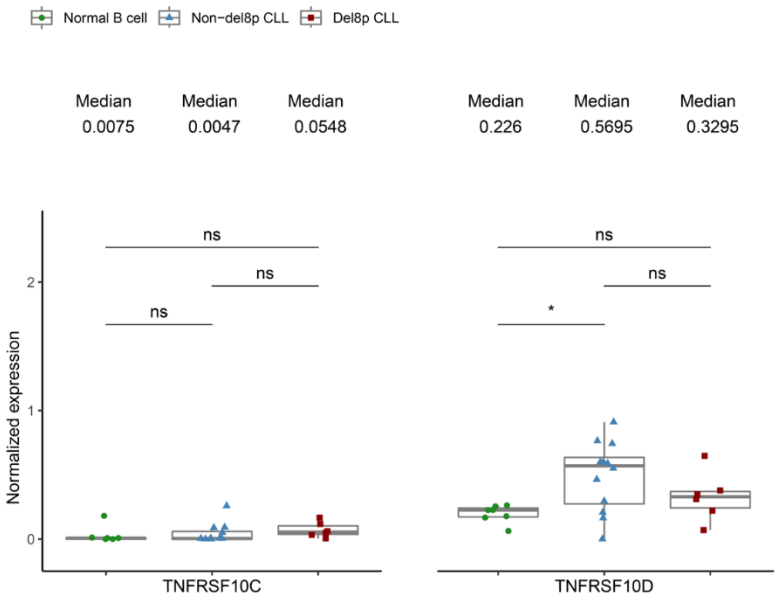

Figure S6. Expression of *TNFRSF10C* and *TNFRSF10D* genes in normal and CLL B-cells. The mRNA was purified from healthy donors (normal B cells, n=7), patients with non-del8p CLL (n=12) or patients with del8p CLL (n=6), and the expression levels were determined by ddPCR. *ABL1* mRNA expression was used to normalize the data. The box corresponds to the interquartile range, the central line corresponds to the median, and the whiskers correspond to the range. Statistical analyses were performed using a Mann-Whitney U test. *, P < .05.

A.

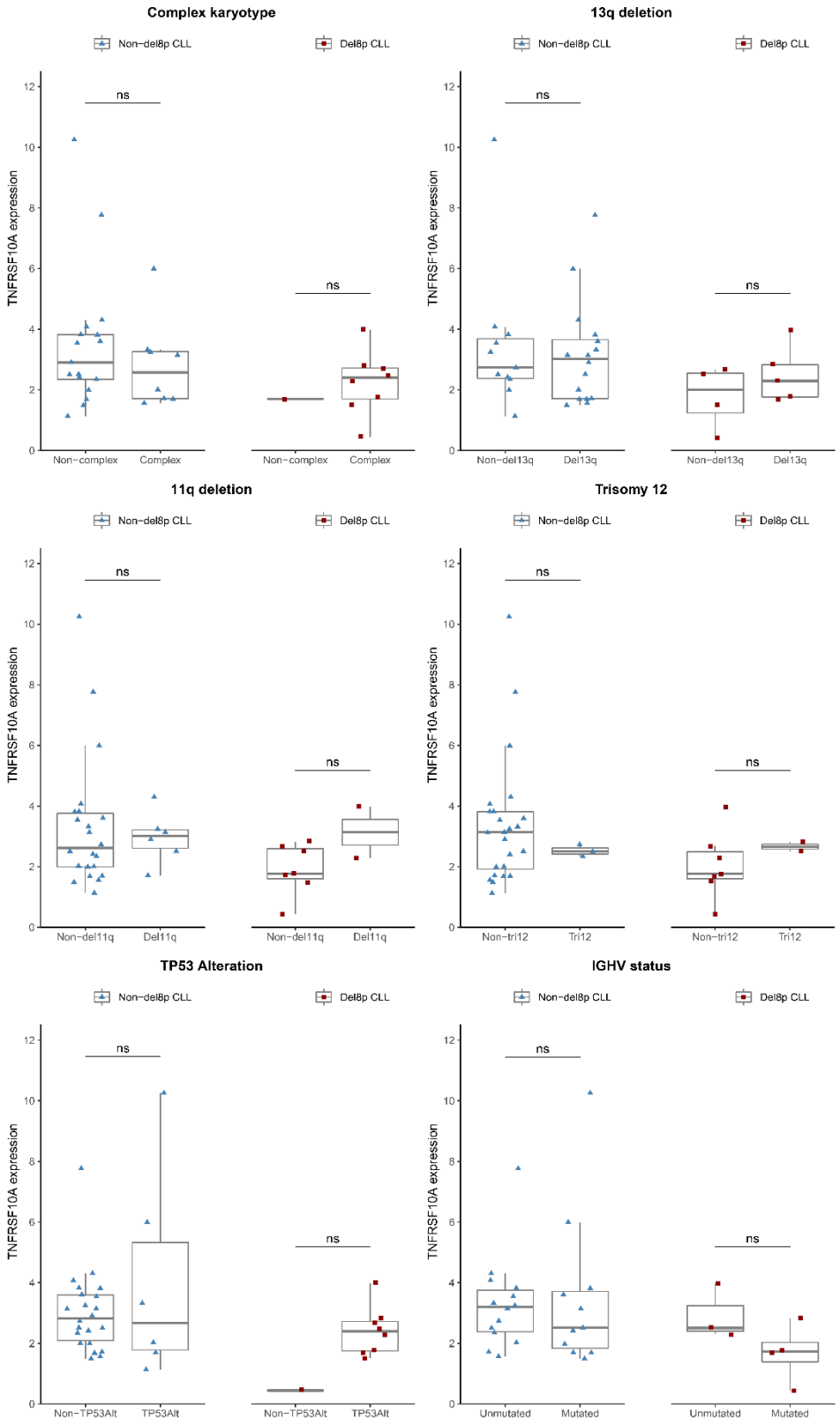
Complex karyotype
13q deletion
11q deletion
Trisomy 12
TP53 Alteration
IGHV status
Non−del8p CLL
Del8p CLL
TNFRSF10A expression
ns
Non−complex
Complex
Non−del13q
Del13q
Non−del11q
Del11q
Non−tri12
Tri12
Non−TP53Alt
TP53Alt
Unmutated
Mutated

B.

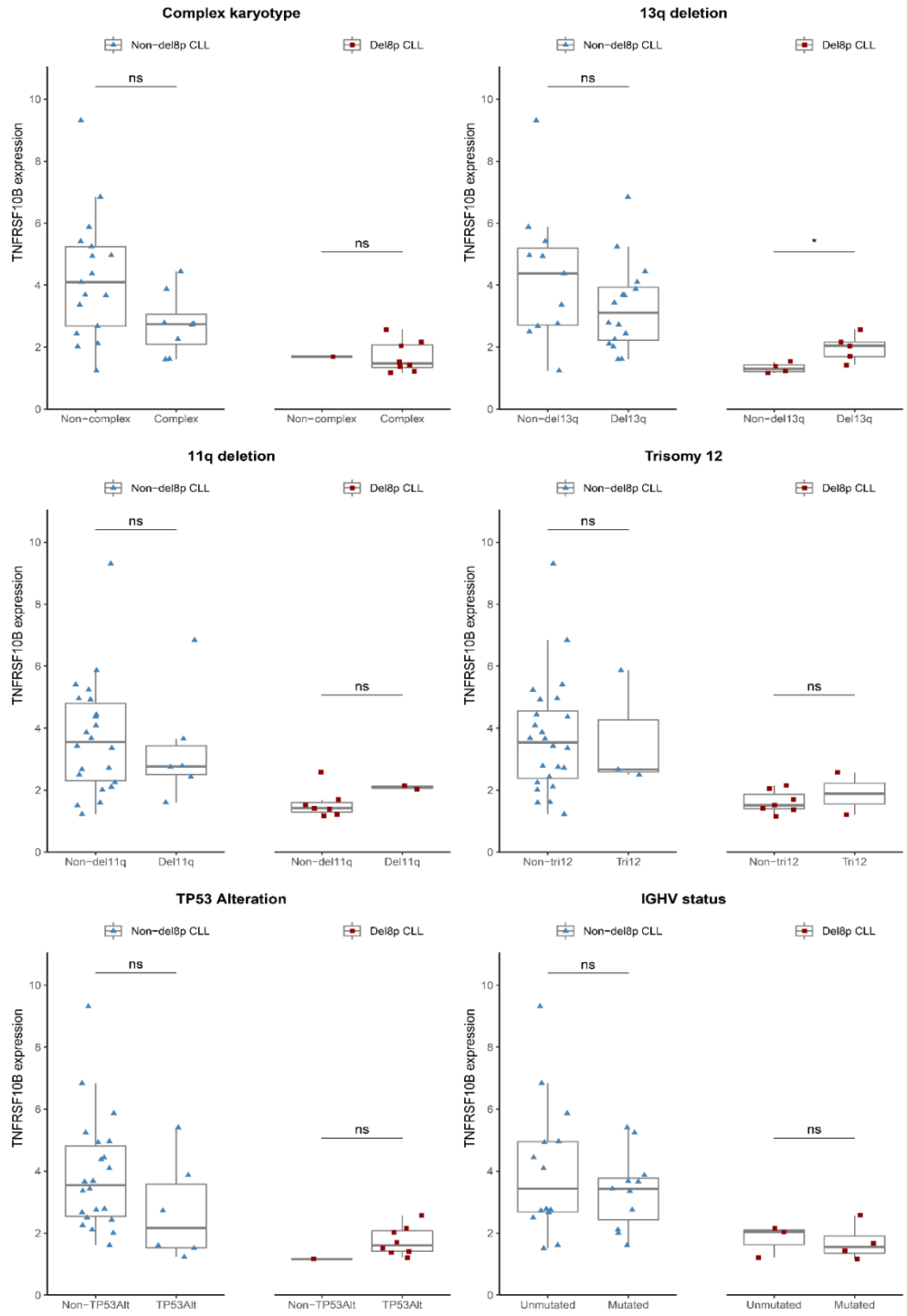

Figure S7. Expression of *TNFRSF10A* and *TNFRSF10B* genes, as a function of the presence of conventional cytogenetic and molecular risk factors in CLL. The mRNA was purified from non-del8p (n=33) or del8p (n=9) CLL patients and the expression levels of *TNFRSF10A* (**A**) and *TNFRSF10B* (**B**) were determined by ddPCR. *ABL1* mRNA expression was used to normalize the data. The box corresponds to the interquartile range, the central line corresponds to the median, and the whiskers correspond to the range. Statistical analyses were performed using a Mann-Whitney U test. With the exception of del13q (associated with a higher (1.5-fold) level of *TNFRSF10B* expression in CLL patients with del8p (*, P < .05)), none of the other abnormalities listed in the Figure appeared to influence *TNFRSF10A* and *TNFRSF10B* mRNA expression levels.

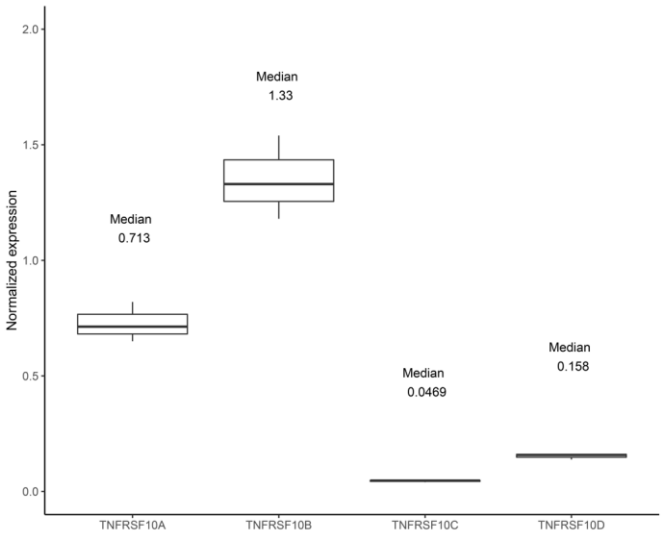

Figure S8. Expression of *TNFRSF10A/B/C/D* genes in the OSU-CLL cell line. The mRNA was purified from the OSU-CLL cell line and the expression levels of *TNFRSF10A/B/C/D* were determined by ddPCR. *ABL1* mRNA expression was used to normalize the data. Note that *TNFRSF10A* and *TNFRSF10B* were more strongly expressed than *TNFRSF10C* and *TNFRSF10D* in OSU-CLL cells and that the expression of *TNFRSF10B* was higher than that of *TNFRSF10A*.

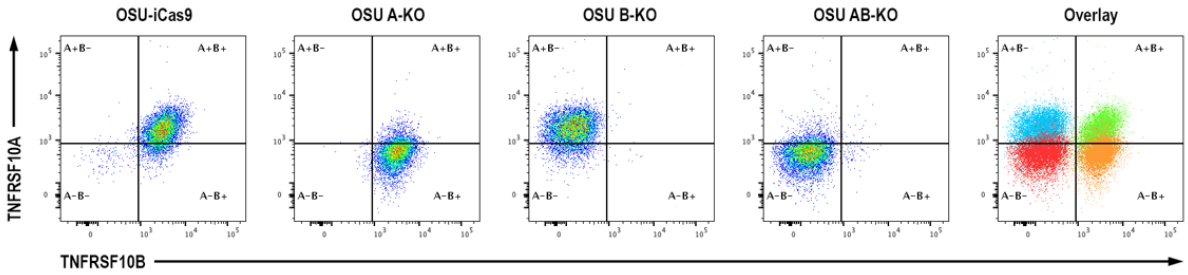

Figure S9. Expression of TNFRSF10A and TNFRSF10B (measured by flow cytometry) in OSU-CLL cells. Representative cytofluorometric plots of TNFRSF10A and TNFRSF10B immunolabeling of OSU-CLL cells transduced with empty vector or edited using CRISPR/Cas9 (as described in the Material and Methods section) to target TNFRSF10A and/or TNFRSF10B (A-KO; B-KO; AB-KO cells). OSU A-KO and OSU B-KO lost TNFRSF10A and TNFRSF10B expression, respectively. OSU AB-KO cells lost both TNFRSF10A and TNFRSF10B. The overlay plot (right panel) represents the labeling of the different cell types.

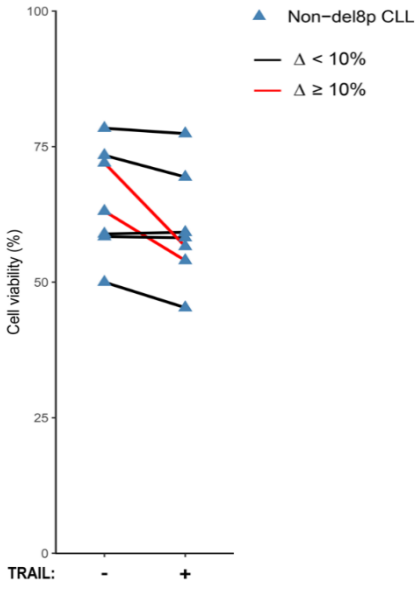

Figure S10. TRAIL fails to induce cell viability loss in non-del8p primary CLL cells. Primary non-del8p CLL B-lymphocytes were treated (or not) for 24h with TRAIL (50 ng/mL), and cell viability was assessed by flow cytometry and annexin-V/PI dual labeling. The graph shows the percentage of viable cells (dual negative annexin-V/PI staining). A decrease in cell viability of 10% or more (relative to control untreated cells) was considered to be significant (red lines).

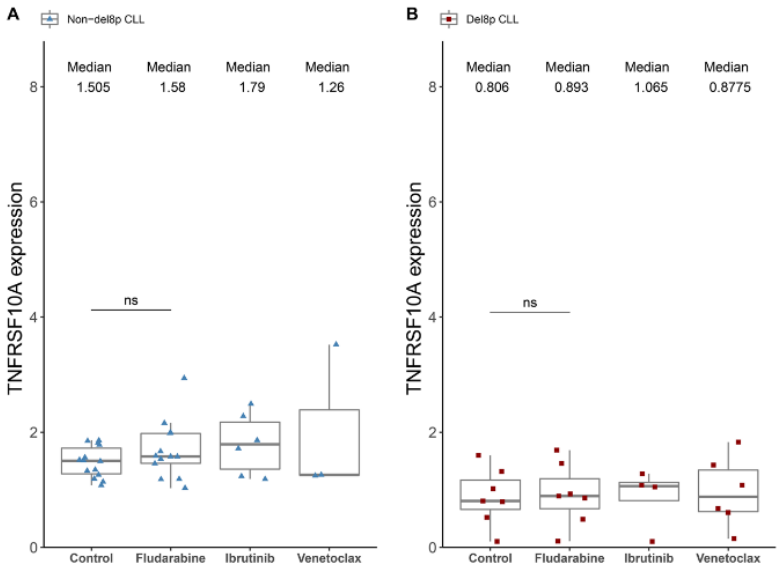

Figure S11. ***TNFRSF10A*** **expression was not modulated in primary CLL cells by treatment with fludarabine, ibrutinib or venetoclax**. (**A**) Non-del8p primary CLL cells were treated with 10 µM fludarabine (n=12), 10 µM ibrutinib (n=6), or 1 nM venetoclax (n=3). The mRNA was purified after 24 h of treatment, and the *TNFRSF10A* expression (relative to control non-treated cells; n=14) was measured using ddPCR. *ABL1* mRNA expression was used to normalize the data. (**B**) Del8p primary CLL cells were treated (or not) with 10 µM fludarabine (n=7), 10 µM ibrutinib (n=4), or 1 nM venetoclax (n=6), mRNA was purified as in (**A**), and the *TNFRSF10A* expression (relative to non-treated cells (n=7)) was measured by ddPCR. *ABL1* mRNA expression was used to normalize the data. Independently of del8p status, no significant increases in TNFRSF10A expression were recorded. The box corresponds to the interquartile range, the central line corresponds to the median, and the whiskers correspond to the range. Statistical analyses were performed using a Mann-Whitney U test.

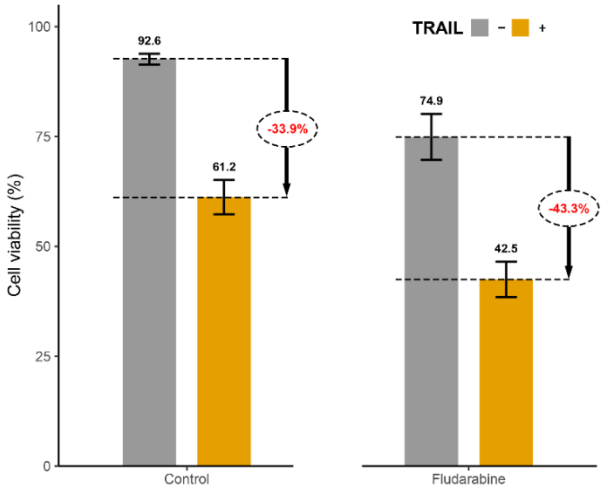

Figure S12. Fludarabine treatment potentiates TRAIL-induced cell death in the wild-type OSU-CLL cell line. Cell viability was measured using flow cytometry (dual negative annexin-V/PI staining) and expressed as the mean ± SD (n=3). For the untreated control samples and fludarabine-treated samples, TRAIL-induced cell death was defined as the viability loss in TRAIL-exposed cells as a proportion of that observed in cells not exposed to TRAIL.

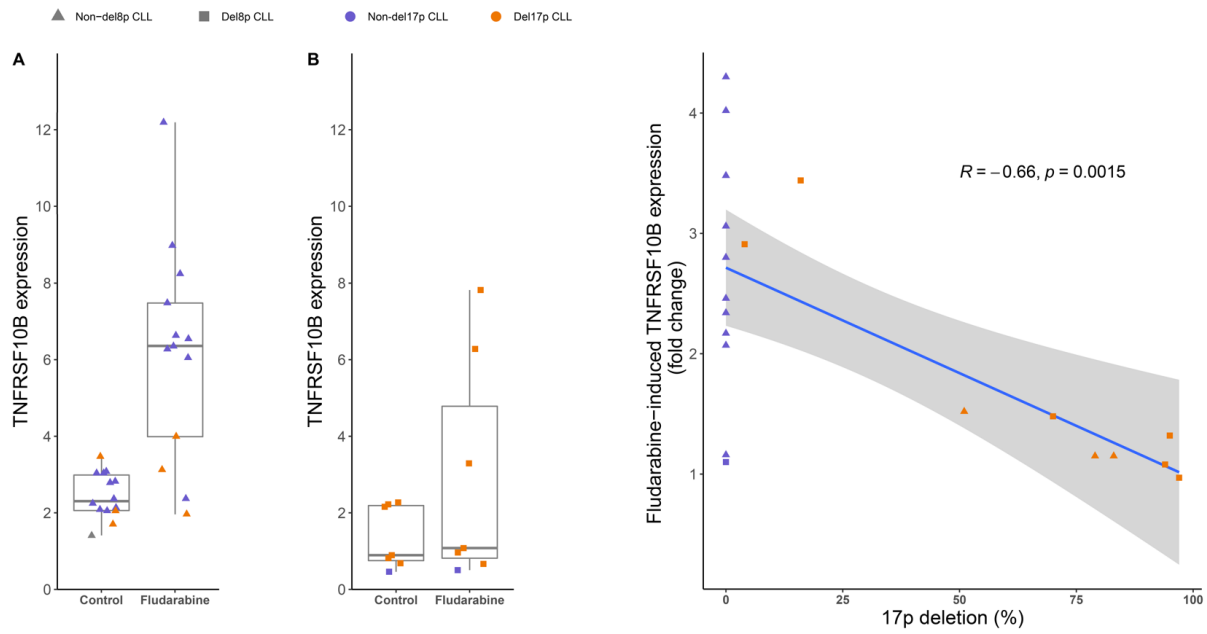

Figure S13. Del8p abolishes fludarabine-induced increase in *TNFRSF10B* expression in CLL cells, independently of del17p status. (**A**) Non-del8p primary CLL cells (n=13, triangles) and (**B**) del8p (n=7, squares) primary CLL cells were treated with fludarabine for 24h, and the *TNFRSF10B* mRNA expression was quantified by ddPCR. *ABL1* mRNA expression was used to normalize the data. del17p B cells are indicated in orange, and non-del17p B cells are indicated in purple. Fludarabine-induced *TNFRSF10B* expression was lower in del8p samples than in non-del8p samples, irrespective of the del17p status. The right panel represents the fludarabine-induced *TNFRSF10B* expression (as a ratio normalized against untreated cells) vs. the percentage of CLL cells harboring del17p. The box corresponds to the interquartile range, the central line corresponds to the median, and the whiskers to the range. Statistical analyses were performed using a Mann-Whitney U test. *, P < .05.

Article 2

Genetic characterization of B-cell prolymphocytic leukemia: a prognostic model involving MYC and TP53

Blood, 2019 Nov 21;134(21):1821-1831

La leucémie prolymphocytaire à cellules B (LPL-B) est une hémopathie lymphoïde B mature rare et généralement considérée comme agressive, présentant de nombreuses similitudes avec d'autres hémopathies lymphoïdes B chroniques comme la leucémie lymphoïde chronique. Par définition, elle se caractérise par une accumulation de prolymphocytes B dans le sang, la moelle osseuse et la rate, jusqu'à représenter au moins 55% des cellules lymphoïdes circulantes, et après exclusion des autres hémopathies lymphoïdes chroniques – en particulier la leucémie lymphoïde chronique et les formes leucémiques de lymphome à cellules du manteau. En plus des marqueurs B classiques exprimés fortement (CD19, CD20, CD22, FMC7), l'immunophénotypage des prolymphocytes identifie le CD5 dans la moitié des cas, et le CD23 dans un tiers des cas (soit un score de Matutes habituellement ≤ 3). Au plan cytogénétique, on retrouve le plus souvent un caryotype complexe (dans plus de 70% des cas), comprenant fréquemment des anomalies impliquant le gène MYC (translocation, gain ; environ 60% des cas) et/ou le gène *TP53* (délétion, mutation ; environ 40% des cas). En raison de la rareté de la maladie, la stratégie thérapeutique ne fait pas consensus : par mimétisme avec la LLC, on peut discuter l'immuno-chimiothérapie par rituximab, fludarabine et cyclophosphamide chez les patients jeunes sans anomalie de *TP53* ; dans les autres cas de figure, les traitements ciblés (ibrutinib, vénétoclax…) peuvent être envisagés. Chez les patients jeunes en rémission, une allogreffe de cellules souches hématopoïétiques peut être discutée.

Dans cet article, nous avons cherché à dépeindre le portrait génétique des LPL-B, afin d'identifier les marqueurs pronostiques les plus significatifs, et leur impact sur la stratégie thérapeutique.

Pour cela, les données cliniques et les échantillons biologiques issus de 34 patients avec un diagnostic confirmé de LPL-B ont été analysés : par caryotype, FISH, biologie moléculaire et tests fonctionnels d'induction d'apoptose in vitro.

Dans notre étude, on mettait en évidence un caryotype complexe chez 73% des patients, voire hypercomplexe chez 45% des patients. L'anomalie la plus fréquente concernait le gène *MYC* (76%), de type translocation (62% ; impliquant les loci IGH, IGL ou IGK) ou plus rarement de type gain (15%). Une del17p impliquant *TP53* était retrouvée chez 38% des patients. L'analyse du statut mutationnel IGHV montrait un profil muté dans près de 80% des cas, et le gène *TP53* était muté chez 38% des patients. Prises ensemble, ces données cytogénétiques et moléculaires ont permis d'identifier 3 sous-groupes : le premier, en présence d'une translocation impliquant *MYC* (62%), souvent associée à des mutations de *MYC* mais rarement aux caryotypes complexes et aux anomalies de *TP53* ; un deuxième, en présence d'un gain *MYC* (15%), fréquemment associé aux caryotypes hypercomplexes ; et un troisième, sans altération de *MYC* (24%), mais au sein duquel on retrouve plus souvent des caryotypes complexes et des délétions 17p.

Au-delà des différences d'ordre cytologique ou phénotypique entre ces sous-groupes, cette stratification a permis d'identifier des différences significatives en matière de survie. Les médianes de survie globale étaient respectivement de 57.5 mois pour le groupe avec translocation impliquant *MYC*, 66.5 mois pour le groupe avec gain *MYC*, et non atteinte en l'absence d'anomalie de *MYC*. L'ensemble des patients porteurs d'une anomalie de *MYC* peut être lui-même divisé en 2 sous-groupes, selon la présence ou non d'une del17p : l'association d'une altération de *MYC* et d'une del17p s'accompagne d'une médiane de survie globale de 11.1 mois, contre 125.7 mois en présence d'une altération de *MYC* sans del17p.

Enfin, des tests d'apoptose induite in vitro sur des échantillons de cellules primaires porteuses d'une translocation impliquant *MYC* ont montré que les traitements classiques (fludarabine, ibrutinib, idélalisib et vénétoclax) permettaient de réduire la viabilité des cellules. L'effet de ces traitements était amplifié par l'ajout d'OTX015 (un inhibiteur de BET ciblant MYC). En revanche, la présence d'une del17p (en l'absence d'anomalie de *MYC*) s'accompagnait d'une résistance à ces mêmes traitements, en présence ou non d'OTX015.

Discussion

Depuis la publication de cet article, la nouvelle classification OMS 2022 (Alaggio et al., *Leukemia*, 2022) a décidé de retirer la LPL-B des entités constituant le spectre des hémopathies lymphoïdes B matures, en séparant les LPL-B CD5+ qui seraient des progressions prolymphocytiques de LLC, et les LPL-B CD5- qui seraient des lymphomes/leucémies spléniques avec nucléole proéminant. Un autre groupe internationalement reconnu de spécialistes a quant à lui gardé la LPL-B comme entité dans la classification consensus internationale des hémopathies matures lymphoïdes (Campo et al., *Blood* 2022). Notre équipe sous l'égide du groupe national de cytogénétique a envoyé un commentaire pour contester la décision de retirer la LPL-B des entités (Nguyen-Khac et al., *Leukemia*, 2022). La réponse est attendue.

blood®
Regular Article

LYMPHOID NEOPLASIA

CME Article

Genetic characterization of B-cell prolymphocytic leukemia: a prognostic model involving *MYC* and *TP53*

Elise Chapiro,[1-3] Elodie Pramil,[1,2] M'boyba Diop,[4] Damien Roos-Weil,[1,2,5] Clémentine Dillard,[1,2] Clémentine Gabillaud,[3] Karim Maloum,[3] Catherine Settegrana,[3] Lucile Baseggio,[6] Jean-François Lesesve,[7] Mélanie Yon,[1,2] Ludovic Jondreville,[1,2] Claude Lesty,[2] Frédéric Davi,[1-3] Magali Le Garff-Tavernier,[1,3] Nathalie Droin,[4] Philippe Dessen,[4] Caroline Algrin,[8] Véronique Leblond,[2,5] Jean Gabarre,[5] Simon Bouzy,[3] Virginie Eclache,[9] Baptiste Gaillard,[10] Evelyne Callet-Bauchu,[6] Marc Muller,[11] Christine Lefebvre,[12] Nathalie Nadal,[13] Antoine Ittel,[14] Stéphanie Struski,[15] Marie-Agnès Collonge-Rame,[16] Benoit Quilichini,[17] Sandra Fert-Ferrer,[18] Nathalie Auger,[19] Isabelle Radford-Weiss,[20] Lena Wagner,[21] Sebastian Scheinost,[21] Thorsten Zenz,[22] Santos A. Susin,[1,2] Olivier A. Bernard,[23,24] and Florence Nguyen-Khac,[1-3] for the Groupe Francophone de Cytogénétique Hématologique (GFCH) and the French Innovative Leukemia Organization (FILO)

[1]Cell Death and Drug Resistance in Lymphoproliferative Disorders Team, Centre de Recherche des Cordeliers, INSERM UMRS 1138, Paris, France; [2]Sorbonne Université, Paris, France; [3]Service d'Hématologie Biologique, Hôpital Pitié-Salpêtrière, Assistance Publique–Hôpitaux de Paris (AP-HP), Paris, France; [4]AMMICa, INSERM US23/Centre National de la Recherche UMS3655, Gustave Roussy, Villejuif, France; [5]Service d'Hématologie Clinique, Hôpital Pitié-Salpêtrière, AP-HP, Paris, France; [6]Service d'Hématologie Biologique, hospices Civils de Lyon, Lyon, France; [7]Service d'Hématologie Biologique, Centre Hospitalier Régionaux et Universitaire Nancy, and INSERM U1256 NGERE, Université de Lorraine, Nancy, France; [8]Service d'Oncologie, Groupe Hospitalier Mutualiste de Grenoble, Grenoble, France; [9]Laboratoire d'Hématologie, Hôpital Avicenne, AP-HP, Bobigny, France; [10]Laboratoire d'Hématologie, Hôpital Robert Debré, Reims, France; [11]Laboratoire de Génétique, Centre Hospitalier Universitaire (CHU) Nancy, Nancy, France; [12]Laboratoire de Cytogénétique Onco-hématologique, CHU Grenoble, Grenoble, France; [13]Service de génétique chromosomique et moléculaire, CHU Dijon, Dijon, France; [14]Cytogénétique, Institut Universitaire du Cancer de Toulouse, Toulouse, France; [15]Laboratoire de Cytogénétique Hématologique, CHU Strasbourg, Strasbourg, France; [16]Service de Génétique Biologique-Histologie, CHU Besançon, Besançon, France; [17]Département Hématologie Cellulaire/Cytogénétique, Biomnis, Lyon, France; [18]Laboratoire de Génétique Chromosomique, Centre Hospitalier Métropole Savoie, Chambéry, France; [19]Laboratoire de Cytogénétique, Institut Gustave Roussy, Villejuif, France; [20]Laboratoire de Cytogénétique, Hôpital Necker-Enfants Malades, AP-HP, Paris, France; [21]National Center for Tumor Diseases and German Cancer Research Centre, Heidelberg, Germany; [22]Department of Medical Oncology and Haematology, University Hospital Zurich and University of Zürich, Zürich, Switzerland; [23]INSERM, U1170, Institut Gustave Roussy, Villejuif, France; and [24]Université Paris-Sud/Paris Saclay, Orsay, France

KEY POINTS

- **B-PLL is tightly linked to *MYC* aberrations (translocation or gain) and 17p (*TP53*) deletion.**
- **Cases of B-PLL with *MYC* aberration and 17p (*TP53*) deletion have the worst prognosis.**

B-cell prolymphocytic leukemia (B-PLL) is a rare hematological disorder whose underlying oncogenic mechanisms are poorly understood. Our cytogenetic and molecular assessments of 34 patients with B-PLL revealed several disease-specific features and potential therapeutic targets. The karyotype was complex (≥3 abnormalities) in 73% of the patients and highly complex (≥5 abnormalities) in 45%. The most frequent chromosomal aberrations were translocations involving *MYC* [t(*MYC*)] (62%), deletion (del)17p (38%), trisomy (tri)18 (30%), del13q (29%), tri3 (24%), tri12 (24%), and del8p (23%). Twenty-six (76%) of the 34 patients exhibited an *MYC* aberration, resulting from mutually exclusive translocations or gains. Whole-exome sequencing revealed frequent mutations in *TP53, MYD88, BCOR, MYC, SF3B1, SETD2, CHD2, CXCR4,* and *BCLAF1*. The majority of B-PLL used the *IGHV3* or *IGHV4* subgroups (89%) and displayed significantly mutated *IGHV* genes (79%). We identified 3 distinct cytogenetic risk groups: low risk (no *MYC* aberration), intermediate risk (*MYC* aberration but no del17p), and high risk (*MYC* aberration and del17p) ($P = .0006$). In vitro drug response profiling revealed that the combination of a B-cell receptor or BCL2 inhibitor with OTX015 (a bromodomain and extra-terminal motif inhibitor targeting *MYC*) was associated with significantly lower viability of B-PLL cells harboring a t(*MYC*). We concluded that cytogenetic analysis is a useful diagnostic and prognostic tool in B-PLL. Targeting *MYC* may be a useful treatment option in this disease. (*Blood*. 2019;134(21):1821-1831)

Medscape, LLC designates this Journal-based CME activity for a maximum of 1.00 *AMA PRA Category 1 Credit(s)*™. Physicians should claim only the credit commensurate with the extent of their participation in the activity.

Successful completion of this CME activity, which includes participation in the evaluation component, enables the participant to earn up to 1.0 MOC points in the American Board of Internal Medicine's (ABIM) Maintenance of Certification (MOC) program. Participants will earn MOC points equivalent to the amount of CME credits claimed for the activity. It is the CME activity provider's responsibility to submit participant completion information to ACCME for the purpose of granting ABIM MOC credit.

All other clinicians completing this activity will be issued a certificate of participation. To participate in this journal CME activity: (1) review the learning objectives and author disclosures; (2) study the education content; (3) take the post-test with a 75% minimum passing score and complete the evaluation at **http://www.medscape.org/journal/blood**; and (4) view/print certificate. For CME questions, see page 1879.

Disclosures

Associate Editor John C. Byrd received grants for clinical research from Acerta; Genentech, Inc.; Janssen Pharmaceuticals, Inc.; and Pharmacyclics, Inc. CME questions author Laurie Barclay, freelance writer and reviewer, Medscape, LLC and the authors declare no competing financial interests.

Learning objectives

Upon completion of this activity, participants will be able to:

1. Describe the genetic portrait of B-cell prolymphocytic leukemia (B-PLL), according to cytogenetic and molecular testing in a case series
2. Determine correlations between cytogenetic and molecular findings and patients' clinical outcomes, according to cytogenetic and molecular testing in a case series
3. Identify primary B-PLL cells' in vitro response to novel targeted therapeutics, according to cytogenetic and molecular testing in a case series

Release date: November 21, 2019; Expiration date: November 21, 2020

Introduction

B-cell prolymphocytic leukemia (B-PLL) is a very rare disease that accounts for <1% of all cases of chronic B-cell leukemia and generally occurs in elderly individuals. According to the World Health Organization criteria, B-PLL can be diagnosed when prolymphocytes comprise >55% of the lymphoid cells in peripheral blood. Diagnosis on the basis of clinical and morphological data can be difficult because B-PLL shares a number of features with other B-cell malignancies, including splenic marginal zone lymphoma (MZL), mantle cell lymphoma (MCL), and chronic lymphocytic leukemia (CLL). For example, an unusual leukemic form of MCL mimicking B-PLL is distinguished by the presence of the t(11;14)(q13;q32) translocation.[1,2] B-PLL does not have a specific immunophenotype and has low Matutes scores,[3,4] as observed for other B lymphoproliferative disorders.

Little is known about the oncogenic events leading to the development and clinical heterogeneity of B-PLL. Given the disease's rarity, its cytogenetic features have only been described in case reports and small series,[5,6] and large-scale genomic sequencing has not yet been performed for this disease.

Rituximab-based chemo-immunotherapy is often used to treat patients who have B-PLL but no *TP53* aberrations. In patients with *TP53* aberrations, alemtuzumab-based regimens have been implemented. Lasting treatment responses are rare, and the prognosis is generally poor.[7] Recent data from case reports and small series suggest that 2 agents targeting B-cell signaling (ibrutinib and idelalisib) are efficacious.[8-10] Hence, allogeneic hematopoietic stem cell transplantation is still the only curative treatment of B-PLL, albeit in younger patients only.[7]

In the present study, we performed cytogenetic and molecular assessments in one of the largest reported series of patients with a validated diagnosis of B-PLL. We further sought correlations between the cytogenetic and molecular findings and the patients' clinical outcomes. Lastly, we studied the in vitro response of the primary B-PLL cells to novel targeted therapeutic agents. To the best of our knowledge, the present study is the first to provide an extensive genetic portrait of B-PLL and to offer insights into prognostic markers and treatment options.

Patients, materials, and methods

Patient selection

Databases from 28 French health care establishments were retrospectively screened for cases of de novo B-PLL. Patients with a history of another B-cell malignancy (CLL or MZL) were excluded. A total of 87 patients with an available blood smear at diagnosis were first identified locally, based on cell morphological criteria. All 87 blood smears were blind-reviewed by 3 independent expert cytologists (L.B., K.M., and C.S.), and 10 representative smears were subsequently reviewed further by a fourth cytologist (J.-F.L.) (supplemental Methods; supplemental Table 1; available on the *Blood* Web site). Only 34 of the 87 cases met the World Health Organization criteria for B-PLL (ie, prolymphocytes accounted for >55% of the lymphoid cells in peripheral blood). A diagnosis of MCL was ruled out according to karyotype (K) and fluorescence in situ hybridization (FISH) assays: no *CCND1* rearrangements or other infrequent translocations involving *CCND2* and *CCND3* were observed.[11,12] Four other patients carrying a translocation t(11;14)(q13;q32) with a *CCND1* rearrangement were diagnosed as having MCL and were excluded. Cytogenetic and molecular analyses were performed on the available material: at diagnosis for 21 patients, during follow-up and before treatment for 10 patients (median time between diagnosis and sampling, 44 months), and at relapse for 3 patients. The study was performed in accordance with the Declaration of Helsinki and was approved by the local investigational review board (CPP-Ile-de-France VI, Paris, France) on 21 May 2014.

Karyotyping and FISH analysis

Standard chromosome banding analyses were used to obtain R- or G-banded chromosomes from peripheral blood (n = 28),

bone marrow (n = 4), or spleen (n = 1) samples. The samples were cultured for 48 to 72 hours with 12-*O*-tetradecanoylphorbol-13-acetate (n = 6) or CpG-oligonucleotides and interleukin-2 (n = 27). All the karyotyping results were reviewed by the members of the Groupe Francophone de Cytogénétique Hématologique and classified according to the International System for Human Cytogenetic Nomenclature (2016). Complex Ks (CKs) and highly complex Ks (HCKs) were defined as the presence of at least 3 or 5 numerical or structural chromosomal abnormalities, respectively. Standard FISH was performed in all cases. The specific probes and procedures used are detailed in the supplemental Methods.

Whole-exome sequencing

DNA extracted from flow-sorted CD19$^+$ tumor cells (and CD5$^+$, IGL, or IGK when appropriate) and nontumor (CD3$^+$) cells (considered to be germinal controls) was used for exome capture according to standard procedures. Paired-end sequencing was performed by using HiSeq2000 sequencing instruments (Illumina, San Diego, CA). More detailed information can be found in the supplemental Methods.

Targeted deep resequencing

Mutation validation using targeted deep resequencing was performed as previously described.[13] Details are available in the supplemental Methods.

IGHV analysis

IGH rearrangement sequencing was performed on DNA extracted from sorted tumor cells or from whole blood, as previously described.[14] Depending on the percentage of identity of the *IGHV* genes with their germline counterparts, sequences were considered as unmutated (100% identity), minimally/borderline mutated (99.9%-97%), or significantly mutated (<97% identity), following criteria proposed by Hadzidimitriou et al[15] for MCL and Bikos et al[16] for MZL.

RNA sequencing

RNA sequencing (RNA-seq) was performed on high-quality RNA from twelve B-PLL as previously described.[17] More detailed information can be found in the supplemental Methods.

In vitro cell viability and programmed cell death assays

The viability of primary B-PLL cells was assessed with the adenosine triphosphate (ATP)-based CellTiter-Glo 2.0 assay (Promega, Madison, WI). Briefly, after pretreatment (or not) with the bromodomain and extra-terminal motif protein inhibitors (iBETs) OTX015 or JQ1 (500 nM), B-PLL cells were exposed for 48 hours to increasing concentrations of fludarabine, ibrutinib, idelalisib, or venetoclax. Viability was determined by normalizing luminescence units against a dimethyl sulfoxide control. Alternatively, programmed cell death was measured by flow cytometry using Annexin-V and propidium iodide colabeling, after B-PLL cell treatment of 48 hours with ibrutinib, idelalisib, venetoclax, or OTX015. Details are provided in the supplemental Methods. All drugs were purchased from Selleckchem (Houston, TX).

Statistical analysis

Overall survival (OS) was defined as the time interval between diagnosis and death or last follow-up. Categorical variables were

Table 1. Characteristics of the patients with B-PLL

Parameter	Whole cohort (N = 34)
Age at diagnosis, median (range), y	72 (46.2-87.9)
Sex, male/female	20/14
Splenomegaly, n/N (%)	18/31 (58)
Lymphadenopathy, n/N (%)	6/31 (19)
Lymphocytosis, median (range), G/L	36 (4.6-244)
Prolymphocytes, median (range), %	79.5 (60-100)
Treated patients, n/N (%)	29/33 (88)
Death, n/N (%)	14/33 (42)
Follow-up, median (range), mo	47 (0.2-141)
OS, median (95% CI), mo	125.7 (52.3-132.1)
TTT, median (95% CI), mo	5.8 (1.5-27.5)
CD38$^+$, n/N (%)	20/33 (61)
Matutes score, n/N (%) 0 1 2 3	 8/33 (25) 11/33 (33) 9/33 (27) 5/33 (15)
CD5$^+$, n/N (%)	19/34 (56)
CD23$^+$, n/N (%)	11/34 (32)
CK (≥3 abnormalities)*, n/N (%)	24/33 (73)
HCK (≥5 abnormalities)*, n/N (%)	15/33 (45)
No. of karyotypic aberrations, median (range)*	4 (1-21)
Unbalanced translocations*, n/N (%)	23/33 (70)
t(*MYC*), n/N (%)	21/34 (62)
del17p (*TP53*), n/N (%)	13/34 (38)
tri12, n/N (%)	8/34 (24)
tri3, n/N (%)	8/33 (24)
tri18, n/N (%)	10/33 (30)
MYC gain, n/N (%)	5/34 (15)
del13q, n/N (%)	10/34 (29)
del8p (*TNFRSF10*), n/N (%)	7/31 (23)
IGHV mutated, n/N (%)	16/19 (84)
TP53 mutated, n/N (%)	6/16 (38)
MYD88 mutated, n/N (%)	4/16 (25)
BCOR mutated, n/N (%)	4/16 (25)
MYC mutated, n/N (%)	3/16 (19)
SF3B1 mutated, n/N (%)	3/16 (19)

CI, confidence interval; TTT, time to first treatment.

*The frequency of chromosomal abnormalities did not differ significantly when comparing patients at diagnosis vs patients during follow-up and treated patients vs untreated patients.

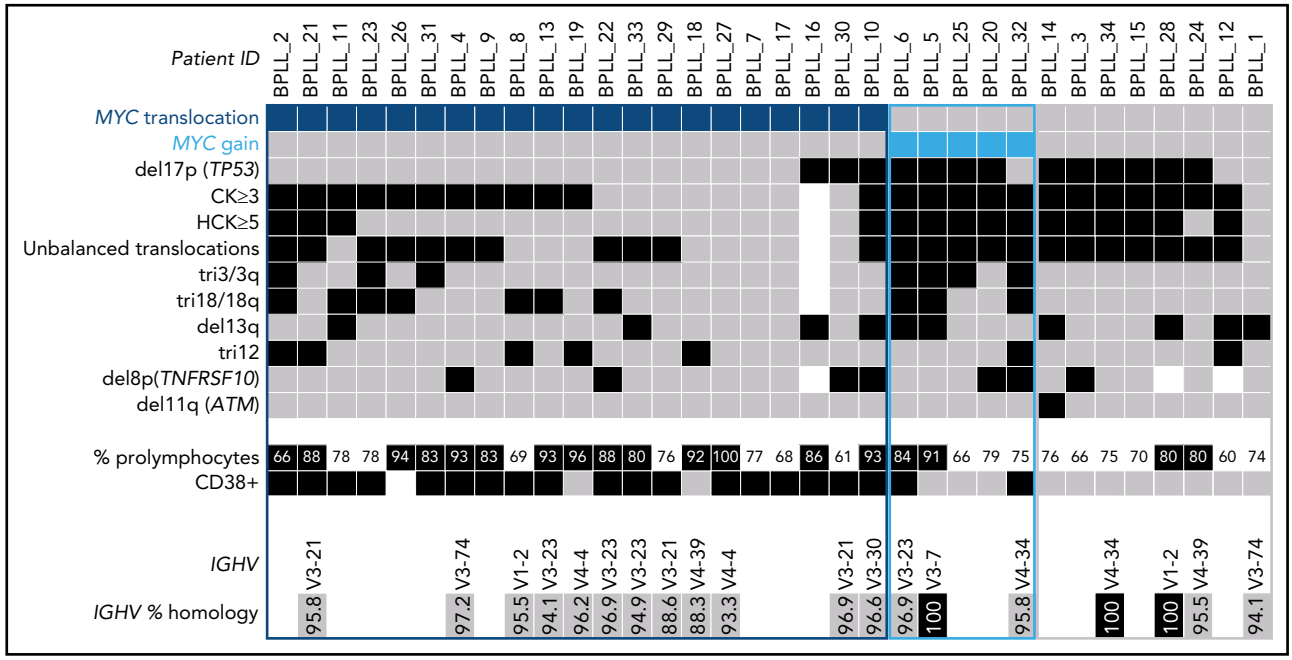

Figure 1. Distribution of chromosomal abnormalities detected in 34 patients with B-PLL with 3 cytogenetic subgroups of patients: *MYC* translocation, *MYC* gain, and no *MYC* aberration. Each column represents 1 patient, and each row 1 particular genetic or laboratory parameter. Color code: black or blue, presence; gray, absence; white, not available. CK, ≥3 chromosomal abnormalities; HCK, ≥5 chromosomal abnormalities. The percentages of prolymphocytes (indicated in black boxes) correspond to above-median values, relative to the cohort as a whole.

compared by using a χ^2 test or Fisher's exact test; continuous variables were compared by using the Mann-Whitney *U* test. Survival analyses were performed by using the Kaplan-Meier method, and the log-rank test was used for intergroup comparisons of OS curves. Two-sided $P < .05$ was considered statistically significant. All statistical analyses were performed by using MedCalc software (version 17.8.6, Ostend, Belgium).

Additional methods are described in the supplemental Methods.

Results

Characteristics of the study population

The study included 34 patients diagnosed with de novo B-PLL between 1992 and 2017 (Table 1). There was a predominance of male subjects (59%), and the median (range) age at diagnosis was 72 (46.2-87.9) years. The median lymphocyte count was 36 (4.6-244) G/L, and the median proportion of prolymphocytes was 79.5 (60-100). Nineteen of the 34 patients (56%) were positive for CD5 (supplemental Table 2). The median follow-up time after diagnosis was 47 (0.2-141) months. Most of the patients had been treated (29 of 33 [88%]) with a median time after diagnosis of 3.2 (0-106) months.

Chromosomal aberrations: *MYC* is the most frequently altered gene in B-PLL

Karyotyping was performed in 33 patients (Table 1; supplemental Table 3). A CK was found in 73% of the patients, and HCK in 45%. By combining K and FISH data, we observed that the most frequent abnormality, found in 21 (62%) of the 34 patients, was a translocation involving the *MYC* gene [t(*MYC*)]. This translocation involved the *IGH* locus in 12 cases, *IGL* in 6, and *IGK* in 1; the *MYC* gene partner was not identified in 2 cases. Five (15%) of the 34 patients had gained copies of the *MYC* gene: three had 3 copies, one had 4 copies, and one had *MYC* amplification. Thus, the majority of the cases (26 of 34 [76%]) had an *MYC* abnormality, *MYC* translocation and *MYC* gain being mutually exclusive. The other frequent chromosomal aberrations were: deletion (del)17p including the *TP53* gene (13 of 34 [38%]), trisomy (tri) 18/18q (10 of 33 [30%]), del13q (10 of 34 [29%]), tri3 (8 of 33 [24%]), tri12 (8 of 34 [24%]), and del8p (7 of 31 [23%]) (Figure 1).

An analysis of copy number values (calculated from the whole-exome sequencing [WES] coverage in 16 patients) confirmed the majority of recurrent losses and gains observed by karyotyping and/or FISH analyses and highlighted other novel recurrent copy number variations: losses of 5q22-23, 9q34, 14q24, and 19p13, and gains of 17q24, 1q31-42, and 4q27-35 (supplemental Table 4).

IGHV analyses: preferential usage of *VH3* and *VH4* genes, and frequently mutated *IGHV* genes

We obtained clonal *IGH* sequences in 19 patients with B-PLL. In 17 (89%) of the 19 B-PLL cases, a member of the *IGHV3* (n = 11, including 4 *IGHV3-23*) or *IGHV4* (n = 6) subgroups was involved; the *IGHV1* subgroup gene (*IGHV1-2*) was used in the 2 remaining cases. Furthermore, the vast majority of B-PLL sequences (15 of 19 [79%]) displayed significantly mutated *IGHV* genes (Figure 1; supplemental Table 5).

The spectrum of somatic mutations

WES of paired tumor-control DNA was performed in 16 patients, and mutations were validated by using targeted deep-resequencing and/or RNA-seq (supplemental Figure 1; supplemental Table 6). We identified 10 genes that were mutated in at least 2 patients

Table 2. Recurrently mutated genes identified by using WES in 16 patients with B-PLL

Gene	No. of cases	No. of mutations identified	Mutations	Biological process
TP53 (NM_000546)	6	7	p.A129Pfs*41 + p.V132L, T205C, V236G, A248D, L275Q, R282P	Cell cycle, apoptosis
MYD88 (NM_002468)	4	4	L265Px2, M232T, S219C	NF-kB pathway
BCOR (NM_001123385)	4	4	F924C, N1459Sx2, P1648Lfs*4	Chromatin remodeling
MYC (NM_002467)	3	3	V160L, S161L, F389L	Cell cycle
SF3B1 (NM_012433)	3	3	K700Ex3	Spliceosome
SETD2 (NM_014159)	2	2	2 p.Gly878Glnfs*14, L1577P	Chromatin remodeling (histone H3K36 methyltransferase)
CHD2 (NM_001271)	2	2	P1387Rfs*13, V1163Gfs*3	Chromatin remodeling
CXCR4 (NM_003467)	2	2	S338X, S325Qfs*22	Cell migration
BCLAF1 (NM_001077440)	2	2	R820C, W211X	RNA processing factor
NFASC (NM_001005388)	2	2	T946I, V644M	Neuronal development

(Table 2). The most frequently mutated gene was *TP53*, with a total of 7 mutations observed in 6 (38%) of the 16 patients. These *TP53* mutations were predicted to affect the protein's DNA-binding domain (supplemental Figure 2). In all cases, these mutations were associated with a del17p. Mutations in *MYD88* were found in 4 patients. Interestingly, the *MYD88* mutation was associated with tri3 in 2 cases, with a variant allele frequency of 66.5% (BPLL_6) and 67.4% (BPLL_32) indicating that the mutated copy was duplicated. Mutations in genes that have a role in chromatin modifications were recurrent, including the X-linked *BCOR* gene encoding a BCL6 corepressor (n = 4), *CHD2* (n = 2), *SETD2* (n = 2), and other genes mutated in 1 patient each (*CREBBP*, *EZH2*, *KMT2D*, *NCOR1*, *SETD1B*, and *TET2*). The *MYC* gene had missense mutations in 3 patients, all of whom harbored a t(*MYC*). Two mutations were just downstream of the transactivation domain, and one was in the bHLH

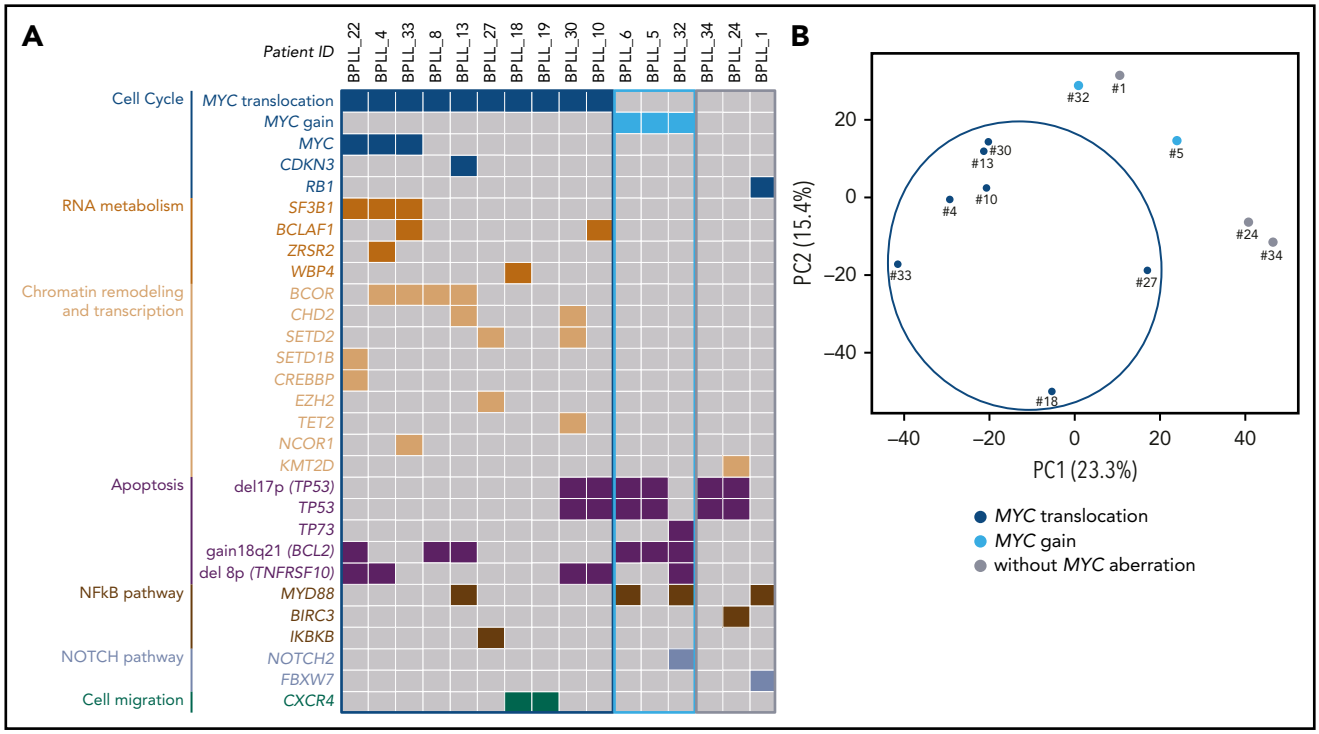

Figure 2. WES and RNA-seq. (A) Distribution of the chromosomal aberrations and mutations in the 3 cytogenetic subgroups (*MYC* translocation, *MYC* gain, and no *MYC* aberration) in the 16 cases analyzed by using WES. Chromosomal abnormalities: gray, absence; color, presence. Mutations: gray, wild type; color, mutated. (B) Principal component analysis of differential gene expression patterns for 12 samples with various cytogenetic abnormalities.

Table 3. Comparison of the 3 cytogenetic subgroups (S) (*MYC* translocation, *MYC* gain, and no *MYC* activation): significant results

Parameter	S1: t(*MYC*) (n = 21 [62%])	S2: *MYC* gain (n = 5 [15%])	S3: no *MYC* (n = 8 [23%])	Comparison	*P*
Prolymphocytes (range), %	86 (61-100)	79 (66-91)	76 (60-80)	S1 vs S2 + S3	.03
				S3 vs S1 + S2	.03
$CD38^+$, n/N (%)	18/20 (90)	2/5 (40)	0/8 (0)	S1 vs S2 + S3	<.0001
				S3 vs S1 + S2	<.001
No. of chromosomal abnormalities (range)	3 (1-9)	6 (5-21)	10 (1-15)	S1 vs S2 + S3	.0005
				S3 vs S1 + S2	.02
HCK (≥5 abnormalities), n/N (%)	4/20 (20)	5/5 (100)	6/8 (75)	S1 vs S2 + S3	.0004
				S2 vs S1 + S3	.01
Unbalanced translocations, n/N (%)	11/20 (55)	5/5 (100)	7/8 (88)	S1 vs S2 + S3	.04
del17p, n/N (%)	3/21 (14)	4/5 (80)	6/8 (75)	S1 vs S2 + S3	.0006
				S3 vs S1 + S2	.03
tri3, n/N (%)	4/20 (20)	4/5 (80)	0/8 (0)	S2 vs S1 + S3	.008

domain. The products of other relevant mutated genes were found to be involved in RNA metabolism (*SF3B1*, *BCLAF1*, *ZRSR2*, and *WBP4*), cell migration (*CXCR4*), cell cycle (*CDKN3* and *RB1*), apoptosis (*TP73*), and NOTCH signaling (*NOTCH2* and *FBXW7*) (Figure 2).

IGL/PVT1 fusions

Using RNA-seq, we detected *IG* fusion transcripts in 3 of 7 patients with t(*MYC*). In case #27 harboring a t(8;14)(q24;q32), *IGHG1* was fused with intron 1 of *MYC*. In cases BPLL_4 and BPLL_30 with a t(8;22)(q24;q11), the *PVT1* gene was fused to *IGLL5* or *IGLV4-69*01*, respectively. The 2 latter fusions were confirmed by using a reverse-transcriptase polymerase chain reaction assay. No other recurrent fusion transcripts were found in the 12 patients with RNA-seq data (supplemental Table 7).

Clonal organization

With a view to identifying early and late oncogenic events, we evaluated the clonal or subclonal nature of chromosomal abnormalities and recurrent somatic mutations. We observed that t(*MYC*), del17p, tri12, and mutations in the *TP53*, *BCOR*, *MYC*, *SF3B1*, and *MYD88* genes were mostly clonal and should be considered as early events in B-PLL. In contrast, *MYC* gain, del8p, and del13q were frequently subclonal, indicating that they are acquired (supplemental Figure 3).

Correlations between cytogenetic aberrations, mutations, and gene expression patterns

Three cytogenetic subgroups were identified (Figure 1; Table 3). The main subgroup of patients (21 of 34 [62%]) had a t(*MYC*). Relative to the patients without t(*MYC*), this subgroup had a higher percentage of prolymphocytes ($P = .03$), a higher proportion of $CD38^+$ cells ($P < .0001$), a lower level of cytogenetic complexity ($P = .0005$), a lower proportion of cases with HCK ($P = .0004$), fewer unbalanced translocations ($P = .04$), and fewer cases with del17p ($P = .0006$). Mutations in *MYC* and in genes involved in RNA metabolism, chromatin remodeling and transcription were almost exclusively observed in the t(*MYC*) subgroup, whereas mutations in *TP53* were less frequent (Figure 2A). A principal component analysis of gene expression data from the 12 cases analyzed by using RNA-seq showed that the 7 patients with t(*MYC*) clustered together (Figure 2B). Taken as a whole, these results suggest that patients with t(*MYC*) form a homogeneous subgroup of B-PLL. A second subgroup of B-PLL with *MYC* gain (5 of 34 [15%]) was associated with HCK ($P = .01$) and tri3 ($P = .008$). The remaining 8 patients corresponded to a third subgroup lacking an *MYC* aberration. Compared with patients with the *MYC* aberration, this third subgroup had a lower percentage of prolymphocytes ($P = .03$), no $CD38^+$ expression ($P < .001$), a higher number of chromosomal aberrations ($P = .02$), and a higher frequency of del17p ($P = .03$) (Table 3).

Survival analyses: the prognostic values of MYC aberrations and del17p

The median OS for the entire study cohort was 125.7 months. Patients with t(*MYC*) had a median (95% CI) OS of 57.5 months (25.7-132.1), which did not differ significantly from the value observed for patients with *MYC* gain (median, 66.5 months) (Figure 3A). Hence, we pooled patients with an *MYC* aberration for subsequent OS comparisons and found that they had a significantly shorter OS than patients without *MYC* aberrations ($P = .03$) (Figure 3B).

With regard to the combination of *MYC* and del17p aberrations, 3 distinct prognostic groups were identified with significant differences in OS ($P = .0006$) (Figure 3C). The patients without an *MYC* aberration (n = 8) had the lower risk (median not reached). Patients with an *MYC* aberration (translocation or gain) but no del17p (n = 18) had an intermediate risk (125.7 months). The high-risk group corresponded to patients with both *MYC* and del17p (n = 7; 11.1 months).

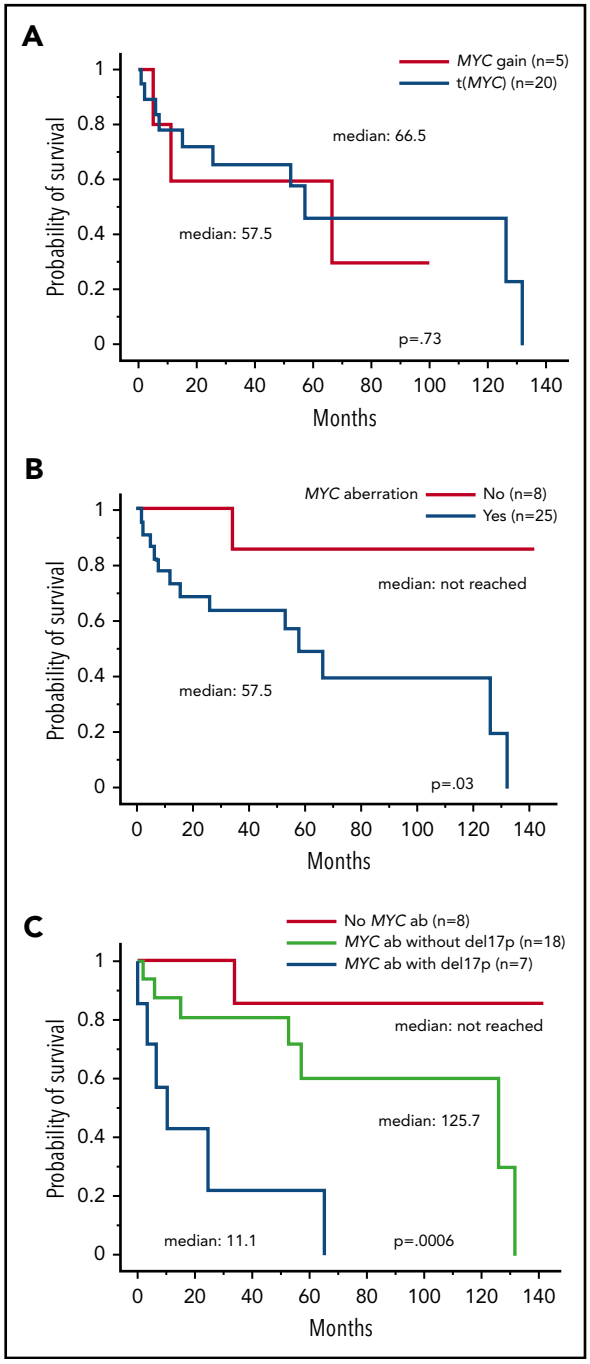

Figure 3. Overall survival in patients with B-PLL. Panels A-B as a function of *MYC* aberrations [t(*MYC*) or gain] and the presence or absence of *MYC* aberration; the t(*MYC*) and *MYC* gain data were pooled. (A) t(*MYC*) median (95% CI), 57.5 months (25.7-132.1); *MYC* gain median (95% CI), 66.5 months (4.7-undetermined). (B) *MYC* aberration [t(*MYC*) + *MYC* gain] median (95% CI), 57.5 (25.7-132.1). (C) *MYC* and del17p status. *MYC* aberration without del17p median (95% CI), 125.7 months (52.2-132.1); MYC aberration with del17p median (95% CI), 11.1 months (4.7-66.5). ab, aberration.

Other chromosomal abnormalities and K complexity had no significant impact on OS. Patients with del17p tended to have a shorter OS than those without del17p (supplemental Figure S4).

In vitro drug response assays

To evaluate the sensitivity of B-PLL cells to drugs used in the treatment of B-cell malignancies, we first used a cell viability assay based on the quantification of cellular ATP levels (an indicator of metabolic activity[18]) on primary B-PLL cells after 48 hours of exposure to ibrutinib, idelalisib (both B-cell receptor inhibitors), venetoclax (a highly specific inhibitor of the antiapoptotic protein BCL2), and fludarabine. The drugs were tested alone or in combination with OTX015 (an iBET known to suppress *MYC* expression in leukemia and lymphoma cell lines).[19-21] Treatment with increasing doses of single drugs resulted in reduced cell viability in the 3 cases with t(*MYC*) (BPLL_8, BPLL_13, and BPLL_18) but varied from one drug to another and from one patient to another. Relative to treatments with single drugs, OTX015 cotreatment with low doses of fludarabine, ibrutinib, or venetoclax was associated with a much lower level of viability (<30%) in patients with t(*MYC*) (Figure 4A). In contrast, the patient harboring a del17p but not an *MYC* aberration (BPLL_34) was significantly more resistant to single drugs and OTX015 cotreatments than patients with t(*MYC*) (Figure 4B).

To confirm these results, a complementary cytofluorometric approach was used. In BPLL_8 with t(*MYC*), treatments with drugs alone killed between 13% and 27% of the cells. An additive effect of OTX015 was observed; between 48% and 63% of the cells were killed (Figure 4C). Cells from patient BPLL_34 (del17p but no *MYC* aberration) were less sensitive to all drugs tested in both the presence and absence of OTX015 (Figure 4D). Thus, the ATP assay and flow cytometry assay results highlighted the efficacy of combined drug + iBET treatment of cells from patients with t(*MYC*). The enhancing effect of the iBETs on the programmed cell death induced by fludarabine, ibrutinib, and venetoclax was fully corroborated by the results of cotreatment with JQ1, another well-known iBET (supplemental Figure 5B-C). It should be noted that we did not test any cases with *MYC* gain.

Discussion

In the present study, 34 patients with B-PLL were genetically characterized. Given that the diagnosis of B-PLL is challenging, a thorough morphological review of blood smears was performed by 3 independent cytologists. Although patients with a history of MZL were excluded, the absence of a biopsy analysis means that we cannot fully rule out the possible presence of MZL with a prolymphocytoid transformation, an extremely rare situation.[22]

To the best of our knowledge, the present series is the largest yet to have undergone a comprehensive genomic characterization of B-PLL. We found that the most frequent aberrations are related to *MYC* alterations (in 76% of cases), highlighting the major role of *MYC* in the pathogenesis of B-PLL. Strikingly, *MYC* translocations and *MYC* gain were found to be mutually exclusive. Translocations in which the *MYC* gene is repositioned under the control of an enhancer (usually immunoglobulin gene enhancers) result in the overexpression of *MYC*, as does the gain of one or more copies of *MYC*.[23] Although *MYC* translocations and mutations are classically associated with Burkitt lymphoma (BL), aberrations in *MYC* have also been linked to almost all B-cell neoplasms. With regard to B-PLL, *MYC* translocations and *MYC* gain have been reported in a few cases.[24-29] In the present series, t(*MYC*) was present in the major clone, but *MYC* gain was mainly subclonal and/or overlooked as part of a CK. Thus, performing FISH with a specific probe is

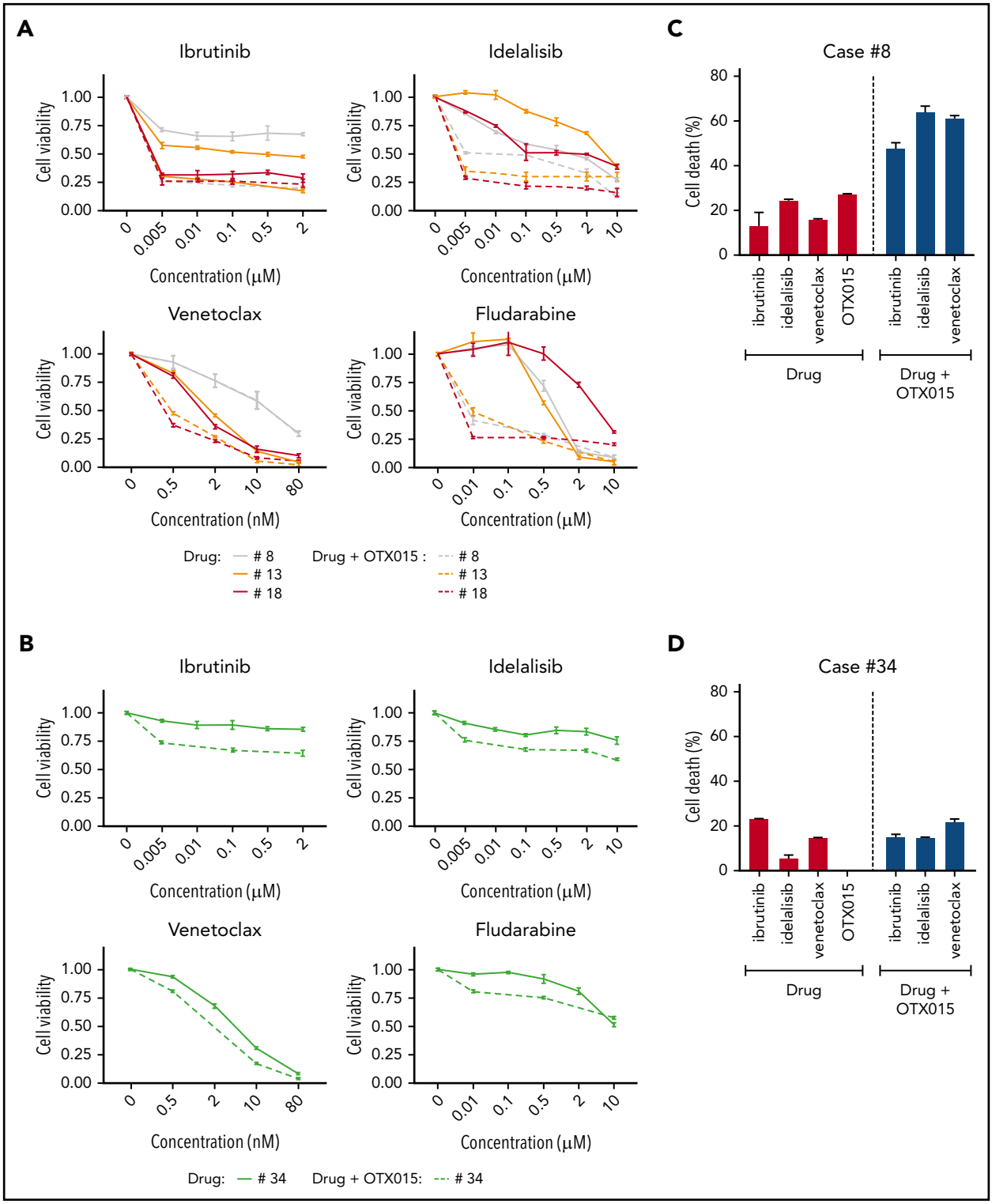

Figure 4. The combination of drugs frequently used to treat B-cell malignancies with iBETs enhances the killing of primary B-PLL cells with t(*MYC*). (A) B-PLL cells from 3 patients with t(*MYC*) were treated with the indicated concentrations of ibrutinib, idelalisib, venetoclax, or fludarabine in the presence or absence of OTX015 (500 nM). Viability was assessed with an ATP-based CellTiter-Glo 2.0 kit. (B) B-PLL cell viability was measured and analyzed as in panel A in a patient with del17p but no *MYC* aberration. (C) Cell death was quantified in primary B-PLL cells from patient BPLL_8 [with t(*MYC*)] with or without pretreatment with OTX015 (500 nM) and exposure for 48 hours to ibrutinib (7.5 μM), idelalisib (50 μM), or venetoclax (10 nM). The percentages refer to Annexin-V–positive or Annexin-V–/propidium iodine–positive cells. (D) Primary B-PLL cells from BPLL_34 (with del17p but no *MYC* aberration) were treated with drugs and analyzed as in panel C. Bars represent the mean ± SEM.

essential to identify *MYC* gain or amplification. *MYC* gene mutations were found in 3 cases, all of which also had t(*MYC*). These mutations were not located in the transactivation domain (the hot spot for *MYC* mutations in BL). However, it is likely that *MYC* mutations have a role in the physiopathology of B-PLL (as they do in BL) by enhancing the oncogenicity of Myc.[30] We found a fusion transcript between *PVT1* and an *IGL* gene in 2 patients with a variant *MYC* translocation t(8;22). This fusion subsequently disrupted the *PVT1* gene, a long intergenic noncoding RNA located 55 kb downstream of *MYC* and which has been identified as a recurrent breakpoint in BL harboring variant translocations t(2;8) or t(8;22).[31,32] In a recent study, the *PVT1* promoter was found to behave like a tumor-suppressor DNA element: silencing the *PVT1* promoter increased *MYC* transcription and cell proliferation.[33] As with *MYC* mutations, disruption of the *PVT1* gene in some patients with B-PLL might cooperate functionally with translocations to increase *MYC*-mediated oncogenesis.

Our present results confirmed previous case reports in which a CK was frequent in B-PLL.[24,27,34] The frequency of a CK in B-PLL (73% in the present study) is higher than that reported in BL (34%),[35] MCL (40%-60%),[36,37] MZL (53%),[38] and CLL at diagnosis (15%)[39-42] and is similar to that observed in high-risk CLL.[43] Whereas t(*MYC*) is the main abnormality in B-PLL (62%), it is rare in other chronic B-cell disorders (ie, <5% in MCL, MZL, and CLL).[28,38,44] The frequency of del17p in B-PLL (38%) observed here is higher than for MCL and MZL (both ~20%)[37,38] or for CLL (5%-7% at diagnosis).[39,45] In addition to *MYC* and *TP53* abnormalities, several other recurrent chromosomal aberrations were found in B-PLL, including trisomies 3, 12, and 18, del13q, and del8p. None of the chromosomal abnormalities observed in B-PLL are specific and thus can be observed in other mature B-cell malignancies, albeit at different frequencies. Similarly, all the driver genes recurrently mutated in B-PLL are also involved in other chronic B-cell disorders but not with the same prevalence. In line with previous studies,[5,6] we found a high frequency of *TP53* mutations (38%) in B-PLL; this frequency is higher than that observed for other B-cell malignancies such as MCL (18%),[46] LZM (14%),[47] CLL (10%),[48] and BL (24%).[49]

We identified a high frequency of clonal *BCOR* mutations, which were present only in t(*MYC*) patients. *BCOR* encodes a Bcl6 co-repressor that silences *BCL6* targets by epigenetic modifications.[50] Inactivating mutations of *BCOR* have been found in myeloid disorders[51,52] but are very unusual in B-cell diseases, except in the rare splenic diffuse red pulp lymphoma.[53] The association of *BCOR* mutations and t(*MYC*) might be a specific feature of B-PLL. Indeed, a recent study of Eμ-*Myc* lymphomas in a mouse model revealed a high frequency of *Bcor* mutations and showed that Bcor was a cooperative tumor suppressor gene, the disruption of which can accelerate *Myc*-driven lymphomagenesis.[54]

Our data showed that patients with B-PLL and t(*MYC*) form a homogeneous subgroup, with a less K complexity, a higher proportion of prolymphocytes, and a higher frequency of CD38 expression. Interestingly, clonal mutations in the *MYC*, *BCOR*, and *SF3B1* genes clustered together in some patients with t(*MYC*), suggesting oncogenic cooperation in the development of B-PLL. *MYC* aberration is a feature shared with BL; however, in contrast to BL, no mutation was found in *TCF3*, *ID3*, or *CCND3* genes in B-PLL.[49]

van der Velden et al[55] have suggested that B-PLL is a specific subgroup of t(11;14)-negative MCL, based on similarities in the immunophenotype, immunogenotype, and gene expression profile. We did not find any *CCND1* or *ATM* mutations (the most frequent mutations in MCL[56]) in our patients with B-PLL. The vast majority of B-PLL expressed significantly mutated *IGHV* genes belonging to the *IGHV3* and *IGHV4* subgroups, in keeping with previous reports.[57,58] This finding contrasts with that of MCL, which exhibits predominantly no or minimal somatic hypermutations.[15]

Taken as a whole, our data show that the genomic profile of B-PLL shares similarities with that of chronic B-cell malignancies but also displays unique combinations of alterations, thus confirming that B-PLL is a distinct entity.

The median OS time in the study cohort was 125.7 months, longer than the times reported in 2 earlier studies.[6,59] This difference might be due to our patients' treatments with rituximab, alemtuzumab, or fludarabine, all of which are reportedly efficacious in B-PLL.[60,61] In light of our results, we propose a hierarchical prognostic model that depends on *MYC* aberration (translocation or gain) and del17p. Patients without an *MYC* aberration have indolent disease (regardless of their 17p status), whereas patients with an *MYC* aberration have a significantly shorter OS time. A combination of *MYC* aberration and del17p confers the worse outcome, with a median OS of <1 year. By analogy with the "double-hit" form of CLL involving del17p and *MYC* gain,[43] these patients may be considered as having a very-high-risk form of B-PLL. Due to the rarity of this disease, our data were obtained with a relatively small number of patients and thus need to be confirmed in future studies.

Our in vitro data showed that a combination of ibrutinib, idelalisib, or venetoclax with OTX015 is more cytotoxic than the drugs used alone, especially in patients with *MYC* translocation. This scenario is concordant with the known effects of OTX015, an inhibitor of the bromodomain-containing proteins BRD2, BRD3, and BRD4. These proteins act as epigenetic readers and have an important role in the regulation of transcription and the modulation of oncogene expression. As with other iBETs, OTX015 strongly downregulates the transcription of genes regulated by super-enhancers such as *MYC*.[20] Current approaches to the treatment of B-PLL (as with CLL) are based on del17p. However, our results strongly suggest that *MYC* should be taken into account and could be targeted. OTX015 is already in phase 1 clinical studies with a relatively good safety profile[62]; when combined with targeted drugs, it might constitute an epigenetic treatment option in patients with B-PLL and *MYC* translocation. In any case, further investigations with a larger number of patients (especially those with *MYC* gain) are required to make progress in this field.

In conclusion, we found that patients with B-PLL have CKs and HCKs, a high frequency of *MYC* aberration (by translocation or gain), frequent del17p, and frequent mutations in the *TP53*, *BCOR*, *MYD88*, and *MYC* genes. We identified 3 prognostic subgroups, depending on *MYC* and 17p status. Patients with both *MYC* aberration and del17p had the shortest OS and should be considered as a high-risk subgroup. These results showed that cytogenetic analysis is a useful diagnostic and prognostic tool in B-PLL. We recommend karyotyping and FISH (for *MYC* and *TP53*) analyses whenever B-PLL is suspected. Moreover, these in vitro data strongly

suggest that drugs targeting the BCR and BCL2 in combination with an iBET might be a treatment option for patients with B-PLL.

Acknowledgments

The authors thank Hélène Merle-Béral for fruitful discussions; Remi Brissiaud, Philippe Rameau, Marie-Claire Grison, Laurent Merlin, Myriam Boudjoghra, Claire Quiney, and Marc Le Lorch for technical assistance; Nadia Bougacha for preliminary assessments; and Stéphanie Mathis, Chantal Brouze, Justine Siavellis, Catherine Godon, Pierre Lemaire, Xavier Troussard, Valérie Bardet, Eric Jeandidier, Dominique Penther, Jean-Baptiste Gaillard, Vincent Leymarie, Annie Brion, Catherine Thieblemont, Cécile Tomowiak, David Ghez, Jean-Marc Zini, and Kamel Laribi for their contribution in the patient selection, the Groupe Francophone d'Hématologie Cellulaire.

This project was funded by the Institut Thématique Multi-Organisme Cancer, the Institut National du Cancer, GEFLUC, Association Laurette Fugain (ALF 14/08), and Roche Diagnostics. E.P. and L.J. received fellowships from the French Research Ministry and Société Française d'Hématologie and Fondation ARC, respectively. This project is part of the International Cancer Genome Consortium program. This work was supported by CURAMUS (Cancer United Research Associating Medicine, University and Society; INCA-DGOS-Inserm_12560).

Authorship

Contribution: F.N.-K., O.A.B, S.A.S., and E.C. designed the study; E.C., E.P., M.D., D.R.-W., C.D., C.G., M.Y., L.J., C.L., F.D., M.L.G.-T., N.D., P.D., S.B., L.W., and S. Scheinost performed experiments and analyzed data; K.M., C.S., L.B., and J.-F.L. performed the morphological review; C.A., V.L., J.G., V.E., B.G., E.C.-B., M.M., C.L., N.N., A.I., S. Struski, M.-A.C.-R., B.Q., S.F.-F., N.A., and I.R.-W. provided samples and clinical data; and E.C., F.D., T.Z., S.A.S., O.A.B. and F.N.-K. wrote the manuscript.

Conflict-of-interest disclosure: The authors declare no competing financial interests.

A complete list of the members of the Groupe Francophone de Cytogénétique Hématologique (GFCH) and the French Innovative Leukemia Organization (FILO) appears in the supplemental appendix.

ORCID profiles: E.C., 0000-0003-3427-7596; D.R.-W., 0000-0002-7767-755X; K.M., 0000-0001-8864-4801; L.B., 0000-0001-7543-6480; F.D., 0000-0002-3764-063X; M.L.G.-T., 0000-0002-3131-3240; S.A.S., 0000-0002-3366-1628; F.N.-K., 0000-0003-3107-6668.

Correspondence: Florence Nguyen-Khac, Service d'Hématologie Biologique, Bâtiment Pharmacie, Pitié-Salpêtrière/Charles Foix University Hospital, 83 Bd de l'Hôpital, F-75013 Paris, France; e-mail: florence.nguyen-khac@aphp.fr.

Footnotes

Submitted 17 April 2019; accepted 12 August 2019. Prepublished online as *Blood* First Edition paper, 16 September 2019; DOI 10.1182/blood.2019001187.

The WES and RNA-seq data have been deposited in the European Genome-phenome Archive database (accession numbers EGAD00001002323, EGAD00001002438, and EGAD00001002476).

The online version of this article contains a data supplement.

There is a *Blood* Commentary on this article in this issue.

The publication costs of this article were defrayed in part by page charge payment. Therefore, and solely to indicate this fact, this article is hereby marked "advertisement" in accordance with 18 USC section 1734.

REFERENCES

1. Ruchlemer R, Parry-Jones N, Brito-Babapulle V, et al. B-prolymphocytic leukaemia with t(11;14) revisited: a splenomegalic form of mantle cell lymphoma evolving with leukaemia. *Br J Haematol*. 2004;125(3):330-336.
2. Swerdlow SH, Campo E, Harris NL, et al. WHO Classification of Tumours of Haematopoietic and Lymphoid Tissues. Revised 4th Edition. Lyon, France: International Agency for Research on Cancer; 2017.
3. Matutes E, Owusu-Ankomah K, Morilla R, et al. The immunological profile of B-cell disorders and proposal of a scoring system for the diagnosis of CLL. *Leukemia*. 1994;8(10):1640-1645.
4. Moreau EJ, Matutes E, A'Hern RP, et al. Improvement of the chronic lymphocytic leukemia scoring system with the monoclonal antibody SN8 (CD79b). *Am J Clin Pathol*. 1997;108(4):378-382.
5. Lens D, De Schouwer PJ, Hamoudi RA, et al. p53 abnormalities in B-cell prolymphocytic leukemia. *Blood*. 1997;89(6):2015-2023.
6. Hercher C, Robain M, Davi F, et al; Groupe Français d'Hématologie Cellulaire. A multicentric study of 41 cases of B-prolymphocytic leukemia: two evolutive forms. *Leuk Lymphoma*. 2001;42(5):981-987.
7. Dearden C. How I treat prolymphocytic leukemia. *Blood*. 2012;120(3):538-551.
8. Gordon MJ, Raess PW, Young K, Spurgeon SEF, Danilov AV. Ibrutinib is an effective treatment for B-cell prolymphocytic leukaemia. *Br J Haematol*. 2017;179(3):501-503.
9. Eyre TA, Fox CP, Boden A, et al. Idelalisib-rituximab induces durable remissions in TP53 disrupted B-PLL but results in significant toxicity: updated results of the UK-wide compassionate use programme. *Br J Haematol*. 2019;184(4):667-671.
10. Damlaj M, Al Balwi M, Al Mugairi AM. Ibrutinib therapy is effective in B-cell prolymphocytic leukemia exhibiting MYC aberrations. *Leuk Lymphoma*. 2018;59(3):739-742.
11. Wlodarska I, Dierickx D, Vanhentenrijk V, et al. Translocations targeting CCND2, CCND3, and MYCN do occur in t(11;14)-negative mantle cell lymphomas. *Blood*. 2008;111(12):5683-5690.
12. Salaverria I, Royo C, Carvajal-Cuenca A, et al. CCND2 rearrangements are the most frequent genetic events in cyclin D1(-) mantle cell lymphoma. *Blood*. 2013;121(8):1394-1402.
13. Cosson A, Chapiro E, Belhouachi N, et al; Groupe Francophone de Cytogénétique Hématologique. 14q deletions are associated with trisomy 12, NOTCH1 mutations and unmutated IGHV genes in chronic lymphocytic leukemia and small lymphocytic lymphoma. *Genes Chromosomes Cancer*. 2014;53(8):657-666.
14. Ghia P, Stamatopoulos K, Belessi C, et al; European Research Initiative on CLL. ERIC recommendations on IGHV gene mutational status analysis in chronic lymphocytic leukemia. *Leukemia*. 2007;21(1):1-3.
15. Hadzidimitriou A, Agathangelidis A, Darzentas N, et al. Is there a role for antigen selection in mantle cell lymphoma? Immunogenetic support from a series of 807 cases. *Blood*. 2011;118(11):3088-3095.
16. Bikos V, Darzentas N, Hadzidimitriou A, et al. Over 30% of patients with splenic marginal zone lymphoma express the same immunoglobulin heavy variable gene: ontogenetic implications. *Leukemia*. 2012;26(7):1638-1646.
17. Merlevede J, Droin N, Qin T, et al. Mutation allele burden remains unchanged in chronic myelomonocytic leukaemia responding to hypomethylating agents. *Nat Commun*. 2016;7(1):10767.
18. Dietrich S, Oleś M, Lu J, et al. Drug-perturbation-based stratification of blood cancer. *J Clin Invest*. 2018;128(1):427-445.
19. Mertz JA, Conery AR, Bryant BM, et al. Targeting MYC dependence in cancer by inhibiting BET bromodomains. *Proc Natl Acad Sci U S A*. 2011;108(40):16669-16674.
20. Chapuy B, McKeown MR, Lin CY, et al. Discovery and characterization of super-enhancer-associated dependencies in diffuse large B cell lymphoma [published correction appears in Cancer Cell. 2014;25(4):545-546]. *Cancer Cell*. 2013;24(6):777-790.
21. Boi M, Gaudio E, Bonetti P, et al. The BET bromodomain inhibitor OTX015 affects pathogenetic pathways in preclinical B-cell tumor models and synergizes with targeted drugs. *Clin Cancer Res*. 2015;21(7):1628-1638.

22. Hoehn D, Miranda RN, Kanagal-Shamanna R, Lin P, Medeiros LJ. Splenic B-cell lymphomas with more than 55% prolymphocytes in blood: evidence for prolymphocytoid transformation. *Hum Pathol*. 2012;43(11):1828-1838.

23. Klapproth K, Wirth T. Advances in the understanding of MYC-induced lymphomagenesis. *Br J Haematol*. 2010;149(4):484-497.

24. Lens D, Coignet LJ, Brito-Babapulle V, et al. B cell prolymphocytic leukaemia (B-PLL) with complex karyotype and concurrent abnormalities of the p53 and c-MYC gene. *Leukemia*. 1999;13(6):873-876.

25. Merchant S, Schlette E, Sanger W, Lai R, Medeiros LJ. Mature B-cell leukemias with more than 55% prolymphocytes: report of 2 cases with Burkitt lymphoma-type chromosomal translocations involving c-myc. *Arch Pathol Lab Med*. 2003;127(3):305-309.

26. Kuriakose P, Perveen N, Maeda K, Wiktor A, Van Dyke DL. Translocation (8;14)(q24;q32) as the sole cytogenetic abnormality in B-cell prolymphocytic leukemia. *Cancer Genet Cytogenet*. 2004;150(2):156-158.

27. Crisostomo RH, Fernandez JA, Caceres W. Complex karyotype including chromosomal translocation (8;14) (q24;q32) in one case with B-cell prolymphocytic leukemia. *Leuk Res*. 2007;31(5):699-701.

28. Put N, Van Roosbroeck K, Konings P, et al; BCGHo and the GFCH. Chronic lymphocytic leukemia and prolymphocytic leukemia with MYC translocations: a subgroup with an aggressive disease course. *Ann Hematol*. 2012; 91(6):863-873.

29. Flatley E, Chen AI, Zhao X, et al. Aberrations of MYC are a common event in B-cell prolymphocytic leukemia. *Am J Clin Pathol*. 2014; 142(3):347-354.

30. Hemann MT, Bric A, Teruya-Feldstein J, et al. Evasion of the p53 tumour surveillance network by tumour-derived MYC mutants. *Nature*. 2005;436(7052):807-811.

31. Graham M, Adams JM. Chromosome 8 breakpoint far 3′ of the c-myc oncogene in a Burkitt's lymphoma 2;8 variant translocation is equivalent to the murine pvt-1 locus. *EMBO J*. 1986;5(11):2845-2851.

32. Shtivelman E, Henglein B, Groitl P, Lipp M, Bishop JM. Identification of a human transcription unit affected by the variant chromosomal translocations 2;8 and 8;22 of Burkitt lymphoma. *Proc Natl Acad Sci U S A*. 1989; 86(9):3257-3260.

33. Cho SW, Xu J, Sun R, et al. Promoter of lncRNA Gene PVT1 is a tumor-suppressor DNA boundary element. *Cell*. 2018;173(6): 1398-1412.e1322.

34. Solé F, Woessner S, Espinet B, et al. Cytogenetic abnormalities in three patients with B-cell prolymphocytic leukemia. *Cancer Genet Cytogenet*. 1998;103(1):43-45.

35. Haberl S, Haferlach T, Stengel A, Jeromin S, Kern W, Haferlach C. MYC rearranged B-cell neoplasms: impact of genetics on classification. *Cancer Genet*. 2016;209(10):431-439.

36. Cohen JB, Ruppert AS, Heerema NA, et al. Complex karyotype is associated with aggressive disease and shortened progression-free survival in patients with newly diagnosed mantle cell lymphoma. *Clin Lymphoma Myeloma Leuk*. 2015;15(5):278-285.e271.

37. Sarkozy C, Terré C, Jardin F, et al. Complex karyotype in mantle cell lymphoma is a strong prognostic factor for the time to treatment and overall survival, independent of the MCL international prognostic index. *Genes Chromosomes Cancer*. 2014;53(1):106-116.

38. Salido M, Baró C, Oscier D, et al. Cytogenetic aberrations and their prognostic value in a series of 330 splenic marginal zone B-cell lymphomas: a multicenter study of the Splenic B-Cell Lymphoma Group. *Blood*. 2010;116(9): 1479-1488.

39. Sutton L, Chevret S, Tournilhac O, et al; Société Française de Greffe de Moelle et de Thérapie Cellulaire (SFGM-TC) and Groupe Français d'étude de la Leucémie Lymphoïde Chronique (GFLLC). Autologous stem cell transplantation as a first-line treatment strategy for chronic lymphocytic leukemia: a multicenter, randomized, controlled trial from the SFGM-TC and GFLLC. *Blood*. 2011; 117(23):6109-6119.

40. Lepretre S, Aurran T, Mahé B, et al. Excess mortality after treatment with fludarabine and cyclophosphamide in combination with alemtuzumab in previously untreated patients with chronic lymphocytic leukemia in a randomized phase 3 trial. *Blood*. 2012;119(22): 5104-5110.

41. Baliakas P, Iskas M, Gardiner A, et al. Chromosomal translocations and karyotype complexity in chronic lymphocytic leukemia: a systematic reappraisal of classic cytogenetic data. *Am J Hematol*. 2014;89(3):249-255.

42. Baliakas P, Jeromin S, Iskas M, et al; ERIC, the European Research Initiative on CLL. Cytogenetic complexity in chronic lymphocytic leukemia: definitions, associations, and clinical impact. *Blood*. 2019;133(11): 1205-1216.

43. Chapiro E, Lesty C, Gabillaud C, et al; GroupeFrancophone de Cytogénétique Hématologique(GFCH) and the French Innovative Leukemia Organization (FILO) group. "Double-hit" chronic lymphocytic leukemia: an aggressive subgroup with 17p deletion and 8q24 gain. *Am J Hematol*. 2018;93(3): 375-382.

44. Hu Z, Medeiros LJ, Chen Z, et al. Mantle cell lymphoma with MYC rearrangement: a report of 17 patients. *Am J Surg Pathol*. 2017;41(2):216-224.

45. Döhner H, Stilgenbauer S, Benner A, et al. Genomic aberrations and survival in chronic lymphocytic leukemia. *N Engl J Med*. 2000; 343(26):1910-1916.

46. Beà S, Valdés-Mas R, Navarro A, et al. Landscape of somatic mutations and clonal evolution in mantle cell lymphoma. *Proc Natl Acad Sci U S A*. 2013;110(45):18250-18255.

47. Rossi D, Trifonov V, Fangazio M, et al. The coding genome of splenic marginal zone lymphoma: activation of NOTCH2 and other pathways regulating marginal zone development. *J Exp Med*. 2012;209(9):1537-1551.

48. Guièze R, Wu CJ. Genomic and epigenomic heterogeneity in chronic lymphocytic leukemia. *Blood*. 2015;126(4):445-453.

49. Love C, Sun Z, Jima D, et al. The genetic landscape of mutations in Burkitt lymphoma. *Nat Genet*. 2012;44(12):1321-1325.

50. Huynh KD, Fischle W, Verdin E, Bardwell VJ. BCoR, a novel corepressor involved in BCL-6 repression. *Genes Dev*. 2000;14(14): 1810-1823.

51. Grossmann V, Tiacci E, Holmes AB, et al. Whole-exome sequencing identifies somatic mutations of BCOR in acute myeloid leukemia with normal karyotype. *Blood*. 2011;118(23): 6153-6163.

52. Damm F, Chesnais V, Nagata Y, et al. BCOR and BCORL1 mutations in myelodysplastic syndromes and related disorders. *Blood*. 2013;122(18):3169-3177.

53. Jallades L, Baseggio L, Sujobert P, et al. Exome sequencing identifies recurrent *BCOR* alterations and the absence of *KLF2, TNFAIP3* and *MYD88* mutations in splenic diffuse red pulp small B-cell lymphoma. *Haematologica*. 2017;102(10):1758-1766.

54. Lefebure M, Tothill RW, Kruse E, et al. Genomic characterisation of Eμ-Myc mouse lymphomas identifies Bcor as a Myc cooperative tumour-suppressor gene. *Nat Commun*. 2017;8(1):14581.

55. van der Velden VH, Hoogeveen PG, de Ridder D, et al. B-cell prolymphocytic leukemia: a specific subgroup of mantle cell lymphoma. *Blood*. 2014;124(3):412-419.

56. Zhang J, Jima D, Moffitt AB, et al. The genomic landscape of mantle cell lymphoma is related to the epigenetically determined chromatin state of normal B cells. *Blood*. 2014; 123(19):2988-2996.

57. Davi F, Maloum K, Michel A, et al. High frequency of somatic mutations in the VH genes expressed in prolymphocytic leukemia. *Blood*. 1996;88(10):3953-3961.

58. Del Giudice I, Davis Z, Matutes E, et al. IgVH genes mutation and usage, ZAP-70 and CD38 expression provide new insights on B-cell prolymphocytic leukemia (B-PLL). *Leukemia*. 2006;20(7):1231-1237.

59. Shvidel L, Shtalrid M, Bassous L, Klepfish A, Vorst E, Berrebi A. B-cell prolymphocytic leukemia: a survey of 35 patients emphasizing heterogeneity, prognostic factors and evidence for a group with an indolent course. *Leuk Lymphoma*. 1999;33(1-2):169-179.

60. Chow KU, Kim SZ, von Neuhoff N, et al. Clinical efficacy of immunochemotherapy with fludarabine, epirubicin and rituximab in the treatment for chronic lymphocytic leukaemia and prolymphocytic leukaemia. *Eur J Haematol*. 2011;87(5):426-433.

61. Bowen AL, Zomas A, Emmett E, Matutes E, Dyer MJ, Catovsky D. Subcutaneous CAMPATH-1H in fludarabine-resistant/relapsed chronic lymphocytic and B-prolymphocytic leukaemia. *Br J Haematol*. 1997;96(3):617-619.

62. Amorim S, Stathis A, Gleeson M, et al. Bromodomain inhibitor OTX015 in patients with lymphoma or multiple myeloma: a dose-escalation, open-label, pharmacokinetic, phase 1 study. *Lancet Haematol*. 2016;3(4): e196-e204.

Supplementary Information

Supplementary Methods

Patient selection

We studied 87 cases with a blood smear available at diagnosis. The cases were first identified locally on the basis of a routine cell morphology screen. In blinded review by three independent cytologist (LB, CS, and KM), cases were only included if all three reviewers agreed with the diagnosis of B-PLL. A fourth blinded review of ten representative cases (five cases of B-PLL: BPLL_24, BPLL_26, BPLL_28, BPLL_33, BPLL_34; and 5 excluded cases) validated our approach. The four cytologists agreed on all five cases of B-PLL and on one excluded case (N°45). For the excluded cases N°76 and N°80, only two of the four cytologists diagnosed B-PLL; for the excluded cases N°49 and N°67, only one of the four cytologists diagnosed B-PLL (see Supplemental Table S1). A diagnosis of MCL was ruled out by karyotyping (K) and FISH assays: no *CCND1* rearrangements or other infrequent translocations involving *CCND2* and *CCND3* were observed. Unfortunately, bone marrow biopsies were not available for CCND1 or SOX11 immunostaining.

FISH

Standard FISH was performed on interphase nuclei and metaphases in all 34 cases. The specific probes were *ATM* (11q22), *TP53* (17p13), IGH/CCND3 (Cytocell, Cambridge, UK), D13S319 (13q14), centromere of chromosome 12 (Metasystems, Altlussheim, Germany), *MYC* (8q24) (DAKO, Santa Clara, CA and/or Zytovision, Bremerhaven, Germany), *MYCN* (2p24) (Abbott Molecular, Des Plaines, IL), *CCND1* (11q13) (DAKO). A break-apart probe for detecting *CCND2* (12p13) rearrangements was built using the home-grown bacterial artificial chromosome clones RP11-578L13 and RP11-388F6. A deletion probe targeting *TNFRSF10A-D* genes (8p21) was built with clones RP11-599A17 and RP11-692J4. Clones were selected using the University of California Santa Cruz Genome Bioinformatic database (NCBI38/hg38 build) and obtained from Genoscope (Evry, France). Extraction, labeling, and hybridization procedures were performed as described previously[1].

Cell sorting

The samples used for WES, targeted deep sequencing and RNA-Seq were obtained from fresh or cryopreserved mononuclear cells, when available. The CD19+ (and CD5+, IGL or IGK when appropriate) B-cells and CD3+ T-cells were sorted as described previously[2]. The purity of the cell fractions was assessed by flow cytometry, and was always greater than 96%. DNA and RNA were extracted from sorted cell fractions using the All Prep DNA/RNA kit (Qiagen, Courtaboeuf, France), according to the manufacturer's recommendations.

Whole Exome Sequencing

DNA extracted from sorted CD19+ tumor cells (and CD5+, IGL or IGK when appropriate) and nontumor (CD3+) cells was used for exome capture with the SureSelect V5 Mb All Exon Kit (Agilent Technologies, Les Ulis, France) following the standard protocols. Paired-end sequencing (2 x 100 bp) was performed using HiSeq2000 sequencing instruments (Illumina, San Diego, CA).The mean coverage in the targeted regions was 106X (Supplemental Table S8). Reads were mapped to the reference genome hg19 using the Burrows–Wheeler Aligner (BWA) alignment tool version 0.7.10. PCR duplicates were removed using Picard Tools - MarkDuplicates (1.119). Local realignment around indels and base quality score recalibration were performed using GATK 3.2 (Genome Analysis ToolKit). Reads with a mapping quality score < 30 were ignored. SNVs and indels were called with VarScan2 somatic 2.3.7. The null hypothesis of equal allele frequencies between tumor and reference was tested using the two-tailed Fisher exact test. The variants were adopted as candidate mutations when P value was <0.01 and allele frequency was <0.1 in the reference sample. Variants were annotated with Annovar. We excluded synonymous single nucleotide variants (SNVs), variants located in intergenic, intronic, untranslated regions and non-coding RNA regions, and removed variants with mapping ambiguities. Mutations were searched in Catalogue of Somatic Mutations in Cancer database (http://cancer.sanger.ac.uk/cosmic/). The effect of the mutation was predicted by SIFT (http://sift.jcvi.org/) and PolyPhen2 (http://genetics.bwh.harvard.edu/pph2/) algorithms.
Somatic copy number variations (CNV) were identified with Control-FREEC (v9.1).

Targeted deep sequencing

Primers flanking exons containing candidate somatic variants were designed using Primer3 (http://frodo.wi.mit.edu/primer3/). Short fragments of 100 to 200 bp were PCR-amplified from genomic DNA of sorted fractions and were subsequently pooled for library construction. PCR products were end-repaired, extended with an 'A' base on the 3' end, ligated with indexed paired-end adaptors (NEXTflex, Bioo Scientific) using the Bravo Platform (Agilent) and amplified by PCR for 4 cycles. Amplicon libraries were sequenced in an Illumina MiSeq flow cell using the onboard cluster method, as paired-end sequencing (2x150 bp reads) (Illumina, San Diego, CA). The mean coverage was 2021X. Quality of reads was evaluated using FastQC 0.11.2. (http://www.bioinformatics.bbsrc.ac.uk/projects/fastqc/). Reads were mapped to the reference genome hg19 using the Burrows–Wheeler Aligner (BWA) alignment tool version 0.7.10. Local realignment around indels and base quality score recalibration were performed using GATK 3.2 (Genome Analysis ToolKit). SNVs and indels were called with VarScan2 somatic 2.3.7.

Clonal organization

Evaluation of the clonal or subclonal nature of chromosomal abnormalities was performed by comparing the percentage of abnormal cells in interphasic FISH analyses (when available) with the percentage of monotypic (IGL or IGK) CD19+ cells defined by immunophenotyping. We considered an abnormality to be clonal when the difference between the two percentages did not exceed 20%, and subclonal when the difference was greater. For mutations detected in purified tumor cell fractions, we used the variant allele frequency (VAF) to distinguish between clonal and subclonal mutations with a threshold of 40% (or 80%, when combined with copy loss) to take account of the potential contamination by non-tumor cells.

RNA Sequencing and data analysis

RNA-Seq libraries were prepared using the SureSelect Automated Strand Specific RNA Library Preparation Kit as per manufacturer's instructions (Agilent technologies) and subjected to paired-end (101 bp) sequencing on HiSeq2000 (Illumina). Quality of reads was evaluated using FastQC 0.11.2. Sequences were filtered with Trimommatic and alignment was performed with Tophat2 version 2.0.14 and Bowtie1 version 1.0.0. The filtered reads were aligned to a reference genome hg19. In average, 88.95% of reads were aligned and counted with HTSeq (v0.5.4p5).

Differential expression analysis: raw counts of reads per Human GENCODE transcripts (GRCh37 release 24)[3] were quantified with Salmon version 0.8.2[4]. These transcripts level raw counts have been aggregated to obtain gene level raw counts. Differential expression analysis was performed using DESeq2 package version 1.6.3[5] with R statistical software version 3.1.2. Differentially expressed genes have been selected with an adjusted p-value of 0.01.

Gene Set Enrichment Analysis (GSEA)[6] was performed using the GSEAPreranked tool (v3.0). Prior to conducting gene set enrichment analysis, differential expression analysis has been conducted using DESeq2 taking into account the batch effect observed in RNA-seq of B-PLL, CLL and pMCL cells. Only genes with an adjusted p-value lower than 5% have been considered. These genes have been ranked by log2 fold-change and captured in an RNK-formatted file. GSEAPreranked tool has been launched with the following option: 'scoring_scheme classic' using hallmark gene (H) and curated gene (C2) sets available from MSigDB (v6.2)[7].

Functional analysis of the differential gene list has been explored for the GO gene sets with the Investigate application (http://software.broadinstitute.org/gsea/msigdb) to compute the statistical score of the overlaps between gene list and GO gene sets.

Fusion transcripts detection: sequences were aligned with Tophat2 version 2.0.14[8] and Bowtie1 version 1.0.0 to a reference genome hg19. In average, 88.95% of reads were aligned. The potential

fusion transcripts were evaluated using Tophat2 –fusion-search option. A minimum of 10 supporting (spanning) reads was used as a threshold for fusion transcripts and the sequence around donor and acceptor sites of potential chimeric reads was manually evaluated to discard potential false positives.

In vitro cell viability and programmed cell death (PCD) assays

The viability of primary B-PLL cells was assessed with the ATP-based CellTiter-Glo 2.0 assay (Promega, Madison, WI). After pretreatment (or not) with the BET proteins inhibitors (iBET) OTX015 or JQ1 (500 nM), B cells were seeded onto 96-well plates (at a density 50×10^3 cells per well) and exposed for 48h to increasing concentrations of fludarabine, ibrutinib, idelalisib or venetoclax. We used drugs concentrations as previously described[9]. The OTX015 and JQ1 concentrations of 500 nM were the lowest with a significant *in vitro* effect on B-PLL cell viability (50% loss of viability; Supp Fig S5A and data not shown). The cells were then incubated for 15 minutes with 50 µl of CellTiter-Glo® reagent. Next, the luminescence was measured in an Infinite M1000 Pro plate reader (TECAN), using an integration time of 500 ms. Viability was determined by normalizing luminescence units against a DMSO control (the solvent used for drug dilution). Alternatively, PCD was measured by flow cytometry. Briefly, 2×10^6 B-PLL cells/ml were treated for 48h with ibrutinib (7.5 µM), idelalisib (50 µM), venetoclax (10 nM), or OTX015 (500 nM), and PCD was measured by annexin-V-APC (0.1 µg/ml; BD Biosciences) and propidium iodide (PI, 0.5 µg/ml; Sigma) co-labeling. All drugs were purchased from Selleckchem (Houston, TX). All these analyses were performed on stored cells resulting in spontaneous apoptosis rates of 10-15%.

Supplementary References

1. Cosson A, Chapiro E, Belhouachi N, et al. 14q deletions are associated with trisomy 12, NOTCH1 mutations and unmutated IGHV genes in chronic lymphocytic leukemia and small lymphocytic lymphoma. *Genes Chromosomes Cancer*. 2014;53(8):657-666.
2. Damm F, Mylonas E, Cosson A, et al. Acquired initiating mutations in early hematopoietic cells of CLL patients. *Cancer Discov*. 2014;4(9):1088-1101.
3. Frankish A, Diekhans M, Ferreira AM, et al. GENCODE reference annotation for the human and mouse genomes. *Nucleic Acids Res*. 2019;47(D1):D766-D773.
4. Patro R, Duggal G, Love MI, Irizarry RA, Kingsford C. Salmon provides fast and bias-aware quantification of transcript expression. *Nat Methods*. 2017;14(4):417-419.
5. Love MI, Huber W, Anders S. Moderated estimation of fold change and dispersion for RNA-seq data with DESeq2. *Genome Biol*. 2014;15(12):550.
6. Subramanian A, Tamayo P, Mootha VK, et al. Gene set enrichment analysis: a knowledge-based approach for interpreting genome-wide expression profiles. *Proc Natl Acad Sci U S A*. 2005;102(43):15545-15550.
7. Liberzon A, Birger C, Thorvaldsdottir H, Ghandi M, Mesirov JP, Tamayo P. The Molecular Signatures Database (MSigDB) hallmark gene set collection. *Cell Syst*. 2015;1(6):417-425.
8. Kim D, Pertea G, Trapnell C, Pimentel H, Kelley R, Salzberg SL. TopHat2: accurate alignment of transcriptomes in the presence of insertions, deletions and gene fusions. *Genome Biol*. 2013;14(4):R36.

9. Cosson A, Chapiro E, Bougacha N, et al. Gain in the short arm of chromosome 2 (2p+) induces gene overexpression and drug resistance in chronic lymphocytic leukemia: analysis of the central role of XPO1. *Leukemia*. 2017;31(7):1625-1629.

Supplementary Tables

Table S1. Results of the morphologic review

ID	ID article	Reviewer 1		Reviewer 2		Reviewer 3		Level of agreement between the first 3 reviewers	Reviewer 4		Level of agreement between the 4 reviewers
		% of prolymphocytes	Diagnosis	% of prolymphocytes	Diagnosis	% of prolymphocytes	Diagnosis		% of prolymphocytes	Diagnosis	
1	BPLL_1	68	B-PLL	80	B-PLL	73	B-PLL	B-PLL: 3/3			
2	BPLL_2	57	B-PLL	60	B-PLL	80	B-PLL	B-PLL: 3/3			
3	BPLL_3	71	B-PLL	72	B-PLL	56	B-PLL	B-PLL: 3/3			
4	BPLL_4	90	B-PLL	92	B-PLL	97	B-PLL	B-PLL: 3/3			
5	BPLL_5	90	B-PLL	94	B-PLL	89	B-PLL	B-PLL: 3/3			
6	BPLL_6	74	B-PLL	90	B-PLL	88	B-PLL	B-PLL: 3/3			
7	BPLL_7	74	B-PLL	80	B-PLL	76	B-PLL	B-PLL: 3/3			
8	BPLL_8	76	B-PLL	64	B-PLL	67	B-PLL	B-PLL: 3/3			
9	BPLL_9	70	B-PLL	85	B-PLL	93	B-PLL	B-PLL: 3/3			
10	BPLL_10	95	B-PLL	97	B-PLL	88	B-PLL	B-PLL: 3/3			
11	BPLL_11	83	B-PLL	73	B-PLL	79	B-PLL	B-PLL: 3/3			
12	BPLL_12	63	B-PLL	60	B-PLL	58	B-PLL	B-PLL: 3/3			
13	BPLL_13	90	B-PLL	93	B-PLL	96	B-PLL	B-PLL: 3/3			
14	BPLL_14	85	B-PLL	68	B-PLL	77	B-PLL	B-PLL: 3/3			
15	BPLL_15	82	B-PLL	73	B-PLL	55	B-PLL	B-PLL: 3/3			
16	BPLL_16	70	B-PLL	92	B-PLL	95	B-PLL	B-PLL: 3/3			
17	BPLL_17	70	B-PLL	66	B-PLL	67	B-PLL	B-PLL: 3/3			
18	BPLL_18	95	B-PLL	89	B-PLL	93	B-PLL	B-PLL: 3/3			
19	BPLL_19	97	B-PLL	98	B-PLL	93	B-PLL	B-PLL: 3/3			
20	BPLL_20	70	B-PLL	84	B-PLL	75	B-PLL	B-PLL: 3/3			
21	BPLL_21	75	B-PLL	96	B-PLL	93	B-PLL	B-PLL: 3/3			
22	BPLL_22	80	B-PLL	93	B-PLL	92	B-PLL	B-PLL: 3/3			
23	BPLL_23	80	B-PLL	81	B-PLL	72	B-PLL	B-PLL: 3/3			
24	BPLL_24	80	B-PLL	91	B-PLL	68	B-PLL	B-PLL: 3/3	62	B-PLL	B-PLL: 4/4
25	BPLL_25	68	B-PLL	66	B-PLL	63	B-PLL	B-PLL: 3/3			
26	BPLL_26	90	B-PLL	95	B-PLL	96	B-PLL	B-PLL: 3/3	92	B-PLL	B-PLL: 4/4
27	BPLL_27	100	B-PLL	100	B-PLL	99	B-PLL	B-PLL: 3/3			
28	BPLL_28	84	B-PLL	86	B-PLL	70	B-PLL	B-PLL: 3/3	78	B-PLL	B-PLL: 4/4
29	BPLL_29	79	B-PLL	74	B-PLL	75	B-PLL	B-PLL: 3/3			
30	BPLL_30	56	B-PLL	65	B-PLL	63	B-PLL	B-PLL: 3/3			
31	BPLL_31	80	B-PLL	85	B-PLL	83	B-PLL	B-PLL: 3/3			
32	BPLL_32	71	B-PLL	83	B-PLL	71	B-PLL	B-PLL: 3/3			
33	BPLL_33	71	B-PLL	78	B-PLL	90	B-PLL	B-PLL: 3/3	80	B-PLL	B-PLL: 4/4
34	BPLL_34	75	B-PLL	72	B-PLL	79	B-PLL	B-PLL: 3/3	75	B-PLL	B-PLL: 4/4
35	excluded (MCL)	57	B-PLL	64	B-PLL	55	B-PLL	B-PLL: 3/3			
36	excluded (MCL)	61	B-PLL	57	B-PLL	58	B-PLL	B-PLL: 3/3			
37	excluded (MCL)	88	B-PLL	78	B-PLL	75	B-PLL	B-PLL: 3/3			
38	excluded (MCL)	75	B-PLL	79	B-PLL	80	B-PLL	B-PLL: 3/3			
39	excluded	<10	Other	<10	MZL ?	<10	MZL ?	B-PLL: 0/3			
40	excluded	<10	Other	23	MZL ?	<10	Other	B-PLL: 0/3			
41	excluded	46	Other	13	Other	13	Other	B-PLL: 0/3			
42	excluded	<10	MZL ?	<10	MZL ?	<10	Other	B-PLL: 0/3			
43	excluded	<10	Other	<10	Other	<10	Other	B-PLL: 0/3			
44	excluded	53	Other	66	B-PLL	53	Other	B-PLL: 1/3			

ID	ID article	Reviewer 1		Reviewer 2		Reviewer 3		Level of agreement between the first 3 reviewers	Reviewer 4		Level of agreement between the 4 reviewers
		% of prolymphocytes	Diagnosis	% of prolymphocytes	Diagnosis	% of prolymphocytes	Diagnosis		% of prolymphocytes	Diagnosis	
45	excluded	<10	Other	<10	MZL	<10	MZL	B-PLL: 0/3	40	other	B-PLL: 0/4
46	excluded	48	HCL_V ?	<10	MZL	<10	MZL	B-PLL: 0/3			
47	excluded	50	Other	<10	MZL	<10	MZL	B-PLL: 0/3			
48	excluded	35	Other	25	Other	45	Other	B-PLL: 0/3			
49	excluded	35	Other	64	B-PLL	23	Other	B-PLL: 1/3	45	other	B-PLL: 1/4
50	excluded	8	Other	64 atypical	Other	73 atypical	Other	B-PLL: 0/3			
51	excluded	50	Other	<10	MZL	47	MZL?	B-PLL: 0/3			
52	excluded	46	Other	31	Other	24	Other	B-PLL: 0/3			
53	excluded	15	Other	<10	atypical LPD	9	Other	B-PLL: 0/3			
54	excluded	65 atypical	Other	48 atypical	Other	49 atypical	Other	B-PLL: 0/3			
55	excluded	38	Other	47	Other	<10	Other	B-PLL: 0/3			
56	excluded	<10	Other	36	Other	17	Other	B-PLL: 0/3			
57	excluded	36	Other	51	Other	42	Other	B-PLL: 0/3			
58	excluded	30	Other	30	MCL?	24	Other	B-PLL: 0/3			
59	excluded	35	Other	14	MZL	25	MZL	B-PLL: 0/3			
60	excluded	50	Other	39	Other	33	Other	B-PLL: 0/3			
61	excluded	45	Other	31	Other	43	Other	B-PLL: 0/3			
62	excluded	28	Other	<10	Other	5	Other	B-PLL: 0/3			
63	excluded	30	Other	<10	Other	<10	MZL?	B-PLL: 0/3			
64	excluded	5	Other	<10	Other	<10	Other	B-PLL: 0/3			
65	excluded	67 atypical	Other	20	Other	18	Other	B-PLL: 0/3			
66	excluded	22	Other	0	Other	<10	Other	B-PLL: 0/3			
67	excluded	75	B-PLL	49	MZL	42	MZL	B-PLL: 1/3	40	MZL	B-PLL: 1/4
68	excluded	25	Other	15	Other	<10	Other	B-PLL: 0/3			
69	excluded	30	Other	41	Other	13	Other	B-PLL: 0/3			
70	excluded	35	Other	39	MCL?	29	Other	B-PLL: 0/3			
71	excluded	50	Other	35	Other	15	Other	B-PLL: 0/3			
72	excluded	29	Other	37	Other	19	Other	B-PLL: 0/3			
73	excluded	<10	Other	7	Other	<10	Other	B-PLL: 0/3			
74	excluded	30	Other	17	Other	25	Other	B-PLL: 0/3			
75	excluded	20	Other	7	Other	<10	Other	B-PLL: 0/3			
76	excluded	77	B-PLL	52	Other	52	Other	B-PLL: 1/3	60	B-PLL	B-PLL: 2/4
77	excluded	<10	Other	<10	Other	<10	Other	B-PLL: 0/3			
78	excluded	67	B-PLL	47	MZL?	49	Other	B-PLL: 1/3			
79	excluded	50	Other	32	Other	26	Other	B-PLL: 0/3			
80	excluded	70	B-PLL	50	MZL?	52	MZL?	B-PLL: 1/3	68	B-PLL	B-PLL: 2/4
81	excluded	25	Other	33	MZL?	12	Other	B-PLL: 0/3			
82	excluded	45	Other	50	Other	32	Other	B-PLL: 0/3			
83	excluded	15	Other	34	Other	<10	Other	B-PLL: 0/3			
84	excluded	40	Other	25	MZL?	38	Other	B-PLL: 0/3			
85	excluded	15	Other	7	Other	10	Other	B-PLL: 0/3			
86	excluded	28	Other	20	Other	<10	Other	B-PLL: 0/3			
87	excluded	32	Other	18	Other	<10	Other	B-PLL: 0/3			

Other: not B-PLL

Atypical: lymphocyte with nucleolus but not a typical prolymphocyte

MZL: marginal zone lymphoma; MCL: mantle cell lymphoma, LPD: lymphoproliferative disorder

Reviewer 4 conducted a blinded morphological review of 10 cases in a second round

Table S2. Immunophenotyping results for the patients with B-PLL

ID Patient	% CD5+ / CD19+	CD5 expression	% CD23+ / CD19+	CD23 expression	Matutes' score
BPLL_1	85	+	24	-	2
BPLL_2	4	-	96	+	1
BPLL_3	99	+	32	+	3
BPLL_4	99	+	44	+	3
BPLL_5	98	+	10	-	1
BPLL_6	70	+	85	+	3
BPLL_7	0	-	0	-	0
BPLL_8	76	+	21	-	2
BPLL_9	0	-	0	-	0
BPLL_10	97	+	5	-	1
BPLL_11	75	+	30	+	2
BPLL_12	0	-	0	-	1
BPLL_13	2	-	62	+	1
BPLL_14	10	-	11	-	1
BPLL_15	74	+	0	-	1
BPLL_16	63	+	8	-	2
BPLL_17	na	-	na	-	0
BPLL_18	0	-	0	-	0
BPLL_19	na	-	na	-	0
BPLL_20	53	+	2	-	2
BPLL_21	3	-	6	-	na
BPLL_22	na	+	na	-	1
BPLL_23	69	+	12	-	3
BPLL_24	32	+	10	-	1
BPLL_25	3	-	25	-	1
BPLL_26	na	+	na	-	na
BPLL_27	0	-	5	-	0
BPLL_28	0	-	78	+	2
BPLL_29	93	+	34	+	2
BPLL_30	97	+	17	-	3
BPLL_31	45	+	99	+	2
BPLL_32	7	-	98	+	1
BPLL_33	96	+	100	+	2
BPLL_34	0	-	7	-	0

A cut-off of 30% of CD19+ cells was used to define CD5 and CD23 positivity
na: not available

Table S3. Karyotype and FISH results for patients with B-PLL

ID Patient	Karyotype (according to ISCN 2016)	*MYC* (0: normal, 1:translocation, 2: gain) *	17p deletion (TP53) *	Trisomy 18/18q	Trisomy 3/3q	13q14 deletion *	Trisomy 12 *	8p deletion (*TNFRSF10*) *	11q deletion (*ATM*) *
BPLL_1	46,XY,del(13)(q12q14)[8]/46,XY[31]	0	0	0	0	1 (64%)	0	0	0
BPLL_2	49,XY,+i(3)(q10),t(4;8)(q21;q24),del(9)(q21q32),+12,+18[20]	1 (67%)	0	1	1	0	1 (41%)	0	0
BPLL_3	44,XY,add(7)(q31),-9,del(14)(q24),-15,del(17)(p13),add(21)(p11)[3]/44,sl,t(5;10)(q?21;p?11)[8]/44~46,sdl1,-del(14)(q24),der(14)del(14)(q24)add(14)(p10),+1~2mar[cp7]	0	1 (89%)	0	0	0	0	1 (5%)	0
BPLL_4	45,X,-Y,der(8)t(1;8)(q11;p21),t(8;22)(q24;q11)[6]/45,X,-Y,der(8)t(1;8)(q11;p21)t(8;22)(q24;q11),t(8;22)(q24;q11)[15]	1 (74%)	0	0	0	0	0	1 (83%)	0
BPLL_5	46,XY,add(1)(q2?5),?inv(2)(p24q14) or der(2) or dic(2.?),add(3)(p21),add(7)(p22),add(10)(q22),add(11)(q13),del(13)(q13q14),add or del(17)(p11),der(18)?t(11;18)(q13;q21)[10]/47,sl,+add(3)(p21)[2]	2 (3 copies, 5%)	1 (93%)	1**	1	1 (93%)	0	0	0
BPLL_6	46-47,XY,+3[10],ins(8)(q?22;?)[8],-9[8],+18[4],+mar1[3],+mar2[2][cp10]	2 (3 copies, 81%)	1 (18%)	1	1	1 (32%)	0	0	0
BPLL_7	46,XY,t(8;22)(q24;q11)[13]/46,XY[1]	1 (not quantified)	0	0	0	0	0	0	0
BPLL_8	48,XY,t(8;22)(q24;q11),+12,+18[15]	1 (89%)	0	1	0	0	1 (78%)	0	0
BPLL_9	46,XX,t(8;14)(q24;q32),del(10)(q23q25)[20]/45,idem,-15,der(16)t(15;16)(q1?4;p13)[8]/46,XX[2]	1 (80%)	0	0	0	0	0	0	0
BPLL_10	45,XX,t(2;8)(p11;q24),del(3)(p12),+add(3)(q11),der(8)t(8;9)(p12;q?21),-9,-17,der(19)t(9;19)(?p;q13)[20]	1 (94%)	1 (96 %)	0	0	1 (9%)	0	1 (89%)	0
BPLL_11	48,XX,t(8;14)(q24;q32),+12,del(13)(q13q22),+18[9]/47,sl,-X[8]/47,sdl1,t(1;6)(q43;q11),t(11;14)(q13;q32)[3]	1 (90%)	0	1	0	1 (80%)	1 (82%)	0	0
BPLL_12	49,XX,add(1)(q11),der(2)add(2)(p1?2)add(2)(q2?3),-8,+der(12)add(12)(p1?2)add(12)(q?11),del(13)(q14q21),add(14)(q32),?add(20)(q13),+mar1,+mar2x2[cp6]	0	0	0	0	1 (56%)	1 (56%)	ND	0
BPLL_13	46-47,X,-Y,+3,t(8;14)(q24;q32),+18[cp12]/46,XY[3]	1 (80%)	0	1	1	0	0	0	0
BPLL_14	44,XX,del(4)(q11),del(6)(q14q24),-7,add(9)(p24),-10,-17,add(20)(q13),-21,+2mar[24]/44,XX,idem,add(3)(q25)[2]	0	1 (79%)	0	0	1 (12%)	0	0	1 (85%)
BPLL_15	46,XX,der(4)?t(4;5)(q32;q15~21),-5,add(6)(q12),del(17)(p11),-19,-20,+3mar[8]/46,XX,t(5;8)(p15;q11)[4]/46,XX[3]	0	1 (75%)	0	0	0	0	0	0
BPLL_16	not done	1 (88%)	1 (89%)	ND	ND	1 (90%)	0	ND	0
BPLL_17	46,XY,t(8;22)(q24;q11),del(10)(q22q26)[17]	1 (94%)	0	0	0	0	0	0	0
BPLL_18	47,XY,t(8;14;19)(q24;q32;p1?3),+12[15]	1 (94%)	0	0	0	0	1 (82%)	0	0
BPLL_19	48,XX,+4,t(8;14)(q24;q32),+12[17]	1 (78%)	0	0	0	0	1 (82%)	0	0
BPLL_20	47,XY,+15,add(17)(p12)[7]/46,sl,-Y[4]/46,XY,add(8)(q32)[5]/46,XY,der(12)t(8;12)(p13;q21),add(17)(p12)[2]/46,XY[3]	2 (3 copies, 20%)	1 (90%)	0	0	0	0	1 (6%)	0
BPLL_21	48,XY,add(4)(p12),t(8;14)(q24;q32),del(11)(p13p15),+12,t(13;16)(q14;p13),del(17)(p11p13),-21,+2mar[9]/46,XY[1]	1 (74%)	0	0	0	0	1 (75%)	0	0
BPLL_22	46,X,add(X)(p21),der(8)add(8)(p11)t(8;22)(q24;q11),der(22)t(8;22)(q24:q11)[20]	1 (92%)	0	1**	0	0	0	1	0
BPLL_23	48,XY,t(8;14)(q24;q32),add(16)(q24),+der(18)t(3;18)(q?11;q?)x2[4]/46,XY[22]	1 (61%)	0	1	1	0	0	0	0
BPLL_24	46,XX,del(6)(q14q24),i(17)(q10)[11]/46,XX,t(7;7;14)(q11;q3?3;q32),del(17)(p12)[8]/46,XX[1]	0	1 (92%)	0	0	0	0	0	0
BPLL_25	40,X,add(X)(q21),t(1;8)(p10;p10),-5,-6,add(7)(q31),der(9)t(3;9)(q13;q13),der(10)t(9;10)(q13;p12),add(12)(q14),der(13;22)(q10;q10)del(13)(q13q21),-15,add(15)(p11),-16,tr(16),-17,add(17)(p13),-21,add(21)(p11),add(22)(q13),+1~2mar[16]/80,slx2[4]/46,XX[9]	2 (4 copies, 42%; 8 copies, 5%)	1 (62%)	0	1	0	0	0	0

ID Patient	Karyotype (according to ISCN 2016)	*MYC* (0: normal, 1:translocation, 2: gain) *	17p deletion (TP53) *	Trisomy 18/18q	Trisomy 3/3q	13q14 deletion *	Trisomy 12 *	8p deletion (*TNFRSF10*) *	11q deletion (*ATM*) *
BPLL_26	48,XY,t(8;14)(q24;q32),+der(18)x2[4]/48,sl,del(3)(p11p22)[15]	1 (92%)	0	1	0	0	0	0	0
BPLL_27	46,XY,t(8;14)(q24;q32)[20]	1 (78%)	0	0	0	0	0	0	0
BPLL_28	44~46,XY,+Y,der(2)t(2;8)(p11;?),der(3)t(3;6)(p11;?),-6,der(7)t(7;14)(p22;q11),-8,der(12)t(12;15)(p12;?),der(14)t(8;14)(q22;q32),der(15)t(15;17)(p11;q23)x2,der(16)t(15;16)(q23;q22),+2~3mar[cp20].	0	1 (51%)	0	0	1 (27%)	0	ND	0
BPLL_29	47,XX,t(8;14)(q24;q32),+mar[19]	1 (78%)	0	0	0	0	0	0	0
BPLL_30	46,XX,t(8;22)(q24;q11)[2]/46,XX[34]	1 (52%)	1 (70%)	0	0	0	0	1 (6%)	0
BPLL_31	48,XY,+3,t(8;14)(q24;q32),+mar1[12]/49,sl,+mar2[2]	1 (not quantified)	0	0	1	0	0	0	0
BPLL_32	49,XY,+3,der(7)t(7;8)(p21;?)del(7)(q33q35),r(8),+12,+18[13]/46,XY[7]	2 (amplification, 79%)	0	1	1	0	1 (74%)	1 (80%)	0
BPLL_33	46,XX,t(8;14)(q24;q32),der(10)t(1;10)(q11;p14)[16]/46,XX[7]	1 (86%)	0	0	0	1 (25%)	0	0	0
BPLL_34	45,XY,t(1;10)(p2?1;q25),t(3;11)(q23;p15),der(9)t(9;17)(q?22;q11),der(14)t(14;17)(p11;q?),-17[16]/45,XY,der(9)t(9;17),t(10;20)(q24;p13),t(12;21)(q11;q22),der(14)t(14;17),-17[3]/46,XY[1]	0	1 (87%)	0	0	0	0	0	0

0: absence; 1: presence; tri: trisomy; ND: not determined

* % of cells bearing the abnormality determined by interphase FISH analysis

** determined by WES and confirmed by FISH

Table S4. Recurrent copy-number variations from WES coverage data in 16 patients with B-PLL. The minimally altered regions are cited with regard to the hg19 reference genome.

Losses	Start	End	Length	Number of cases	Candidate genes
17p13	1629307	7677922	6048616	6	*TP53*
8p21	21924203	23432383	1508181	4	*TNFRSF10A/B/C/D, EGR3*
5q32-q33.1	149755481	149827491	72011	3	*TCOF1, RPS14, CD74*
9q21	71002296	79999625	8997329	3	no candidate genes
Xq28	152613014	153881710	1268697	2	no candidate genes
9q34	134379493	138927656	4548164	2	*NOTCH1*
13q14	45517397	53422012	7904616	2	*RB1, MIR15A, MIR16-1*
14q24	68758421	69263126	504706	2	*ZFP36L1, RAD51B*
19p13	1592411	2823326	1230916	2	no candidate genes

Gains	Start	End	Length	Number of cases	Candidate genes
18q21.32-q23	56702915	77960906	21257991	6	*BCL2*
chromosome 3	361267	197762956	197401689	4	no candidate genes
chromosome 12	175960	133808310	133632350	4	no candidate genes
17q24	63923550	67243919	3320369	4	no candidate genes
1q31.3-q42	197063118	225140263	28077146	3	no candidate genes
8q24	127569322	128753330	1184009	3	*MYC*
4q27-q35.2	121828503	190947668	69119165	2	no candidate genes

Table S5. *IGHV* sequencing data for patients with B-PLL

patient ID	*IGHV*	% homology		Unmutated/ minimally
BPLL_8	V1-2	95.5	significantly mutated	
BPLL_28	V1-2	100	unmutated	x
BPLL_30	V3-21	96.9	significantly mutated	
BPLL_21	V3-21	95.8	significantly mutated	
BPLL_29	V3-21	88.6	significantly mutated	
BPLL_6	**V3-23**	96.9	significantly mutated	
BPLL_22	**V3-23**	96.9	significantly mutated	
BPLL_33	**V3-23**	94.9	significantly mutated	
BPLL_13	**V3-23**	94.1	significantly mutated	
BPLL_10	V3-30	96.6	significantly mutated	
BPLL_5	V3-7	100	unmutated	x
BPLL_4	V3-74	97.2	minimally mutated	x
BPLL_1	V3-74	94.1	significantly mutated	
BPLL_32	V4-34	95.8	significantly mutated	
BPLL_34	V4-34	100	unmutated	x
BPLL_24	V4-39	95.5	significantly mutated	
BPLL_18	V4-39	88.3	significantly mutated	
BPLL_19	V4-4	96.2	significantly mutated	
BPLL_27	V4-4	93.3	significantly mutated	

Table S6. List of variants detected by WES in 16 patients with B-PLL. A total of 309 non-synonymous somatic mutations were identified in 287 genes. We validated 299 mutations by using targeted deep resequencing and/or RNA-Seq.

Patient ID	Gene	Mutation Type	Mutation	#Chr	Position	BaseRef	BaseCalled	nbBases RefNorm	nbBases AltN	VAF Norm	nbBases RefTumo	nbBases	VAF Tumor	Somatic_p-value	Confirmed (y/n)	Confirmation method	Sift score	Polyphen score
BPLL_1	ZBTB40	missense	ZBTB40:NM_014870:exon2:c.T557G:p.M186R.	chr1	22816998	T	G	197	2	1.01	70	68	49.28	1.45E-29	y	MiSeq+RNA-Seq	NA	0.899
BPLL_1	NFASC	missense	NFASC:NM_001005388:exon25:c.C2837T:p.T946I.	chr1	2.05E+08	C	T	234	1	0.43	84	74	46.84	4.98E-34	y	MiSeq	NA	NA
BPLL_1	LRRTM4	missense	LRRTM4:NM_024993:exon3:c.C577T:p.L193F.	chr2	77746418	G	A	325	0	0	113	108	48.87	4.67E-52	y	MiSeq	NA	NA
BPLL_1	LRRTM1	missense	LRRTM1:NM_178833:exon2:c.G160A:p.A54T.	chr2	80530785	C	T	129	0	0	50	35	41.18	4.79E-17	y	MiSeq	NA	0
BPLL_1	MYD88	missense	MYD88:NM_002468:exon5:c.T794C:p.L265P	chr3	38182641	T	C	264	0	0	88	77	46.67	8.37E-39	y	MiSeq+RNA-Seq	NA	0.999
BPLL_1	SLMAP	missense	SLMAP:NM_007159:exon2:c.G341A:p.R114Q.	chr3	57817252	G	A	391	16	3.93	187	158	45.8	1.20E-45	y	MiSeq+RNA-Seq	NA	0.993
BPLL_1	SPICE1	missense	SPICE1:NM_144718:exon2:c.G10T:p.V4F.	chr3	1.13E+08	C	A	182	2	1.09	94	53	36.05	2.41E-19	y	MiSeq+RNA-Seq	NA	0.427
BPLL_1	FBXW7	frameshift insertion	FBXW7:NM_018315:exon8:c.1156_1157insCCGATGCGGT:p.C386fs.	chr4	1.53E+08	-	ACCGCATCGG	243	0	0	86	47	35.34	5.17E-25	y	MiSeq+RNA-Seq	NA	1
BPLL_1	FBXW7	missense	FBXW7:NM_018315:exon8:c.C1153G:p.R385G.	chr4	1.53E+08	G	C	257	2	0.77	85	56	39.72	6.39E-27	y	MiSeq+RNA-Seq	NA	0.06
BPLL_1	LIFR	missense	LIFR:NM_001127671:exon17:c.G2435A:p.R812Q.	chr5	38485983	C	T	273	0	0	111	69	38.33	1.44E-32	y	MiSeq	0.47	0.081
BPLL_1	NFIB	missense	NFIB:NM_001190738:exon8:c.G1307T:p.S436I.	chr9	14120455	C	A	72	0	0	23	25	52.08	7.42E-13	y	MiSeq	NA	0.063
BPLL_1	SVEP1	missense	SVEP1:NM_153366:exon38:c.A7958T:p.H2653L.	chr9	1.13E+08	T	A	322	3	0.92	131	95	42.04	4.00E-39	y	MiSeq	NA	NA
BPLL_1	LDB1	stopgain SNV	LDB1:NM_001113407:exon11:c.G1057T:p.E353X.	chr10	1.04E+08	C	A	261	2	0.76	88	70	44.3	1.26E-32	y	MiSeq+RNA-Seq	NA	0.73539
BPLL_1	WDR11	missense	WDR11:NM_018117:exon24:c.T2936G:p.F979C.	chr10	1.23E+08	T	G	122	0	0	55	63	53.39	3.18E-25	y	MiSeq+RNA-Seq	0.11	0.84
BPLL_1	MUC6	missense	MUC6:NM_005961:exon31:c.A5057G:p.N1686S.	chr11	1017744	T	C	1983	204	9.33	1304	198	13.18	1.51E-04	y	RNA-Seq	0.48	NA
BPLL_1	RB1	frameshift insertion	RB1:NM_000321:exon7:c.707_708insAG:p.K236fs.	chr13	48934252	-	AG	71	2	2.74	8	31	79.49	6.41E-18	y	MiSeq+RNA-Seq	NA	NA
BPLL_1	SHC4	missense	SHC4:NM_203343:exon8:c.C1174T:p.R392W.	chr15	49148218	G	A	268	1	0.37	97	71	42.26	1.93E-33	y	MiSeq	NA	1
BPLL_1	PITPNM3	missense	PITPNM3:NM_031220:exon3:c.G142T:p.A48S.	chr17	6428760	C	A	138	4	2.82	47	56	54.37	8.91E-22	y	MiSeq	0.05	0.956
BPLL_4	CAPN13	missense	CAPN13:NM_144575:exon11:c.G1162A:p.V388I.	chr2	30974043	C	T	294	5	1.67	138	128	48.12	2.96E-44	y	MiSeq	0.35	NA
BPLL_4	SF3B1	missense	SF3B1:NM_012433:exon15:c.A2098G:p.K700E.	chr2	1.98E+08	T	C	125	6	4.58	59	58	49.57	4.35E-17	y	MiSeq+RNA-Seq	NA	0.999
BPLL_4	VHL	missense	VHL:NM_000551:exon2:c.G430A:p.G144R.	chr3	10188287	G	A	274	1	0.36	133	78	36.97	1.54E-31	y	MiSeq+RNA-Seq	NA	0.786
BPLL_4	NBEAL2	missense	NBEAL2:NM_015175:exon14:c.G1948A:p.G650R.	chr3	47037253	G	A	226	0	0	97	64	39.75	4.80E-29	y	MiSeq	NA	NA
BPLL_4	PLCH1	splice site	NA	chr3	1.55E+08	T	A	120	2	1.64	57	40	41.24	1.04E-14	y	MiSeq	NA	NA
BPLL_4	LNX1	missense	LNX1:NM_032622:exon1:c.G61A:p.V21M.	chr4	54424072	C	T	169	8	4.52	93	75	44.64	8.11E-20	y	MiSeq	0.13	0.53509
BPLL_4	ARHGAP10	missense	ARHGAP10:NM_024605:exon7:c.C643A:p.H215N.	chr4	1.49E+08	C	A	94	1	1.05	61	34	35.79	3.41E-11	y	MiSeq	NA	0.97
BPLL_4	NSD1	missense	NSD1:NM_022455:exon20:c.A6085G:p.T2029A.	chr5	1.77E+08	A	G	236	1	0.42	121	93	43.46	6.58E-35	y	MiSeq+RNA-Seq	NA	0.997
BPLL_4	JARID2	missense	JARID2:NM_004973:exon7:c.T1742C:p.V581A.	chr6	15497138	T	C	163	2	1.21	44	29	39.73	3.52E-15	y	MiSeq+RNA-Seq	0.95	0.02
BPLL_4	KHDRBS2	missense	KHDRBS2:NM_152688:exon6:c.C775T:p.P259S.	chr6	62604575	G	A	102	2	1.92	30	28	48.28	3.83E-13	y	MiSeq+RNA-Seq	NA	0.979
BPLL_4	IYD	missense	IYD:NM_001164695:exon3:c.A479G:p.N160S.	chr6	1.51E+08	A	G	103	2	1.9	36	34	48.57	1.93E-14	y	MiSeq	NA	0.926
BPLL_4	PAX4	splice site	NA	chr7	1.27E+08	C	G	217	5	2.25	83	79	48.77	7.69E-30	y	MiSeq	NA	NA
BPLL_4	MYC	missense	MYC:NM_002467:exon2:c.G478C:p.V160L.	chr8	1.29E+08	G	C	216	6	2.7	15	112	88.19	4.32E-66	y	MiSeq+RNA-Seq	NA	0.92
BPLL_4	CCDC67	missense	CCDC67:NM_181645:exon12:c.A1390C:p.N464H.	chr11	93141460	A	C	143	0	0	71	50	41.32	1.13E-20	y	MiSeq	NA	NA
BPLL_4	BTG4	missense	BTG4:NM_017583:exon2:c.A158T:p.K53I.	chr11	1.11E+08	T	A	146	4	2.67	66	52	44.07	8.21E-18	y	MiSeq	NA	0.997
BPLL_4	UPK2	missense	UPK2:NM_006760:exon4:c.A356G:p.Y119C.	chr11	1.19E+08	A	G	196	4	2	83	69	45.39	2.26E-25	y	MiSeq	NA	0.997
BPLL_4	TRHDE	missense	TRHDE:NM_013381:exon1:c.C485T:p.T162I.	chr12	72667043	C	T	119	1	0.83	17	30	63.83	6.61E-20	y	MiSeq	0.13	0.548
BPLL_4	TBC1D4	missense	TBC1D4:NM_014832:exon2:c.G607A:p.E203K.	chr13	75936635	C	T	198	4	1.98	99	92	48.17	3.02E-30	y	MiSeq	NA	0.98
BPLL_4	HYDIN	missense	HYDIN:NM_032821:exon42:c.G6659A:p.R2220Q.	chr16	70977722	C	T	359	5	1.37	266	80	23.12	1.16E-21	y	MiSeq	NA	0.44481
BPLL_4	FBN3	missense	FBN3:NM_032447:exon18:c.C2396G:p.P799R.	chr19	8191617	G	C	172	5	2.82	16	14	46.67	5.80E-10	y	MiSeq	NA	0.99
BPLL_4	ZNF208	missense	ZNF208:NM_007153:exon4:c.A509G:p.K170R.	chr19	22157327	T	C	252	8	3.08	105	102	49.28	2.37E-34	y	MiSeq	NA	NA
BPLL_4	ZRSR2	frameshift deletion	ZRSR2:NM_005089:exon8:c.571_572del:p.191_191del.	chrX	15833813	AT	-	96	3	3.03	2	87	97.75	3.19E-47	y	MiSeq+RNA-Seq	NA	NA
BPLL_4	BCOR	missense	BCOR:NM_001123385:exon10:c.A4376G:p.N1459S.	chrX	39921444	T	C	56	3	5.08	5	39	88.64	2.56E-19	y	MiSeq+RNA-Seq	NA	0.92
BPLL_5	KIF1B	missense	KIF1B:NM_015074:exon19:c.G1879A:p.D627N.	chr1	10357110	G	A	182	0	0	72	35	32.71	1.27E-17	y	MiSeq	NA	0.98
BPLL_5	FLNB	missense	FLNB:NM_001164317:exon21:c.C3356T:p.P1119L.	chr3	58109049	C	T	160	0	0	155	102	39.69	1.87E-26	y	MiSeq	NA	0.955
BPLL_5	USO1	missense		chr4	76703985	G	T	181	0	0	23	23	50	1.66E-21	y	MiSeq+RNA-Seq	NA	NA
BPLL_5	PPIP5K2	missense	PPIP5K2:NM_015216:exon13:c.T1474G:p.S492A.	chr5	1.02E+08	T	G	195	1	0.51	25	35	58.33	1.01E-25	y	MiSeq+RNA-Seq	NA	0.021
BPLL_5	ZNF425	missense	ZNF425:NM_001001661:exon4:c.G1931A:p.G644D.	chr7	1.49E+08	C	T	203	1	0.49	130	140	51.85	1.94E-42	y	MiSeq	NA	0.031
BPLL_5	RP1	missense	RP1:NM_006269:exon4:c.G1726A:p.V576M.	chr8	55538168	G	A	358	1	0.28	98	49	33.33	2.51E-28	y	MiSeq	NA	0.334
BPLL_5	GDF6	missense	GDF6:NM_001001557:exon1:c.G330T:p.K110N.	chr8	97172591	C	A	319	9	2.74	85	104	55.03	5.80E-45	y	MiSeq	NA	0.932
BPLL_5	KIF27	frameshift deletion	KIF27:NM_017576:exon14:c.3083delA:p.D1028fs.	chr9	86474138	C	-	414	0	0	80	67	45.58	9.68E-46	y	MiSeq	NA	NA
BPLL_5	TNC	missense	TNC:NM_002160:exon8:c.G2693C:p.R900P.	chr9	1.18E+08	C	G	98	2	2	102	58	36.25	1.83E-12	y	MiSeq	NA	0.999
BPLL_5	NUP214	missense	NUP214:NM_005085:exon18:c.C2455A:p.Q819K.	chr9	1.34E+08	C	A	330	2	0.6	40	16	28.57	5.58E-13	y	MiSeq+RNA-Seq	NA	0.08
BPLL_5	TM9SF3	missense	TM9SF3:NM_020123:exon2:c.G109C:p.D37H.	chr10	98336580	C	G	252	1	0.4	56	15	21.13	4.85E-10	y	MiSeq+RNA-Seq	0.06	0.423
BPLL_5	NAV2	missense	NAV2:NM_001111018:exon7:c.C1288T:p.R430W.	chr11	19955270	C	T	153	0	0	117	110	48.46	1.15E-31	y	MiSeq	NA	0.988
BPLL_5	OR8H2	missense	OR8H2:NM_001005200:exon1:c.C284T:p.T95M.	chr11	55872802	C	T	260	3	1.14	170	156	47.85	2.40E-45	y	MiSeq	0.13	0.001
BPLL_5	AHNAK	missense	AHNAK:NM_001620:exon5:c.C4994T:p.P1665L.	chr11	62296895	G	A	141	1	0.7	53	54	50.47	2.32E-23	y	MiSeq	NA	0.60018
BPLL_5	ARHGEF12	missense	ARHGEF12:NM_001198665:exon14:c.C1198T:p.R400C.	chr11	1.2E+08	C	T	428	0	0	102	56	35.44	2.90E-36	y	MiSeq+RNA-Seq	NA	1
BPLL_5	FGF6	missense	FGF6:NM_020996:exon2:c.C443T:p.T150M.	chr12	4553300	G	A	158	1	0.63	130	100	43.48	7.97E-27	y	MiSeq	NA	0.954

Patient ID	Gene	Mutation Type	Mutation	#Chr	Position	BaseRef	BaseCalled	nbBases RefNorm	nbBases AltNor	VAF Norma	nbBases RefTumor	nbBases	VAF Tumor	Somatic_p-value	Confirmed (y/n)	Confirmation method	Sift score	Polyphen score
BPLL_5	MLXIP	missense	MLXIP:NM_014938:exon1:c.G268C:p.E90Q.	chr12	1.23E+08	G	C	218	1	0.46	151	83	35.47	1.39E-26	y	MiSeq	NA	NA
BPLL_5	INTS6	missense	INTS6:NM_012141:exon14:c.A1838G:p.H613R.	chr13	51948824	T	C	53	0	0	0	12	100	2.48E-13	y	MiSeq+RNA-Seq	NA	0.999
BPLL_5	TP53	missense	NM_000546:exon6.T205C	chr17	7578235	T	C	148	1	0.67	0	67	100	9.43E-56	y	MiSeq+RNA-Seq	NA	0.998
BPLL_5	TANC2	missense	TANC2:NM_025185:exon25:c.C5596T:p.R1866W.	chr17	61498933	C	T	173	2	1.14	213	121	36.23	9.19E-24	y	MiSeq	NA	NA
BPLL_5	STRN4	stopgain SNV	STRN4:NM_001039877:exon5:c.C727T:p.Q243X.	chr19	47236306	G	A	230	3	1.29	143	91	38.89	2.84E-28	y	MiSeq	0.06	0.639802
BPLL_6	TNR	missense	TNR:NM_003285:exon5:c.C1111A:p.Q371K.	chr1	1.75E+08	G	T	166	3	1.78	104	65	38.46	1.53E-19	y	MiSeq	0.25	0.989
BPLL_6	NYAP2	missense	NYAP2:NM_020864:exon4:c.C704T:p.A235V.	chr2	2.26E+08	C	T	263	1	0.38	158	124	43.97	8.36E-42	y	MiSeq	0.07	NA
BPLL_6	MYD88	missense	MYD88:NM_002468:exon5:c.T794C:p.L265P	chr3	38182641	T	C	200	11	5.21	102	203	66.56	2.25E-50	y	MiSeq	NA	0.999
BPLL_6	ACSL1	frameshift deletion	ACSL1:NM_001995:exon18:c.1666_1681delp.556_561del.	chr4	1.86E+08	ATGTGCT	-	353	1	0.28	254	108	29.83	5.85E-35	y	MiSeq	NA	NA
BPLL_6	SLC6A19	missense	SLC6A19:NM_001003841:exon6:c.G815A:p.G272D.	chr5	1214108	G	A	162	2	1.22	77	95	55.23	8.06E-33	y	MiSeq	NA	0.998
BPLL_6	PDE4D	missense	PDE4D:NM_001197218:exon1:c.G194T:p.R65M.	chr5	59064142	C	A	259	2	0.77	138	98	41.53	6.33E-35	y	MiSeq	0.06	NA
BPLL_6	RIN1	missense	RIN1:NM_004292:exon3:c.A292C:p.T98P.	chr11	66103323	T	G	148	8	5.13	144	31	17.71	2.60E-04	y	MiSeq	NA	0.025
BPLL_6	KLRF2	missense	KLRF2:NM_001190765:exon5:c.C462G:p.H154Q.	chr12	10046123	C	G	314	5	1.57	147	144	49.48	6.93E-50	y	MiSeq	NA	NA
BPLL_6	SLITRK5	missense	SLITRK5:NM_015567:exon2:c.A1101C:p.K367N.	chr13	88328744	A	C	301	7	2.27	174	178	50.57	4.98E-51	y	MiSeq	NA	0.968
BPLL_6	KIF23	missense	KIF23:NM_004856:exon12:c.A1259T:p.Y420F	chr15	69728097	A	T	301	1	0.33	272	34	11.11	5.24E-10	y	MiSeq	0.1	0.488
BPLL_6	TP53	missense	TP53:NM_000546:exon8:c.G845C.R282P	chr17	7577093	C	G	135	2	1.46	78	84	51.85	7.41E-26	y	MiSeq	NA	1
BPLL_6	KRTAP9-9	missense	KRTAP9-9:NM_030975:exon1:c.C482A:p.S161Y.	chr17	39412119	C	A	342	0	0	177	22	11.06	1.29E-10	y	MiSeq	0.08	NA
BPLL_8	CACHD1	missense	CACHD1:NM_020925:exon14:c.A1909G:p.N637D.	chr1	65129488	A	G	192	0	0	41	33	44.59	7.47E-22	n		0.14	0.889
BPLL_8	POLR2B	missense	POLR2B:NM_000938:exon7:c.T832C:p.F278L.	chr4	57865879	T	C	213	1	0.47	63	49	43.75	1.23E-25	y	MiSeq	NA	0.999
BPLL_8	FAM160A1	missense	FAM160A1:NM_001109377:exon11:c.G2296A:p.A766T.	chr4	1.53E+08	G	A	166	1	0.6	56	28	33.33	3.15E-14	y	MiSeq	1	NA
BPLL_8	TRDN	frameshift deletion	TRDN:NM_001251987:exon13:c.1067delC:p.A356fs.	chr6	1.24E+08	C	-	239	2	0.66	124	78	38.61	3.52E-33	y	MiSeq	NA	NA
BPLL_8	BCLAF1	missense	BCLAF1:NM_014739:exon12:c.C2611T:p.R871C.	chr6	1.37E+08	G	A	661	1	0.15	249	76	23.38	1.69E-38	y	MiSeq	NA	0.992
BPLL_8	PC	missense	PC:NM_001040716:exon18:c.C2295G:p.D765E.	chr11	66618323	G	C	62	0	0	20	15	42.86	2.10E-08	y	MiSeq	0.1	0.001
BPLL_8	BCL7A	missense	BCL7A:NM_020993:exon1:c.G86A:p.R29H.	chr12	1.22E+08	G	A	121	1	0.82	15	44	74.58	5.87E-28	n		NA	0.985
BPLL_8	F7	missense	F7:NM_000131:exon8:c.C752T:p.A251V.	chr13	1.14E+08	C	T	224	0	0	50	44	46.81	6.34E-28	n		NA	0.994
BPLL_8	PPM1A	missense	PPM1A:NM_021003:exon2:c.G625A:p.G209S.	chr14	60750046	G	A	172	1	0.58	34	39	53.42	6.95E-24	y	MiSeq	0.28	0.57173
BPLL_8	RNFT1	missense	RNFT1:NM_016125:exon2:c.C358T:p.H120Y.	chr17	58040344	G	A	169	2	1.17	44	46	51.11	1.87E-23	y	MiSeq	NA	0.03
BPLL_8	DOK5	missense	DOK5:NM_018431:exon3:c.A183C:p.E61D.	chr20	53205030	A	C	325	2	0.61	64	54	45.76	1.11E-33	y	MiSeq	0.15	0.384
BPLL_8	BCOR	missense	BCOR:NM_001123385:exon4:c.T2771G:p.F924C.	chrX	39931828	A	C	101	2	1.94	0	39	100	6.15E-33	y	MiSeq	NA	0.997
BPLL_10	MAGI1	missense	MAGI1:NM_001033057:exon23:c.G3874A:p.G1292R.	chr3	65342568	C	T	227	2	0.87	68	75	52.45	1.33E-35	y	MiSeq	NA	0.024
BPLL_10	MRPS30	missense	MRPS30:NM_016640:exon5:c.G1234A:p.G412S.	chr5	44815218	G	A	117	0	0	52	76	59.38	5.92E-29	y	MiSeq+RNA-Seq	NA	0.74
BPLL_10	TRAPPC13/C5Or	missense	C5orf44:NM_024941:exon3:c.G215T:p.G72V.	chr5	64931870	G	T	151	4	2.58	94	98	51.04	9.36E-27	y	RNA-Seq	0.07	NA
BPLL_10	HLA-DRB5	missense	HLA-DRB5:NM_002125:exon2:c.T286A:p.F96I.	chr6	32489766	A	T	73	10	12.05	52	31	37.35	1.28E-04	y	RNA-Seq	0.9	0
BPLL_10	BCLAF1	stopgain SNV	BCLAF1:NM_001077440:exon4:c.G632A:p.W211X.	chr6	1.37E+08	C	T	660	2	0.3	328	122	27.11	5.36E-50	y	MiSeq	NA	0.73327
BPLL_10	POM121L12	missense	POM121L12:NM_182595:exon1:c.G488A:p.R163H.	chr7	53103852	G	A	108	0	0	57	36	38.71	9.77E-15	y	MiSeq	0.14	0.737
BPLL_10	MSR1	splice site	NA	chr8	16035500	T	G	99	2	1.98	51	62	54.87	7.88E-20	y	MiSeq	NA	NA
BPLL_10	RBM17	missense	RBM17:NM_032905:exon8:c.G823A:p.G275S.	chr10	6154291	G	A	151	5	3.21	68	55	44.72	4.18E-18	y	MiSeq+RNA-Seq	NA	0.999
BPLL_10	PABPC3	missense	PABPC3:NM_030979:exon1:c.C832T:p.R278C.	chr13	25671172	C	A	572	53	8.48	285	63	18.1	1.06E-05	y	RNA-Seq	NA	0.991
BPLL_10	ZFHX2	missense	ZFHX2:NM_033400:exon2:c.G1301A:p.G434D.	chr14	24003234	C	T	79	1	1.25	50	42	45.65	3.33E-13	y	MiSeq	NA	NA
BPLL_10	GSG2	missense	GSG2:NM_031965:exon1:c.A1345G:p.T449A.	chr17	3628574	A	G	204	5	2.39	3	108	97.3	8.59E-75	y	MiSeq	NA	0.108
BPLL_10	TP53	missense	TP53:NM_000546:exon7:c.C743A:p.A248D	chr17	7577538	C	T	84	1	1.18	0	42	100	5.65E-33	y	MiSeq+RNA-Seq	NA	1
BPLL_10	RSAD1	missense	RSAD1:NM_018346:exon7:c.G1090A:p.V364M.	chr17	48561104	G	A	69	2	2.82	39	30	43.48	2.11E-09	y	MiSeq+RNA-Seq	0.05	0.208
BPLL_10	C19orf44	missense	C19orf44:NM_032207:exon2:c.C25T:p.R9C.	chr19	16611628	C	T	55	6	9.84	40	40	50	1.99E-07	y	RNA-Seq	NA	0.006
BPLL_10	ZFX	frameshift deletion	ZFX:NM_001178086:exon6:c.663_682del:p.221_228del	chrX	24228425	AGAAGA	-	485	3	0.61	139	93	40.09	2.72E-48	y	MiSeq+RNA-Seq	NA	NA
BPLL_13	MTOR	missense	MTOR:NM_004958:exon30:c.T4358C:p.L1453P.	chr1	11217320	A	G	357	2	0.56	169	149	46.86	2.02E-56	y	MiSeq	NA	0.992
BPLL_13	CCDC28B	missense	CCDC28B:NM_024296:exon4:c.A503T:p.N168I.	chr1	32669958	A	T	116	0	0	56	46	45.1	6.09E-19	y	MiSeq+RNA-Seq	NA	0.996
BPLL_13	IQCA1	missense	IQCA1:NM_024726:exon2:c.G190A:p.V64I.	chr2	2.37E+08	C	T	215	2	0.92	79	76	49.03	1.44E-32	y	MiSeq	0.07	NA
BPLL_13	IQSEC1	stopgain SNV	IQSEC1:NM_001134382:exon3:c.C402A:p.Y134X.	chr3	12978114	G	T	323	1	0.31	326	167	33.87	2.18E-41	y	MiSeq+RNA-Seq	0.09	0.735421
BPLL_13	MYD88	missense	MYD88:NM_002468:exon3:c.C656G:p.S219C	chr3	38182032	C	G	183	0	0	173	121	34.75	1.69E-31	y	MiSeq+RNA-Seq	NA	0.955
BPLL_13	TP63	missense	TP63:NM_001114980:exon8:c.T1013C:p.I338T.	chr3	1.9E+08	T	C	234	1	0.43	176	95	35.06	8.03E-29	y	MiSeq	NA	0.725
BPLL_13	COL25A1	missense	COL25A1:NM_198721:exon20:c.C1090T:p.R364W	chr4	1.1E+08	G	A	87	0	0	55	16	22.54	9.74E-07	y	MiSeq	NA	0.999
BPLL_13	DCHS2	missense	DCHS2:NM_017639:exon25:c.G7819C:p.V2607L.	chr4	1.55E+08	C	G	248	0	0	141	104	42.45	1.95E-38	y	MiSeq	0.11	0.013
BPLL_13	GUCY1A3	missense	GUCY1A3:NM_001130682:exon6:c.T960G:p.F320L	chr4	1.57E+08	T	G	384	1	0.26	221	222	50.11	3.40E-74	y	MiSeq	0.16	0.999
BPLL_13	SPATS1	missense	SPATS1:NM_145026:exon5:c.G481A:p.G161R.	chr6	44329636	G	A	137	1	0.72	69	64	48.12	2.44E-23	y	MiSeq	NA	0.995
BPLL_13	COL9A1	missense	COL9A1:NM_001851:exon28:c.A1826G:p.Q609R	chr6	70961869	T	C	150	0	0	56	62	52.54	4.02E-28	y	MiSeq	0.32	0.463
BPLL_13	CSMD3	missense	CSMD3:NM_198123:exon18:c.T2955G:p.F985L	chr8	1.14E+08	A	C	195	1	0.51	93	85	47.75	2.02E-32	y	MiSeq	NA	0.999
BPLL_13	GLIS3	missense	GLIS3:NM_152629:exon3:c.C542A:p.A181D	chr9	4118471	G	T	229	1	0.43	103	119	53.6	2.75E-45	y	MiSeq	NA	0.754

Patient ID	Gene	Mutation Type	Mutation	#Chr	Position	BaseRef	BaseCalled	nbBases RefNorm	nbBases AltNor	VAF Norma	nbBases RefTumor	nbBases	VAF Tumor	Somatic_p-value	Confirmed (y/n)	Confirmation method	Sift score	Polyphen score
BPLL_13	PCSK5	missense	PCSK5:NM_001190482:exon30:c.G4008C:p.E1336D.	chr9	78936542	G	C	223	0	0	157	61	27.98	1.54E-21	y	MiSeq	0.39	NA
BPLL_13	OR5R1	missense	OR5R1:NM_001004744:exon1:c.G59A:p.R20Q.	chr11	56185650	C	T	321	1	0.31	181	148	44.98	6.61E-52	y	MiSeq	0.23	0.081
BPLL_13	C14orf93	missense	C14orf93:NM_001130708:exon3:c.A724G:p.N242D	chr14	23465351	T	C	204	8	3.77	122	88	41.9	6.20E-23	y	MiSeq+RNA-Seq	0.09	0.168
BPLL_13	CDKN3	missense	CDKN3:NM_001130851:exon4:c.C190T:p.H64Y	chr14	54878318	C	T	229	3	1.29	105	108	50.7	9.28E-39	y	MiSeq	NA	1
BPLL_13	AK7	missense	AK7:NM_152327:exon16:c.C1856T:p.A619V.	chr14	96949438	C	T	196	2	1.01	126	100	44.25	1.42E-30	y	MiSeq	0.09	0.721
BPLL_13	CHD2	frameshift insertion	CHD2:NM_001271:exon28:c.3485_3486insG:p.L1162fs.	chr15	93536118	-	G	74	0	0	51	19	27.14	2.62E-07	y	MiSeq	NA	
BPLL_13	NFAT5	missense	NFAT5:NM_173215:exon13:c.A3502G:p.N1168D	chr16	69727512	A	G	82	0	0	38	41	51.9	1.51E-16	y	MiSeq	NA	0.474
BPLL_13	CTAGE1	missense	CTAGE1:NM_172241:exon1:c.T2215C:p.F739L.	chr18	19995560	A	G	256	0	0	355	53	12.99	1.52E-12	y	MiSeq	NA	NA
BPLL_13	ITGB1BP3	missense	ITGB1BP3:NM_170678:exon8:c.C599T:p.P200L.	chr19	3942177	C	T	182	2	1.09	103	89	46.35	3.31E-29	y	MiSeq	NA	0.988
BPLL_13	CYP4F12	missense	CYP4F12:NM_023944:exon7:c.C814T:p.R272W.	chr19	15794469	C	T	403	2	0.49	213	229	51.81	2.48E-78	y	MiSeq	NA	0.771
BPLL_13	HAUS5	stopgain SNV	HAUS5:NM_015302:exon13:c.C1171T:p.Q391X.	chr19	36109943	C	T	42	0	0	14	13	48.15	5.19E-07	y	RNA-Seq	0.96	0.640922
BPLL_13	PAX1	missense	PAX1:NM_006192:exon2:c.C573G:p.I191M.	chr20	21687362	C	G	353	1	0.28	218	197	47.47	6.68E-64	y	MiSeq	0.33	0.926
BPLL_13	BCOR	frameshift insertion	BCOR:NM_001123385:exon14:c.4942_4943insA:p.P1648fs	chrX	39913173	-	T	70	2	2.78	2	67	97.1	3.31E-35	y	MiSeq+RNA-Seq	NA	NA
BPLL_18	PCNXL2	missense	PCNXL2:NM_014801:exon2:c.C284G:p.P95R.	chr1	2.33E+08	G	C	117	0	0	158	129	44.95	8.10E-25	y	MiSeq+RNA-Seq	NA	NA
BPLL_18	TPO	missense	TPO:NM_001206744:exon12:c.G2029A:p.V677I.	chr2	1499783	G	A	143	2	1.38	72	65	47.45	1.34E-22	y	MiSeq	NA	0.562
BPLL_18	CXCR4	stopgain SNV	CXCR4:NM_003467:exon2:c.C1013G:p.S338X	chr2	1.37E+08	G	C	73	0	0	77	82	51.57	2.79E-18	y	MiSeq+RNA-Seq	0.06	0.732383
BPLL_18	COBLL1	missense	COBLL1:NM_014900:exon5:c.T718G:p.F240V.	chr2	1.66E+08	A	C	30	0	0	42	41	49.4	7.71E-08	y	MiSeq+RNA-Seq	NA	0.986
BPLL_18	TTLL4	missense	TTLL4:NM_014640:exon3:c.G2107A:p.A703T.	chr2	2.2E+08	G	A	192	2	1.03	167	135	44.7	3.66E-33	y	MiSeq+RNA-Seq	0.36	0.001
BPLL_18	SPDL1	missense	CCDC99:NM_017785:exon8:c.C905T:p.T302M.	chr5	1.69E+08	C	T	218	0	0	218	212	49.3	3.84E-49	y	MiSeq	NA	0.944
BPLL_18	VARS2	missense	VARS2:NM_001167733:exon4:c.G83A:p.R28H	chr6	30883641	G	A	72	0	0	31	52	62.65	9.92E-20	y	RNA-Seq	NA	1
BPLL_18	FIBIN	missense	FIBIN:NM_203371:exon1:c.A583G:p.R195G.	chr11	27016656	A	G	117	0	0	59	46	43.81	1.38E-18	y	MiSeq	NA	0.996
BPLL_18	CLECL1	missense	CLECL1:NM_172004:exon2:c.A440G:p.H147R.	chr12	9875286	G	C	69	0	0	93	46	33.09	4.24E-10	y	MiSeq+RNA-Seq	0.1	0.263
BPLL_18	WBP4	frameshift deletion	WBP4:NM_007187:exon5:c.356delG:p.R119fs.	chr13	41642790	A	-	89	0	0	80	55	40.74	2.87E-15	y	MiSeq	NA	NA
BPLL_18	GPHN	missense	GPHN:NM_001024218:exon22:c.C2110T:p.R704C	chr14	67647553	C	T	215	0	0	127	83	39.52	1.31E-30	y	MiSeq+RNA-Seq	NA	0.986
BPLL_18	MUC16	missense	MUC16:NM_024690:exon3:c.G28442A:p.S9481N.	chr19	9059004	C	T	111	0	0	73	82	52.9	1.86E-25	y	MiSeq	NA	NA
BPLL_18	IGLL5	missense	IGLL5:NM_001178126:exon1:c.C133T:p.P45S.	chr22	23230366	C	T	49	0	0	13	16	55.17	3.95E-09	y	MiSeq+RNA-Seq	0.37	NA
BPLL_19	RAVER2	frameshift deletion	RAVER2:NM_018211:exon10:c.1735_1753del:p.579_585del.	chr1	65278514	TTATCATI	-	244	0	0	101	35	25.74	9.96E-18	y	MiSeq	NA	NA
BPLL_19	NR1I3	missense	NR1I3:NM_001077482:exon4:c.G283T:p.A95S.	chr1	1.61E+08	C	A	475	8	1.66	63	62	49.6	2.13E-40	y	MiSeq	0.11	0.011
BPLL_19	CXCR4	frameshift deletion	CXCR4:NM_003467:exon2:c.960_961del:p.320_321del. p.Ser325Glnfs	chr2	1.37E+08	CA	-	93	0	0	43	12	21.82	3.01E-06	y	MiSeq	NA	NA
BPLL_19	LGI2	missense	LGI2:NM_018176:exon6:c.C613G:p.L205V.	chr4	25019653	G	C	385	0	0	190	113	37.29	3.35E-47	y	MiSeq	0.46	0.003
BPLL_19	UTP15	missense	UTP15:NM_032175:exon6:c.T553C:p.Y185H.	chr5	72866416	T	C	98	0	0	65	33	33.67	4.51E-12	y	MiSeq	NA	0.999
BPLL_19	CLINT1	missense	CLINT1:NM_014666:exon1:c.C22G:p.R8G	chr5	1.57E+08	G	C	102	0	0	61	43	41.35	7.26E-16	y	MiSeq	NA	NA
BPLL_19	HOXA5	missense	HOXA5:NM_019102:exon1:c.G202A:p.E68K.	chr7	27183025	C	T	132	0	0	74	37	33.33	5.18E-15	y	MiSeq	NA	0.474
BPLL_19	UNC5D	missense	UNC5D:NM_080872:exon9:c.G1267A:p.G423S.	chr8	35579877	G	A	60	0	0	20	16	44.44	1.10E-08	y	MiSeq	NA	0.98
BPLL_19	SSTR5	missense	SSTR5:NM_001053:exon1:c.G1048A:p.A350T	chr16	1129916	G	A	45	0	0	53	58	52.25	5.20E-12	y	MiSeq	1	0
BPLL_19	PPL	missense	PPL:NM_002705:exon22:c.C3020T:p.A1007V.	chr16	4935636	G	A	1297	77	5.6	52	53	50.48	1.97E-32	y	MiSeq	0.23	0.001
BPLL_19	RAB37	missense	RAB37:NM_001163990:exon3:c.C178T:p.H60Y	chr17	72739310	C	T	94	0	0	52	41	44.09	1.18E-15	y	MiSeq	NA	0.999
BPLL_19	CCDC137	missense	CCDC137:NM_199287:exon3:c.C381G:p.H127Q.	chr17	79637367	C	G	2789	63	2.21	39	35	47.3	1.89E-34	y	MiSeq	0.64	0.008
BPLL_19	HSBP1L1	missense	HSBP1L1:NM_001136180:exon3:c.T128A:p.M43K.	chr18	77728098	T	A	86	0	0	41	25	37.88	3.74E-11	y	MiSeq	NA	NA
BPLL_19	FTHL17	missense	FTHL17:NM_031894:exon1:c.G451A:p.G151S.	chrX	31089620	C	T	325	5	1.52	128	111	46.44	2.08E-43	y	MiSeq	NA	0.108
BPLL_19	GPKOW	missense	GPKOW:NM_015698:exon7:c.C947A:p.T316N.	chrX	48972644	G	T	1159	0	0	98	103	51.24	1.56E-98	y	MiSeq	NA	0.125
BPLL_22	ARHGEF11	frameshift insertion	ARHGEF11:NM_198236:exon30:c.2963_2964insGG:p.A988fs	chr1	1.57E+08	-	CC	58	0	0	35	29	45.31	1.44E-10	y	MiSeq	NA	NA
BPLL_22	TGFBRAP1	missense	TGFBRAP1:NM_004257:exon12:c.T2459C:p.I820T	chr2	1.06E+08	A	G	235	0	0	132	142	51.82	4.25E-49	y	MiSeq	0.08	0
BPLL_22	SF3B1	missense	SF3B1:NM_012433:exon15:c.A2098G:p.K700E.	chr2	1.98E+08	T	C	141	0	0	69	82	54.3	1.04E-30	y	MiSeq	NA	0.999
BPLL_22	GLB1	missense	GLB1:NM_001135602:exon6:c.G538A:p.G180R	chr3	33093274	C	T	143	0	0	81	63	43.75	2.14E-23	y	MiSeq	NA	1
BPLL_22	MITF	missense	MITF:NM_198158:exon2:c.T71C:p.I24T	chr3	69987010	T	C	145	3	2.03	99	90	47.62	2.47E-24	y	MiSeq	NA	0.996
BPLL_22	PCDHB4	missense	PCDHB4:NM_018938:exon1:c.C76T:p.R26C.	chr5	1.41E+08	C	T	142	2	1.39	80	93	53.76	8.25E-29	y	MiSeq	0.15	0
BPLL_22	HMMR	splice site	NA	chr5	1.63E+08	A	T	74	0	0	48	37	43.53	7.60E-13	y	MiSeq	NA	NA
BPLL_22	TCP11	missense	TCP11:NM_001093728:exon7:c.C895T:p.L299F	chr6	35088283	G	A	176	0	0	103	93	47.45	1.31E-32	y	MiSeq	0.12	0.137
BPLL_22	PKHD1	missense	PKHD1:NM_170724:exon39:c.A6335G:p.Y2112C	chr6	51776752	T	C	55	0	0	35	29	45.31	3.27E-10	y	MiSeq	NA	0.998
BPLL_22	SYNE1	missense	SYNE1:NM_033071:exon52:c.G7789A:p.G2597S	chr6	1.53E+08	C	T	100	0	0	83	78	48.45	2.33E-21	y	MiSeq	0.08	0.002
BPLL_22	ABCA13	missense	ABCA13:NM_152701:exon17:c.G2312A:p.S771N.	chr7	48311575	G	A	206	1	0.48	115	112	49.34	4.39E-38	y	MiSeq	NA	NA
BPLL_22	COBL	missense	COBL:NM_015198:exon10:c.G2041A:p.A681T.	chr7	51096752	C	T	168	1	0.59	104	117	52.94	7.05E-36	y	MiSeq	NA	0.108
BPLL_22	PCLO	missense	PCLO:NM_033026:exon3:c.C2326T:p.P776S	chr7	82764540	G	A	215	0	0	121	150	55.35	3.61E-50	y	MiSeq	NA	NA
BPLL_22	MYC	missense	MYC:NM_002467:exon3:c.T1167G:p.F389L.	chr8	1.29E+08	T	G	242	1	0.41	151	126	45.49	6.50E-41	y	MiSeq	NA	0.761143
BPLL_22	CACNA2D4	missense	CACNA2D4:NM_172364:exon1:c.A103C:p.I35L.	chr12	2027537	T	G	106	0	0	54	43	44.33	3.02E-17	y	MiSeq	0.14	NA

Patient ID	Gene	Mutation Type	Mutation	#Chr	Position	BaseRef	BaseCalled	nbBases RefNorm	nbBase sAltNor	VAF Norma	nbBases RefTumor	nbBase s	VAF Tumor	Somatic_p-value	Confirmed (y/n)	Confirmation method	Sift score	Polyphen score
BPLL_22	CD4	missense	CD4:NM_000616:exon5:c.G511A:p.V171M.	chr12	6924062	G	A	109	0	0	51	62	54.87	6.05E-24	y	MiSeq	0.28	0
BPLL_22	KIAA1551/C12orf3	frameshift deletion	C12orf35:NM_018163:exon4:c.2959_2962del:p.987_988del.	chr12	32136848	AAAC	-	173	0	0	120	84	41.18	1.72E-27	y	MiSeq	NA	NA
BPLL_22	SETD1B	frameshift insertion	SETD1B:NM_015048:exon5:c.1635_1636insT:p.P545fs.	chr12	1.22E+08	-	T	46	0	0	47	42	47.19	2.74E-10	y	MiSeq	NA	NA
BPLL_22	CREBBP	frameshift insertion	CREBBP:NM_004380:exon7:c.1640_1641insT:p.S547fs	chr16	3831241	-	A	79	0	0	36	45	55.56	9.67E-18	y	MiSeq	NA	NA
BPLL_22	PRKCB 2	missense	PRKCB:NM_212535:exon1:c.G87T:p.K29N	chr16	23847583	G	T	78	2	2.5	36	21	36.84	9.21E-08	y	MiSeq	NA	0.998
BPLL_22	PRKCB 1	missense	PRKCB:NM_212535:exon9:c.A1054G:p.S352G	chr16	24135291	A	G	155	4	2.52	114	94	45.19	1.59E-23	y	MiSeq	NA	0.926
BPLL_22	SPATA20	missense	SPATA20:NM_022827:exon10:c.A1138G:p.I380V.	chr17	48627936	A	G	113	0	0	65	42	39.25	4.06E-16	y	MiSeq	0.2	0.119
BPLL_22	CBLN2	missense	CBLN2:NM_182511:exon3:c.C331T:p.R111C.	chr18	70209065	G	A	75	0	0	48	44	47.83	8.09E-15	y	MiSeq	NA	0.984
BPLL_24	PPP1R21	missense	PPP1R21:NM_152994:exon10:c.G935A:p.R312H	chr2	48698263	G	A	103	3	2.83	65	34	34.34	9.98E-10	y	MiSeq	NA	0.999
BPLL_24	ZDBF2	missense	ZDBF2:NM_020923:exon5:c.C2507T:p.P836L.	chr2	2.07E+08	C	T	185	2	1.07	118	85	41.87	2.26E-26	n		NA	NA
BPLL_24	STAC	missense	STAC:NM_003149:exon2:c.G188A:p.R63Q.	chr3	36484932	G	A	196	0	0	93	76	44.97	3.06E-31	y	MiSeq	NA	0.202
BPLL_24	MRPS27	missense	MRPS27:NM_015084:exon10:c.G853A:p.A285T.	chr5	71519662	C	T	114	1	0.87	83	27	24.55	1.06E-08	y	RNA-Seq	0.58	0
BPLL_24	WRNIP1	missense	WRNIP1:NM_020135:exon2:c.A959C:p.K320T	chr6	2769061	A	C	53	0	0	21	29	58	1.99E-12	y	MiSeq+RNA-Seq	0.1	0.712
BPLL_24	OPRK1	missense	OPRK1:NM_000912:exon4:c.G853A:p.V285I.	chr8	54142147	C	T	223	3	1.33	123	92	42.79	2.07E-30	y	MiSeq	0.83	0
BPLL_24	KIAA0020	missense	KIAA0020:NM_014878:exon18:c.C1816T:p.L606F.	chr9	2804462	G	A	145	0	0	93	73	43.98	8.19E-25	y	MiSeq+RNA-Seq	NA	0.96
BPLL_24	ANP32B	onframeshift deletic	ANP32B:NM_006401:exon6:c.653_655del:p.218_219del.	chr9	1.01E+08	TGA	-	90	0	0	68	22	24.44	5.53E-08	y	MiSeq+RNA-Seq	NA	NA
BPLL_24	ZNF33A	missense	ZNF33A:NM_006954:exon5:c.T943A:p.C315S	chr10	38343995	T	A	196	0	0	138	80	36.7	1.06E-26	y	MiSeq+RNA-Seq	0.41	0.152
BPLL_24	C11orf74	missense	C11orf74:NM_138787:exon3:c.C262T:p.R88C.	chr11	36654959	C	T	113	2	1.74	66	65	49.62	6.04E-20	y	MiSeq	NA	0.987
BPLL_24	SYT12	missense	SYT12:NM_001177880:exon3:c.G103A:p.A35T	chr11	66802184	G	A	110	1	0.9	40	43	51.81	1.02E-18	y	MiSeq	NA	0.157
BPLL_24	BIRC3	frameshift insertion	BIRC3:NM_182962:exon10:c.1643_1644insG:p.L548fs	chr11	1.02E+08	-	G	116	0	0	98	16	14.04	7.50E-06	y	MiSeq	NA	NA
BPLL_24	MLL2/KMT2D	frameshift deletion	MLL2:NM_003482:exon19:c.4884delT:p.G1628fs.	chr12	49438606	C	-	112	1	0.88	82	38	31.67	8.67E-12	y	MiSeq+RNA-Seq	NA	NA
BPLL_24	PPM1H	missense	PPM1H:NM_020700:exon5:c.G941C:p.R314P.	chr12	63131295	C	G	69	0	0	67	19	22.09	5.08E-06	y	MiSeq	NA	NA
BPLL_24	AHNAK2	missense	AHNAK2:NM_138420:exon7:c.A5465G:p.K1822R.	chr14	1.05E+08	T	C	129	6	4.44	130	34	20.73	1.82E-05	y	RNA-Seq	0.12	NA
BPLL_24	PMM2	missense	PMM2:NM_000303:exon6:c.A462T:p.R154S.	chr16	8905509	A	T	91	0	0	64	32	33.33	2.61E-11	y	MiSeq+RNA-Seq	NA	1
BPLL_24	NFATC3	missense	NFATC3:NM_173163:exon5:c.G1688T:p.R563I.	chr16	68200832	G	T	248	0	0	261	58	18.18	2.65E-16	y	MiSeq+RNA-Seq	NA	1
BPLL_24	TP53	missense	TP53:NM_000546:exon5:c.G394C:p.V132L	chr17	7578536	T	G	75	0	0	30	7	18.92	2.84E-04	y	MiSeq	NA	0.991
BPLL_24	TP53	frameshift deletion	TP53:NM_000546:exon5:c.384delT:p.P128fs	chr17	7578546	G	-	73	0	0	6	30	83.33	3.20E-21	y	MiSeq+RNA-Seq	NA	NA
BPLL_24	GRB7	missense	GRB7:NM_005310:exon5:c.G523A:p.G175R	chr17	37839492	G	A	239	1	0.42	281	67	19.25	9.66E-16	y	MiSeq	NA	0.849
BPLL_24	PITPNC1	missense	PITPNC1:NM_012417:exon3:c.G850A:p.A284T.	chr17	65688855	G	A	283	2	0.7	307	172	35.91	2.81E-38	y	MiSeq+RNA-Seq	0.06	NA
BPLL_24	ZNF416	missense	ZNF416:NM_017879:exon4:c.C889G:p.P297A.	chr19	58084383	G	C	226	0	0	142	104	42.28	5.52E-36	y	MiSeq	NA	0.939
BPLL_24	PTPRA	missense	PTPRA:NM_080840:exon13:c.A1040G:p.D347G	chr20	3001980	A	G	183	1	0.54	154	57	27.01	1.60E-16	y	MiSeq+RNA-Seq	NA	0.049
BPLL_24	RBL1	missense	RBL1:NM_002895:exon19:c.A2641T:p.S881C	chr20	35646763	T	A	208	0	0	170	26	13.27	2.73E-09	y	MiSeq	NA	0.99
BPLL_24	PHACTR3	missense	PHACTR3:NM_001199505:exon5:c.G547T:p.A183S	chr20	58342255	G	T	112	1	0.88	103	30	22.56	2.96E-08	y	MiSeq	0.19	0.002
BPLL_24	SON 1	frameshift deletion	SON:NM_032195:exon3:c.3742delG:p.V1248fs	chr21	34925279	T	-	205	0	0	174	47	21.27	2.87E-15	y	MiSeq	NA	NA
BPLL_24	SON 2	missense	SON:NM_032195:exon3:c.C3745G:p.P1249A	chr21	34925282	C	G	209	0	0	174	46	20.91	3.50E-15	y	MiSeq	NA	0.943
BPLL_24	TLR7	missense	TLR7:NM_016562:exon3:c.C917T:p.P306L.	chrX	12904544	C	T	308	5	1.6	347	92	20.96	5.78E-18	y	MiSeq	NA	0.244
BPLL_24	MAGEB16	stopgain SNV	MAGEB16:NM_001099921:exon2:c.G679T:p.E227X.	chrX	35820992	G	T	155	1	0.64	130	45	25.71	4.14E-13	y	MiSeq	0.1	0.58003
BPLL_24	EFNB1	missense	EFNB1:NM_004429:exon3:c.T431C:p.V164A.	chrX	68059591	T	C	93	0	0	97	40	29.2	6.50E-11	y	MiSeq	NA	0.997
BPLL_27	SYPL2	onframeshift deletic	SYPL2:NM_001040709:exon6:c.723_752del:p.241_251del.	chr1	1.1E+08	CAGGAC	-	447	2	0.45	64	62	49.21	7.00E-45	y	MiSeq	NA	NA
BPLL_27	PPP1R1C	missense	PPP1R1C:NM_001080545:exon3:c.G151T:p.D51Y.	chr2	1.83E+08	G	T	46	0	0	43	27	38.57	9.65E-08	y	MiSeq	NA	NA
BPLL_27	GHRL	missense	GHRL:NM_001134941:exon4:c.G307A:p.D103N	chr3	10328412	C	T	274	0	0	117	75	39.06	3.62E-34	n		NA	0.847
BPLL_27	SETD2	missense	SETD2:NM_014159:exon6:c.T4730C:p.L1577P.	chr3	47147596	A	G	105	2	1.87	65	49	42.98	6.57E-15	y	MiSeq+RNA-Seq	NA	1
BPLL_27	RNF180	missense	RNF180:NM_001113561:exon3:c.A161G:p.Q54R	chr5	63507317	A	G	146	1	0.68	76	73	48.99	6.43E-26	n		NA	0.017
BPLL_27	BTN2A1	missense	BTN2A1:NM_078476:exon3:c.G247C:p.E83Q	chr6	26459873	G	C	189	1	0.53	104	84	44.68	9.75E-30	y	RNA-Seq	NA	0.988
BPLL_27	ACAT2	missense	ACAT2:NM_005891:exon4:c.G373T:p.A125S.	chr6	1.6E+08	G	T	258	3	1.15	204	100	32.89	4.31E-27	n		0.32	0.229
BPLL_27	LIMK1	missense	LIMK1:NM_002314:exon6:c.C617T:p.P206L	chr7	73520213	C	T	136	0	0	76	90	54.22	8.12E-31	y	MiSeq+RNA-Seq	0.09	0.02
BPLL_27	EZH2	missense	EZH2:NM_152998:exon19:c.A2102G:p.E701G	chr7	1.49E+08	T	C	175	1	0.57	72	54	42.86	2.84E-23	y	MiSeq+RNA-Seq	NA	0.999
BPLL_27	IKBKB	missense	IKBKB:NM_001190720:exon6:c.A506T:p.K169M	chr8	42163895	A	T	145	0	0	96	39	28.89	1.59E-14	y	MiSeq+RNA-Seq	NA	0.973
BPLL_27	SCAI	missense	SCAI:NM_173690:exon15:c.C1321T:p.P441S	chr9	1.28E+08	G	A	209	3	1.42	106	117	52.47	1.09E-38	y	MiSeq+RNA-Seq	NA	0.999
BPLL_27	FADS3	missense	FADS3:NM_021727:exon5:c.G703A:p.V235M.	chr11	61646028	C	T	226	0	0	100	95	48.72	1.36E-39	y	MiSeq+RNA-Seq	NA	0.977
BPLL_27	LMO7	missense	LMO7:NM_015842:exon11:c.G1855A:p.D619N	chr13	76395659	G	A	337	7	2.03	140	109	43.78	9.01E-40	y	MiSeq	NA	0.98
BPLL_27	CHD8	missense	CHD8:NM_020920:exon38:c.A6517C:p.S2173R	chr14	21854164	T	G	261	4	1.51	104	85	44.97	2.05E-33	y	MiSeq+RNA-Seq	NA	NA
BPLL_27	RBM25	frameshift deletion	RBM25:NM_021239:exon11:c.1194_1195del:p.398_399del.	chr14	73572606	AG	-	103	2	1.9	55	28	33.73	1.05E-09	y	RNA-Seq	NA	NA
BPLL_27	RYR3	missense	RYR3:NM_001243996:exon88:c.T12479C:p.L4160P	chr15	34130675	T	C	143	0	0	89	76	46.06	6.04E-26	y	MiSeq	NA	NA
BPLL_27	CSK	missense	CSK:NM_004383:exon11:c.G953A:p.R318H	chr15	75094101	G	A	140	0	0	101	67	39.88	1.16E-21	y	MiSeq+RNA-Seq	NA	1
BPLL_27	SREBF1	frameshift deletion	SREBF1:NM_001005291:exon3:c.283delG:p.D95fs	chr17	17723734	G	-	202	3	1.46	64	73	53.28	5.15E-32	y	MiSeq	NA	NA

Patient ID	Gene	Mutation Type	Mutation	#Chr	Position	BaseRef	BaseCalled	nbBases RefNorm	nbBases AltN	VAF Norm	nbBases RefTumo	nbBases	VAF Tumor	Somatic_p-value	Confirmed (y/n)	Confirmation method	Sift score	Polyphen score
BPLL_27	MAPK4	missense	MAPK4:NM_002747:exon2:c.G122A:p.R41Q.	chr18	48190450	G	A	491	3	0.61	163	142	46.56	3.56E-66	y	MiSeq	0.61	0.06
BPLL_27	IZUMO4	missense	IZUMO4:NM_001039846:exon3:c.G593A:p.R198K.	chr19	2099013	G	A	93	0	0	66	46	41.07	3.93E-15	y	MiSeq+RNA-Seq	0.11	0.08
BPLL_27	ICAM1	missense	ICAM1:NM_000201:exon6:c.C1361T:p.T454I.	chr19	10395639	C	T	98	0	0	43	38	46.91	1.63E-16	y	MiSeq+RNA-Seq	NA	0.998
BPLL_27	EMR2	missense	EMR2:NM_152919:exon13:c.G1309A:p.V437M	chr19	14866540	C	T	306	0	0	133	91	40.62	1.70E-40	n		NA	0.315
BPLL_30	CSMD2	missense	CSMD2:NM_052896:exon65:c.G9808T:p.G3270W.	chr1	33990638	C	A	165	2	1.2	59	50	45.87	7.79E-22	y	MiSeq	NA	0.648
BPLL_30	ADAM30	missense	ADAM30:NM_021794:exon1:c.C1396A:p.L466I.	chr1	1.2E+08	G	T	129	1	0.77	63	69	52.27	7.00E-25	y	MiSeq	NA	0.993
BPLL_30	NFASC	missense	NFASC:NM_001005388:exon18:c.G1930A:p.V644M.	chr1	2.05E+08	G	A	135	1	0.74	64	58	47.54	4.36E-22	y	MiSeq	NA	0.921
BPLL_30	MSH6	missense	MSH6:NM_000179:exon1:c.C71T:p.S24L.	chr2	48010443	C	T	302	2	0.66	149	130	46.59	1.05E-47	y	MiSeq+RNA-Seq	0.22	0.008
BPLL_30	DES	missense	DES:NM_001927:exon1:c.C65T:p.P22L.	chr2	2.2E+08	C	T	142	7	4.7	59	64	52.03	5.56E-20	y	MiSeq	NA	0.43725
BPLL_30	SETD2	frameshift insertion	SETD2:NM_014159:exon3:c.2628_2629insAG:p.S876fs.	chr3	47163498	-	CT	126	1	0.79	84	45	34.88	1.10E-14	y	MiSeq+RNA-Seq	NA	NA
BPLL_30	TET2	frameshift deletion	TET2:NM_001127208:exon3:c.4179_4182del:p.1393_1394del.	chr4	1.06E+08	TGGGCTC	-	56	0	0	64	33	34.02	2.53E-08	y	MiSeq	NA	NA
BPLL_30	IL6ST	missense	IL6ST:NM_001190981:exon16:c.T2302G:p.S768A	chr5	55237182	A	C	23	0	0	15	18	54.55	4.88E-06	y	MiSeq+RNA-Seq	0.3	0.588
BPLL_30	MYOT	missense	MYOT:NM_006790:exon3:c.A1284C:p.E428D	chr5	1.37E+08	A	C	73	2	2.67	50	40	44.44	5.40E-11	y	MiSeq	NA	0.465
BPLL_30	FZD6	missense	FZD6:NM_001164615:exon4:c.A1179C:p.L393F	chr8	1.04E+08	A	C	201	4	1.95	132	105	44.3	2.45E-29	y	MiSeq	NA	0.853
BPLL_30	COL27A1	missense	COL27A1:NM_032888:exon10:c.C2237T:p.P746L.	chr3	1.17E+08	C	T	146	1	0.68	84	71	45.81	4.30E-24	y	MiSeq	0.09	1
BPLL_30	ABLIM1	missense	ABLIM1:NM_002313:exon4:c.C650T:p.P217L	chr10	1.16E+08	G	A	108	0	0	37	31	24.22	8.67E-10	y	MiSeq	NA	0.004
BPLL_30	OR51E1	missense	OR51E1:NM_152430:exon2:c.T18G:p.N6K.	chr11	4673774	T	G	37	1	2.63	18	18	50	1.65E-06	y	MiSeq	NA	0.264
BPLL_30	SORL1	missense	SORL1:NM_003105:exon25:c.C3514T:p.R1172C.	chr11	1.21E+08	C	T	214	2	0.93	120	79	39.7	3.36E-27	y	MiSeq	0.11	0.999
BPLL_30	TMPO	missense	TMPO:NM_003276:exon4:c.C1025T:p.P342L.	chr12	98927060	C	T	93	0	0	54	64	54.24	1.57E-21	y	MiSeq+RNA-Seq	0.08	0
BPLL_30	BNIP2	missense	BNIP2:NM_004330:exon6:c.A886G:p.M296V.	chr15	59964888	T	C	100	3	2.91	68	29	29.9	7.00E-08	y	MiSeq+RNA-Seq	NA	0.904
BPLL_30	CHD2	frameshift deletion	CHD2:NM_001271:exon33:c.4160_4178del:p.1387_1393del.	chr15	93545429	AAAAAAAA	-	84	1	1.18	45	40	47.06	5.70E-14	y	MiSeq+RNA-Seq		
BPLL_30	TP53	missense	TP53:NM_000546:exon8:c.T824A:p.L275Q	chr17	7577114	C	T	92	1	1.08	2	46	95.83	1.55E-33	y	MiSeq+RNA-Seq	NA	1
BPLL_30	JUP	missense	JUP:NM_021991:exon11:c.C1853T:p.A618V	chr17	39913957	G	A	109	0	0	42	53	55.79	4.78E-23	y	MiSeq+RNA-Seq	NA	0.838
BPLL_30	ZNF134	missense	ZNF134:NM_003435:exon3:c.A803G:p.Y268C.	chr19	58132290	A	G	105	1	0.94	53	59	52.68	1.16E-20	y	MiSeq+RNA-Seq	0.18	0.987
BPLL_32	TP73	missense	TP73:NM_001204190:exon3:c.G466A:p.E156K	chr1	3638768	G	A	91	0	0	27	23	46	6.89E-13	y	MiSeq	NA	0.096
BPLL_32	NOTCH2	stopgain SNV	NOTCH2:NM_024408:exon34:c.A6397T:p.K2133X.	chr1	1.2E+08	T	A	193	0	0	68	82	54.67	1.13E-37	y	MiSeq+RNA-Seq	NA	0.73513
BPLL_32	MYD88	missense	MYD88:NM_002468:exon4:c.T695C:p.M232T	chr3	38182259	T	C	147	0	0	68	141	67.46	3.91E-47	y	MiSeq+RNA-Seq	NA	1
BPLL_32	DROSHA	missense	DROSHA:NM_013235:exon25:c.T3140C:p.L1047S	chr5	31431688	A	G	222	0	0	126	121	48.99	1.32E-42	y	MiSeq+RNA-Seq	NA	NA
BPLL_32	TTC1	nonframeshift deletio	TTC1:NM_003314:exon8:c.864_866del:p.288_289del.	chr5	1.59E+08	AAT	-	182	1	0.55	96	50	34.25	2.80E-19	y	MiSeq+RNA-Seq	NA	NA
BPLL_32	DNAH11	missense	DNAH11:V973A	chr7	21639655	T	C	250	0	0	109	116	51.56	1.28E-47	y	MiSeq	NA	NA
BPLL_32	TNFRSF10C	nonframeshift deletio	TNFRSF10C:NM_003841:exon5:c.641_685del:p.214_229del.	chr8	22974405	GCCCCAG	-	31	0	0	2	37	94.87	7.39E-18	n		NA	NA
BPLL_32	PLEC	missense	PLEC:NM_201383:exon14:c.C1670T:p.A557V	chr8	1.45E+08	G	A	243	1	0.41	98	69	41.32	1.51E-30	y	RNA-Seq	NA	0.66782
BPLL_32	PARD3	missense	PARD3:NM_001184787:exon8:c.G998A:p.R333Q	chr10	34673075	C	T	111	0	0	55	52	48.6	1.83E-20	y	MiSeq	NA	0.999
BPLL_32	ARAP1	missense	ARAP1:NM_001040118:exon14:c.G1932C:p	chr11	72415197	C	G	158	0	0	45	45	50	1.55E-24	y	MiSeq	0.12	0.05
BPLL_32	PDZD3	missense	PDZD3:NM_001168468:exon3:c.G100A:p.E34K	chr11	1.19E+08	G	A	219	2	0.9	102	91	47.15	4.56E-34	y	MiSeq	NA	0.629
BPLL_32	PUS7L	missense	PUS7L:NM_001098615:exon7:c.C1489T:p.R497C	chr12	44130420	G	A	106	2	1.85	119	48	28.74	4.98E-10	y	RNA-Seq	NA	1
BPLL_32	TENC1	missense	TENC1:NM_170754:exon18:c.C1924T:p.R642C	chr12	53453349	C	T	227	0	0	160	80	33.33	3.25E-27	y	MiSeq	NA	0.999
BPLL_32	NCKAP1L	missense	NCKAP1L:NM_001184976:exon6:c.C422T:p.T141I	chr12	54903518	C	T	109	1	0.91	106	50	32.05	1.35E-12	y	MiSeq+RNA-Seq	0.41	0.28
BPLL_32	N4BP2L2	missense	N4BP2L2:NM_033111:exon7:c.A1443T:p.K483N.	chr13	33017225	T	A	117	0	0	38	44	53.66	1.10E-21	y	RNA-Seq	NA	NA
BPLL_32	ATP10A	missense	ATP10A:NM_024490:exon10:c.G2164A:p.V722M.	chr15	25953001	C	T	314	0	0	128	117	47.76	1.54E-51	y	MiSeq	NA	0.971
BPLL_32	UBR1	missense	UBR1:NM_174916:exon22:c.T2408G:p.V803G.	chr15	43319998	A	C	118	0	0	55	51	48.11	5.96E-21	y	MiSeq+RNA-Seq	NA	0.992
BPLL_32	BRCA1	missense	BRCA1:NM_007294:exon10:c.C2317T:p.P773S	chr17	41245231	G	A	339	9	2.59	150	137	47.74	8.39E-46	y	MiSeq	0.06	0.296
BPLL_32	KIF2B	missense	KIF2B:NM_032559:exon1:c.C547A:p.P183T.	chr17	51900941	C	A	404	3	0.74	184	127	40.84	9.46E-50	y	MiSeq	NA	0.099
BPLL_32	ACTG1	missense	ACTG1:NM_001199954:exon2:c.C56A:p.A19D	chr17	79479325	G	T	277	0	0	111	112	50.22	5.24E-49	y	MiSeq+RNA-Seq	NA	0.443
BPLL_32	ANKRD12	missense	ANKRD12:NM_015208:exon9:c.T3054A:p.D1018E	chr18	9256319	T	A	58	0	0	71	24	25.26	3.01E-06	y	RNA-Seq	NA	0.99
BPLL_32	MATK	missense	MATK:NM_139354:exon7:c.C571G:p.L191V	chr19	3781653	G	C	166	2	1.19	67	49	42.24	3.07E-20	y	MiSeq	0.46	0.001
BPLL_32	GPR112	missense	GPR112:NM_153834:exon21:c.C8444A:p.A2815E.	chrX	1.35E+08	C	A	43	0	0	0	44	100	7.62E-26	y	MiSeq	NA	0.754
BPLL_33	DPYD	stopgain SNV	DPYD:NM_000110:exon11:c.A1252T:p.K418X.	chr1	98039403	T	A	529	1	0.19	99	94	48.7	5.72E-62	y	MiSeq	0.56	0.66176
BPLL_33	LRIF1	missense	LRIF1:NM_018372:exon4:c.A1957G:p.I653V	chr1	1.11E+08	T	C	212	0	0	51	41	44.57	2.16E-25	y	MiSeq+RNA-Seq	1	0
BPLL_33	SMG5	missense	SMG5:NM_015327:exon18:c.G2636A:p.R879H.	chr1	1.56E+08	C	T	177	0	0	63	34	35.05	5.37E-18	y	MiSeq+RNA-Seq	NA	0.976
BPLL_33	IL1RL1	missense	IL1RL1:NM_016232:exon11:c.G1328A:p.R443Q.	chr2	1.03E+08	G	A	228	3	1.3	22	26	54.17	2.68E-20	y	MiSeq	NA	1
BPLL_33	SF3B1	missense	SF3B1:NM_012433:exon15:c.A2098G:p.K700E.	chr2	1.98E+08	T	C	158	1	0.63	25	30	54.55	2.28E-20	y	MiSeq+RNA-Seq	NA	0.999
BPLL_33	AFF4	missense	AFF4:NM_014423:exon3:c.C457T:p.R153C.	chr5	1.32E+08	G	A	205	1	0.49	22	21	48.84	1.22E-17	y	MiSeq+RNA-Seq	NA	1
BPLL_33	MUC17	missense	MUC17:NM_001040105:exon3:c.C5138T:p.T1713I.	chr7	1.01E+08	C	T	432	0	0	61	42	40.78	2.61E-34	y	MiSeq	NA	0.25442
BPLL_33	MET	missense	MET:NM_000245:exon2:c.G911T:p.R304I	chr7	1.16E+08	G	T	433	1	0.23	80	71	47.02	2.10E-47	y	MiSeq	NA	0.999
BPLL_33	MYC	missense	MYC:NM_002467:exon2:c.C482T:p.S161L.	chr8	1.29E+08	C	T	529	2	0.38	44	44	50	4.33E-40	y	MiSeq+RNA-Seq	NA	0.983

Patient ID	Gene	Mutation Type	Mutation	#Chr	Position	BaseRef	BaseCalled	nbBases RefNorm	nbBases AltN	VAF Norm	nbBases RefTumo	nbBases	VAF Tumor	Somatic_p-value	Confirmed (y/n)	Confirmation method	Sift score	Polyphen score
BPLL_33	COL5A1	missense	COL5A1:NM_000093:exon65:c.C5293T:p.R1765C.	chr9	1.38E+08	C	T	260	6	2.26	63	49	43.75	1.07E-23	y	MiSeq	NA	0.77514
BPLL_33	DDB1	missense	DDB1:NM_001923:exon21:c.C2660T:p.T887M.	chr11	61076456	G	A	79	0	0	16	16	50	7.37E-11	y	RNA-Seq	NA	0.031
BPLL_33	FAT3	missense	FAT3:NM_001008781:exon6:c.G4277A:p.R1426K.	chr11	92507288	G	A	325	1	0.31	86	62	41.89	4.34E-35	y	MiSeq	1	NA
BPLL_33	NCOR1	stopgain SNV	NCOR1:NM_001190440:exon36:c.C5459G:p.S1820X	chr17	15965185	G	C	132	1	0.75	29	28	49.12	1.40E-16	y	MiSeq+RNA-Seq	0.08	0.73546
BPLL_33	SMG8	missense	SMG8:NM_018149:exon3:c.T2665A:p.L889I.	chr17	57290849	T	A	202	1	0.49	38	31	44.93	1.77E-20	y	MiSeq+RNA-Seq	NA	0.963
BPLL_33	SLC39A6	missense	SLC39A6:NM_012319:exon2:c.G329A:p.R110H.	chr18	33706642	C	T	313	1	0.32	75	19	20.21	2.74E-12	y	RNA-Seq	0.2	0.39595
BPLL_33	BCOR	missense	BCOR:NM_001123385:exon10:c.A4376G:p.N1459S.	chrX	39921444	T	C	147	1	0.68	28	24	46.15	1.41E-15	y	MiSeq+RNA-Seq	NA	0.92
BPLL_34	UBR3	missense	UBR3:NM_172070:exon23:c.A3468G:p.I1156M.	chr2	1.71E+08	A	G	463	12	2.53	209	200	48.9	1.20E-65	y	MiSeq+RNA-Seq	NA	0.82
BPLL_34	PGM2	missense	PGM2:NM_018290:exon6:c.T554G:p.I185S.	chr4	37841716	T	G	245	3	1.21	226	29	11.37	9.38E-07	y	RNA-Seq	NA	0.336
BPLL_34	ZSWIM6	missense	ZSWIM6:NM_020928:exon8:c.C1915G:p.L639V.	chr5	60825956	C	G	97	6	5.83	44	46	51.11	3.44E-13	y	RNA-Seq	0.11	NA
BPLL_34	TINAG	missense	TINAG:NM_014464:exon7:c.G1024A:p.V342I.	chr6	54214638	G	A	130	3	2.26	78	92	54.12	5.95E-26	y	MiSeq	0.4	0
BPLL_34	FAM120B	missense	FAM120B:NM_032448:exon2:c.T1213A:p.S405T.	chr6	1.71E+08	T	A	282	1	0.35	324	38	10.5	2.23E-09	y	RNA-Seq	NA	0
BPLL_34	OCM	missense	OCM:NM_001097622:exon2:c.T89C:p.F30S.	chr7	5922151	T	C	252	4	1.56	126	126	50	5.34E-42	y	MiSeq	NA	1
BPLL_34	PGAM2	nonframeshift deletion	PGAM2:NM_000290:exon1:c.314_316del:p.105_106del.	chr7	44104813	GGC	-	133	6	4.32	75	69	47.92	1.96E-18	y	RNA-Seq	NA	NA
BPLL_34	MLLT3	nonframeshift deletion	MLLT3:NM_004529:exon5:c.502_504del:p.168_168del.	chr9	20414340	CTA	-	105	0	0	60	42	41.18	5.41E-16	n		NA	NA
BPLL_34	DDIT4	missense	DDIT4:NM_019058:exon3:c.C271T:p.H91Y.	chr10	74034518	C	T	226	9	3.83	130	137	51.31	5.22E-36	y	MiSeq+RNA-Seq	0.29	0.653
BPLL_34	DOCK1	missense	DOCK1:NM_001380:exon10:c.G910A:p.V304M.	chr10	1.29E+08	G	A	162	0	0	71	71	50	1.20E-29	y	MiSeq	NA	NA
BPLL_34	KRT3	missense	KRT3:NM_057088:exon1:c.G251A:p.R84Q.	chr12	53189576	C	T	141	8	5.37	62	77	55.4	2.79E-22	y	MiSeq	NA	NA
BPLL_34	PIWIL1	missense	PIWIL1:NM_004764:exon16:c.C1921T:p.R641W	chr12	1.31E+08	C	T	148	3	1.99	77	51	39.84	4.82E-17	y	MiSeq	NA	0.985
BPLL_34	TMEM63C	missense	TMEM63C:NM_020431:exon8:c.G515A:p.R172Q.	chr14	77693816	G	A	63	4	5.97	41	33	44.59	7.04E-08	y	RNA-Seq	NA	NA
BPLL_34	CILP	missense	CILP:NM_003613:exon3:c.C2729G:p.A910G.	chr15	65489835	G	C	227	6	2.58	123	140	53.23	6.60E-41	y	MiSeq	0.48	0
BPLL_34	TP53	missense	TP53:NM_000546:exon7:c.T707G:p.V236G	chr17	7577574	T	C	224	4	1.75	0	99	100	7.66E-80	y	MiSeq+RNA-Seq	NA	0.999
BPLL_34	PYCR1	missense	PYCR1:NM_153824:exon4:c.G508A:p.V170I	chr17	79892834	C	T	55	0	0	39	51	56.67	9.84E-15	y	MiSeq+RNA-Seq	0.1	0.014
BPLL_34	LAMA1	missense	LAMA1:NM_005559:exon50:c.G7079A:p.R2360H.	chr18	6965403	C	T	492	11	2.19	256	203	44.23	3.78E-63	y	MiSeq	NA	0
BPLL_34	ADNP2	missense	ADNP2:NM_014913:exon4:c.C3145T:p.R1049C.	chr18	77896441	C	T	105	2	1.87	61	27	30.68	6.09E-09	y	MiSeq	NA	0.994
BPLL_34	SPTBN4	missense	SPTBN4:NM_020971:exon14:c.C1852A:p.R618S.	chr19	41018548	C	A	52	0	0	19	16	45.71	3.43E-08	y	MiSeq	NA	1
BPLL_34	LTN1	missense	LTN1:NM_015565:exon23:c.A4269T:p.E1423D.	chr21	30316078	T	A	279	7	2.45	127	110	46.41	8.10E-37	y	MiSeq+RNA-Seq	0.6	0.008

Table S7. Fusions detected by RNA-Seq. The coordinates refer to the hg19 reference genome.

Patient ID	ChrA	Gene A	Band	ChrB	Gene B	Band	Number of spanning reads	Strand orientation (forward:f / reverse:r)	Confirmation by RT-PCR	Corresponding abnormalities by karyotype
BPLL_32	chr13:114514709	FAM70B exon 8	13q34	chr13:114536552	GAS6 intron 2	13q34	161	rr	ND	
BPLL_34	chr10:104161003	NFKB2 exon 19	10q24.32	chr10:105232917	CALHM3 3'UTR exon 3	10q24.33	676	fr	ND	
BPLL_27	chr14:106213663	IGHG1	14q32.33	chr8:128750494	MYC intron 1	8q24.21	20	rf	ND	t(8;14)(q24;q32)
BPLL_30	chr8: 127794677	PVT1 intron 1	8q24.21	chr22:22792944	IGLV4-69*01	22q11.22	11	ff	**yes**	t(8;22)(q24;q11)
BPLL_4	chr8:128078031	PVT1 intron 5	8q24.21	chr22:22888886	IGLL5 intron 1	22q11.22	38	ff	**yes**	t(8;22)(q24;q11)
BPLL_30	chr10:93558648	TNKS2 intron 1	10q23.32	chr14:78177178	SLIRP intron 1	14q24.3	18	ff	ND	
BPLL_5	chr3:75832457	ZNF717 exon 2	3p12.3	chr18:56686740	no gene	18q21.32	16	rf	ND	der(18), add(3)(p22)

ND: not done

Table S8. Quality control data for WES.

Patient ID	Fraction	Total reads	%Unmapped	Mean depth	% Targeted exome covered by at least 1 read	% Targeted exome covered by at least 10 reads
BPLL_1	CD19+/CD5+	1.48E+08	0.12137	106 x	91.62	86.179
BPLL_1	CD3+	1.82E+08	0.032739	146 x	91.671	88.545
BPLL_4	CD19+	1.45E+08	0.041366	95 x	87.118	80.568
BPLL_4	CD3+	2.01E+08	0.069637	109 x	89.508	84.935
BPLL_5	CD19+	1.54E+08	0.5213	94 x	89.387	81.924
BPLL_5	CD3+	2.23E+08	0.50716	119 x	91.843	87.29
BPLL_6	CD19+	1.65E+08	0.043966	129 x	91.641	87.596
BPLL_6	CD3+	1.80E+08	0.067951	119 x	91.672	87.647
BPLL_8	CD19+	1.02E+08	0.022356	54 x	91.552	80.11
BPLL_8	CD3+	1.59E+08	0.02019	105 x	91.855	87.253
BPLL_10	CD19+/CD5+	2.86E+08	0.031002	107 x	91.578	89.399
BPLL_10	CD3+	1.59E+08	0.029828	121 x	91.54	88.282
BPLL_13	CD19+	1.53E+08	0.043803	122 x	91.514	86.481
BPLL_13	CD3+	1.79E+08	0.037851	130 x	91.692	88.968
BPLL_18	CD19+/IGK+	1.84E+08	0.022249	98 x	91.829	87.161
BPLL_18	CD3+	9.57E+07	0.021904	69 x	91.728	83.383
BPLL_19	CD19+	1.22E+08	0.021803	86 x	91.71	85.768
BPLL_19	CD3+	1.95E+08	0.042149	131 x	91.705	86.44
BPLL_22	CD19+	1.74E+08	0.2666	116 x	88.184	80.881
BPLL_22	CD3+	1.58E+08	0.46315	92 x	88.921	81.941
BPLL_24	CD19+/IGK+	1.76E+08	0.042913	117 x	86.75	79.931
BPLL_24	CD3+	1.71E+08	0.060721	103 x	87.321	81.548
BPLL_27	CD19+	1.61E+08	0.040653	127 x	91.645	88.275
BPLL_27	CD3+	1.88E+08	0.041159	143 x	91.574	86.851
BPLL_30	CD19+/CD5+	1.12E+08	0.019185	89 x	91.463	85.493
BPLL_30	CD3+	1.06E+08	0.021597	88 x	91.396	84.335
BPLL_32	CD19+	1.30E+08	0.04556	97 x	91.578	86.2
BPLL_32	CD3+	1.43E+08	0.038769	108 x	91.615	87.074
BPLL_33	CD19+/CD5+	1.12E+08	0.0185	51 x	91.319	78.561
BPLL_33	CD3+	1.87E+08	0.020833	129 x	91.837	89.375
BPLL_34	CD19+/IGK+	1.35E+08	0.016767	94 x	91.781	85.962
BPLL_34	CD3+	1.58E+08	0.01649	99 x	91.833	86.756

Supplementary Figures

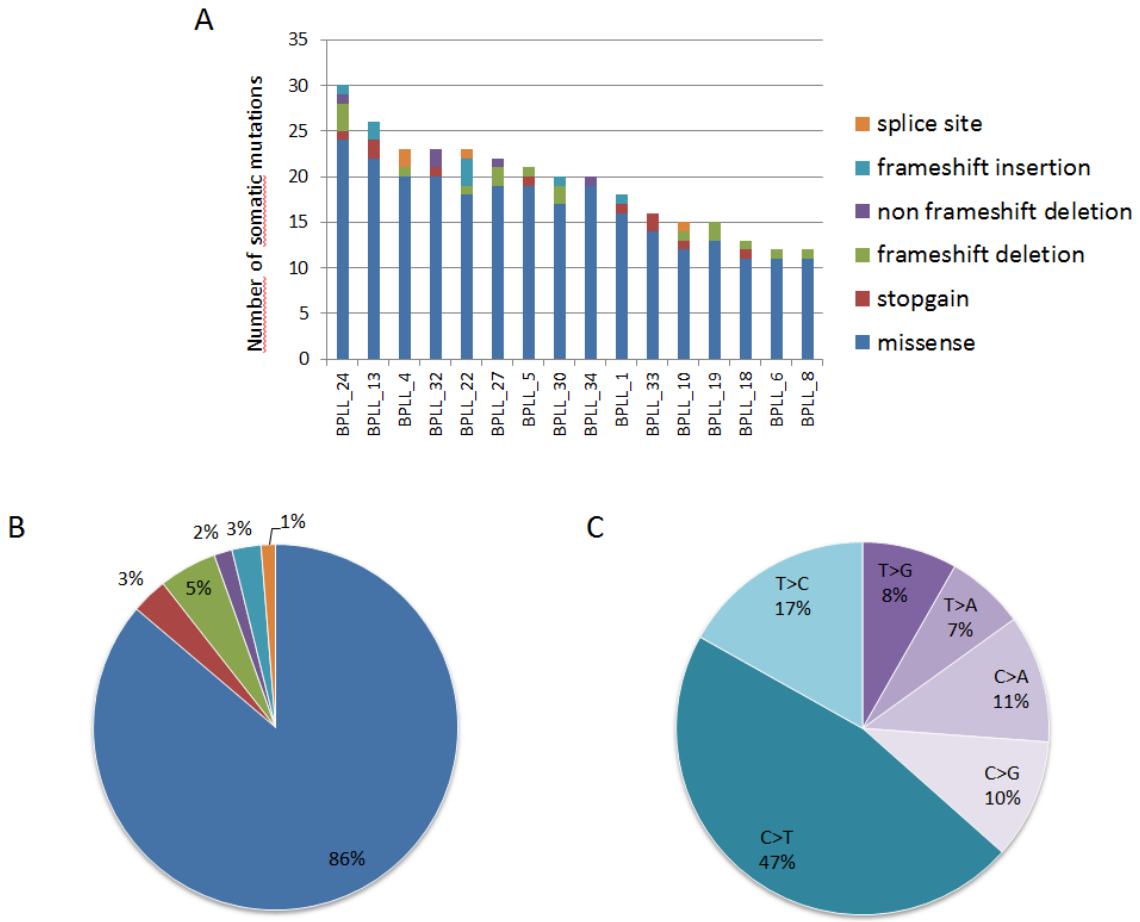

Figure S1. Somatic variants in coding regions identified by WES in 16 patients with B-PLL. A. Numbers and types of somatic mutations identified in each patient. The median number of somatic mutation was 20 per patient (range: 12-30). B. Distribution of the 309 somatic mutations identified in the 16 patients with B-PLL. The most frequent alterations were somatic missense mutations (n=266, 86%) and insertions/deletions (n=29, 10%). C. Distribution of base changes, with transitions in purple and transversions in blue.

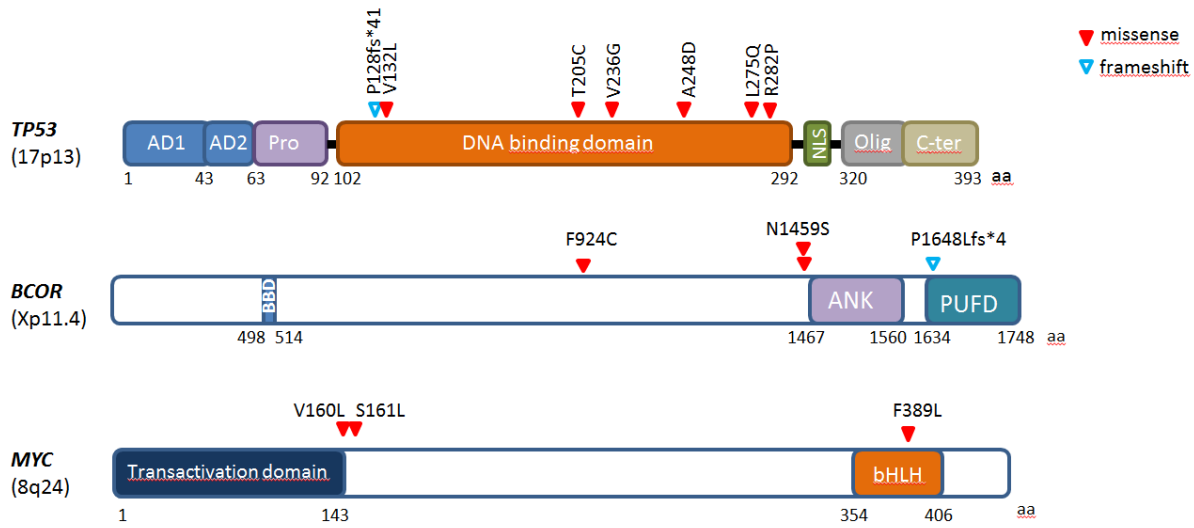

Figure S2. Genes with recurrent somatic mutations, in patients with B-PLL.

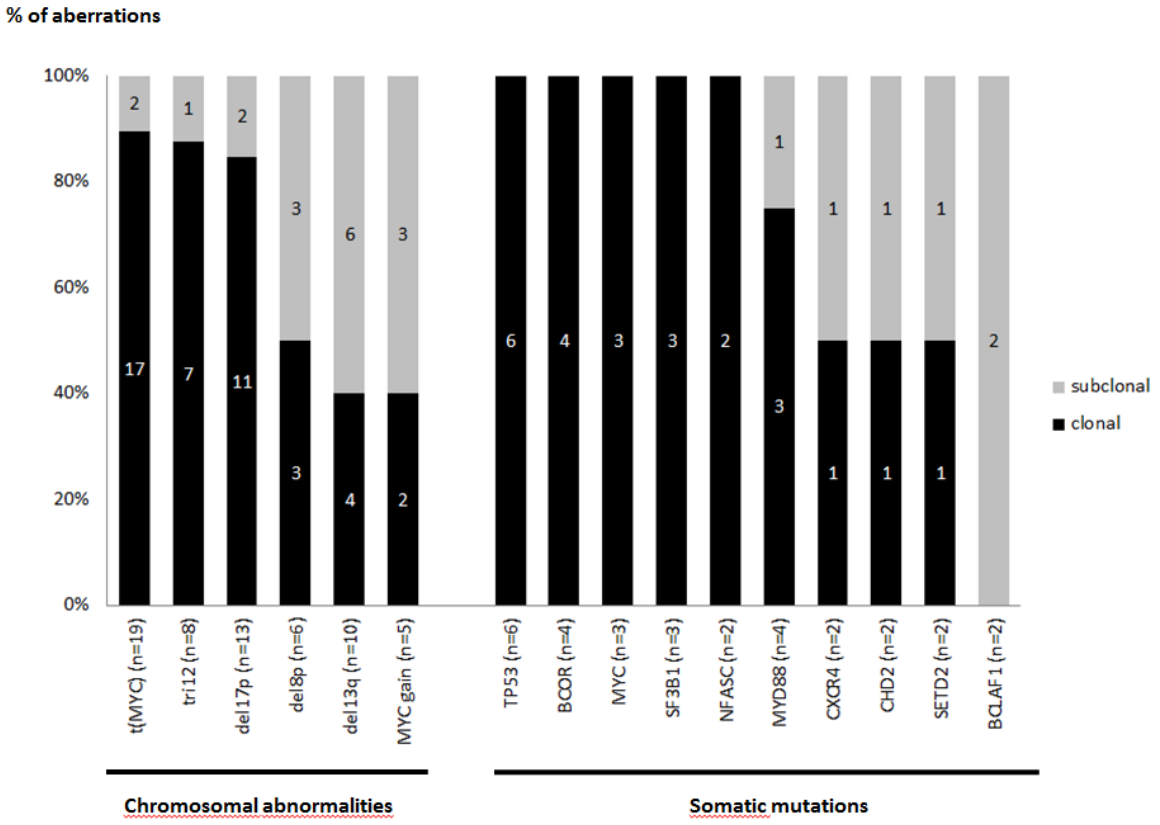

Figure S3. Clonal and subclonal aberrations. Histograms represent the percentage of the aberrations classified as clonal (black) or subclonal (grey). The n corresponds to the number of patients with the genomic abnormality. For example, the translocation t(*MYC*) was observed in 19 cases with available data (see the Supplementary Methods above). The aberration was clonal in 17 of the 19 cases (89.5%).

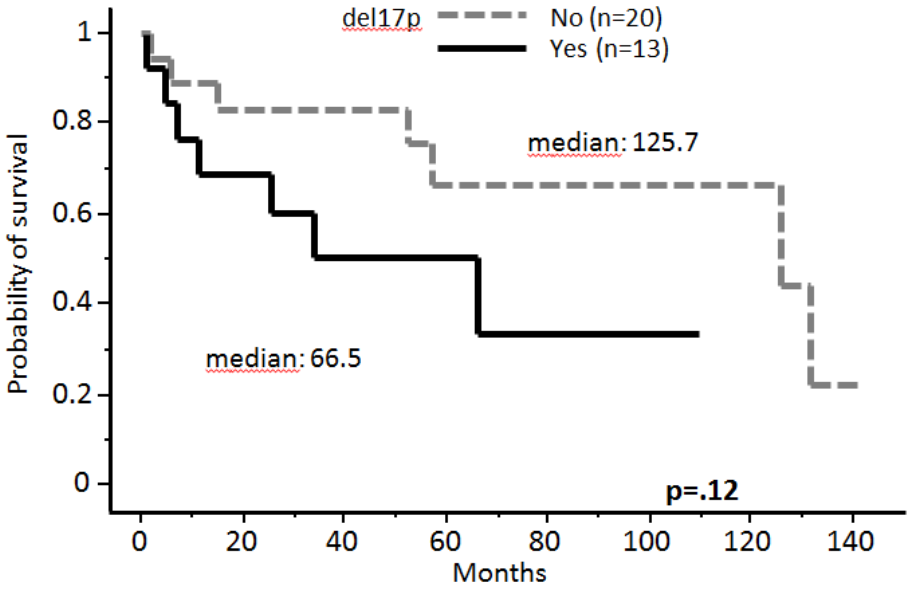

Figure S4. Overall survival in patients with B-PLL, according to the presence (median [95%CI]: 66.5 [11.1-66.5] or absence (median [95%CI]: 125.7 [57.5-132.1] of del17p.

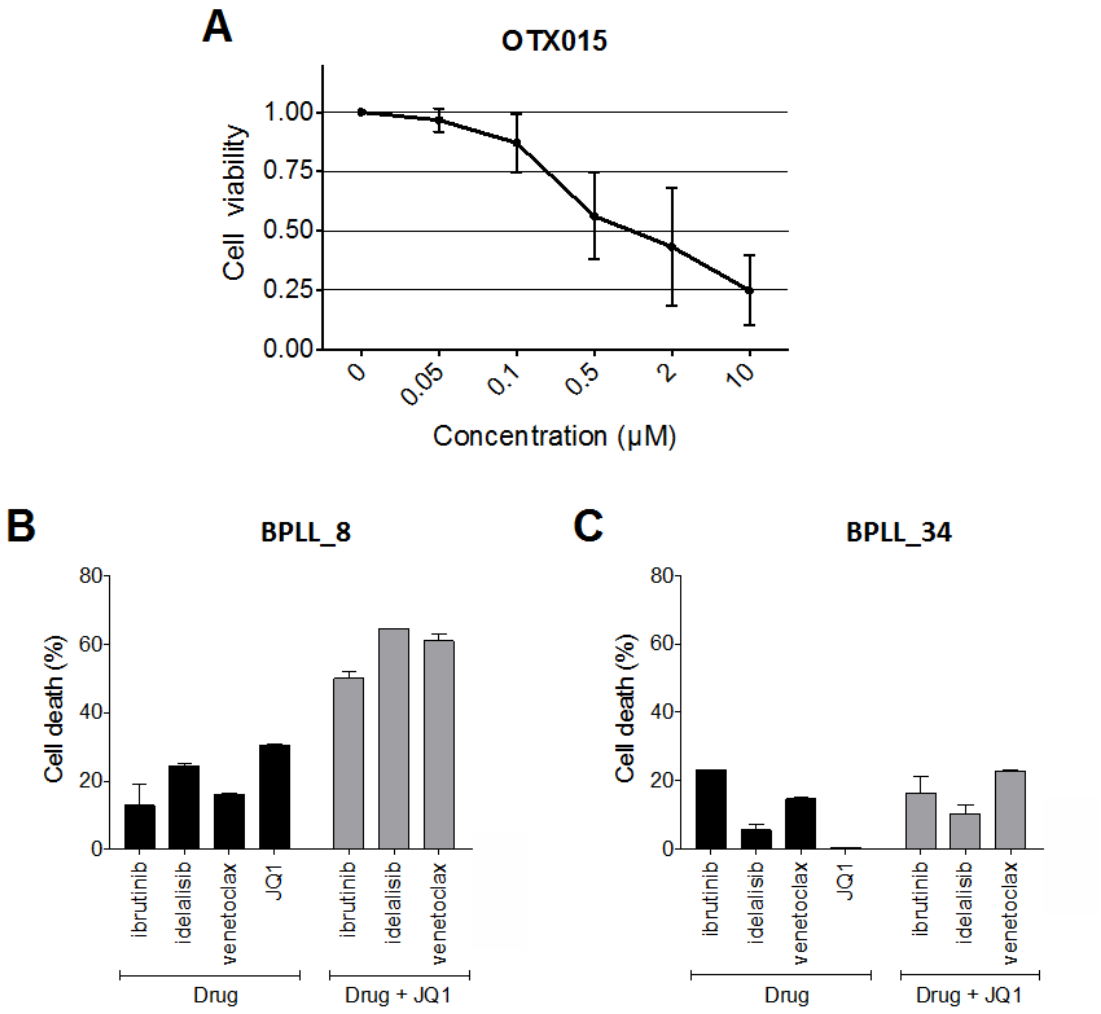

Figure S5. (A) Mean of cell viability assessed by ATP-based CellTiter-Glo 2.0 kit in B-PLL cells from 3 patients (B_PLL8, BPLL_13 and BPLL_18) exposed to increasing doses of OTX015. (B) Cell death was quantified in primary B-PLL cells from patient BPLL_8 (with t(*MYC*)) with or without pretreatment with JQ1 (500 nM) and and exposure for 48h to ibrutinib (7.5 µM), idelalisib (50 µM), or venetoclax (10 nM). The percentages refer to annexin-V-positive or annexin-V-/PI-positive cells. (C) Primary B-PLL cells from patient BPLL_34 (with del17p but no *MYC* activation) were treated and analyzed as in (B). Bars represent the mean ± SEM.

GFCH (Groupe Francophone de Cytogénétique Hématologique) members

Nassera ABERMIL (Paris); Lucille ALTOUNIAN (Metz) ; Geneviève AMEYE (Leuven) ; Nathalie AUGER (Villejuif); Estelle BALDUCCI (Villejuif); Zsofia BALOGH (Villejuif); Laurence BARANGER (Angers); Carole BARIN (Tours); Audrey BASINKO (Brest); Beatrice GRANGE (Lyon) ; Martine BECKER (Rouen); Audrey BIDET (Bordeaux); Chrystele BILHOU-NABERA (Paris); Rossana BONOMI (Montevideo); Claire BORIE (Villejuif); Elise BOUDRY (lille); Evelyne CALLET-BAUCHU (Lyon); Helene CANNONI (Marseille); Élise CHAPIRO (Paris); COLLONGE-RAME Marie-Agnes (Besancon); Lucie COSTER (Toulouse); Sophie COTTERET (villejuif); Wendy CUCCUINI (Paris); Laurent DANO (strasbourg); Agnes DAUDIGNON (Lille); Mathieu DECAMP (Caen); Sabine DEFASQUE (Cergy-Pontoise); Barbara DEWAELE (Leuven); Nathalie DOUET-GUILBERT (Brest); Olivier DUPUY (Toulon); Virginie ECLACHE (Paris); Yann FERRET (Amiens); Sandra FERT-FERRER (Chambery); Nathalie GACHARD (Limoges); Baptiste GAILLARD (Reims); Carine GERVAIS (Strasbourg); Catherine GODON (nantes); Ellen HAMMOUCHE (Tours); Nazha HDA (Casablanca); Catherine HELIAS (Strasbourg); Catherine HENRY (Rennes); Jean-Loup HURET (Poitiers); Antoine ITTEL (Marseille); Eric JEANDIDIER (Mulhouse) ; Mélanie JIMENEZ (Tours) ; Sophie KALTENBACH (Paris); Stephan KEMENY (Clermont-Ferrand); Emilie KLEIN (Bordeaux); Marina LAFAGE (Marseille); Elodie LAHARANNE (Bordeaux); Sophy LAIBE (Marseille); Erika LAUNAY (Rennes); Christine LEFEBVRE (Grenoble) ; CORNILLET-LEFEBVRE Pascale (Reims); Geneviève LEFORT (Brest); Isabelle LUQUET (Toulouse) ; Odile MAAREK (Paris); Mélanie MARTIN (Nimes); Catherine MENTEN (Liège); Lucienne MICHAUX (Leuven); Marie-Joelle MOZZICONACCI (Marseille); Marc MULLER (Nancy); Nathalie NADAL (Dijon); Florence NGUYEN-KHAC (Paris); Marie-Pierre PAGES (Lyon); Agathe PAUBEL (Chambray); Dominique PENTHER (Rouen); Benoit QUILICHINI (Lyon); Isabelle RADFORD-WEISS (Paris); Sophie RAYNAUD (Nice); Bénédicte RIBOURTOUT (Angers); Steven RICHEBOURG (Nantes); Lauren RIGOLLET (St Etienne); Catherine ROCHE-LESTIENNE (Lille); Serge ROMANA (Paris); Véronique SAADA (Villejuif); Gwendoline SOLER (Clermont-Ferrand); Anne STAAL-VILIARE (Metz); Stéphanie STRUSKI (Toulouse) ; Andrei TCHIRKOV (Clermont-Ferrand); Christine TERRE (Versailles); Isabelle TIGAUD (Lyon); Sylvie TONDEUR (Grenoble); Saloua TOUJANI (Rennes); Lauren VERONESE (Clermont-Ferrand)

FILO (French Innovative Leukemia Organization) members

Alain DELMER (Reims), Thérèse Aurran-Schleinitz (Marseille) ; Marie-Christine Béné (Nantes) ; Annie Brion (Besançon); Guillaume Cartron (Montpellier) ; Aline Clavert, (Angers) ; Florence Cymbalista (Bobigny); David Ghez (Villejuif) ; Sophie de Guibert (Rennes); Marie-Sarah Dilhuydy, (Bordeaux) ; Bernard Drenou (Mulhouse) ; Charles Dumontet (Lyon) ; Jehan Dupuis (Creteil); Pierre Feugier (Nancy) ; Fontanet Bijou(Bordeaux) ; Luc-Matthieu Fornecker (Strasbourg) ; Romain Guieze (Clermont-Ferrand); Katell Ledu (Le Mans); Magali LE GARFF TAVERNIER (Paris); Véronique LEBLOND (Paris); Stephane Lepretre (Rouen) ; Rémi LETESTU (Bobigny) ; Vincent Levy (Bobigny); Béatrice Mahé (Nantes) ; Karim MALOUM (Paris); Marc

Maynadié (Dijon) ; Fatiha Merabet, (Versailles); Anne-Sophie MICHALLET (Lyon); Pierre Morel (Amiens); Florence NGUYEN-KHAC (Paris) ; Delphine Nollet (Tour); Brigitte Pégourie (Grenoble); Bertrand Pollet (Boulogne sur Mer); Stéphanie Poulain (Valenciennes) ; Anne Quinquenel (Reims) ; Sophie Raynaud, (Nice); Daniel Ré (Antibes); Philippe Rodon (Périgueux); Valérie Rouille (Montpellier.fr); Laurence Sanhes (Perpignan); Cécile Tomowiak (Poitiers); Olivier Tournilhac (Clermont Ferrand); Xavier Troussard (Caen); Eric Van Den Neste, (Bruxelles) Sandrine Vaudaux (Rouen); Marguerite VIGNON (Paris); Jean-Pierre Vilque (Caen); Maud Voldoire (La Roche sur Yon); Lise WILLEMS (Paris); Loic Ysebaert (Toulouse) ; Jean-Marc ZINI (Paris)

Article 3

The complex karyotype and chronic lymphocytic leukemia: prognostic value and diagnostic recommendations.

American Journal of Hematology, 2020; 95:1361–1367. Critical Review.

Les anomalies du gène *TP53* (délétion/mutation) et le statut mutationnel du gène *IGHV* sont les deux marqueurs pronostiques utilisés à l'heure actuelle en pratique clinique pour orienter la décision thérapeutique. A l'instar de nombreuses hémopathies myéloïdes, la mise en évidence d'un caryotype complexe est de plus en plus communément admise comme un facteur pronostique péjoratif dans la LLC.

Dans cette revue, nous avons cherché à synthétiser les connaissances actuelles sur l'impact pronostique du caryotype complexe dans la LLC.

Dans la LLC, le caryotype complexe a été associé avec une réduction de la survie globale dès 1985 (Juliusson et al., *Blood*, 1985), ce qui a été confirmé par de nombreuses études ultérieures. Une réduction du temps au premier traitement a également été rapportée. De plus, les patients porteurs d'un caryotype hypercomplexe ont été décrits comme ayant une survie globale et un temps au premier traitement encore diminué par rapport aux patients ayant un caryotype complexe (Baliakas et al., *Blood*, 2019).

La question de l'indépendance de ce paramètre vis-à-vis des autres facteurs de mauvais pronostic que sont la del17p, la del11q et le statut *IGHV* non muté reste sujette à débat. Cependant, Puiggros et al. ont montré que les patients porteurs d'un caryotype complexe sans anomalie de *TP53* ni d'*ATM* avaient tout de même un pronostic défavorable (Puiggros et al., *Oncotarget*, 2017). Des observations similaires ont été faites en présence d'un caryotype complexe chez des patients présentant par ailleurs une del13q sans anomalie 17p/11q, ou encore un statut *IGHV* muté (Baliakas et al., *Am J Hematol*, 2014). Enfin, le caryotype complexe a été rapporté comme aggravant le pronostic déjà défavorable des patients porteurs d'anomalies de TP53 (Blanco et al., *Oncotarget*, 2016 ; Chapiro et al., *Am J Hematol*, 2018).

Le caryotype complexe a été décrit à plusieurs reprises comme associé à des survies globale et sans progression plus courtes après traitement par immunochimiothérapie (fludarabine-cyclophosphamide-rituximab) (Le Bris et al., *Hematol Oncol*, 2017 ; Badoux et al., *Blood*, 2011). Les résultats sont plus contrastés après un traitement ciblé par inhibiteur de Bruton tyrosine kinase (ibrutinib) : certaines études mettant en évidence une réduction de survie globale et sans progression (Thompson et al., *Cancer*, 2015 ; Woyach et al., *J Clin Oncol*, 2017), et d'autres non (Kipps et al*., Clin Lymphoma Myeloma Leuk*, 2019). De même, l'étude de l'impact du caryotype complexe sur la survie après traitement par inhibiteur de BCL2 (vénétoclax) a produit des résultats à ce jour contradictoires (Anderson et al., Blood, 2017 ; Mato et al., *Haematologica*, 2018), et nécessitera une réévaluation avec davantage de recul.

A défaut de recommandations claires de l'ISCN (International System for Human Cytogenomic Nomenclature), la définition du caryotype complexe n'est pas universelle et peut ainsi varier d'une étude à l'autre. Afin d'uniformiser cette définition, nous avons proposé des recommandations pour le comptage des anomalies chromosomiques de nombre et de structure, applicables pour l'ensemble des hémopathies myéloïdes et lymphoïdes. Sur la base de ce compte, on définit un caryotype complexe en présence de 3 ou 4 anomalies. A partir de 5, on parlera de caryotype hypercomplexe.

Discussion

Bien que le concept de caryotype complexe soit utilisé par cliniciens, biologistes et chercheurs depuis plusieurs décennies, l'absence de définition consensuelle internationale explique certaines divergences entre les études, ce qui pourrait altérer leur comparabilité. Pour pallier cette difficulté, nous avons proposé une méthode de comptage standardisée. Le concept de caryotype hypercomplexe est plus récent, et de nombreux auteurs ne les distinguent pas des caryotypes complexes. Pourtant, de plus en plus d'études récentes viennent appuyer l'idée d'un impact pronostique encore plus péjoratif des caryotypes hypercomplexes au sein des caryotypes complexes.

Il semble clair que la présence d'un caryotype complexe voire hypercomplexe constitue un facteur de mauvais pronostic dans la LLC, en raison d'un intervalle de temps au premier traitement plus court et d'une survie globale diminuée.

Received: 9 June 2020 | Revised: 31 July 2020 | Accepted: 4 August 2020

DOI: 10.1002/ajh.25956

CRITICAL REVIEW

The complex karyotype and chronic lymphocytic leukemia: prognostic value and diagnostic recommendations

Ludovic Jondreville[1] | Daphné Krzisch[1] | Elise Chapiro[1,2] | Florence Nguyen-Khac[1,2]

[1]INSERM, Cell Death and Drug Resistance in Lymphoproliferative Disorders Team, Centre de Recherche des Cordeliers, Paris, France

[2]Service d'Hématologie Biologique, Sorbonne Université, Hôpital Pitié-Salpêtrière, APHP, Paris, France

Correspondence
Florence Nguyen-Khac, Service d'Hématologie Biologique, Bâtiment Pharmacie, 3e étage, Pitié-Salpêtrière/Charles Foix University Hospital, 83 Bd de l'Hôpital, F-75013 Paris, France.
Email: florence.nguyen-khac@aphp.fr

Abstract

Chromosomal abnormalities are frequently observed in patients with chronic lymphocytic leukemia (CLL) and have prognostic value. Deletions of the short arm of chromosome 17 (and/or mutations *TP53*) predict resistance to chemoimmunotherapy and shorter progression-free survival after targeted therapies. Although the complex karyotype (CK) is strongly predictive of a poor prognosis in hematologic malignancies such acute myeloid leukemia or myelodysplastic syndrome, its value in CLL is subject to debate. Here, we review the literature on the CK in CLL and examine its prognostic value with different treatments. We also propose a standardized method for defining a CK in all types of hematopoietic neoplasm.

1 | CHRONIC LYMPHOCYTIC LEUKEMIA

Chronic lymphocytic leukemia (CLL) is the most common form of leukemia among adults in Western countries. The leukemic monomorphic small mature B cells in CLL co-express CD5 and CD23. The disease is typically diagnosed at an early stage and is then monitored in the absence of treatment until the symptoms worsen. The Rai and Binet clinical staging systems are used[1,2] to decide when to initiate treatment. At present, allogeneic stem cell transplantation is the only potentially curative treatment option for CLL. The most commonly administered cancer treatments include chemoimmunotherapy (such as fludarabine, cyclophosphamide plus rituximab (FCR), bendamustine plus rituximab (BR), and rituximab plus chlorambucil), Bruton tyrosine kinase (BTK) inhibitors, and B-cell leukemia/lymphoma-2 (BCL2) inhibitors. Until now, the only prognostic parameter used to choose between chemoimmunotherapy or targeted therapy is *TP53* gene status (17p deletion/*TP53* mutation). Indeed, *TP53* disruption is the strongest predictor of refractoriness to chemotherapy. The mutational status of the *IGHV* gene is also a known prognostic marker that helps clinicians to fine-tune the treatment of CLL. The clinical outcome is worse for patients whose CLL cells use an unmutated *IGHV* gene, relative to those whose CLL cells use a mutated *IGHV* gene.[3,4] However, *IGHV3-21* gene usage (in stereotype subset 2) may be associated with a poor prognosis, independently of the *IGHV* mutational status.[5,6] Among patients lacking *TP53* disruption, individuals carrying mutated *IGHV* genes experience a longer-lasting response to FCR than those with unmutated *IGHV* gene[7]; hence, the latter may benefit more from targeted therapy. A large number of recurrent gene mutations have been discovered in patients with CLL since 2011,[8,9] however, none of these mutations have clear prognostic value. It has been reported that *NOTCH1* mutations reduced the benefit of adding rituximab (anti-CD20) to fludarabine.[10] Pozzo et al. have shown that *NOTCH1* mutations in CLL are associated with low CD20 expression, and with relative resistance to anti-CD20 immunotherapy in vitro.[11]

Although the prognostic value of *TP53* and *IGHV* markers is well established, a growing number of studies performed over the past 10 years have highlighted the prognostic and predictive value of the complex karyotype (CK) in CLL. A recent analysis of a very large cohort has again raised the question of whether or not the CK should be incorporated in the risk stratification algorithm for CLL in routine clinical practice.[12] The objective of the present review was to assess the prognostic value of a karyotype analysis and the CK in the management of CLL.

2 | THE KARYOTYPE AND B CELL STIMULATION

Given that B cells have a low proliferation index, the first chromosomal abnormalities in CLL were only detected in the 1980s.[13-17] A

broad range of mitogens have since been used to stimulate CLL B cells; for example, the use of 12-0-tetradecanoylphorbol-13-acetate (TPA) led to the detection of clonal aberrations in 40% to 50% of CLL cases.[18] Since 2006, stimulation with CpG oligodeoxynucleotides (CpG-ODN) and interleukin 2 permit detection of clonal aberrations in about 80% of cases of CLL.[19-21] Improved cytogenetic techniques in CLL have prompted renewed interest in the karyotype in this setting.

3 | CHROMOSOMAL ABNORMALITIES IN CLL

Although no specific chromosomal abnormalities have been observed in CLL, the disease does appear to have a particular cytogenomic profile. A number of recurrent aberrations have been characterized by karyotyping, fluorescence in situ hybridization (FISH), comparative genomic hybridization (CGH), single nucleotide polymorphism (SNP) arrays, and other molecular analyses. The four classical abnormalities are deletions of the long arm (q) of chromosomes 13 (55%) and 11 (6%-20%), deletion of the short arm (p) of chromosome 17 (found in 5%-8% of chemotherapy-naïve patients with CLL), and trisomy 12 (11%-25%).[22,23] In 2000, Döhner et al. published a hierarchical model based on four FISH probes: 17p deletion and 11q deletion were associated with a poor prognosis, 13q deletion was associated with the best prognosis when it was the sole anomaly present, and trisomy 12 was associated with an intermediate prognosis.[22] Other frequent, recurrent abnormalities in CLL include 6q deletion (5%)[21,22] and 2p gain (5%-16%).[21,24,25] Lastly, recurrent but rare (<5%) abnormalities include 8q gain, 14q deletion, t(14;19)(q32;q13), t(14;18)(q32;q24), t(8;14)(q24;q32), 8p deletion, 15q deletion, trisomy 18, and trisomy 19.[21]

4 | THE CK: DEFINITION AND FREQUENCY

The International System for Human Cytogenomic Nomenclature (ISCN) does not currently define a CK. The complexity of a karyotype is defined by its negative prognostic impact on a disease, as described in myelodysplastic syndromes and in acute myeloid leukemia.[26,27] Another aspect relates to how the chromosomal aberrations are counted; again, this is not specified in the ISCN and is not always clearly explained in research publications. With regard to a CK, some researchers count only the abnormalities present in the same clone and other researchers count only "unrelated" cytogenetic abnormalities, but do not clearly explain these options or cite a reference [28, 29]. We consider that a simple, standardized procedure for counting chromosomal abnormalities according to the ISCN would be of great value not only for CLL but also for all other hematologic malignancies. For example, one could count each item between commas in the description of the karyotype as an aberration, regardless of whether these abnormalities were present in the same (sub)clone or in different (sub)clones.[30] One could also adopt the guidelines for MDS karyotypes by (a) counting each item between commas (numerical change, balanced translocation, and structural change) as an aberration, (b) not counting constitutional aberrations; (c) counting a single change only once when two or more clones are present, and (d) counting tetraploidy as an aberration.[31] Lastly, some abnormalities may reflect an underlying effect of age in some settings, such as trisomy 15 and loss of chromosome Y. In our opinion, these abnormalities must be counted if they are crucial for diagnosis and treatment decisions in complex cases but should be clearly flagged up as being precautionary factors only.[32,33] Lastly, chromosomal abnormalities must be counted by a cytogeneticist, and have to be explained in the cytogenetic report, with a clear conclusion for the clinician[31] (Table 1).

TABLE 1 Guidelines for counting aberrations in karyotypes

In all hematologic malignancies:
1. Count one (1) aberration[a] for each item between commas, in all clones and subclones[b]
2. Count a single change only once if it is present in several subclones[c]
3. Count each numerical change (including -Y, -X, +15)[d], balanced translocation, simple structural change and each complex structural change[e] as one (1) aberration
4. Count each chromosome marker as one (1) aberration[a]
5. Count one (1) aberration for tetraploidy (92 chromosomes) or near-tetraploidy (81-103 chromosomes)[f]
6. Do not count constitutional aberrations[g]
In CLL, additionally:
7. Distinguish between a CK with three (3) to four (4) abnormalities and a high CK with five (5) or more abnormalities
8. -Y, -X and +15 have to be flagged up in the cytogenetics report[d]
9. Count one (1) aberration for FISH abnormalities [del(13)(q), +12, del (11)(q) and del(17)(p)] only if they are observed in the karyotype[h]
10. CKs with +12,+19 have to be classified separately

Note: Reminder: according to the ISCN nomenclature, a clone must have at least two cells with the same aberration (for chromosome gain or a structural rearrangement) or at least three cells with the same aberration (for chromosome loss). However, two cells with identical losses of one or more chromosomes and the same chromosome gain or the same structural abnormality may be considered to be clonal.

[a]Exceptions: marker chromosomes, multiple copies of rearranged chromosomes; for example: +3mar or +1~3mar: count three (3) aberrations; del(6)(q21)x2: count two (2) aberrations.

[b]Regardless of whether these abnormalities are present in the same (sub)clone or in different (sub)clones.

[c]This change must be identical. If the aberration is not identical in two clones or subclones, count two (2) aberrations; for example, count two (2) aberrations for del(11)(q23) and del(11)(q13).

[d]The abnormalities -Y, -X, and +15 may reflect an underlying age effect in some cases.

[e]If the structural change is complex, count one (1) aberration for each change between commas; for example, count two (2) aberrations for der(3)t(3;13) and der(13)t(3;13).

[f]For example, count five (5) aberrations for 94,XXYY,+12,+12,t(14;19)(q32;q13)x2.

[g]Even if not strictly proven (not always performed with T lymphocytes).

[h]However, FISH abnormalities must be mentioned in the cytogenetics report.

In 1985, Juliusson et al. reported that the presence of three or more abnormalities was associated with poor overall survival (OS) in mature B cell disorders, including CLL.[34] In the early 1990s, the same research group defined several prognostic subgroups in CLL as a function of the chromosomal abnormalities.[18] Even though a few patients in this series (10 out of 391, 2.5%) had a t(11;14)(q13;q32) (which may reflect mantle cell lymphoma than CLL cases), the researchers again showed that presence of a CK with three or more abnormalities (n = 53 out of 391 patients, 13.5%) was associated with a shorter OS, relative to patients with zero, one or two abnormalities. Following on from this work and on the basis of definitions for other hematological diseases, a CK in CLL was defined in 2006-2007 as the presence of three or more clonal aberrations.[18,21,26,34,35] Thus, Mayr et al. observed that CLL patients with a CK (n = 24 out of 92, 26%) had a shorter treatment-free survival time (median: 26 months, vs 106 months in patients without a CK; $P < .001$). Furthermore, the CK had a significant influence on the OS time (median: 107 months, vs 346 months in patients without a CK; $P < .001$).[19] Based on a large international study (n = 1001), Baliakas et al. reported in 2014 that a CK (n = 157 out of 1001 patients, 15.5%) was associated with a significantly shorter time to first treatment (TTFT) ($P = .009$).[36] The researchers also noted that within the CK group, cases with five or more abnormalities (n = 40 out of 1001, 4%) exhibited an even shorter TTFT ($P < .001$). Furthermore, the CK was significantly associated with a poor prognosis in both patients with a mutated *IGHV* gene ($P = .009$) and those without ($P = .017$). In a multivariate analysis, the CK was an independent, prognostic factor for TTFT ($P < .001$).[36] Rigolin et al. suggested differentiating between two types of CK: those with major structural aberrations (including unbalanced translocations, chromosome additions, insertions, duplications, and ring, dicentric and marker chromosomes, defining a "CK2" subset in 66 of the 90 CKs, 73.5%) were associated with worse outcomes (shorter OS and TTFT) than CKs with balanced translocations, deletions, monosomy or trisomy (the "CK1" subset in 24 of the 90 CKs, 26.5%).[37] In a larger study, the same research group confirmed that CK2 patients (n = 69 out of 522, 13%) had a worst prognosis with regard to the TTFT, the time to next treatment, and OS.[28] At the same time, the study by Baliakas et al. led to the development of a hierarchical model in which "high-CK" patients (five or more abnormalities; n = 233 out of 3539, 6.5%) exhibited the shortest OS, whereas patients with a CK with +12,+19 (as well as cases of mutated CLL lacking a CK, or *TP53* abnormalities) had the longest OS time. A high-CK (with five or more chromosomal aberrations) emerged as an independent prognostic marker.[12]

In conclusion, a CK in CLL can be defined as three or four abnormalities, whereas a high-CK in CLL corresponds to five or more abnormalities - with the exception of cases with +12,+19 and other aberrations associated with a good prognosis. It remains to be determined whether the presence of a CK with major structural aberrations corresponds to a subset of cases with particularly aggressive disease. Overall, a CK is observed in 11% to 18% of treatment-naïve patients with CLL and in up to 40% of patients with relapsed/refractory (R/R) CLL.[38-42]

5 | PROGNOSTIC VALUE OF THE CK IN CLL

5.1 | Is the CK an independent prognostic factor?

Several studies have found that the CK was associated with classical factors for poor outcomes, such as unmutated *IGHV* status, del17p, and del11q.[21,36,43-45] Interestingly, the same studies showed that the CK was an independent marker of a poor prognosis. Herling et al. showed that the interaction between *TP53* abnormalities and CK was not statistically significant in their patient population (n = 16 out of 147, 11%, for *TP53* abnormalities, and 30 out of 147, 20.5%, for the CK).[46] Moreover, Puiggros et al. did not observe differences in OS when comparing cases with a CK but without del17p/del11q (n = 42 out of 1039, 4%), and cases with del17p/del11q but without a CK (n = 111 out of 1039, 10.5%).[44] Hence, one can reasonably assume that factors other than 17p/TP53 and 11q abnormalities are associated with a poor outcome in CLL patients with a CK.

Hence, with regard to classical prognostic markers in CLL, it seems that the CK may have additional prognostic value. Indeed, Baliakas et al. have shown that among cases with an isolated del13q in a FISH analysis (ie, the cases with the best prognosis, according to the hierarchical model of Döhner et al.), those found with a CK in a metaphase cytogenetic analysis (19 out of 249, 7.6%) had a significantly shorter OS time ($P = .021$). This was also true for the *IGHV* status: CK was associated with a significantly shorter TTFT even when the patient carried a mutated *IGHV* (40 out of 447 [8.9%], $P = .009$).[36] Lastly, the combination of a CK and *TP53* abnormalities (del17p and/or *TP53* mutations) appears to be associated with the shortest OS time and/or TTFT.[47,48]

5.2 | The CK and treatments for CLL

Various treatments for CLL are available. The CK appears to have prognostic value - even with the new targeted therapies. The great majority of clinical studies defined CK as three or more chromosomal abnormalities and did not differentiate between CK and high-CK.

In a prospective study of CLL patients treated with first-line chlorambucil-based regimens, Herling et al. showed that CK (n = 30 out of 154, 19.5%) was associated with a shorter OS in a multivariate analysis ($P = .004$); and that the combined occurrence of both CK and TP53 abnormalities resulted in a particularly poor prognosis ($P < .001$).[46] Regarding FCR regimens, Le Bris et al. found that a CK (in 38 out of 110 patients, 34.5%) was associated with shorter progression-free survival (PFS) and 5-year OS in a multivariate analysis ($P = .005$ and $P = .03$ respectively) in a cohort of patients with CLL treated with first-line FCR.[43] In the study by Badoux et al. of 182 FCR-treated patients with R/R CLL, a CK (not including chromosome 17 abnormalities) was found in 22 individuals (12%) and was associated with shorter PFS and OS ($P < .001$ and $P = .02$, respectively).[49] We conclude that a CK predicts a poor outcome in patients with CLL receiving chemotherapy and/or immunochemotherapy.

The study by Thompson et al. of patients with ibrutinib (BTK inhibitor)-treated R/R CLL showed that a CK (n = 21 out of 56, 37.5%) was associated with shorter event-free survival (EFS) (P = .006) and OS (P = .008), after a median follow-up of 28 months. In contrast, the RESONATE prospective study of previously treated patients with CLL or small lymphocytic lymphoma (SLL) did not reveal any significant differences in PFS and OS between patients with a CK (n = 39 out of 153, 25.5%) and those without, after a median follow-up of 19 months.[50] However, long-term follow-up (median: 44 months) of the same patients showed that the median PFS was 40.8 months among patients with a CK but was not reached for patients without a CK (hazard ratio [95% confidence interval] = 1.292 [0.770-2.168]).[51] The pooled analysis by Kipps et al. of patients with treatment-naïve or R/R CLL/SLL from three Phase III studies (RESONATE-2, RESONATE, and HELIOS) showed that there was no significant difference in PFS and OS between patients with a CK (not including del17p; n = 41 out of 379, 10.8%) and those without, after a median follow-up of 47 months.[52] Lastly, Woyach et al. included four sequential studies (including the RESONATE prospective trial) of ibrutinib-treated patients with treatment-naïve or R/R CLL. At a follow-up time of 3.4 years, the researchers observed that patients with a CK (n = 172 out of 295, 58%) had a higher risk of CLL progression or transformation (P = .006 and P = .008 respectively).[53] The new BTK inhibitor acalabrutinib is expected to have minimal off-target activity. In a multicenter Phase I/II study in patients with R/R CLL/SLL and a median follow-up time of 41 months, the overall response rate with acalabrutinib was high (94%); however, the PFS was shorter for patients with a CK (n = 20 out of 57, 35%) and for patients with del17p (median PFS: 36 and 33 months, respectively) than for the cohort as a whole (median PFS: not reached).[54] Even though the study parameters differed somewhat, one can conclude that the CK need to be evaluated with BTK inhibitors.

Anderson et al. showed that a CK (n = 16 out of 38, 42%) was associated with a shorter PFS in patients with R/R CLL treated with the BCL2 inhibitor venetoclax (median follow-up: 23 months[2-46]).[55] In contrast, an analysis performed after a shorter follow-up time (median [IQR]: 7 months [0;1-38;4]), found that a CK (n = 52 out of 130, 26.8%) was not associated with a shorter PFS in cases of treatment-naïve and R/R CLL.[56] Further studies (and especially prospective ones) are required before firm conclusions can be drawn.

The clinical development of the PI3-kinase inhibitor idelalisib has been limited by a high incidence of adverse events.[57] In a study of both treatment-naive and previously treated patients, Mato et al. found that individuals with a CK (n = 12 out of 49 (25%) and those without CK did not differ significantly with regard to the PFS.[58] Similarly, in a study of relapsed CLL, Kreutzer et al. did not observe differences in PFS or OS when comparing patients with a CK (n = 26 out of 63, 41.2%) or without after treatment with idelalisib plus rituximab.[59] New PI3-kinase inhibitors are now available (eg, duvelisib and umbralisib), and so further studies are needed to establish the impact of CK in treated patients with CLL.[60,61]

Lastly, only one study has been conducted in patients with CLL after allogeneic stem cell transplantation. The recipients with a CK (defined as five or more abnormalities; n = 19 out of 51, 37.2%) had shorter OS and EFS times in a bivariate analysis. A CK was also predictive of worse OS and EFS in patients with high-risk interphase cytogenetics (del(17p) and del(11q)).[62]

5.3 | The CK and the risk of Richter transformation

Richter syndrome (RS) is defined as the transformation of CLL or small lymphocytic lymphoma into an aggressive lymphoma - usually diffuse large B-cell lymphoma (2%-8% of cases of CLL) or Hodgkin lymphoma (<1% of cases of CLL). Few biomarkers are reportedly associated with risk of RS, including *NOTCH1* mutations, *TP53* abnormalities, the use of subset eight immunoglobulin genes, near-tetraploidy, and a CK.[63-67] Further studies are required to confirm that CK is a risk factor for Richter transformation.

6 | USE OF OTHER TECHNIQUES TO PROBE GENOME COMPLEXITY IN CLL?

Genomic arrays (such as CGH and SNP arrays) allow the entire genome to be screened in a single experiment. These techniques does not require cultured cells, and have a greater resolution (~50 kb or less) than karyotyping (10 Mb), and can identify novel gains or losses. A number of genomic array studies have highlighted an association between genomic complexity and a poor outcome in CLL.[68-70] However, the threshold for clinically relevant copy-number variations (5 Mb, 1 Mb, or less) has not been defined, and array techniques miss balanced translocations and low-level clones (accounting for <10%–15% of cells) with regard to a low tumor cell percentage or a low level of subclones. We are now waiting for the arrival of new techniques such as next generation sequencing currently in development and that will have to be validated in clinical practice.[71] At present, karyotyping can be easily performed worldwide and is supported by a large body of experience and by national and international guidelines. Moreover, it is easy to request another sample if karyotyping fails because a blood test is not highly invasive.

7 | RECOMMENDATIONS

The International Workshop on Chronic Lymphocytic Leukemia (iwCLL) recommends the four-probe FISH panel for the pre-treatment evaluation of CLL.[6] In a context of economic crisis, one could suggest that it might be acceptable to not systematically perform cytogenetic analyses upon diagnosis of CLL. However, for clinical and psychological reasons, it is important for the patient to know whether his/her cancer disease is associated with a good prognosis. We think that along with the four-probe FISH analyses prior to treatment, karyotyping should be mandatory - especially in clinical trials - as a

TABLE 2 Recommendations for karyotyping and FISH in CLL

	Routine clinical practice	Clinical trials
On diagnosis		
Karyotype (K)[a]	Recommended	Mandatory
4-probe FISH[b]	Recommended	Mandatory
Other FISH probes	Depending on the K[c]	Depending on the purpose[d]
Before treatment		
Karyotype (K)[a]	Mandatory	Mandatory
4-probe FISH[b]	Mandatory	Mandatory
Other FISH probes	Depending on the K[c]	Depending on the purpose[d]

[a]In peripheral blood lymphocytes after in vitro stimulation with CpG oligodeoxynucleotides and interleukin 2.
[b]To detect del(13)(q14)(D13S319), +12, del(11)(q22)(*ATM*) and del(17)(p13)(*TP53*).
[c]To detect/confirm other chromosomal abnormalities (within the CK or not) with a prognostic impact, for example, 2p gain, 8q gain, and 8p deletion.
[d]For example, clinical trial can focus on one abnormality of interest.

definitive guide to the prognosis (Table 2). In routine clinical practice, the physician and patient currently have to choose (on the basis of the 17p/*TP53* and *IGHV* status) between immunochemotherapy and targeted therapies. Even though the choice of treatment does not strictly require karyotyping, we consider that these data should be integrated into the decision and the follow up. As we have seen above, a CK can modify the good prognosis associated with a single del13q detected by FISH or with mutated *IGHV* status, and CLL patients with a CK respond less well than patients without a CK. Lastly, it is important to karyotype the CLL B cells after in vitro stimulation with CpG oligodeoxynucleotides and interleukin 2; and the cytogeneticist must detect the specific chromosomal abnormalities within these CKs - for example, 2p gain, 8q gain, or 8p deletion - that might flag patients who could potentially be treated with novel drugs in the near future.[25,48,72,73]

8 | CONCLUSION

According to the current guidelines issued by the iwCLL and European cytogenetics guidelines, targeted FISH is mandatory and karyotyping is recommended for patients with CLL.[6,74] However, karyotyping would also be useful in clinical trials so that the prognostic value of chromosomal aberrations could be assessed. In addition to the classic four-probe panel, we recommend systematic karyotyping before treatment initiation. Firstly, karyotyping can reveal chromosomal aberrations not covered by the FISH probes and can help to determine whether or not a CK is present. Secondly, it appears that patients with a CK do not respond as well as other patients to targeted therapies. In patients without *TP53* abnormalities, however, knowledge of the CK could help the physician to choose the appropriate targeted therapy. If this treatment is initiated, close follow-up is required.

CONFLICT OF INTERESTS

The authors declare no potential conflict of interest.

DATA AVAILABILITY STATEMENT

Data sharing not applicable - no new data generated

ORCID

Elise Chapiro https://orcid.org/0000-0003-3427-7596
Florence Nguyen-Khac https://orcid.org/0000-0003-3107-6668

REFERENCES

1. Binet JL, Auquier A, Dighiero G, et al. A new prognostic classification of chronic lymphocytic leukemia derived from a multivariate survival analysis. *Cancer*. 1981;48:198-206.
2. Rai KR, Sawitsky A, Cronkite EP, Chanana AD, Levy RN, Pasternack BS. Clinical staging of chronic lymphocytic leukemia. *Blood*. 1975;46:219-234.
3. Damle RN, Wasil T, Fais F, et al. Ig V gene mutation status and CD38 expression as novel prognostic indicators in chronic lymphocytic leukemia. *Blood*. 1999;94:1840-1847.
4. Hamblin TJ, Davis Z, Gardiner A, Oscier DG, Stevenson FK. Unmutated Ig V(H) genes are associated with a more aggressive form of chronic lymphocytic leukemia. *Blood*. 1999;94:1848-1854.
5. Baliakas P, Agathangelidis A, Hadzidimitriou A, et al. Not all IGHV3-21 chronic lymphocytic leukemias are equal: prognostic considerations. *Blood*. 2015;125:856-859.
6. Hallek M, Cheson BD, Catovsky D, et al. iwCLL guidelines for diagnosis, indications for treatment, response assessment, and supportive management of CLL. *Blood*. 2018;131:2745-2760.
7. Fischer K, Bahlo J, Fink AM, et al. Long-term remissions after FCR chemoimmunotherapy in previously untreated patients with CLL: updated results of the CLL8 trial. *Blood*. 2016;127:208-215.
8. Puente XS, Pinyol M, Quesada V, et al. Whole-genome sequencing identifies recurrent mutations in chronic lymphocytic leukaemia. *Nature*. 2011;475:101-105.
9. Fabbri G, Rasi S, Rossi D, et al. Analysis of the chronic lymphocytic leukemia coding genome: role of NOTCH1 mutational activation. *J Exp Med*. 2011;208:1389-1401.
10. Stilgenbauer S, Schnaiter A, Paschka P, et al. Gene mutations and treatment outcome in chronic lymphocytic leukemia: results from the CLL8 trial. *Blood*. 2014;123:3247-3254.
11. Pozzo F, Bittolo T, Arruga F, et al. NOTCH1 mutations associate with low CD20 level in chronic lymphocytic leukemia: evidence for a NOTCH1 mutation-driven epigenetic dysregulation. *Leukemia*. 2016;30:182-189.
12. Baliakas P, Jeromin S, Iskas M, et al. Cytogenetic complexity in chronic lymphocytic leukemia: definitions, associations, and clinical impact. *Blood*. 2019;133:1205-1216.
13. Gahrton G, Robert KH, Friberg K, et al. Extra chromosome 12 in chronic lymphocytic leukaemia. *Lancet*. 1980;1:146-147.
14. Gahrton G, Robert KH, Friberg K, Zech L, Bird AG. Nonrandom chromosomal aberrations in chronic lymphocytic leukemia revealed by polyclonal B-cell-mitogen stimulation. *Blood*. 1980;56:640-647.
15. Callen DF, Ford JH. Chromosome abnormalities in chronic lymphocytic leukemia revealed by TPA as a mitogen. *Cancer Genet Cytogenet*. 1983;10:87-93.
16. Pittman S, Catovsky D. Prognostic significance of chromosome abnormalities in chronic lymphocytic leukaemia. *Br J Haematol*. 1984;58:649-660.

17. Fitchett M, Griffiths MJ, Oscier DG, Johnson S, Seabright M. Chromosome abnormalities involving band 13q14 in hematologic malignancies. *Cancer Genet Cytogenet*. 1987;24:143-150.
18. Juliusson G, Oscier DG, Fitchett M, et al. Prognostic subgroups in B-cell chronic lymphocytic leukemia defined by specific chromosomal abnormalities. *N Engl J Med*. 1990;323:720-724.
19. Mayr C, Speicher MR, Kofler DM, et al. Chromosomal translocations are associated with poor prognosis in chronic lymphocytic leukemia. *Blood*. 2006;107:742-751.
20. Dicker F, Schnittger S, Haferlach T, Kern W, Schoch C. Immunostimulatory oligonucleotide-induced metaphase cytogenetics detect chromosomal aberrations in 80% of CLL patients: a study of 132 CLL cases with correlation to FISH, IgVH status, and CD38 expression. *Blood*. 2006;108:3152-3160.
21. Haferlach C, Dicker F, Schnittger S, Kern W, Haferlach T. Comprehensive genetic characterization of CLL: a study on 506 cases analysed with chromosome banding analysis, interphase FISH, IgV(H) status and immunophenotyping. *Leukemia*. 2007;21:2442-2451.
22. Dohner H, Stilgenbauer S, Benner A, et al. Genomic aberrations and survival in chronic lymphocytic leukemia. *N Engl J Med*. 2000;343:1910-1916.
23. Letestu R, Levy V, Eclache V, et al. Prognosis of Binet stage A chronic lymphocytic leukemia patients: the strength of routine parameters. *Blood*. 2010;116:4588-4590.
24. Schwaenen C, Nessling M, Wessendorf S, et al. Automated array-based genomic profiling in chronic lymphocytic leukemia: development of a clinical tool and discovery of recurrent genomic alterations. *Proc Natl Acad Sci U S A*. 2004;101:1039-1044.
25. Cosson A, Chapiro E, Bougacha N, et al. Gain in the short arm of chromosome 2 (2p+) induces gene overexpression and drug resistance in chronic lymphocytic leukemia: analysis of the central role of XPO1. *Leukemia*. 2017;31:1625-1629.
26. Greenberg P, Cox C, LeBeau MM, et al. International scoring system for evaluating prognosis in myelodysplastic syndromes. *Blood*. 1997;89:2079-2088.
27. Grimwade D, Walker H, Oliver F, et al. The importance of diagnostic cytogenetics on outcome in AML: analysis of 1,612 patients entered into the MRC AML 10 trial. The Medical Research Council Adult and Children's Leukaemia Working Parties. *Blood*. 1998;92:2322-2333.
28. Visentin A, Bonaldi L, Rigolin GM, et al. The combination of complex karyotype subtypes and IGHV mutational status identifies new prognostic and predictive groups in chronic lymphocytic leukaemia. *Br J Cancer*. 2019;121:150-156.
29. Woyach JA, Ruppert AS, Heerema NA, et al. Ibrutinib regimens versus chemoimmunotherapy in older patients with untreated CLL. *N Engl J Med*. 2018;379:2517-2528.
30. Breems DA, Van Putten WL, De Greef GE, et al. Monosomal karyotype in acute myeloid leukemia: a better indicator of poor prognosis than a complex karyotype. *J Clin Oncol*. 2008;26:4791-4797.
31. Chun K, Hagemeijer A, Iqbal A, Slovak ML. Implementation of standardized international karyotype scoring practices is needed to provide uniform and systematic evaluation for patients with myelodysplastic syndrome using IPSS criteria: An International Working Group on MDS Cytogenetics Study. *Leuk Res*. 2010;34:160-165.
32. Loss of the Y chromosome from normal and neoplastic bone marrows. United Kingdom Cancer Cytogenetics Group (UKCCG). *Genes Chromosomes Cancer*. 1992;5:83-88.
33. Sinclair EJ, Potter AM, Watmore AE, Fitchett M, Ross F. Trisomy 15 associated with loss of the Y chromosome in bone marrow: a possible new aging effect. *Cancer Genet Cytogenet*. 1998;105:20-23.
34. Juliusson G, Robert KH, Ost A, et al. Prognostic information from cytogenetic analysis in chronic B-lymphocytic leukemia and leukemic immunocytoma. *Blood*. 1985;65:134-141.
35. Schoch C, Haferlach T, Haase D, et al. Patients with de novo acute myeloid leukaemia and complex karyotype aberrations show a poor prognosis despite intensive treatment: a study of 90 patients. *Br J Haematol*. 2001;112:118-126.
36. Baliakas P, Iskas M, Gardiner A, et al. Chromosomal translocations and karyotype complexity in chronic lymphocytic leukemia: a systematic reappraisal of classic cytogenetic data. *Am J Hematol*. 2014;89:249-255.
37. Rigolin GM, Saccenti E, Guardalben E, et al. In chronic lymphocytic leukaemia with complex karyotype, major structural abnormalities identify a subset of patients with inferior outcome and distinct biological characteristics. *Br J Haematol*. 2018;181:229-233.
38. Sutton L, Chevret S, Tournilhac O, et al. Autologous stem cell transplantation as a first-line treatment strategy for chronic lymphocytic leukemia: a multicenter, randomized, controlled trial from the SFGM-TC and GFLLC. *Blood*. 2011;117:6109-6119.
39. Lepretre S, Aurran T, Mahe B, et al. Excess mortality after treatment with fludarabine and cyclophosphamide in combination with alemtuzumab in previously untreated patients with chronic lymphocytic leukemia in a randomized phase 3 trial. *Blood*. 2012;119:5104-5110.
40. Dartigeas C, Van Den Neste E, Leger J, et al. Rituximab maintenance versus observation following abbreviated induction with chemoimmunotherapy in elderly patients with previously untreated chronic lymphocytic leukaemia (CLL 2007 SA): an open-label, randomised phase 3 study. *Lancet Haematol*. 2018;5:e82-e94.
41. Michallet AS, Dilhuydy MS, Subtil F, et al. Obinutuzumab and ibrutinib induction therapy followed by a minimal residual disease-driven strategy in patients with chronic lymphocytic leukaemia (ICLL07 FILO): a single-arm, multicentre, phase 2 trial. *Lancet Haematol*. 2019;6:e470-e479.
42. Guieze R, Robbe P, Clifford R, et al. Presence of multiple recurrent mutations confers poor trial outcome of relapsed/refractory CLL. *Blood*. 2015;126:2110-2117.
43. Le Bris Y, Struski S, Guieze R, et al. Major prognostic value of complex karyotype in addition to TP53 and IGHV mutational status in first-line chronic lymphocytic leukemia. *Hematol Oncol*. 2017;35:664-670.
44. Puiggros A, Collado R, Calasanz MJ, et al. Patients with chronic lymphocytic leukemia and complex karyotype show an adverse outcome even in absence of TP53/ATM FISH deletions. *Oncotarget*. 2017;8:54297-54303.
45. Rigolin GM, Cavallari M, Quaglia FM, et al. In CLL, comorbidities and the complex karyotype are associated with an inferior outcome independently of CLL-IPI. *Blood*. 2017;129:3495-3498.
46. Herling CD, Klaumunzer M, Rocha CK, et al. Complex karyotypes and KRAS and POT1 mutations impact outcome in CLL after chlorambucil-based chemotherapy or chemoimmunotherapy. *Blood*. 2016;128:395-404.
47. Blanco G, Puiggros A, Baliakas P, et al. Karyotypic complexity rather than chromosome 8 abnormalities aggravates the outcome of chronic lymphocytic leukemia patients with TP53 aberrations. *Oncotarget*. 2016;7:80916-80924.
48. Chapiro E, Lesty C, Gabillaud C, et al. "Double-hit" chronic lymphocytic leukemia: an aggressive subgroup with 17p deletion and 8q24 gain. *Am J Hematol*. 2018;93:375-382.
49. Badoux XC, Keating MJ, Wang X, et al. Fludarabine, cyclophosphamide, and rituximab chemoimmunotherapy is highly effective treatment for relapsed patients with CLL. *Blood*. 2011;117:3016-3024.
50. Brown JR, Hillmen P, O'Brien S, et al. Extended follow-up and impact of high-risk prognostic factors from the phase 3 RESONATE study in patients with previously treated CLL/SLL. *Leukemia*. 2018;32:83-91.
51. Byrd JC, Hillmen P, O'Brien S, et al. Long-term follow-up of the RESONATE phase 3 trial of ibrutinib vs ofatumumab. *Blood*. 2019;133:2031-2042.
52. Kipps TJ, Fraser G, Coutre SE, et al. Long-term studies assessing outcomes of ibrutinib therapy in patients with del(11q) chronic lymphocytic leukemia. *Clin Lymphoma Myeloma Leuk*. 2019;19:715-722 e716.

53. Woyach JA, Ruppert AS, Guinn D, et al. BTK(C481S)-mediated resistance to ibrutinib in chronic lymphocytic leukemia. *J Clin Oncol*. 2017; 35:1437-1443.
54. Byrd JC, Wierda WG, Schuh A, et al. Acalabrutinib monotherapy in patients with relapsed/refractory chronic lymphocytic leukemia: updated phase 2 results. *Blood*. 2020;135(15):1204-1213.
55. Anderson MA, Tam C, Lew TE, et al. Clinicopathological features and outcomes of progression of CLL on the BCL2 inhibitor venetoclax. *Blood*. 2017;129:3362-3370.
56. Mato AR, Thompson M, Allan JN, et al. Real-world outcomes and management strategies for venetoclax-treated chronic lymphocytic leukemia patients in the United States. *Haematologica*. 2018;103: 1511-1517.
57. Lampson BL, Kasar SN, Matos TR, et al. Idelalisib given front-line for treatment of chronic lymphocytic leukemia causes frequent immune-mediated hepatotoxicity. *Blood*. 2016;128:195-203.
58. Mato AR, Hill BT, Lamanna N, et al. Optimal sequencing of ibrutinib, idelalisib, and venetoclax in chronic lymphocytic leukemia: results from a multicenter study of 683 patients. *Ann Oncol*. 2017;28:1050-1056.
59. Kreuzer KA, Furman RR, Stilgenbauer S, et al. The impact of complex karyotype on the overall survival of patients with relapsed chronic lymphocytic leukemia treated with idelalisib plus rituximab. *Leukemia*. 2020;34:296-300.
60. Flinn IW, Hillmen P, Montillo M, et al. The phase 3 DUO trial: duvelisib vs ofatumumab in relapsed and refractory CLL/SLL. *Blood*. 2018;132:2446-2455.
61. Burris HA 3rd, Flinn IW, Patel MR, et al. Umbralisib, a novel PI3Kdelta and casein kinase-1epsilon inhibitor, in relapsed or refractory chronic lymphocytic leukaemia and lymphoma: an open-label, phase 1, dose-escalation, first-in-human study. *Lancet Oncol*. 2018; 19:486-496.
62. Jaglowski SM, Ruppert AS, Heerema NA, et al. Complex karyotype predicts for inferior outcomes following reduced-intensity conditioning allogeneic transplant for chronic lymphocytic leukaemia. *Br J Haematol*. 2012;159:82-87.
63. Fabbri G, Khiabanian H, Holmes AB, et al. Genetic lesions associated with chronic lymphocytic leukemia transformation to Richter syndrome. *J Exp Med*. 2013;210:2273-2288.
64. Rossi D, Rasi S, Spina V, et al. Different impact of NOTCH1 and SF3B1 mutations on the risk of chronic lymphocytic leukemia transformation to Richter syndrome. *Br J Haematol*. 2012;158:426-429.
65. Rossi D, Spina V, Cerri M, et al. Stereotyped B-cell receptor is an independent risk factor of chronic lymphocytic leukemia transformation to Richter syndrome. *Clin Cancer Res*. 2009;15:4415-4422.
66. Maddocks KJ, Ruppert AS, Lozanski G, et al. Etiology of ibrutinib therapy discontinuation and outcomes in patients with chronic lymphocytic leukemia. *JAMA Oncol*. 2015;1:80-87.
67. Miller CR, Ruppert AS, Heerema NA, et al. Near-tetraploidy is associated with Richter transformation in chronic lymphocytic leukemia patients receiving ibrutinib. *Blood Adv*. 2017;1:1584-1588.
68. Gunnarsson R, Mansouri L, Isaksson A, et al. Array-based genomic screening at diagnosis and follow-up in chronic lymphocytic leukemia. *Haematologica*. 2011;96:1161-1169.
69. Ouillette P, Collins R, Shakhan S, et al. Acquired genomic copy number aberrations and survival in chronic lymphocytic leukemia. *Blood*. 2011;118:3051-3061.
70. Leeksma AC, Baliakas P, Moysiadis T, et al. Genomic arrays identify high-risk chronic lymphocytic leukemia with genomic complexity: a multi-center study. *Haematologica*. 2020. https://doi.org/10.3324/haematol.2019.239947. [Epub ahead of print].
71. Klintman J, Barmpouti K, Knight SJL, et al. Clinical-grade validation of whole genome sequencing reveals robust detection of low-frequency variants and copy number alterations in CLL. *Br J Haematol*. 2018; 182:412-417.
72. Chapiro E, Pramil E, Diop M, et al. Genetic characterization of B-cell prolymphocytic leukemia: a prognostic model involving MYC and TP53. *Blood*. 2019;134:1821-1831.
73. Burger JA, Landau DA, Taylor-Weiner A, et al. Clonal evolution in patients with chronic lymphocytic leukaemia developing resistance to BTK inhibition. *Nat Commun*. 2016;7:11589.
74. Rack KA, van den Berg E, Haferlach C, et al. European recommendations and quality assurance for cytogenomic analysis of haematological neoplasms. *Leukemia*. 2019;33:1851-1867.

How to cite this article: Jondreville L, Krzisch D, Chapiro E, Nguyen-Khac F. The complex karyotype and chronic lymphocytic leukemia: prognostic value and diagnostic recommendations. *Am J Hematol*. 2020;95:1361–1367. https://doi.org/10.1002/ajh.25956

Conclusions

Conclusions

La LLC est une entité polymorphe, dont le pronostic repose sur une grande variété d'altérations génétiques possibles, acquises au cours de l'évolution de la maladie. Les caractéristiques cytogénétiques et moléculaires restent à ce jour les facteurs pronostiques les plus pertinents dans la prise en charge des patients, en raison de leur impact sur la résistance aux traitements. Mon travail de thèse a contribué à améliorer la compréhension de certaines des formes les plus agressives de LLC.

L'essentiel de mes travaux ont porté sur la caractérisation de la del8p dans la LLC. J'ai montré que la del8p était associée à des facteurs de mauvais pronostic, une survie raccourcie, et un risque accru de transformation en lymphome agressif. Cette anomalie étant parfois difficile à détecter au sein d'un caryotype souvent complexe, et associée à une survie sans rechute plus courte après chimiothérapie indépendamment des autres facteurs de risques, nous proposons sa recherche systématique par FISH chez tout patient candidat à un traitement par immunochimiothérapie.

Je me suis particulièrement concentré sur les gènes *TNFRSF10*, codant les protéines homonymes, dont la perte d'un haplotype a été identifiée chez plus de 90% des patients LLC porteurs d'une del8p. Le fonctionnement de ces récepteurs est complexe : leur activation par le ligand TRAIL induit un signal pro-apoptotique, mais une stimulation prolongée associée à une altération de la fonction apoptotique (habituelle dans la LLC) active d'autres voies de survie cellulaire. Ceci pourrait expliquer l'expression augmentée en particulier de *TNFRSF10B* dans les cellules LLC non-del8p. Après exposition à la fludarabine, les cellules LLC non-del8p sont capables de surexprimer *TNFRSF10B*, et deviennent sensibles à l'apoptose induite par TRAIL. En revanche, en présence d'une del8p, l'expression de *TNFRSF10B* à l'état basal est réduite, et ne peut être augmentée par l'exposition à la fludarabine, ce qui s'accompagne d'une résistance à TRAIL in vitro. Ces données montrent que l'haplo-insuffisance de *TNFRSF10B* est suffisante pour perdre la synergie entre fludarabine et l'apoptose induite par TRAIL.

Afin d'analyser les effets de TRAIL in vitro, j'ai généré des lignées cellulaires KO pour les gènes *TNFRSF10A*, *TNFRSF10B* et double-KO, à partir de cellules OSU-CLL éditées par CRISPR/Cas9. J'ai montré dans ces modèles que TNFRSF10A et TNFRSF10B sont tous deux capables d'induire une réponse apoptotique en réponse à TRAIL dans la LLC. Ces lignées KO pourront être utilisées pour des analyses fonctionnelles ultérieures, en particulier pour tester la réponse aux traitements activateurs de la voie TRAIL, ou pour l'étude des voies de signalisation en aval.

J'ai également participé à un travail ayant permis la caractérisation du profil génétique des LPL-B, une forme rare et agressive de LLC. Dans notre étude, on retrouvait un caryotype complexe chez 73% des patients, une anomalie des gènes *MYC* ou *TP53* chez respectivement 76% et 38% des patients. Ces données cytogénétiques et moléculaires ont permis d'identifier 3 sous-groupes pronostiques : le premier, en présence d'une anomalie de *MYC* et de *TP53* ; le second, en présence d'une anomalie de *MYC* sans anomalie de *TP53* ; et le troisième, sans altération de *MYC*. Une discussion est lancée actuellement sur la reconnaissance de l'entité LPL-B dans la nouvelle classification OMS 2022 (Alaggio et al., *Leukemia*, 2022), qui propose de séparer les LPL-B CD5+, qui seraient des LLC en progression, et les LPL-B CD5-, qui apparentés à des lymphomes B spléniques à nucléole proéminant. Une autre classification internationale a décidé de conserver la LPL-B comme entité (Campo et al., *Blood*, 2022). Une étude du méthylome par notre équipe est en cours, qui pourrait aider à avancer dans la compréhension de cette maladie.

Enfin, par une revue de la littérature, j'ai essayé de synthétiser les données disponibles afin d'étudier le rôle de facteur pronostique indépendant des caryotypes complexes et hypercomplexes dans la LLC, en particulier en regard des autres facteurs de mauvais pronostic que sont la del17p, la del11q et le statut *IGHV* non muté. Il semble clair que les caryotypes complexes / hypercomplexes sont associés à une réduction des survies globale et sans progression après traitement par immunochimiothérapie. Quant à leur impact sur la survie après traitement ciblé (ibrutinib, vénétoclax…), les données apparaissent encore contradictoires, et nécessiteront d'autres études avec un suivi plus important.

Tous ces travaux partant d'observations cytogénétiques soulignent l'importance de l'exploration des anomalies génomiques, même rares, permettant d'approfondir nos connaissances et notre compréhension des mécanismes oncogéniques. L'apparition des thérapies ciblées dans la LLC a révolutionné la prise en charge de cette maladie. Cependant, on s'aperçoit que toutes les LLC ne répondent pas de la même façon à ces nouveaux traitements, avec des résistances et des rechutes qu'il est important d'explorer et de comprendre, afin de proposer d'autres alternatives thérapeutiques.

Références bibliographiques

Références bibliographiques

1. Wasnik S, Tiwari A, Kirkland MA, Pande G. Osteohematopoietic stem cell niches in bone marrow. *Int Rev Cell Mol Biol*. 2012;298:95-133. doi:10.1016/B978-0-12-394309-5.00003-1

2. Kurosaki T, Shinohara H, Baba Y. B cell signaling and fate decision. *Annu Rev Immunol*. 2010;28:21-55. doi:10.1146/annurev.immunol.021908.132541

3. Matutes E, Owusu-Ankomah K, Morilla R, et al. The immunological profile of B-cell disorders and proposal of a scoring system for the diagnosis of CLL. *Leukemia*. 1994;8(10):1640-1645.

4. Binet JL, Auquier A, Dighiero G, et al. A new prognostic classification of chronic lymphocytic leukemia derived from a multivariate survival analysis. *Cancer*. 1981;48(1):198-206. doi:10.1002/1097-0142(19810701)48:1<198::aid-cncr2820480131>3.0.co;2-v

5. Rai KR, Sawitsky A, Cronkite EP, Chanana AD, Levy RN, Pasternack BS. Clinical staging of chronic lymphocytic leukemia. *Blood*. 1975;46(2):219-234.

6. SPF. Estimations nationales de l'incidence et de la mortalité par cancer en France métropolitaine entre 1990 et 2018 - Hémopathies malignes : Étude à partir des registres des cancers du réseau Francim. Accessed December 4, 2022. https://www.santepubliquefrance.fr/import/estimations-nationales-de-l-incidence-et-de-la-mortalite-par-cancer-en-france-metropolitaine-entre-1990-et-2018-hemopathies-malignes-etude-a-pa

7. Goldin LR, Pfeiffer RM, Li X, Hemminki K. Familial risk of lymphoproliferative tumors in families of patients with chronic lymphocytic leukemia: results from the Swedish Family-Cancer Database. *Blood*. 2004;104(6):1850-1854. doi:10.1182/blood-2004-01-0341

8. Hanada M, Delia D, Aiello A, Stadtmauer E, Reed JC. bcl-2 gene hypomethylation and high-level expression in B-cell chronic lymphocytic leukemia. *Blood*. 1993;82(6):1820-1828.

9. Messmer BT, Messmer D, Allen SL, et al. In vivo measurements document the dynamic cellular kinetics of chronic lymphocytic leukemia B cells. *J Clin Invest*. 2005;115(3):755-764. doi:10.1172/JCI23409

10. Chiorazzi N. Cell proliferation and death: Forgotten features of chronic lymphocytic leukemia B cells. *Best Practice & Research Clinical Haematology*. 2007;20(3):399-413. doi:10.1016/j.beha.2007.03.007

11. Takata M, Sabe H, Hata A, et al. Tyrosine kinases Lyn and Syk regulate B cell receptor-coupled Ca2+ mobilization through distinct pathways. *The EMBO Journal*. 1994;13(6):1341-1349. doi:10.1002/j.1460-2075.1994.tb06387.x

12. Xiong S, Xu W. 10.06 - Human Immune System. In: Brahme A, ed. *Comprehensive Biomedical Physics*. Elsevier; 2014:91-114. doi:10.1016/B978-0-444-53632-7.01008-X

13. Niiro H, Clark EA. Regulation of B-cell fate by antigen-receptor signals. *Nat Rev Immunol*. 2002;2(12):945-956. doi:10.1038/nri955

14. Minden MD von, Übelhart R, Schneider D, et al. Chronic lymphocytic leukaemia is driven by antigen-independent cell-autonomous signalling. *Nature*. 2012;489(7415):309-312. doi:10.1038/nature11309

15. ten Hacken E, Burger JA. Molecular Pathways: Targeting the Microenvironment in Chronic Lymphocytic Leukemia—Focus on the B-Cell Receptor. *Clinical Cancer Research*. 2014;20(3):548-556. doi:10.1158/1078-0432.CCR-13-0226

16. Montserrat E, Sanchez-Bisono J, Viñolas N, Rozman C. Lymphocyte doubling time in chronic lymphocytic leukaemia: analysis of its prognostic significance. *Br J Haematol*. 1986;62(3):567-575. doi:10.1111/j.1365-2141.1986.tb02969.x

17. Fasola G, Fanin R, Gherlinzoni F, et al. Serum LDH concentration in non-Hodgkin's lymphomas. Relationship to histologic type, tumor mass, and presentation features. *Acta Haematol*. 1984;72(4):231-238. doi:10.1159/000206395

18. Gdynia G, Robak T, Kopitz J, et al. Distinct Activities of Glycolytic Enzymes Identify Chronic Lymphocytic Leukemia Patients with a more Aggressive Course and Resistance to Chemo-Immunotherapy. *EBioMedicine*. 2018;32:125-133. doi:10.1016/j.ebiom.2018.05.030

19. Hallek M, Wanders L, Ostwald M, et al. Serum beta(2)-microglobulin and serum thymidine kinase are independent predictors of progression-free survival in chronic lymphocytic leukemia and immunocytoma. *Leuk Lymphoma*. 1996;22(5-6):439-447. doi:10.3109/10428199609054782

20. Deaglio S, Aydin S, Grand MM, et al. CD38/CD31 interactions activate genetic pathways leading to proliferation and migration in chronic lymphocytic leukemia cells. *Mol Med*. 2010;16(3-4):87-91. doi:10.2119/molmed.2009.00146

21. Deaglio S, Vaisitti T, Bergui L, et al. CD38 and CD100 lead a network of surface receptors relaying positive signals for B-CLL growth and survival. *Blood*. 2005;105(8):3042-3050. doi:10.1182/blood-2004-10-3873

22. Vaisitti T, Audrito V, Serra S, et al. The enzymatic activities of CD38 enhance CLL growth and trafficking: implications for therapeutic targeting. *Leukemia*. 2015;29(2):356-368. doi:10.1038/leu.2014.207

23. Hamblin TJ, Davis Z, Gardiner A, Oscier DG, Stevenson FK. Unmutated Ig V(H) genes are associated with a more aggressive form of chronic lymphocytic leukemia. *Blood*. 1999;94(6):1848-1854.

24. Damle RN, Wasil T, Fais F, et al. Ig V gene mutation status and CD38 expression as novel prognostic indicators in chronic lymphocytic leukemia. *Blood*. 1999;94(6):1840-1847.

25. Sagatys EM, Zhang L. Clinical and laboratory prognostic indicators in chronic lymphocytic leukemia. *Cancer Control*. 2012;19(1):18-25. doi:10.1177/107327481201900103

26. Juliusson G, Robèrt KH, Ost A, et al. Prognostic information from cytogenetic analysis in chronic B-lymphocytic leukemia and leukemic immunocytoma. *Blood*. 1985;65(1):134-141.

27. Juliusson G, Oscier DG, Fitchett M, et al. Prognostic Subgroups in B-Cell Chronic Lymphocytic Leukemia Defined by Specific Chromosomal Abnormalities. *N Engl J Med*. 1990;323(11):720-724. doi:10.1056/NEJM199009133231105

28. Dierlamm J, Michaux L, Criel A, Wlodarska I, Berghe HVD, Hossfeld DK. Genetic abnormalities in chronic lymphocytic leukemia and their clinical and prognostic implications. *Cancer Genetics and Cytogenetics*. 1997;94(1):27-35. doi:10.1016/S0165-4608(96)00246-4

29. Baliakas P, Jeromin S, Iskas M, et al. Cytogenetic complexity in chronic lymphocytic leukemia: definitions, associations, and clinical impact. *Blood*. 2019;133(11):1205-1216. doi:10.1182/blood-2018-09-873083

30. Klein U, Lia M, Crespo M, et al. The DLEU2/miR-15a/16-1 Cluster Controls B Cell Proliferation and Its Deletion Leads to Chronic Lymphocytic Leukemia. *Cancer Cell*. 2010;17(1):28-40. doi:10.1016/j.ccr.2009.11.019

31. Roos-Weil D, Nguyen-Khac F, Chevret S, et al. Mutational and cytogenetic analyses of 188 CLL patients with trisomy 12: A retrospective study from the French Innovative Leukemia Organization (FILO) working group. *Genes, Chromosomes and Cancer*. 2018;57(11):533-540. doi:10.1002/gcc.22650

32. Baliakas P, Hadzidimitriou A, Sutton LA, et al. Recurrent mutations refine prognosis in chronic lymphocytic leukemia. *Leukemia*. 2015;29(2):329-336. doi:10.1038/leu.2014.196

33. Rossi D, Fangazio M, Rasi S, et al. Disruption of BIRC3 associates with fludarabine chemorefractoriness in TP53 wild-type chronic lymphocytic leukemia. *Blood*. 2012;119(12):2854-2862. doi:10.1182/blood-2011-12-395673

34. Döhner H, Stilgenbauer S, Benner A, et al. Genomic Aberrations and Survival in Chronic Lymphocytic Leukemia. *New England Journal of Medicine*. 2000;343(26):1910-1916. doi:10.1056/NEJM200012283432602

35. Stilgenbauer S, Bullinger L, Benner A, et al. Incidence and clinical significance of 6q deletions in B cell chronic lymphocytic leukemia. *Leukemia*. 1999;13(9):1331-1334. doi:10.1038/sj.leu.2401499

36. Jarosova M, Hruba M, Oltova A, et al. Chromosome 6q deletion correlates with poor prognosis and low relative expression of FOXO3 in chronic lymphocytic leukemia patients. *Am J Hematol*. 2017;92(10):E604-E607. doi:10.1002/ajh.24852

37. Cuneo A, Rigolin GM, Bigoni R, et al. Chronic lymphocytic leukemia with 6q- shows distinct hematological features and intermediate prognosis. *Leukemia*. 2004;18(3):476-483. doi:10.1038/sj.leu.2403242

38. Tsimberidou AM, Wen S, O'Brien S, et al. Assessment of chronic lymphocytic leukemia and small lymphocytic lymphoma by absolute lymphocyte counts in 2,126 patients: 20 years of experience at the University of Texas M.D. Anderson Cancer Center. *J Clin Oncol*. 2007;25(29):4648-4656. doi:10.1200/JCO.2006.09.4508

39. Jarosova M, Urbankova H, Plachy R, et al. Gain of chromosome 2p in chronic lymphocytic leukemia: significant heterogeneity and a new recurrent dicentric rearrangement. *Leukemia & Lymphoma*. 2010;51(2):304-313. doi:10.3109/10428190903518311

40. Edelmann J, Holzmann K, Miller F, et al. High-resolution genomic profiling of chronic lymphocytic leukemia reveals new recurrent genomic alterations. *Blood*. 2012;120(24):4783-4794. doi:10.1182/blood-2012-04-423517

41. Kostopoulou F, Gabillaud C, Chapiro E, et al. Gain of the short arm of chromosome 2 (2p gain) has a significant role in drug-resistant chronic lymphocytic leukemia. *Cancer Med*. 2019;8(6):3131-3141. doi:10.1002/cam4.2123

42. Cosson A, Chapiro E, Bougacha N, et al. Gain in the short arm of chromosome 2 (2p+) induces gene overexpression and drug resistance in chronic lymphocytic leukemia: analysis of the central role of XPO1. *Leukemia*. 2017;31(7):1625-1629. doi:10.1038/leu.2017.100

43. Edelmann J, Holzmann K, Tausch E, et al. Genomic alterations in high-risk chronic lymphocytic leukemia frequently affect cell cycle key regulators and NOTCH1-regulated transcription. *Haematologica*. 2020;105(5):1379-1390. doi:10.3324/haematol.2019.217307

44. Forconi F, Rinaldi A, Kwee I, et al. Genome-wide DNA analysis identifies recurrent imbalances predicting outcome in chronic lymphocytic leukaemia with 17p deletion. *Br J Haematol*. 2008;143(4):532-536. doi:10.1111/j.1365-2141.2008.07373.x

45. Houldsworth J, Guttapalli A, Thodima V, et al. Genomic imbalance defines three prognostic groups for risk stratification of patients with chronic lymphocytic leukemia. *Leuk Lymphoma*. 2014;55(4):920-928. doi:10.3109/10428194.2013.845882

46. Leeksma AC, Baliakas P, Moysiadis T, et al. Genomic arrays identify high-risk chronic lymphocytic leukemia with genomic complexity: a multi-center study. *Haematologica*. 2021;106(1):87-97. doi:10.3324/haematol.2019.239947

47. Brown JR, Hanna M, Tesar B, et al. Integrative Genomic Analysis Implicates Gain of PIK3CA at 3q26 and MYC at 8q24 in Chronic Lymphocytic Leukemia. *Clin Cancer Res*. 2012;18(14):3791-3802. doi:10.1158/1078-0432.CCR-11-2342

48. Landau DA, Carter SL, Stojanov P, et al. Evolution and impact of subclonal mutations in chronic lymphocytic leukemia. *Cell*. 2013;152(4):714-726. doi:10.1016/j.cell.2013.01.019

49. Burger JA, Landau DA, Taylor-Weiner A, et al. Clonal evolution in patients with chronic lymphocytic leukaemia developing resistance to BTK inhibition. *Nat Commun*. 2016;7(1):1-13. doi:10.1038/ncomms11589

50. Beà S, López-Guillermo A, Ribas M, et al. Genetic imbalances in progressed B-cell chronic lymphocytic leukemia and transformed large-cell lymphoma (Richter's syndrome). *Am J Pathol*. 2002;161(3):957-968. doi:10.1016/S0002-9440(10)64256-3

51. Rubio-Moscardo F, Blesa D, Mestre C, et al. Characterization of 8p21.3 chromosomal deletions in B-cell lymphoma: TRAIL-R1 and TRAIL-R2 as candidate dosage-dependent tumor suppressor genes. *Blood*. 2005;106(9):3214-3222. doi:10.1182/blood-2005-05-2013

52. Kay NE, Eckel-Passow JE, Braggio E, et al. Progressive but previously untreated CLL patients with greater array CGH complexity exhibit a less durable response to chemoimmunotherapy. *Cancer Genet Cytogenet*. 2010;203(2):161-168. doi:10.1016/j.cancergencyto.2010.09.003

53. Rinaldi A, Mian M, Kwee I, et al. Genome-wide DNA profiling better defines the prognosis of chronic lymphocytic leukaemia. *British Journal of Haematology*. 2011;154(5):590-599. doi:10.1111/j.1365-2141.2011.08789.x

54. O'Malley DP, Giudice C, Chang AS, et al. Comparison of array comparative genomic hybridization (aCGH) to FISH and cytogenetics in prognostic evaluation of chronic lymphocytic leukemia. *Int J Lab Hematol*. 2011;33(3):238-244. doi:10.1111/j.1751-553X.2010.01284.x

55. Gunnarsson R, Mansouri L, Isaksson A, et al. Array-based genomic screening at diagnosis and during follow-up in chronic lymphocytic leukemia. *Haematologica*. 2011;96(8):1161-1169. doi:10.3324/haematol.2010.039768

56. Ouillette P, Collins R, Shakhan S, et al. Acquired genomic copy number aberrations and survival in chronic lymphocytic leukemia. *Blood*. 2011;118(11):3051-3061. doi:10.1182/blood-2010-12-327858

57. Kawamata N, Moreilhon C, Saitoh T, et al. Genetic differences between Asian and Caucasian chronic lymphocytic leukemia. *Int J Oncol*. 2013;43(2):561-565. doi:10.3892/ijo.2013.1966

58. Salaverria I, Martín-Garcia D, López C, et al. Detection of chromothripsis-like patterns with a custom array platform for chronic lymphocytic leukemia. *Genes Chromosomes Cancer*. 2015;54(11):668-680. doi:10.1002/gcc.22277

59. Landau DA, Tausch E, Taylor-Weiner AN, et al. Mutations driving CLL and their evolution in progression and relapse. *Nature*. 2015;526(7574):525-530. doi:10.1038/nature15395

60. Blanco G, Puiggros A, Baliakas P, et al. Karyotypic complexity rather than chromosome 8 abnormalities aggravates the outcome of chronic lymphocytic leukemia patients with TP53 aberrations. *Oncotarget*. 2016;7(49):80916-80924. doi:10.18632/oncotarget.13106

61. Ramos-Campoy S, Puiggros A, Beà S, et al. Chromosome banding analysis and genomic microarrays are both useful but not equivalent methods for genomic complexity risk stratification in chronic lymphocytic leukemia patients. *Haematologica*. 2022;107(3):593-603. doi:10.3324/haematol.2020.274456

62. Goede V, Fischer K, Busch R, et al. Obinutuzumab plus chlorambucil in patients with CLL and coexisting conditions. *N Engl J Med*. 2014;370(12):1101-1110. doi:10.1056/NEJMoa1313984

63. Wang E, Mi X, Thompson MC, et al. Mechanisms of Resistance to Noncovalent Bruton's Tyrosine Kinase Inhibitors. *N Engl J Med*. 2022;386(8):735-743. doi:10.1056/NEJMoa2114110

64. Byrd JC, Harrington B, O'Brien S, et al. Acalabrutinib (ACP-196) in Relapsed Chronic Lymphocytic Leukemia. *N Engl J Med*. 2016;374(4):323-332. doi:10.1056/NEJMoa1509981

65. Mato AR, Shah NN, Jurczak W, et al. Pirtobrutinib in relapsed or refractory B-cell malignancies (BRUIN): a phase 1/2 study. *Lancet*. 2021;397(10277):892-901. doi:10.1016/S0140-6736(21)00224-5

66. Furman RR, Sharman JP, Coutre SE, et al. Idelalisib and rituximab in relapsed chronic lymphocytic leukemia. *N Engl J Med*. 2014;370(11):997-1007. doi:10.1056/NEJMoa1315226

67. Lampson BL, Kasar SN, Matos TR, et al. Idelalisib given front-line for treatment of chronic lymphocytic leukemia causes frequent immune-mediated hepatotoxicity. *Blood*. 2016;128(2):195-203. doi:10.1182/blood-2016-03-707133

68. Seymour JF, Ma S, Brander DM, et al. Venetoclax plus rituximab in relapsed or refractory chronic lymphocytic leukaemia: a phase 1b study. *The Lancet Oncology*. 2017;18(2):230-240. doi:10.1016/S1470-2045(17)30012-8

69. Al-Sawaf O, Zhang C, Tandon M, et al. Venetoclax plus obinutuzumab versus chlorambucil plus obinutuzumab for previously untreated chronic lymphocytic leukaemia (CLL14): follow-up results from a multicentre, open-label, randomised, phase 3 trial. *The Lancet Oncology*. 2020;21(9):1188-1200. doi:10.1016/S1470-2045(20)30443-5

70. Deng J, Paulus A, Fang DD, et al. Lisaftoclax (APG-2575) Is a Novel BCL-2 Inhibitor with Robust Antitumor Activity in Preclinical Models of Hematologic Malignancy. *Clin Cancer Res*. 2022;28(24):5455-5468. doi:10.1158/1078-0432.CCR-21-4037

71. Buccheri V, Barreto WG, Fogliatto LM, Capra M, Marchiani M, Rocha V. Prognostic and therapeutic stratification in CLL: focus on 17p deletion and p53 mutation. *Ann Hematol*. 2018;97(12):2269-2278. doi:10.1007/s00277-018-3503-6

72. Rafei H, Kharfan-Dabaja MA. Treatment of Del17p and/or aberrant TP53 chronic lymphocytic leukemia in the era of novel therapies. *Hematol Oncol Stem Cell Ther*. 2018;11(1):1-12. doi:10.1016/j.hemonc.2017.04.002

73. Woyach JA, Furman RR, Liu TM, et al. Resistance Mechanisms for the Bruton's Tyrosine Kinase Inhibitor Ibrutinib. *N Engl J Med*. 2014;370(24):2286-2294. doi:10.1056/NEJMoa1400029

74. Blombery P, Thompson ER, Lew TE, et al. Enrichment of BTK Leu528Trp mutations in patients with CLL on zanubrutinib: potential for pirtobrutinib cross-resistance. *Blood Adv*. 2022;6(20):5589-5592. doi:10.1182/bloodadvances.2022008325

75. Blombery P, Anderson MA, Gong J nan, et al. Acquisition of the Recurrent Gly101Val Mutation in BCL2 Confers Resistance to Venetoclax in Patients with Progressive Chronic Lymphocytic Leukemia. *Cancer Discov*. 2019;9(3):342-353. doi:10.1158/2159-8290.CD-18-1119

76. Lucas F, Larkin K, Gregory CT, et al. Novel BCL2 mutations in venetoclax-resistant, ibrutinib-resistant CLL patients with BTK/PLCG2 mutations. *Blood*. 2020;135(24):2192-2195. doi:10.1182/blood.2019003722

77. Guièze R, Liu VM, Rosebrock D, et al. Mitochondrial Reprogramming Underlies Resistance to BCL-2 Inhibition in Lymphoid Malignancies. *Cancer Cell*. 2019;36(4):369-384.e13. doi:10.1016/j.ccell.2019.08.005

78. Hallek M, Cheson BD, Catovsky D, et al. iwCLL guidelines for diagnosis, indications for treatment, response assessment, and supportive management of CLL. *Blood*. 2018;131(25):2745-2760. doi:10.1182/blood-2017-09-806398

79. Quinquenel A, Aurran-Schleinitz T, Clavert A, et al. Diagnosis and Treatment of Chronic Lymphocytic Leukemia: Recommendations of the French CLL Study Group (FILO). *Hemasphere*. 2020;4(5):e473. doi:10.1097/HS9.0000000000000473

80. Kerr JFR, Wyllie AH, Currie AR. Apoptosis: A Basic Biological Phenomenon with Wide-ranging Implications in Tissue Kinetics. *Br J Cancer*. 1972;26(4):239-257.

81. Galluzzi L, Vitale I, Aaronson SA, et al. Molecular mechanisms of cell death: recommendations of the Nomenclature Committee on Cell Death 2018. *Cell Death Differ*. 2018;25(3):486-541. doi:10.1038/s41418-017-0012-4

82. Yuan J, Shaham S, Ledoux S, Ellis HM, Horvitz HR. The C. elegans cell death gene ced-3 encodes a protein similar to mammalian interleukin-1 beta-converting enzyme. *Cell*. 1993;75(4):641-652. doi:10.1016/0092-8674(93)90485-9

83. Couzinet A, Hérincs Z, Hueber AO. Régulation de la mort cellulaire programmée : vers une conception plus dynamique. *Med Sci (Paris)*. 2002;18(8-9):841-852. doi:10.1051/medsci/20021889841

84. Pihán P, Carreras-Sureda A, Hetz C. BCL-2 family: integrating stress responses at the ER to control cell demise. *Cell Death Differ*. 2017;24(9):1478-1487. doi:10.1038/cdd.2017.82

85. Shalini S, Dorstyn L, Dawar S, Kumar S. Old, new and emerging functions of caspases. *Cell Death Differ*. 2015;22(4):526-539. doi:10.1038/cdd.2014.216

86. Cabon L, Martinez-Torres AC, Susin SA. La mort cellulaire programmée ne manque pas de vocabulaire. *Med Sci (Paris)*. 2013;29(12):1117-1124. doi:10.1051/medsci/20132912015

87. Krijnen PAJ, Nijmeijer R, Meijer CJLM, Visser CA, Hack CE, Niessen HWM. Apoptosis in myocardial ischaemia and infarction. *J Clin Pathol*. 2002;55(11):801-811.

88. Broughton BRS, Reutens DC, Sobey CG. Apoptotic Mechanisms After Cerebral Ischemia. *Stroke*. 2009;40(5):e331-e339. doi:10.1161/STROKEAHA.108.531632

89. Olivier M, Hollstein M, Hainaut P. TP53 Mutations in Human Cancers: Origins, Consequences, and Clinical Use. *Cold Spring Harbor Perspectives in Biology*. 2010;2(1):a001008-a001008. doi:10.1101/cshperspect.a001008

90. Grønbaek K, Straten PT, Ralfkiaer E, et al. Somatic Fas mutations in non-Hodgkin's lymphoma: association with extranodal disease and autoimmunity. *Blood*. 1998;92(9):3018-3024.

91. Shin MS, Kim HS, Lee SH, et al. Mutations of tumor necrosis factor-related apoptosis-inducing ligand receptor 1 (TRAIL-R1) and receptor 2 (TRAIL-R2) genes in metastatic breast cancers. *Cancer Res*. 2001;61(13):4942-4946.

92. Cimmino A, Calin GA, Fabbri M, et al. miR-15 and miR-16 induce apoptosis by targeting BCL2. *Proc Natl Acad Sci U S A*. 2005;102(39):13944-13949. doi:10.1073/pnas.0506654102

93. Billard C. Apoptosis inducers in chronic lymphocytic leukemia. *Oncotarget*. 2013;5(2):309-325.

94. Roberts AW, Wei AH, Huang DCS. BCL2 and MCL1 inhibitors for hematologic malignancies. *Blood*. 2021;138(13):1120-1136. doi:10.1182/blood.2020006785

95. O'Brien S, Moore JO, Boyd TE, et al. Randomized phase III trial of fludarabine plus cyclophosphamide with or without oblimersen sodium (Bcl-2 antisense) in patients with relapsed or refractory chronic lymphocytic leukemia. *J Clin Oncol*. 2007;25(9):1114-1120. doi:10.1200/JCO.2006.07.1191

96. Andreeff M, Kelly KR, Yee K, et al. Results of the Phase I Trial of RG7112, a Small-Molecule MDM2 Antagonist in Leukemia. *Clinical Cancer Research*. 2016;22(4):868-876. doi:10.1158/1078-0432.CCR-15-0481

97. Loeder S, Zenz T, Schnaiter A, et al. A Novel Paradigm to Trigger Apoptosis in Chronic Lymphocytic Leukemia. *Cancer Research*. 2009;69(23):8977-8986. doi:10.1158/0008-5472.CAN-09-2604

98. Hymowitz SG, Christinger HW, Fuh G, et al. Triggering cell death: the crystal structure of Apo2L/TRAIL in a complex with death receptor 5. *Mol Cell*. 1999;4(4):563-571. doi:10.1016/s1097-2765(00)80207-5

99. Ramamurthy V, Yamniuk AP, Lawrence EJ, et al. The structure of the death receptor 4-TNF-related apoptosis-inducing ligand (DR4-TRAIL) complex. *Acta Crystallogr F Struct Biol Commun*. 2015;71(Pt 10):1273-1281. doi:10.1107/S2053230X15016416

100. MacFarlane M. TRAIL-induced signalling and apoptosis. *Toxicology Letters*. 2003;139(2-3):89-97. doi:10.1016/S0378-4274(02)00422-8

101. Chaudhary PM, Eby M, Jasmin A, Bookwalter A, Murray J, Hood L. Death Receptor 5, a New Member of the TNFR Family, and DR4 Induce FADD-Dependent Apoptosis and Activate the NF-κB Pathway. *Immunity*. 1997;7(6):821-830. doi:10.1016/S1074-7613(00)80400-8

102. Refaat A, Abd-Rabou A, Reda A. TRAIL combinations: The new 'trail' for cancer therapy (Review). *Oncology Letters*. 2014;7(5):1327-1332. doi:10.3892/ol.2014.1922

103. Marsters SA, Sheridan JP, Pitti RM, et al. A novel receptor for Apo2L/TRAIL contains a truncated death domain. *Current Biology*. 1997;7(12):1003-1006. doi:10.1016/S0960-9822(06)00422-2

104. Degli-Esposti MA, Dougall WC, Smolak PJ, Waugh JY, Smith CA, Goodwin RG. The Novel Receptor TRAIL-R4 Induces NF-κB and Protects against TRAIL-Mediated Apoptosis, yet Retains an Incomplete Death Domain. *Immunity*. 1997;7(6):813-820. doi:10.1016/S1074-7613(00)80399-4

105. Zauli G, Rimondi E, Nicolin V, Melloni E, Celeghini C, Secchiero P. TNF-related apoptosis-inducing ligand (TRAIL) blocks osteoclastic differentiation induced by RANKL plus M-CSF. *Blood*. 2004;104(7):2044-2050. doi:10.1182/blood-2004-03-1196

106. Ehrlich S, Infante-Duarte C, Seeger B, Zipp F. Regulation of soluble and surface-bound TRAIL in human T cells, B cells, and monocytes. *Cytokine*. 2003;24(6):244-253. doi:10.1016/S1043-4666(03)00094-2

107. Kemp TJ, Moore JM, Griffith TS. Human B Cells Express Functional TRAIL/Apo-2 Ligand after CpG-Containing Oligodeoxynucleotide Stimulation. *The Journal of Immunology*. 2004;173(2):892-899. doi:10.4049/jimmunol.173.2.892

108. Chaperot L, Blum A, Manches O, et al. Virus or TLR Agonists Induce TRAIL-Mediated Cytotoxic Activity of Plasmacytoid Dendritic Cells. *The Journal of Immunology*. 2006;176(1):248-255. doi:10.4049/jimmunol.176.1.248

109. Kalb ML, Glaser A, Stary G, Koszik F, Stingl G. TRAIL+ Human Plasmacytoid Dendritic Cells Kill Tumor Cells In Vitro: Mechanisms of Imiquimod- and IFN-α–Mediated Antitumor Reactivity. *The Journal of Immunology*. 2012;188(4):1583-1591. doi:10.4049/jimmunol.1102437

110. Mirandola P, Ponti C, Gobbi G, et al. Activated human NK and CD8+ T cells express both TNF-related apoptosis-inducing ligand (TRAIL) and TRAIL receptors but are resistant to TRAIL-mediated cytotoxicity. *Blood*. 2004;104(8):2418-2424. doi:10.1182/blood-2004-04-1294

111. Guan B, Yue P, Clayman GL, Sun SY. Evidence that the death receptor DR4 is a DNA damage-inducible, p53-regulated gene. *Journal of Cellular Physiology*. 2001;188(1):98-105. doi:10.1002/jcp.1101

112. Wu GS, Burns TF, McDonald ER, et al. KILLER/DR5 is a DNA damage–inducible p53–regulated death receptor gene. *Nat Genet*. 1997;17(2):141-143. doi:10.1038/ng1097-141

113. Rossin A, Derouet M, Abdel-Sater F, Hueber AO. Palmitoylation of the TRAIL receptor DR4 confers an efficient TRAIL-induced cell death signalling. *Biochemical Journal*. 2009;419(1):185-194. doi:10.1042/BJ20081212

114. Ouyang X, Shi M, Jie F, et al. Phase III study of dulanermin (recombinant human tumor necrosis factor-related apoptosis-inducing ligand/Apo2 ligand) combined with vinorelbine and cisplatin in patients with advanced non-small-cell lung cancer. *Invest New Drugs*. 2018;36(2):315-322. doi:10.1007/s10637-017-0536-y

115. Marconi M, Ascione B, Ciarlo L, et al. Constitutive localization of DR4 in lipid rafts is mandatory for TRAIL-induced apoptosis in B-cell hematologic malignancies. *Cell Death Dis*. 2013;4(10):e863-e863. doi:10.1038/cddis.2013.389

116. Mollinedo F, Gajate C. Lipid rafts as signaling hubs in cancer cell survival/death and invasion: implications in tumor progression and therapy: Thematic Review Series: Biology of Lipid Rafts. *Journal of Lipid Research*. 2020;61(5):611-635. doi:10.1194/jlr.TR119000439

117. Wu GS, Burns TF, Zhan Y, Alnemri ES, El-Deiry WS. Molecular cloning and functional analysis of the mouse homologue of the KILLER/DR5 tumor necrosis factor-related apoptosis-inducing ligand (TRAIL) death receptor. *Cancer Res*. 1999;59(12):2770-2775.

118. Diehl GE, Yue HH, Hsieh K, et al. TRAIL-R as a negative regulator of innate immune cell responses. *Immunity*. 2004;21(6):877-889. doi:10.1016/j.immuni.2004.11.008

119. Finnberg N, Klein-Szanto AJP, El-Deiry WS. TRAIL-R deficiency in mice promotes susceptibility to chronic inflammation and tumorigenesis. *J Clin Invest*. 2008;118(1):111-123. doi:10.1172/JCI29900

120. Cretney E, Takeda K, Yagita H, Glaccum M, Peschon JJ, Smyth MJ. Increased Susceptibility to Tumor Initiation and Metastasis in TNF-Related Apoptosis-Inducing Ligand-Deficient Mice. *The Journal of Immunology*. 2002;168(3):1356-1361. doi:10.4049/jimmunol.168.3.1356

121. Grosse-Wilde A, Voloshanenko O, Bailey SL, et al. TRAIL-R deficiency in mice enhances lymph node metastasis without affecting primary tumor development. *J Clin Invest*. 2008;118(1):100-110. doi:10.1172/JCI33061

122. Sedger LM, Shows DM, Blanton RA, et al. IFN-gamma mediates a novel antiviral activity through dynamic modulation of TRAIL and TRAIL receptor expression. *J Immunol*. 1999;163(2):920-926.

123. Clarke P, Meintzer SM, Gibson S, et al. Reovirus-Induced Apoptosis Is Mediated by TRAIL. *J Virol*. 2000;74(17):8135-8139.

124. Brincks EL, Katewa A, Kucaba TA, Griffith TS, Legge KL. CD8 T cells utilize TRAIL to control influenza virus infection. *J Immunol*. 2008;181(7):4918-4925. doi:10.4049/jimmunol.181.7.4918

125. Peppa D, Gill US, Reynolds G, et al. Up-regulation of a death receptor renders antiviral T cells susceptible to NK cell-mediated deletion. *J Exp Med*. 2013;210(1):99-114. doi:10.1084/jem.20121172

126. Lamhamedi-Cherradi SE, Zheng SJ, Maguschak KA, Peschon J, Chen YH. Defective thymocyte apoptosis and accelerated autoimmune diseases in TRAIL−/− mice. *Nat Immunol*. 2003;4(3):255-260. doi:10.1038/ni894

127. Chyuan IT, Chu CL, Hsu CL, et al. T Cell–Specific Deletion of TRAIL Receptor Reveals Its Critical Role for Regulating Pathologic T Cell Activation and Disease Induction in Experimental Autoimmune Encephalomyelitis. *The Journal of Immunology*. 2022;208(7):1534-1544. doi:10.4049/jimmunol.2100788

128. Sedger LM, Katewa A, Pettersen AK, et al. Extreme lymphoproliferative disease and fatal autoimmune thrombocytopenia in FasL and TRAIL double-deficient mice. *Blood*. 2010;115(16):3258-3268. doi:10.1182/blood-2009-11-255497

129. Guerreiro-Cacais AO, Levitskaya J, Levitsky V. B cell receptor triggering sensitizes human B cells to TRAIL-induced apoptosis. *J Leukoc Biol*. 2010;88(5):937-945. doi:10.1189/jlb.0510246

130. Crowder RN, Zhao H, Chatham WW, Zhou T, Carter RH. B lymphocytes are resistant to death receptor 5-induced apoptosis. *Clin Immunol*. 2011;139(1):21-31. doi:10.1016/j.clim.2010.12.006

131. Daniels RA, Turley H, Kimberley FC, et al. Expression of TRAIL and TRAIL receptors in normal and malignant tissues. *Cell Res*. 2005;15(6):430-438. doi:10.1038/sj.cr.7290311

132. von Karstedt S, Montinaro A, Walczak H. Exploring the TRAILs less travelled: TRAIL in cancer biology and therapy. *Nat Rev Cancer*. 2017;17(6):352-366. doi:10.1038/nrc.2017.28

133. Sträter J, Walczak H, Pukrop T, et al. TRAIL and its receptors in the colonic epithelium: a putative role in the defense of viral infections. *Gastroenterology*. 2002;122(3):659-666. doi:10.1053/gast.2002.31889

134. van Grevenynghe J, Cubas RA, Noto A, et al. Loss of memory B cells during chronic HIV infection is driven by Foxo3a- and TRAIL-mediated apoptosis. *J Clin Invest*. 2011;121(10):3877-3888. doi:10.1172/JCI59211

135. Staniek J, Lorenzetti R, Heller B, et al. TRAIL-R1 and TRAIL-R2 Mediate TRAIL-Dependent Apoptosis in Activated Primary Human B Lymphocytes. *Front Immunol*. 2019;10:951. doi:10.3389/fimmu.2019.00951

136. Martinez-Climent JA, Vizcarra E, Sanchez D, et al. Loss of a novel tumor suppressor gene locus at chromosome 8p is associated with leukemic mantle cell lymphoma. *Blood*. 2001;98(12):3479-3482. doi:10.1182/blood.V98.12.3479

137. Berglund M, Enblad G, Flordal E, et al. Chromosomal imbalances in diffuse large B-cell lymphoma detected by comparative genomic hybridization. *Mod Pathol*. 2002;15(8):807-816. doi:10.1097/01.MP.0000024375.04135.2B

138. Kohlhammer H, Schwaenen C, Wessendorf S, et al. Genomic DNA-chip hybridization in t(11;14)-positive mantle cell lymphomas shows a high frequency of aberrations and allows a refined characterization of consensus regions. *Blood*. 2004;104(3):795-801. doi:10.1182/blood-2003-12-4175

139. Sutlu T, Alici E, Jansson M, et al. The prognostic significance of 8p21 deletion in multiple myeloma. *Br J Haematol*. 2009;144(2):266-268. doi:10.1111/j.1365-2141.2008.07454.x

140. Gmidène A, Saad A, Avet-Loiseau H. 8p21.3 deletion suggesting a probable role of TRAIL-R1 and TRAIL-R2 as candidate tumor suppressor genes in the pathogenesis of multiple myeloma. *Med Oncol*. 2013;30(2):489. doi:10.1007/s12032-013-0489-8

141. Wistuba II, Behrens C, Virmani AK, et al. Allelic losses at chromosome 8p21-23 are early and frequent events in the pathogenesis of lung cancer. *Cancer Res*. 1999;59(8):1973-1979.

142. Yaremko ML, Kutza C, Lyzak J, Mick R, Recant WM, Westbrook CA. Loss of heterozygosity from the short arm of chromosome 8 is associated with invasive behavior in breast cancer. *Genes Chromosomes Cancer*. 1996;16(3):189-195. doi:10.1002/(SICI)1098-2264(199607)16:3<189::AID-GCC6>3.0.CO;2-V

143. Kagan J, Stein J, Babaian RJ, et al. Homozygous deletions at 8p22 and 8p21 in prostate cancer implicate these regions as the sites for candidate tumor suppressor genes. *Oncogene*. 1995;11(10):2121-2126.

144. Emi M, Fujiwara Y, Nakajima T, et al. Frequent loss of heterozygosity for loci on chromosome 8p in hepatocellular carcinoma, colorectal cancer, and lung cancer. *Cancer Res*. 1992;52(19):5368-5372.

145. Lee SH, Shin MS, Kim HS, et al. Alterations of the DR5/TRAIL receptor 2 gene in non-small cell lung cancers. *Cancer Res*. 1999;59(22):5683-5686.

146. Secchiero P, Tiribelli M, Barbarotto E, et al. Aberrant expression of TRAIL in B chronic lymphocytic leukemia (B-CLL) cells. *J Cell Physiol*. 2005;205(2):246-252. doi:10.1002/jcp.20392

147. Irmler M, Thome M, Hahne M, et al. Inhibition of death receptor signals by cellular FLIP. *Nature*. 1997;388(6638):190-195. doi:10.1038/40657

148. Olsson A, Diaz T, Aguilar-Santelises M, et al. Sensitization to TRAIL-induced apoptosis and modulation of FLICE-inhibitory protein in B chronic lymphocytic leukemia by actinomycin D. *Leukemia*. 2001;15(12):1868-1877. doi:10.1038/sj.leu.2402287

149. Johnston JB, Kabore AF, Strutinsky J, et al. Role of the TRAIL/APO2-L death receptors in chlorambucil- and fludarabine-induced apoptosis in chronic lymphocytic leukemia. *Oncogene*. 2003;22(51):8356-8369. doi:10.1038/sj.onc.1207004

150. MacFarlane M, Inoue S, Kohlhaas SL, et al. Chronic lymphocytic leukemic cells exhibit apoptotic signaling via TRAIL-R1. *Cell Death Differ*. 2005;12(7):773-782. doi:10.1038/sj.cdd.4401649

151. MacFarlane M, Kohlhaas SL, Sutcliffe MJ, Dyer MJS, Cohen GM. TRAIL receptor-selective mutants signal to apoptosis via TRAIL-R1 in primary lymphoid malignancies. *Cancer Res*. 2005;65(24):11265-11270. doi:10.1158/0008-5472.CAN-05-2801

152. Natoni A, MacFarlane M, Inoue S, et al. TRAIL signals to apoptosis in chronic lymphocytic leukaemia cells primarily through TRAIL-R1 whereas cross-linked agonistic TRAIL-R2 antibodies facilitate signalling via TRAIL-R2. *Br J Haematol*. 2007;139(4):568-577. doi:10.1111/j.1365-2141.2007.06852.x

153. Duru AD, Sutlu T, Wallblom A, et al. Deletion of Chromosomal Region 8p21 Confers Resistance to Bortezomib and Is Associated with Upregulated Decoy TRAIL Receptor Expression in Patients with Multiple Myeloma. *PLOS ONE*. 2015;10(9):e0138248. doi:10.1371/journal.pone.0138248

154. Wiley SR, Schooley K, Smolak PJ, et al. Identification and characterization of a new member of the TNF family that induces apoptosis. *Immunity*. 1995;3(6):673-682. doi:10.1016/1074-7613(95)90057-8

155. Walczak H, Miller RE, Ariail K, et al. Tumoricidal activity of tumor necrosis factor-related apoptosis-inducing ligand in vivo. *Nat Med*. 1999;5(2):157-163. doi:10.1038/5517

156. Kelley SK, Harris LA, Xie D, et al. Preclinical studies to predict the disposition of Apo2L/tumor necrosis factor-related apoptosis-inducing ligand in humans: characterization of in vivo efficacy, pharmacokinetics, and safety. *J Pharmacol Exp Ther*. 2001;299(1):31-38.

157. Hylander BL, Pitoniak R, Penetrante RB, et al. The anti-tumor effect of Apo2L/TRAIL on patient pancreatic adenocarcinomas grown as xenografts in SCID mice. *J Transl Med*. 2005;3:22. doi:10.1186/1479-5876-3-22

158. Pollack IF, Erff M, Ashkenazi A. Direct stimulation of apoptotic signaling by soluble Apo2l/tumor necrosis factor-related apoptosis-inducing ligand leads to selective killing of glioma cells. *Clin Cancer Res*. 2001;7(5):1362-1369.

159. Mitsiades CS, Treon SP, Mitsiades N, et al. TRAIL/Apo2L ligand selectively induces apoptosis and overcomes drug resistance in multiple myeloma: therapeutic applications. *Blood*. 2001;98(3):795-804. doi:10.1182/blood.v98.3.795

160. Chinnaiyan AM, Prasad U, Shankar S, et al. Combined effect of tumor necrosis factor-related apoptosis-inducing ligand and ionizing radiation in breast cancer therapy. *Proc Natl Acad Sci U S A*. 2000;97(4):1754-1759. doi:10.1073/pnas.030545097

161. Gliniak B, Le T. Tumor necrosis factor-related apoptosis-inducing ligand's antitumor activity in vivo is enhanced by the chemotherapeutic agent CPT-11. *Cancer Res*. 1999;59(24):6153-6158.

162. Chuntharapai A, Dodge K, Grimmer K, et al. Isotype-dependent inhibition of tumor growth in vivo by monoclonal antibodies to death receptor 4. *J Immunol*. 2001;166(8):4891-4898. doi:10.4049/jimmunol.166.8.4891

163. Ichikawa K, Liu W, Zhao L, et al. Tumoricidal activity of a novel anti-human DR5 monoclonal antibody without hepatocyte cytotoxicity. *Nat Med*. 2001;7(8):954-960. doi:10.1038/91000

164. Herbst RS, Eckhardt SG, Kurzrock R, et al. Phase I dose-escalation study of recombinant human Apo2L/TRAIL, a dual proapoptotic receptor agonist, in patients with advanced cancer. *J Clin Oncol*. 2010;28(17):2839-2846. doi:10.1200/JCO.2009.25.1991

165. Camidge DR, Herbst RS, Gordon MS, et al. A phase I safety and pharmacokinetic study of the death receptor 5 agonistic antibody PRO95780 in patients with advanced malignancies. *Clin Cancer Res*. 2010;16(4):1256-1263. doi:10.1158/1078-0432.CCR-09-1267

166. Hotte SJ, Hirte HW, Chen EX, et al. A phase 1 study of mapatumumab (fully human monoclonal antibody to TRAIL-R1) in patients with advanced solid malignancies. *Clin Cancer Res*. 2008;14(11):3450-3455. doi:10.1158/1078-0432.CCR-07-1416

167. Younes A, Vose JM, Zelenetz AD, et al. A Phase 1b/2 trial of mapatumumab in patients with relapsed/refractory non-Hodgkin's lymphoma. *Br J Cancer*. 2010;103(12):1783-1787. doi:10.1038/sj.bjc.6605987

168. von Pawel J, Harvey JH, Spigel DR, et al. Phase II trial of mapatumumab, a fully human agonist monoclonal antibody to tumor necrosis factor-related apoptosis-inducing ligand receptor 1 (TRAIL-R1), in combination with paclitaxel and carboplatin in patients with advanced non-small-cell lung cancer. *Clin Lung Cancer*. 2014;15(3):188-196.e2. doi:10.1016/j.cllc.2013.12.005

169. Trarbach T, Moehler M, Heinemann V, et al. Phase II trial of mapatumumab, a fully human agonistic monoclonal antibody that targets and activates the tumour necrosis factor apoptosis-inducing ligand receptor-1 (TRAIL-R1), in patients with refractory colorectal cancer. *Br J Cancer*. 2010;102(3):506-512. doi:10.1038/sj.bjc.6605507

170. Paz-Ares L, Bálint B, de Boer RH, et al. A randomized phase 2 study of paclitaxel and carboplatin with or without conatumumab for first-line treatment of advanced non-small-cell lung cancer. *J Thorac Oncol*. 2013;8(3):329-337. doi:10.1097/JTO.0b013e31827ce554

171. Kindler HL, Richards DA, Garbo LE, et al. A randomized, placebo-controlled phase 2 study of ganitumab (AMG 479) or conatumumab (AMG 655) in combination with gemcitabine in patients with metastatic pancreatic cancer. *Ann Oncol*. 2012;23(11):2834-2842. doi:10.1093/annonc/mds142

172. Forero-Torres A, Infante JR, Waterhouse D, et al. Phase 2, multicenter, open-label study of tigatuzumab (CS-1008), a humanized monoclonal antibody targeting death receptor 5, in combination with gemcitabine in chemotherapy-naive patients with unresectable or metastatic pancreatic cancer. *Cancer Med*. 2013;2(6):925-932. doi:10.1002/cam4.137

173. Reck M, Krzakowski M, Chmielowska E, et al. A randomized, double-blind, placebo-controlled phase 2 study of tigatuzumab (CS-1008) in combination with carboplatin/paclitaxel in patients with chemotherapy-naïve metastatic/unresectable non-small cell lung cancer. *Lung Cancer*. 2013;82(3):441-448. doi:10.1016/j.lungcan.2013.09.014

174. Legler K, Hauser C, Egberts JH, et al. The novel TRAIL-receptor agonist APG350 exerts superior therapeutic activity in pancreatic cancer cells. *Cell Death Dis*. 2018;9(5):445. doi:10.1038/s41419-018-0478-0

175. Lemke J, von Karstedt S, Zinngrebe J, Walczak H. Getting TRAIL back on track for cancer therapy. *Cell Death Differ*. 2014;21(9):1350-1364. doi:10.1038/cdd.2014.81

176. Kaplan-Lefko PJ, Graves JD, Zoog SJ, et al. Conatumumab, a fully human agonist antibody to death receptor 5, induces apoptosis via caspase activation in multiple tumor types. *Cancer Biol Ther*. 2010;9(8):618-631. doi:10.4161/cbt.9.8.11264

177. Wilson NS, Yang B, Yang A, et al. An Fcγ receptor-dependent mechanism drives antibody-mediated target-receptor signaling in cancer cells. *Cancer Cell*. 2011;19(1):101-113. doi:10.1016/j.ccr.2010.11.012

178. Thapa B, Kc R, Uludağ H. TRAIL therapy and prospective developments for cancer treatment. *Journal of Controlled Release*. 2020;326:335-349. doi:10.1016/j.jconrel.2020.07.013

179. Schneider P. Production of recombinant TRAIL and TRAIL receptor: Fc chimeric proteins. *Methods Enzymol*. 2000;322:325-345. doi:10.1016/s0076-6879(00)22031-4

180. Pitti RM, Marsters SA, Ruppert S, Donahue CJ, Moore A, Ashkenazi A. Induction of apoptosis by Apo-2 ligand, a new member of the tumor necrosis factor cytokine family. *J Biol Chem*. 1996;271(22):12687-12690. doi:10.1074/jbc.271.22.12687

181. Chae SY, Kim TH, Park K, et al. Improved antitumor activity and tumor targeting of NH(2)-terminal-specific PEGylated tumor necrosis factor-related apoptosis-inducing ligand. *Mol Cancer Ther*. 2010;9(6):1719-1729. doi:10.1158/1535-7163.MCT-09-1076

182. Yuan Z, Kolluri KK, Gowers KHC, Janes SM. TRAIL delivery by MSC-derived extracellular vesicles is an effective anticancer therapy. *J Extracell Vesicles*. 2017;6(1):1265291. doi:10.1080/20013078.2017.1265291

183. Dong F, Wang L, Davis JJ, et al. Eliminating established tumor in nu/nu nude mice by a tumor necrosis factor-alpha-related apoptosis-inducing ligand-armed oncolytic adenovirus. *Clin Cancer Res*. 2006;12(17):5224-5230. doi:10.1158/1078-0432.CCR-06-0244

184. Kock N, Kasmieh R, Weissleder R, Shah K. Tumor therapy mediated by lentiviral expression of shBcl-2 and S-TRAIL. *Neoplasia*. 2007;9(5):435-442. doi:10.1593/neo.07223

185. Luo C, Miao L, Zhao Y, et al. A novel cationic lipid with intrinsic antitumor activity to facilitate gene therapy of TRAIL DNA. *Biomaterials*. 2016;102:239-248. doi:10.1016/j.biomaterials.2016.06.030

186. Huang S, Li J, Han L, et al. Dual targeting effect of Angiopep-2-modified, DNA-loaded nanoparticles for glioma. *Biomaterials*. 2011;32(28):6832-6838. doi:10.1016/j.biomaterials.2011.05.064

187. Sayers TJ, Murphy WJ. Combining proteasome inhibition with TNF-related apoptosis-inducing ligand (Apo2L/TRAIL) for cancer therapy. *Cancer Immunol Immunother*. 2006;55(1):76-84. doi:10.1007/s00262-005-0676-3

188. Ricci MS, Jin Z, Dews M, et al. Direct repression of FLIP expression by c-myc is a major determinant of TRAIL sensitivity. *Mol Cell Biol*. 2004;24(19):8541-8555. doi:10.1128/MCB.24.19.8541-8555.2004

189. Bangert A, Cristofanon S, Eckhardt I, et al. Histone deacetylase inhibitors sensitize glioblastoma cells to TRAIL-induced apoptosis by c-myc-mediated downregulation of cFLIP. *Oncogene*. 2012;31(44):4677-4688. doi:10.1038/onc.2011.614

190. Inoue S, Harper N, Walewska R, Dyer MJS, Cohen GM. Enhanced Fas-associated death domain recruitment by histone deacetylase inhibitors is critical for the sensitization of chronic lymphocytic leukemia cells to TRAIL-induced apoptosis. *Mol Cancer Ther*. 2009;8(11):3088-3097. doi:10.1158/1535-7163.MCT-09-0451

191. Zhou Q, Fukushima P, DeGraff W, et al. Radiation and the Apo2L/TRAIL apoptotic pathway preferentially inhibit the colonization of premalignant human breast cells overexpressing cyclin D1. *Cancer Res*. 2000;60(10):2611-2615.

Résumé

La leucémie lymphoïde chronique (LLC) est la leucémie la plus fréquente de l'adulte caucasien. Le pronostic, très hétérogène, dépend des anomalies cytogénétiques et moléculaires. Certaines de ces anomalies sont associées à des mécanismes de résistance aux traitements, dont la compréhension est primordiale pour adapter les thérapies.

Mon travail de thèse a principalement porté sur l'étude des LLC avec délétion 8p (del8p). Nous avons montré que cette anomalie chromosomique rare, mais récurrente, était non seulement fréquemment associée à d'autres facteurs « classiques » de mauvais pronostic (tels que le caryotype complexe, les anomalies *TP53*, et le statut *IGHV* non muté), mais également à des survies globale et sans progression raccourcies, et un risque de transformation en lymphome agressif (Richter). J'ai montré l'implication de la famille des gènes *TNFRSF10*, récepteurs du ligand TRAIL, dans la grande majorité des patients porteurs de la délétion (91% dans notre cohorte). En utilisant un modèle de lignée cellulaire de LLC (OSU-CLL) que j'ai modifié par CRISPR/Cas9, j'ai montré que TNFRSF10A et TNFRSF10B étaient tous deux fonctionnels dans la LLC, et que la voie TRAIL activée par TNFRSF10B était particulièrement impliqué dans la mort cellulaire induite par la fludarabine, un traitement utilisé dans la LLC. De plus, j'ai montré par des tests d'apoptose induite in vitro que les cellules primaires de LLC del8p perdaient leur capacité à surexprimer TNFRSF10B après exposition à la fludarabine, d'où une réduction significative de la sensibilité à TRAIL. Ces données suggèrent d'une part une efficacité diminuée de la fludarabine chez les patients porteurs d'une del8p, mais également une synergie possible entre la fludarabine et les traitements activateurs de la voie TRAIL en cours de développement qui pourrait être une option thérapeutique.

J'ai également participé à un travail ayant permis la caractérisation du profil génétique des leucémies prolymphocytaires B, une forme rare et agressive de LLC, au sein desquelles nous avons montré qu'une stratification du risque selon les anomalies des gènes *MYC* et *TP53* permettait de définir 3 groupes de pronostic très différent.

Enfin, je me suis intéressé à l'impact du caryotype complexe et hypercomplexe en tant que facteur pronostique indépendant. Une revue de la littérature a confirmé la réduction des survies globale et sans progression après traitement par fludarabine. Les études plus récentes à propos de l'influence du caryotype complexe sur la survie après traitement ciblé (ibrutinib, vénétoclax…), apparaissent encore contradictoires, et nécessiteront davantage de recul.

Abstract

Chronic lymphocytic leukemia (CLL) is the most common leukemia in the West. The prognosis is highly heterogeneous and depends on cytogenetic and molecular abnormalities. Some of these abnormalities involve resistance to CLL treatments, which is crucial to understand for an optimal treatment.

My thesis work mainly focused on CLL with 8p deletion (del8p). We have shown that this rare but recurrent chromosomal abnormality was associated with poor prognostic factors (such as complex karyotype, *TP53* aberrations, and unmutated IGHV status), short overall and progression-free survival, and Richter transformation. I showed the implication of the *TNFRSF10* gene family, receptors for the TRAIL ligand, in the great majority of patients carrying the del8p (91% in our cohort). Using a CLL cell line model (OSU-CLL), which I edited by CISPR/Cas9, I demonstrated that both TNFRSF10A and TNFRSF10B were functional in CLL, and that TRAIL pathway activated by TNFRSF10B was significantly involved in fludarabine-induced cell death – fludarabine being a CLL treatment. Furthermore, I showed by in vitro induced apoptosis assays that primary del8p CLL cells lost their ability to overexpress TNFRSF10B after exposure to fludarabine, resulting in a significant reduction in TRAIL sensitivity. These data suggest a lower efficacy of fludarabine in del8p patients, but also a potential synergy between fludarabine and TRAIL therapies under development, which might benefit non-del8p CLL patients.

I also contributed to the characterization of the genetic profile of B-cell prolymphocytic leukemia, a rare but aggressive type of CLL. We showed that a risk stratification according to *MYC* and *TP53* gene abnormalities allowed to define 3 groups with quite distinct prognosis.

Finally, I investigated the impact of complex and hypercomplex karyotype as an independent prognostic factor. A review of the literature confirmed the reduction of overall and progression-free survival, especially after fludarabine treatment. Recent studies on the influence of complex karyotype after targeted therapy (ibrutinib, venetoclax...) still appear controversial, and will require further research with longer follow-up.